Computational Techniques for Automated Tracking and Analysis of Fish Movement in Controlled Aquatic Environments

Tomasz Hubert Pinkiewicz, BComp(Hons)

Submitted in fulfilment of the requirements for the Degree of
Doctor of Philosophy
University of Tasmania
2012

Declarations and Statements

Declaration of Originality

This thesis contains no material which has been accepted for a degree or diploma by the University or any other institution, except by way of background information and duly acknowledged in the thesis, and to the best of the my knowledge and belief no material previously published or written by another person except where due acknowledgement is made in the text of the thesis, nor does the thesis contain any material that infringes copyright.

Authority of Access

This thesis may be available for loan and limited copying in accordance with Copyright Act 1968.

Statement of Ethical Conduct

The research associated with this thesis abides by the international and Australian codes on human and animal experimentation, the guidelines by the Australian Government's Office of the Gene Technology Regulator and the rulings of the Safety, Ethics and Institutional Biosafety Committees of the University.

Signature _____ Date _____

Acknowledgements

A lot of people supported me throughout my candidature but perhaps the most important was the support of my family. My children, Monique and Michael, have always known me as the "Uni student" and while I can never recoup the time I have missed out with them, at least now I will be able to to devote my time to them. My wife's initial enthusiasm turned into "Hurry up and finish" but she was always there for me, putting up with my moods. Thank you for letting me accomplish this, you will have your old Tom back now. To our parents, for helping our young family during these years - great thanks.

This thesis would not be possible without the great support from my supervisors - Dr. Mike Cameron-Jones, Professor John Purser and Dr. Ray Williams (ret.). Early on, the guidance and our exchange of ideas with John and Ray gave me a two path approach to my research, sea cages and tanks, something which I persevered with for the rest of the thesis. Throughout, our regular meetings kept pushing me forward even in times of poor discipline and feedback was always around the corner. In final stages, the feedback from Mike and John on the structure and content of the thesis was invaluable and helped me get to the end in a timely manner.

Thanks go to support staff at School of Computing and Information Systems and National Centre for Marine Conservation and Resource Sustainability. They have spent lots of time helping me setup software and hardware required for my work. Also thanks go to the administration staff for assistance with all things big and small. Great appreciation to Denis for his very valuable proof-reading in the final stages of thesis writing.

During my travels I have met many people in the area of aquaculture. On the industry side, perhaps the greatest thanks go to staff at Van Diemen Aquaculture Pty Ltd for letting me carry out my recordings on the farm, even when at times I was a nuisance. I also met several aquaculture researchers who have provided me with feedback and encouragement in regards to my work. Thanks Neil, Chris and Sunil.

Final acknowledgements go to University of Tasmania for providing me with a scholarship, which meant that I could conduct a large part of my study full-time, therefore shortening the misery I bestowed upon my family.

Abstract

This thesis presents research on automated video analysis using computer vision systems, for analysing fish movements and behaviours in sea cages and tanks.

Video technology is widely used in aquaculture to observe fish movements, however these observations can be subjective and fish can only be observed for short periods due to the manual labour required and observer fatigue. In research, the analysis of video footage is tedious and very time consuming, requiring sampling to make it feasible. It is therefore desirable to automate such analysis and provide users with a tool that can gather data about fish movements in real-time, continuously, objectively and at a high sampling rate. The aim of this thesis is to develop and validate computer vision systems to track fish automatically in sea cages and tanks.

Three computer vision systems are proposed, one for sea cages and two for tanks, and they consist of two major stages. The first stage extracts fish images from complex backgrounds in video footage through the process of segmentation. The second stage is responsible for tracking multiple detected fish by associating newly extracted objects with existing tracks of fish. The system developed for use in sea cages tracks fish for short periods and generates measures of fish movement - their average swimming speed and direction. The first system used in tanks tracks a small number of fish over a long period of time with the purpose of long-term observation of spatial location and agonistic behaviours between individuals. The second system used in tanks is based on the one developed for sea cages and is used to track small groups of fish, with the purpose of observing groups' spatio-temporal patterns rather than movements of individuals.

When using the sea cage system, variations in swimming speed and direction were observed within days and between days. Some of these variations could be attributed to water current changes due to tides, but no consistent patterns were observed in relation to time of day or feeding. During the transfer of Atlantic salmon smolts from a freshwater hatchery to sea cages, a pattern of non-schooling behaviour during the first 3-5 weeks was observed, followed by a sharp transition to schooling behaviour.

In tanks, tracking of two individuals was possible but maintaining unique identification of fish was not completely achieved. When tracking groups of fish, the tracking system was able to detect variations in swimming speed, while spatio-temporal patterns were observed in relation to the demand feeder and the water

inlet.

The sea cage system has a potential application in the commercial setting, where it can be used to develop behavioural profiles of fish and act as an alarm system if unusual behaviours are detected. From the research point of view, use of these automated systems improves the process of gathering data about fish movements, provides a high level of sampling and increases the speed of video processing, which is currently based on manual observation of fish movement. Time can be spent on analysing the data rather than on extracting it from video. While there is some requirement for data analysis in this system, the benefits in extracting data from the video automatically far outweigh the requirement for data analysis.

Keywords: target tracking, image and video processing, aquaculture, fish behaviour

Contents

List of Tables

List of Figures

CHAPTER 1

INTRODUCTION

This thesis describes research on computer vision systems to automatically analyse fish behaviours in aquaculture sea cages and tanks.

1.1 Research Background

Finfish aquaculture research attempts to understand relationships between fish and their surroundings (Oppedal et al., 2011). This knowledge can be used to evaluate and improve aquaculture management practices and fish welfare. From the commercial point of view, an aquaculture business aims to maximise revenues and minimise operating costs in order to maximise profits, while maintaining environmental sustainability. This is achieved by maintaining healthy stock which grows optimally, while reducing the wastage of feed. Different fish species require different conditions to grow optimally; locality of the site, water flow, temperatures, oxygen levels, and preferred feeding patterns are some major considerations (Ashley, 2007).

Fish vary their behaviour in response to environmental changes, therefore observation of fish behaviour and movement is often a focus of experimental studies (Juell, 1995). Today's advances in technology provide various ways of observing fish behaviour, but possibly the most accessible and cheapest is video technology, due to its widespread commercial and private use, and very large volume of sales. Underwater video cameras are most widely used in aquaculture, because most fish activity is not visible from the surface.

By observing fish behaviour one can evaluate their welfare and examine the impact of the environment on fish (Oppedal et al., 2011). For that reason farm operators observe fish during feeding; the operators' experience allows them to control the feeding, and they can terminate the feeding event early if satiation is reached, or extend feeding if required. However it is impractical for farmers to observe fish all the time. The manual observation is also a subjective procedure,

results differ depending on the level of operator training and experience. Continuous observation of fish is also impractical in aquaculture research but desirable because sampling of observations may affect outcomes of experiments.

1.2 Justification for Research

The finfish aquaculture sector is growing worldwide and farm operators are always interested in technologies which can improve farm operations and maintain a high level of quality of fish and environment. In some countries there is already a requirement to monitor the environment around fish farms through legislation and more countries will soon follow (Oppedal et al., 2011). Practical, on farm monitoring of fish welfare through Operational Welfare Indices is the current focus of fish welfare researchers (First International Workshop on Fish Welfare, Madrid - http://www.fishwelfare.com) and one of the economical ways of doing that is through observation of fish behaviour using video technology. However the observation of fish behaviour is currently a manual process and not cost-effective for commercial purposes.

In aquaculture research, sampling is used when observing fish over long time periods, as it is not practical to undertake continuous observation. For example, Kadri et al. (1991) when investigating daily feeding rhythms, sampled video observations every two hours and observed swimming speeds every hour for 10 days. Observing feeding behaviours usually involves recording only the actual feeding events (Petrell and Ang, 2001).

Automated observation would provide benefits over manual observation. On farms, such automation would enable continuous observation of fish (at least during the daytime). Such a system could be used to evaluate fish welfare, further optimise feeding, provide real-time alerts about unusual behaviours (e.g. due to predators, environmental changes or disease) and provide historical data for long term management. Due to the low cost of video technology, such a system could be applied to every sea cage at an affordable cost, providing farm managers with an improved overall picture of fish activity on the farm. From the research point of view, with such a system continuous data would be available and sampling would not be required. Researchers could spend more time looking at and making sense of the fish behaviour data rather than trying to extract the data from video. Therefore the speed of research would increase and a wider range of experimental parameters could be explored.

1.3 Research Aims

The main aim of this project is to investigate the automation of the analysis of fish behaviour in sea cages and tanks by using video technology. This is achieved by the development of computer vision software and subsequent validation experiments.

The computing aspect of the thesis involves researching existing computer vision techniques, modifying, combining and applying them to suit the unique marine environment where quality of footage is often poor due to various factors outside of experimental control. In sea cages where short term tracking is investigated, visibility is often poor due to restricted light and turbidity and the camera is exposed to constant movement. In tanks, where the aim is to uniquely track small number of fish for prolonged periods of time and also track a small group of fish for prolonged periods of time without identifying individuals, the presence of light reflections and water movement affects the ability to track fish effectively.

The aquaculture aim of the thesis is to demonstrate that computer vision systems developed for sea cages and tanks can effectively monitor fish movement and behaviour. In sea cages, the goal is to analyse dataset generated by the system and combine it with environmental and farm management data. The analysis identifies any patterns of behaviours in relation to time of day, feeding, tides, temperature and visibility. In tanks, the aim is to identify individual fish uniquely and track them for prolonged periods of time. This allows identification of agonistic behaviours between fish, which would inform about social hierarchies. The secondary goal is to observe a group of fish during a self-feeding experiment to observe fish behaviours in relation to the feeder.

1.4 Key Assumptions and Limitations

A key assumption of the thesis is that the observation of fish in a sea cage using a video camera provides a representative subset of the fish population concerned. Therefore placement of the camera is important and farm operators' knowledge was used to determine best depths and locations for the camera. The main limitation was that cage recordings were done on a commercial farm and often commercial operations took precedence over research recordings. Accessibility to the remote site was also an issue and any problems with recordings could not be corrected immediately.

1.5 Animal Ethics Approval

The experimentation reported in this thesis was conducted with the approval of the University of Tasmania Animal Ethics Committee, approval numbers A0007720 and A0009439.

1.6 Outline of the Thesis

The research project is a combination of computer science and aquaculture research. While separating the manuscript in two parts, one for each discipline, would at first seem intuitive, it would create an divide between the two areas that would be difficult to follow. The goal of the thesis structure is to bridge the gap between the disciplines and focus on two areas in the analysis of fish behaviour: analysis in sea cages and analysis in tanks. While work conducted in sea cages is concerned with large numbers of fish in a commercial setting, the work carried out in tanks is concerned with individual fish or small numbers of fish.

The thesis is structured as follows. The first three chapters of the body of the thesis (Chapters 2, 3, 4) provide a literature review for both disciplines. Chapter 2 introduces the aquaculture research on fish behaviours and research methods used to analyse fish movements and behaviours. This chapter also outlines the current use of computer vision and other technologies in aquaculture research and their relevance to the thesis.

The process of separating foreground objects from background is called segmentation. Chapter 3 reviews how objects can be extracted from video sequences and several methods of segmentation are presented, some of which use individual image frames, and others that use the motion within the video sequence to extract shapes. Chapter 4 describes how extracted objects can be tracked within a video sequence. The chapter reviews tracking algorithms such as the Kalman filter and the Particle filter and also covers multi-target tracking where multiple measurements need to be assigned to multiple targets at each time step. These two chapters provide the necessary background for the computer vision algorithms described in later experimental chapters.

The experimental chapters consist of two parts. The focal point of the first part is the analysis of fish movement in sea cages, with Chapter 5 describing the development of the tracking system and Chapter 6 describing experiments in sea cages used to validate the system. Chapter 5 presents the computer system developed, methods used, and how the system deals with the unique challenges of underwater video imaging. The chapter also describes which data are extracted

from the tracking system, how they are manipulated, the accuracy of the system and how data is presented. Chapter 6 focuses on the output generated by the tracking system in the aquaculture context. Four experiments are presented to validate the system by discussing the observed patterns of behaviour.

The second part of the experimental chapters focuses on fish movement in research tanks, with Chapter 7 examining tracking of individual fish in tanks, while Chapter 8 examines tracking of a small group of fish in a tank. Chapter 7 presents a unique tracking system designed to track individuals in a small tank and results from analysing two video sequences are shown to demonstrate the capability of the system and problems encountered. Experiments in Chapter 8 track groups of fish within a tank without a focus on individuals. The tracking system is a modification of the system mentioned in Chapter 5, so the focus is on validating the system in an experiment involving a group of naive fish in a tank adapting to use a demand feeder by pulling on a bead.

In the concluding Chapter 9, a summary of findings is stated along with limitations of the proposed systems and possibilities for future research.

CHAPTER 2

THE USE OF TECHNOLOGY IN FISH BEHAVIOUR RESEARCH

2.1 Introduction

Fish behaviour plays a crucial role in aquaculture. Farm operators need to recognise different behaviours and understand their significance, and encourage certain behaviours, like fish schooling, that are desirable for effective fish production (Brown et al., 2006). Failure to recognise changes in behaviour, or failure to establish certain behaviours, may result in poor growth, poor health and increased mortality rate - an undesirable outcome from both a fish welfare and commercial perspective.

While the definition of fish welfare is still under debate (Damsgård et al., 2006; Ashley, 2007; Huntingford and Kadri, 2008), aquaculture operators and researchers agree that good welfare is important to successful commercial operation, while poor welfare is not desirable. Many issues mentioned in this chapter have a great influence on the welfare of fish. Stress and welfare are related, though the exact relationship is still not well understood (Huntingford and Kadri, 2008). However it is understood that long term stress causes slow growth through loss of appetite and decreases resistance to disease (Ashley, 2007). Another problem facing farmers and researchers is how to measure welfare given different definitions and different perspectives. Experienced farmers can identify which farming practices, fish behaviours and environmental conditions may cause poor welfare and which conditions promote good welfare but the process is subjective and differs between individuals. Recently a focus has been on how to quantify fish welfare through the development of Operational Welfare Indices (Branson, 2008). Researchers are now acknowledging that continuous monitoring of fish welfare is desirable and are looking for methods which can help quantify fish welfare.

This chapter provides the background of previous aquaculture research on fish behaviours with an emphasis on the technology used to analyse these behaviours.

Section 2.2 describes research on fish behaviours in sea cages while Section 2.3 describes research on fish behaviours in small tanks, where the focus is on individuals and small group interactions. Section 2.4 further narrows the topic to the use of computer vision in aquaculture and marine science. As video technology is not the only technology used in aquaculture, Section 2.5 provides background on acoustic and radio telemetry and acoustic based detection.

2.2 Behaviours in Sea Cages

Research on fish behaviours in sea cages has focused mainly on the impact of farm operation on fish behaviour, and an understanding of how these behaviours impact on fish welfare. Management practices such as feeding, cage maintenance and protection from predators have an impact on, or are influenced by, fish behaviour. Feeding behaviours form an important part of aquaculture research because they directly impact the efficiency of aquaculture businesses, where the main objective is to optimise fish growth and minimise food wastage. Feeding behaviours may be observed as activity at the water surface, though observations using underwater video cameras give a better indication of feeding activity (Ang and Petrell, 1997). Underwater cameras can also be used to detect uneaten pellets as they sink towards the bottom of the cage. Operators use this information to cease feeding and minimise wastage. To further increase efficiency, automated feeding systems have been developed and waste feed minimisation technologies also developed (Blyth et al., 1993).

Observation of fish behaviour was instrumental in the evaluation of these new systems and gave researchers an understanding of which behaviours are desirable during feeding to achieve the most effective results (Ang and Petrell, 1998). One of the indicators of fish behaviour that has been investigated over the years in relation to feeding is swimming speed. A diurnal pattern in swimming speed of Atlantic salmon has been observed with swimming speeds higher in the early morning and evening, and much lower in early afternoon (Kadri et al., 1991; Blyth et al., 1993). Kadri et al. (1991) also found that time of day had more influence on the swimming speed of fish than the state of the tide. However a study by Smith et al. (1993) determined that such a pattern, related to time of day, was not evident when experiments were conducted during different seasons of the year. Both studies concluded that these differences could have been due to different light conditions and therefore different visibility in the water. Swimming speed also varies between feeding and non-feeding periods, and is affected by different feeding regimes. It has been demonstrated that the use of on-demand feeding, as opposed to normal time-based feeding, decreases competition during feeding

and decreases the swimming speed, and therefore decreases the variation in size and improves growth (Andrew et al., 2002). On-demand feeding also results in different search strategies being applied by fish with resultant lower swimming speeds (Andrew et al., 2002). Thus, swimming speed can be used as a descriptor of fish behaviour.

Another aspect of sea cage aquaculture is the impact of the environment on the welfare of fish and on their ability to feed and grow optimally. Fish react to their surroundings in a behavioural way, therefore the observation of fish behaviour becomes important to understanding the relationship between fish farming and the environment. In salmonid aquaculture, the main influencing environmental variables are dissolved oxygen (DO) levels, temperature, water current speed and direction, salinity, turbidity and algal concentration. These variables may be manually or automatically sampled on a regular basis, providing good historical data, or may be observed on an ad-hoc basis. Dissolved oxygen levels are inversely related to temperature and salinity, and are critical to the survival of fish. Higher temperatures cause lower DO levels and often aeration is required to maintain sufficient oxygen supply, especially during periods of low water flow or exchange. Care also needs to be taken when feeding fish in higher temperatures, as the post-prandial oxygen requirement increases substantially (Purser and Forteath, 2003).

While video technology provides a suitable method of observing fish behaviour directly, currently it requires manual analysis, making it time consuming and costly. Researchers can use other tools to indirectly observe fish behaviours in relation to environmental changes. For example, the analysis of feed intake using adaptive feeder technology (AQ1 Systems, Tasmania, Australia) has allowed researchers to examine the relationship between feeding habits and day-length, seasons, and water temperature. Daily ration was used as an indirect representation of feeding activity and it was analysed against the above mentioned variables. Analysis showed that feeding rhythms change with seasons and are influenced by temperature changes and the length of day (Noble et al., 2007). Another element important in cage-rearing is light intensity, which can include the use of artificial lights to delay the maturation process. Swimming at depths displaying a high intensity of light forces fish to compromise between increased risk of predators and hunger (Juell and Fosseidengen, 2004). Investigating these relationships can be difficult, as it requires continuous observation of fish, which is only feasible if an automated system exists to analyse such behaviours.

Understanding how fish react to predator attacks is important because sea cages are often subject to attacks from seals and other predators. Even when predator attacks are limited by measures undertaken by farmers (e.g. exclusion

nets), it is possible for fish to be stressed due to the presence of predators attempting to breach cage defences (Brännäs et al., 2001). Prolonged exposure to predators may cause chronic stress and this will inhibit growth and affect fish welfare (Purser and Forteath, 2003). Researchers are investigating the link between predation risk, feeding and environmental conditions, and farmers employ measures to minimise exposure to predators, to avoid or minimise long term stress (Ashley, 2007). The understanding of farmed fish anti-predator behaviours often comes from observing natural behaviours of wild fish. However it has been observed that anti-predator responses of wild origin brown trout differed from those of sea-ranched origin trout (Petersson and Järvi, 2006). Two possible explanations were offered. The first was a non-genetic maternal influence, the second plausible explanation was a genetic difference which might occur within a single-year class despite both wild and sea-ranched fish coming from a very similar genetic pool.

An important aspect of aquaculture research focuses on fish welfare. The research community has been trying to reach a consensus on what constitutes fish welfare (Damsgård et al., 2006), with the focus shifted towards the measurement of fish welfare in a practical manner on commercial farms. This led to the development of Operational Welfare Indices (OWIs), a set of indicators which can be measured on farms to provide farmers with real-time and historical feedback of fish welfare (Oppedal et al., 2011). Rather than trying to measure all variables which may contribute to the evaluation of fish welfare, the challenge is to pick a limited number of indices which can provide an effective evaluation of welfare at an affordable cost to farmers. Fish movement could be one of these indicators. Oppedal et al. (2011) used echo sounders to evaluate the vertical distribution of fish in sea cages and suggested that an OWI could be based on these vertical behaviours, where the fish welfare index would relate to the deviation from expected behaviour. Another method of observing fish movement could be using video technology, but until now there has been no automated way to observe fish behaviour using video. While the above mentioned indicators relate to groups of fish in sea cages, it is also important to understand fish welfare for individuals (Juell, 1995). This leads to the use of RF, acoustic and video technologies on a smaller scale where individuals are observed.

Fish behaviour in sea cages is a result of complex interactions between man-induced management practices and numerous environmental variables. Determining these interactions in sea cages can be difficult, hence behavioural studies are often carried out on a much smaller scale - in research tanks.

2.3 Behaviours in Small Research Tanks

Tanks offer a smaller scale and controlled environment, providing an ideal setting in which to conduct behavioural research on fish. The smaller scale lets researchers examine how individuals and small groups respond to experimental stimuli. It is also easier to achieve replication in space for experimental purposes.

Feeding behaviours have been investigated in tanks in order to understand which methods of feed delivery yield optimal fish growth. Observations of rainbow trout (*Oncorhynchus mykiss*) interactions have shown that when using demand feeders, only a few individuals are responsible for activating the feeder (Brännäs and Alanärä, 1993), which leads to uneven feed intake and consequently uneven growth (Gélineau et al., 1998). A high reward level might mitigate this, allowing feeding by fish from low-weight classes. In a hand fed scenario, trout had better access to feed, with better growth and better size distribution (Gélineau et al., 1998). However when feeding, the rate of delivery has to be considered, because low rations may cause increased competition and low growth, while high rations when fish are fed to satiation lead to decreased competition and better growth but increased waste (Andrew et al., 2004).

Fish also establish social hierarchies, with dominant fish having better access to feed, often forcing subordinate fish to forage at times of increased predation risk, trading off safety for hunger (Alanärä et al., 2001). Comparison between wild origin and sea-ranched origin brown trout fry revealed that the number of agonistic behaviours was higher in wild origin fish (Hedenskog et al., 2002). One explanation offered by Hedenskog et al. (2002) was that the selection of fish for rapid growth may indirectly select for passiveness. Another was that wild fish may be more aggressive due to competition for food or space.

Another topic that is suitable for small scale tank research is fish adaptability and ability to learn. For example Atlantic salmon can adapt to stimuli of light flashes during feeding within 6 days (Bratland et al., 2010). On a commercial farm, this knowledge can be used to condition salmon to various farm management practices. Another application of light stimuli is for exercise purposes. Herbert et al. (2011) exposed Atlantic salmon to moving lights in the centre of the tank at a speed of 1.5 Body Lengths/s. Fish increased the swimming speed from the original 0.6 BL/s to $\geq$1.8 BL/s after 28 days. Swimming at such speeds for sustained periods of time improved the growth, and the quality (slender body shape), and lowered stress (lower cortisol levels).

The small scale of tanks allows the background conditions to remain the same while varying only treatment data. Short term stress response is not unexpected in aquaculture but chronic stress is usually associated with poor welfare. Density

of fish is one of the variables which can affect fish welfare (Ashley, 2007). For adult Atlantic halibut (*Hippoglossus hippoglossus L.*) a high density may induce unusual surface activity, lower feed intake and inhibit growth (Kristiansen et al., 2004). Movements of rainbow trout in a high density system caused fish to alter direction often, and a higher incidence of fin damage was also observed (Bégout Anras and Lagardère, 2004). Crowding also forced fish to swim within the inner part of the tank, while fish in a less crowded tank had an ability to swim in the outer areas of the tank where the feeder and water inlet were located. Crowded fish also lost their day-night activity rhythm, something that was visible in less crowded fish (Bégout Anras and Lagardère, 2004).

2.4 Computer Vision in Aquaculture/Marine Science

Video technology is widely used both in commercial aquaculture and in aquaculture research (Kadri et al., 1996; Ang and Petrell, 1997). The technology is appealing because its cost is continually decreasing due to commercial demand (high volume) and quality is increasing due to advances in manufacturing. Farm operators mainly use cameras during feeding events to observe fish movement and pellet wastage. Observations at other times are carried out on an ad-hoc basis only. With advances in computer technology, the ability to use computers to analyse images and video sequences has improved. Current technology allows real-time video processing for long periods of time. Aquaculture researchers have realised this potential and began developing systems which would make farm management and research easier (Israeli and Kimmel, 1996; Dunn, 2008). This section will review the field and include technologies peripheral to the framework of the thesis in order to place the behavioural work in the context of current advances and technologies.

2.4.1 Size Measurement and Stock Assessment

One of the most important tasks in aquaculture is the estimation of biomass of all fish in a cage. An accurate estimate provides input into farm management to determine feed requirements and monitor growth. It also has an impact on financial planning, allowing determination of the expected commercial value of the stock and the cost required to feed the stock. The earliest application of computer vision to the challenge of biomass estimation dates back to the early 1990s. This research centred on the task of estimating the size of swimming fish from stereo images (Naiberg, 1994); given the size of the fish and stock inventory, the overall biomass could be estimated. The system matched heads and tails in

stereo images and provided a length measurement for detected fish. At the same time, a semi-automated system called Fish Image Capturing And Sizing System (FICASS) was developed, as real-time processing of images was not viable at the time (Petrell et al., 1997). FICASS allowed an operator to manually mark important features of a fish within a video frame (using a computer mouse) and the program would then calculate fish weight according to a mathematical relationship with the length and height of the fish specific to fish species. The key objective since then has been to replace manual marking with automated marking allowing a biomass system to gather more samples with less effort and provide more accurate estimates of fish biomass within a sea cage.

More recent work has focused on this specific aspect of detecting and extracting fish shapes in a reliable manner. Point Distribution Models have been used to accurately extract fish shapes (Tillett et al., 2000). The concept was based on the Active Shape Model (ASM) (Cootes et al., 1995) where a fish shape can be described as a statistical model using training images. The method was capable of statistically deforming the model to deal with variations in shape. Applied to testing images, the system was capable of wrapping the model around the candidate fish and giving its correct shape as an output. This shape was then used to calculate fish dimensions and therefore the biomass.

A similar approach was taken by Williams et al. (2006) but they applied a variation of ASM called the Active Appearance Model (AAM) (Cootes and Taylor, 2001) to detect fish in sea cages. Side-on footage used aquaculture nets as a unique background which assisted in separating fish from the background. Once fish were extracted, their centroids, and ellipses approximating their outline, were calculated. An eccentricity statistic of an ellipse around fish shape was used to eliminate unlikely matches, and for the remaining candidate matches, ellipses provided a starting point for the AAM. This final procedure would further eliminate any shapes that could not be fitted successfully. Costa et al. (2006) provided another example of determining fish size using Artificial Neural Networks to decrease the error associated with camera distortions. This method improved the shape modelling of detected fish and therefore increased the accuracy of body size measurements. Another important aspect of underwater image processing, uneven illumination, was addressed by Martinez-de Dios et al. (2003). The specific nature of the marine environment causes variability in light intensity in different areas of an image or video. This variability is affected by the depth and orientation of the camera, turbidity of the water and the intensity of the light source. With the camera in the water facing sideways, Martinez-de Dios et al. (2003) compensated for variability in illumination between the upper region of the image frame (close to the surface and the light source) and the bottom of the image frame (where less light penetrates, due to fish occlusion and attenuation

of light) by modifying a histogram transformation to even out the illumination and contrast in each row. Accounting for uneven illumination allows for a more accurate extraction of fish shapes and therefore better size estimation.

2.4.2 Fish Behaviour

Computer vision has been used to analyse fish behaviours and this subsection introduces current research trends and relates them to the research carried out in this thesis. Early work on behavioural research using computer vision was undertaken by Kato et al. (1996) and Israeli and Kimmel (1996). Kato et al. (1996) developed an image processing system to track a single goldfish in three dimensions using two orthogonal cameras. This was an advance on previous rodent tracking systems, which worked in two dimensions. However data storage capacities were low compared with those of today, so tracking was carried out for only 60 minutes. Israeli and Kimmel (1996) investigated how goldfish in a tank dealt with hypoxia, by detecting the school of fish within each video frame from two perpendicular cameras. This produced a three dimensional distribution of the school and allowed researchers to observe variations in the school size. In addition, frame differencing was used to create a motion image called a Projected Mobility Picture (PMP) to describe the changing location of the fish. The system detected fish movement to the surface when subjected to the effect of hypoxia. PMP was further improved in another study to produce a numerical indication of Tilapia activity - speed normalised in terms of body lengths per unit of time (Xu et al., 2006). The authors used a glass aquarium in which to conduct the experiment and contented with shadows, uneven illumination and turbidity. As fish quickly adapt their colour to surroundings, a blue background was used for better contrast out of white, blue and green colours investigated. This experiment showed that with careful consideration of experimental set-up (suitable light and background), computer vision techniques can provide useful research data with a small number of fish. However as the number of fish increased, problems of occlusion occurred and these needed to be addressed to differentiate individual fish.

A fish species popular in behavioural studies is the zebra fish. Kato et al. (2004) used computer vision techniques to detect several zebra fish in a research tank. They successfully tracked a single fish, providing activity tracks and also tracked two fish and their interactions. However they did not attempt to track these fish for extended periods of time and maintain their unique identifications. Instead their focus was on shorter chasing behaviours. Automated tracking of large numbers of zebra fish is difficult due to their size relative to the area covered by a camera which makes unique identification of individuals impossible. How-

ever Miller and Gerlai (2007) used a semi-automated approach where the fish were marked manually on each image frame and a computer vision system then calculated statistics of the shoal behaviour. This compromise allowed generation of an accurate set of measurements and increased speed of calculations.

Automated behavioural analysis of large numbers of fish has described vertical distribution of fish in tanks (Stien et al., 2007). Thick markers were painted on the side of the wall, and software was used to detect the level of coverage of these markers by the fish. The result of the analysis was an activity graph showing the percentage of the marker coverage. As a case study Stien et al. (2007) observed the process of fish being exposed to flashing lights, with the aim of determining the length of time for fish to associate lights with feeding. In a study by Duarte et al. (2009) the activity of flatfish was described using frame differencing. While the density of fish was high and tracking of individuals was not possible, the frame difference between two consecutive frames did provide an activity index. The index was a ratio between the total number of pixels and the number of pixels deemed to represent motion. There was a high correlation between the activity determined by the automated method and the manual method (operator measurement). Though the automated method was not able to distinguish different types of activities, it could be used as an alarm to detect unusual behaviours.

2.5 Other Technologies

While the use of video technology has been widespread due to its relatively low cost, other technologies which complement or often outperform video technology are used in aquaculture. This section will review some of the aquaculture research carried out using these technologies outlining their advantages but also discussing their limitations. The studies in this section will be outlined individually, in turn, to highlight applications.

2.5.1 Acoustics and Acoustic Telemetry

The effective performance of acoustics (sound) in the water makes the technology a natural choice for use in aquaculture research. This is especially important for salt water, where the effectiveness of radio telemetry is severely degraded (Section 2.5.2). In tank based research there are two main types of such work: tracking of individuals using acoustic tags, and detecting movement (or noise) of the whole tank population. Bégout Anras and Lagardère (2004) used small

ultrasonic tags on rainbow trout to monitor fish swimming behaviour at different densities. They tracked nine fish in three tanks of 116, 333 and 583 fish, three tagged fish per tank. The tracking system sampled every 5 seconds with an accuracy to $<$ 10cm producing data on distance travelled, turning angles, swimming trajectories, space utilisation and activity patterns. In other work Lagardère et al. (2004) recorded the feeding sounds of brown trout, rainbow trout and turbot using hydrophones. The aim of the experiment was to identify sounds characteristic of feeding, specifically suction feeding, which is commonly associated with teleost fish. While the research identified some unique sounds related to feeding, the authors observed noise generated by aquaculture systems (water flows, pumps, etc.) and meteorological noise.

Fitting between the above mentioned areas of studies was a non-invasive way of tracking fish in tanks using acoustics (Conti et al., 2006). The problem however was scattering of acoustic signals within a tank. Conti et al. (2006) developed a set of equations that would allow a system to differentiate between a true signal and its echo. They suggested this technique may be suitable to track the activity of fish in tanks and fish growth, and be used as an alarm if unusual events are detected.

Sea cage aquaculture usually involves larger fish to which acoustic tags could be attached. Cubitt et al. (2003) used acoustic tags to track the movement of 39 chinook salmon within 3 cages (with an average of 6000 fish in each) - 13 fish per cage. Using 8 hydrophones in total, they were able to provide three-dimensional data of fish movement. Their results showed differences in fish movement between day and night, and also change in activity during feeding. The influences of various sources of noise (eg. boats, feeders, generators and natural noise within the environment) were identified, as noise affected the possible frequency of sampling as well as the accuracy. In addition the positioning of hydrophones, which had an effect on the triangulation, influenced the signal, with a recommendation that arranging hydrophones in a cube gives better accuracy than a rectangular box arrangement.

More recent research on tracking fish in open sea cages was conducted as part of the Open Ocean Aquaculture program at the University of New Hampshire (Rillahan et al., 2009). The project investigated the use of acoustic technology to monitor fish behaviours in sea cages. A four hydrophone system capable of tracking hundreds of tagged fish was deployed to allow Atlantic cod to be tracked in a submerged cage. It was observed that the environmental noise affected the sampling rate. A daily activity pattern, similar to the one reported by Cubitt et al. (2003), was observed - higher activity during the daytime than during night time. One important feature of this research project was the very small size of the

tag used, minimising the effect on physical attributes of fish. The tag operated at a different frequency to that which is traditionally used, which resulted in a smaller detection range (not a problem due to the size of the cage) but the accuracy of the system allowed fine movements of tracked fish, like turns and accelerations to be recorded - something not achievable with traditional systems where tags are larger, and also made the system applicable to juvenile fish.

While tagging systems can provide accurate three dimensional data, there are draw-backs especially when considering widespread commercial use. These systems are expensive and they are difficult to set-up (especially compared with video systems) because they require careful positioning in three dimensions and calibration. The implantation of tags is an invasive procedure and while the above mentioned research has not found evidence that the procedure was detrimental to the fish, it is possible that in larger scale commercial settings stress levels could increase. This would mean that tagged fish would behave differently from non-tagged fish, e.g. tagged fish which are stressed may not feed as much or occupy the same area of the cage as non-tagged fish. In a commercial system this has obvious problems as a management tool because the fish being used as a representative sample of the population, are not actually representing the behaviour of the majority of the fish in the whole system. Also tags have a limited life span and would require continuous maintenance and costly replacement. While the cost of the technology will decrease over time, currently such systems are restricted to research-oriented deployments.

Other sonar technologies provide an alternative to tagging. An earlier study as part of the Open Ocean Aquaculture program, undertaken by Michel et al. (2002), examined the feasibility of a multi-frequency/multi-beam sonar capable of detecting objects at up to 50 metres. Several problems were encountered with the system used. Tests of different frequencies proved inconclusive and problems were encountered in detecting fish, especially moving fish as the scan period was too long. While this research looked at cost effective methods of detecting fish in sea cages, another related technology exists which while costly can provide very good results in detecting and tracking of fish. The device, called Dual-frequency IDentification SONar (DIDSON) from Sound Metrics Corporation, is a multi-beam sonar (96 beams) capable of generating video-like sequences of acoustic data. So far its use in aquaculture research has been limited. McKinnon et al. (2008) used DIDSON in Northern Australia to examine the impacts of sea cage farming on wild fish surrounding the cages. Work in Australia, conducted by the New South Wales Department of Primary Industries, on the migration of fish in Australian freshwaters (Baumgartner et al., 2006), produced video sequences of acoustic data generated by DIDSON. The fact that DIDSON generates video means that research undertaken in visual systems may be applicable to the anal-

ysis of acoustic video sequences with only minor modifications. DIDSON could provide a powerful all weather monitoring system capable of tracking fish movements in sea cages. While the effectiveness of DIDSON has been praised in the reports, personal communications with researchers revealed that DIDSON is not capable of penetrating through the school of fish and so it may be of limited use. Additionally the cost of the device (which was AU$120,000 in March 2010) means that substantial funding would be required to purchase a unit for research purposes and it is likely not to be feasible for commercial aquaculture use on a per cage basis.

2.5.2 Radio Telemetry

The use of radio and acoustic telemetry has been reviewed by Baras and Lagardère (1995). The review covered active tags which use batteries to power circuitry sending out periodic signals. Tagging involves handling fish (Baras and Lagardère, 1995) and can have an effect on fish physiology and behaviour of fish (Bridger and Booth, 2003). While radio tags can perform reasonably well in freshwater, salt water operation is limited due to the conductivity of salt water (Koehn, 1999), hence acoustic tags are preferred in salt water (Section 2.5.1). Also the cost of equipment (tags and readers) is somewhat more expensive than video because the price of radio tagging systems is dependent on demand. Higher volumes of production usually mean lower costs. While this is achievable in video technology where consumer demand is high, radio tagging systems are not directly sought by the general public. However the advent of Radio Frequency Identification (RFID) technology is bringing radio telemetry to the mainstream population through supermarkets and other sectors wanting to tag their products for the purpose of identifying and streamlining supply systems. This will increase the demand for radio telemetry and drive the cost down, potentially making it more attractive to researchers and farmers.

Advances in RFID development have produced tags which have no battery of their own but are activated by an energy signal sent from the scanner. This technology is called Passive Integrated Transponders (PIT). Because there is no need for a battery, tags are very small and can be easily inserted into the fish. Also, the effects on fish physiology and behaviour are negligible (Prentice et al., 1990). However the main downside of the tags is the limited detection range (< 30cm), requiring experiments to have strategic points such as near demand feeders (Covès et al., 2006) and water inlets, where antennae will be located such that the system will determine the presence of fish close to the point of interest.

Fish can also be channelled into narrow passageways for the system to detect

their presence. A narrow channel ensures fish passing through will be registered by the readers. Using this setup, Alanärä et al. (2001) examined the passage of Brown Trout between foraging and refuge areas and determined the influence of social rank and temperature on foraging fish behaviours. They noted patterns in foraging behaviours with dominant fish feeding mainly during the night, while subordinate fish either fed in the later part of the night at lower temperatures or during the day at higher temperature, thereby compromising between the risk of predators and the need to feed. A PIT system was used to observe habitat selection by juvenile burbot between four different quadrants with different habitats (Fischer et al., 2001). The use of passageways between habitats allowed fish to swim to a different habitat through an electronic gate, which was used to decide if the transition actually occurred or if fish withdrew to a previous habitat. A study of bottom dwelling Atlantic halibut used PIT tags to examine the surface activity (Kristiansen et al., 2004). The PIT antenna was placed just under the surface of the water and it was used to detect fish swimming on the surface. They found a negative correlation between surface activity and growth rate and suggested that surface activity might be an indication of poor welfare.

PIT systems have also been used to tag a subset of fish in a larger experimental system. Dempster et al. (2008) tagged 400 fish out of a population of 2000 to ensure that these 400 fish could be identified during later stages of the experiment. During transfers, tagged fish were identified and dealt with according to the experiment design. There was no attempt to track or detect fish in water, tags were simply used to identify tagged fish from non-tagged fish. This is the most common application of PIT systems in aquaculture research (Dempster et al., 2008).

2.6 Summary

As the aquaculture industry and aquaculture research continue to grow, there is a need for continuous monitoring of not only environmental variables but also fish behaviour (Oppedal et al., 2011). While video technology has limitations, one of which is its restriction to day-time (or illuminated periods) use only , its relatively low cost and current wide-spread use means that it could be deployed on each cage or tank. Other technologies (DIDSON for example) may be more successful at detecting fish in all weather conditions, but currently their cost restricts them to funded research on a limited scale. The current issue in the use of video technology is how to use it for continuous analysis of fish behaviour. Computer vision techniques provide a solution to continuous analysis, the approach taken in this thesis. While this chapter provided some examples of the use of computer

vision in aquaculture research, to date there has been no such work done on long term, automated analysis of fish behaviour in tanks or sea-cages, the goal of the work in this thesis. The following chapter describes computer vision concepts relevant to extracting foreground objects from complex backgrounds.

CHAPTER 3

IMAGE AND VIDEO SEGMENTATION

3.1 Introduction

The previous chapter introduced the use of computer vision in aquaculture in Section 2.4. This chapter's aim is to introduce the computer vision techniques used in extraction of foreground objects from complex backgrounds.

Advances in computing over the last two decades and decreasing hardware costs have had a significant impact on image and video processing especially in real-time situations. The main objective of image and video segmentation in the context of the thesis is to extract regions of interest (foreground objects) from video sequences, while ignoring background areas (remaining areas of an image not relevant to the application). Research in image and video segmentation has been driven by several major applications and these are discussed in Section 3.1.1. Section 3.2 introduces the concepts behind segmentation of single images while Section 3.3 discusses segmentation of sequences of images and how the temporal dimension is utilised to improve segmentation outcomes. A stabilisation of camera to enhance segmentation outcomes is covered briefly in Section 3.4. A summary in Section 3.5 provides an explanation of how motion segmentation can link with tracking methods, which are described in the next chapter.

3.1.1 Computer Vision Applications

Perhaps the most prominent area where image and video processing plays an important role is security and surveillance. Airports, city malls and motorways are all monitored using video technology. Over the years, the push has been towards automation of these systems for various purposes, such as detection of faces or detection of suspicious items left unattended. There are several challenges which surveillance systems must overcome to be effective (Xu et al., 2004). While back-

grounds may be static (a motorway for example), more often backgrounds will vary with time (especially outdoors). Movement of trees, rain and fog, as well as movement of the camera (intentional or unintentional) all cause the background to be of a dynamic nature. In addition some objects may not be relevant to the application and will need to be treated as background. Even static backgrounds will change their appearance over time due to illumination changes, caused by sunlight and cloud cover. The number of objects to be detected can be high (e.g. heavy traffic) and often these objects are close together (e.g. people in a crowd). This poses a challenge in detecting and separating individual objects, as occlusions will be unavoidable. In addition, objects of interest will cast shadows and this further complicates the computer vision task. Rosin and Ellis (1995) proposed a shadow detection method based on a region growing algorithm. Xu et al. (2004) used colour-based information combined with texture information to reconstruct foreground shapes without shadows included.

In the late 1990's the Video and Surveillance Monitoring (VASM) project was undertaken at Carnegie Mellon University (Collins et al., 2000). The goal of this project was to develop a multi-camera integrated video surveillance system able to provide continuous tracking of people and vehicles over a wide area in a multi-building situation. The project was sponsored by a DARPA initiative which looked at multi-sensor surveillance in battlefield situations. The system was required to deal with a variety of backgrounds, with varying degrees of dynamics. Researchers developed a method that allowed computed backgrounds to adapt to temporal changes caused by illumination, environment changes (e.g. trees and rain) and camera motion. The method is covered in more detail in Section 3.3.3. The system was also capable of tracking multiple objects and identifying types of cars by using neural network algorithms. The VASM project also dealt with human activity analysis (using gait analysis), moving camera tracking, airborne tracking, scene representation, visualisation and geolocation. Results were shown not only in a military setting but also in civilian situations. Another military surveillance system was proposed by Boult et al. (2001). The system used a background modelling algorithm which allowed detection of slow moving targets deliberately trying to avoid detection, such as camouflaged snipers, while at the same time dealing with the fact that the environment was also visually dynamic (moving trees, branches, grass, changes in illumination, etc.). A similar background management to the VSAM model has also been applied in hardware-based video encoding (Chien et al., 2004). The key idea in these systems was methods of separating objects of interest from various dynamic backgrounds. The following sections present some of the more commonly used techniques used in detecting objects in backgrounds of various complexities.

3.2 Image Segmentation Techniques

3.2.1 Image Pre-processing

Images are often captured in less than ideal conditions. Before they can be analysed they require some form of "cleaning" to reduce the effects of noise, blur or uneven illumination. This is known as image pre-processing or image enhancement. Simple contrast adjustment is the linear scaling of an image between specified lower and upper limits. This may allow the brightness of darker areas of the image to be increased and decrease the intensity in bright areas. More complex contrast adjustment can also be carried out, such as using histogram equalisation which works by evaluating the histogram of the original image and transforming it into a histogram with uniform intensity levels (Gonzalez et al., 2004). The original image is then remapped using the new histogram to create a contrast enhanced image. A further improvement of this method, called Adaptive Histogram Equalisation (AHE), uses multiple histograms for different parts of an image to provide more local contrast adjustment. However the drawback of this method is that it produces additional noise in parts of the image. To deal with this problem Contrast Limited Adaptive Histogram Equalisation (CLAHE) was proposed by (Pizer et al., 1987). More recently Jin et al. (2001) offered an alternative method called Multi-scale Adaptive Histogram Equalisation (MAHE) based on wavelets.

Many images are captured with noise which filtering can be used to remove. A spatial filter uses a mask which is centred around a pixel and extracts neighbouring pixels for processing. Filter operations are then carried out on this neighbourhood of pixels. A spatial filter algorithm moves through each pixel in an image and based on the mask and the filter operation, it generates a new, transformed image. Blurring is one of the most commonly used operations in image filtering. It allows the removal of small details from an image, reducing the effect of noise on segmentation (Gonzalez and Woods, 2008). An averaging filter (or low pass filter) can be used to blur (smooth) an image by averaging pixels contained in a neighbourhood mask. A very different, commonly used type of filter, is the sharpening filter, where the aim is to highlight intensity transitions. It can be used in photograph enhancement to alleviate blur caused by a shaky camera.

Different types of image analysis require different enhancements. In this thesis, the purpose of enhancements is to strengthen the difference between image areas corresponding to foreground objects and the background. A segmentation process is used to extract these regions from images. The following subsections will describe two commonly used methods of image segmentation: thresholding

and edge detection.

3.2.2 Thresholding

Image thresholding is a basic method for examining an image's intensity levels and deciding on an appropriate threshold that may allow differentiation between foreground and background. The thresholding operation transforms a grey-scale image f (Fig. 3.1) into a binary image g where the value of each transformed pixel $g(x, y)$ is determined by the value of the original pixel $f(x, y)$ and the threshold value. This transformation generates a black and white image g, in which pixels in areas detected as foreground will have value of 1 (white) and pixels in areas detected as background will have value of 0 (black) (Eq. 3.1).

$$g(x,y) = \begin{cases} 1 & \text{if } f(x,y) \leq T \\ 0 & \text{if } f(x,y) > T \end{cases} \tag{3.1}$$

Figure 3.1: Grey-scale, unthresholded image

Global Thresholding

When a single threshold is applied to the whole image, this method is called global thresholding (Fig. 3.2). One of the best known methods for selecting a

global threshold is the one proposed by Otsu (1979). It operates directly on the histogram of the grey-level image. The main assumption of this method is that the histogram is bimodal. This is a statistical method which maximises between-class variance of the histogram values (Gonzalez and Woods, 2008, p. 742). Global thresholding can be used in images where there is a clear distinction between the foreground and background (the histogram is bimodal) and the image has constant illumination levels. Otherwise the threshold achieved will not separate objects of interest from the background completely. Because thresholding requires relatively low computing resources this method can be used effectively in industrial inspection applications. In this case illumination levels can be controlled and background can be adjusted so that foreground objects can be easily detected by thresholding. Global thresholding may also be enhanced by prior smoothing of an image to eliminate noise.

Figure 3.2: Global thresholding of Figure 3.1

Adaptive Thresholding

Local thresholding is an adaptive thresholding method and can deal better with varying illumination levels (Fig. 3.3). It works by finding the mean and maximum of the neighbourhood surrounding each pixel and calculating the local threshold according to the following equation (Davies, 2005):

$$T_{pixel} = mean_{nbrhood} - (maximum_{nbrhood} - mean_{nbrhood})$$

The key choice here is to select a neighbourhood size that will cover enough foreground and background pixels. This neighbourhood size is problem dependent and often it will be a compromise between accuracy (satisfactory segmentation) and performance (speed of execution). This type of thresholding is useful when illumination across the image is non-uniform. An example can be optical character recognition (OCR), where an image of a page of text has varying illumination levels due to the position of the light source and the objective is to extract the binary image including all the text. The light source produces a white background that is brighter closer to the light source and darker further away from the source blending in with the dark text. While global thresholding would produce poor results in this case, segmenting bright background from dark background without effectively segmenting the text, adaptive thresholding will be applied locally and it will produce a better result by successfully extracting text from regions of different background intensity.

Figure 3.3: Adaptive thresholding of Figure 3.1

3.2.3 Edge Detection

Image segmentation can also be based on edge detection. The principle behind edge detection methods is that they look for sharp, local transitions in intensity (bright to dark and vice-versa). These changes can be detected using first- or

second-order derivatives which for two-dimensional images provide a gradient of change. Two popular algorithms for edge detection are the gradient detection algorithm and Canny edge detector. A gradient detection algorithm based on the Sobel operator uses a simple 3x3 mask to calculate a gradient based on the first-order derivative. This has some noise suppression capabilities that make it slightly preferable to older operators (Roberts and Prewitt operators). The Canny edge detector is a more sophisticated method which applies a Gaussian mask to calculate the gradient and also uses corrective measures to thin edges and decrease the error rate of detection (Fig. 3.4). Gonzalez and Woods (2008) give a fuller description of gradient and Canny algorithms and references to original papers. They also describe other gradient operators like Roberts, Prewitt and the Marr-Hildreth edge detector. It is important to note that although the Canny edge detector is a superior algorithm, it is also more computationally intensive. Therefore simpler methods (such as using the Sobel operator) may be preferred for real-time image processing.

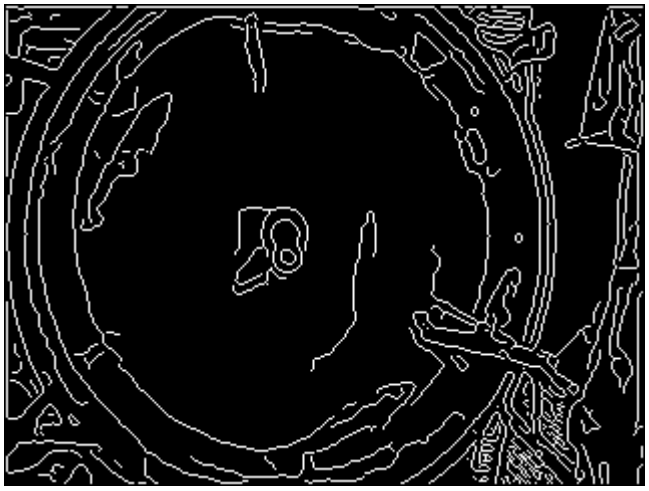

Figure 3.4: Edge detection of Figure 3.1

3.3 Motion segmentation

Motion segmentation uses the temporal dimension to separate moving objects of interest from the static background. The addition of the third dimension gives an ability to detect change. The general assumption is that foreground objects will change their position or shape over time while the background will remain constant. As this assumption often does not hold, there is a requirement to manage a dynamic background and ensure that stationary foreground objects

do not become part of the background. The assumption of moving objects and a static background may still be used during the initialisation stage when the initial background is being established. The background may then be modified over time to include changes in illumination e.g. associated with movement of the sun or changes in cloud cover. The following two subsections (3.3.1 and 3.3.2) describe two methods of extracting foreground objects from a sequence of images. Subsection 3.3.3 describes methods which combine various other methods to provide a hybrid solution for motion segmentation.

3.3.1 Temporal differencing

The most basic way of detecting motion in a sequence of images is by taking an absolute difference between a frame at time k and a frame at time $k-1$. The difference image shows which areas have changed between frames. However this method does not detect the entire object, leaving undesirable holes. In addition the difference image may contain noise from background motion or sensor errors. To reduce the effects of this noise three-frame differencing can be applied rather than just comparing two frames. Let $I_k(x, y)$ be a pixel intensity at time k. The pixel at (x, y) is determined to be moving if

$$|I_k(x,y) - I_{k-1}(x,y)| > T_k(x,y) \text{ and } |I_k(x,y) - I_{k-2}(x,y)| > T_k(x,y) \qquad (3.2)$$

where $T_k(x, y)$ is a threshold, which may be constant or evolve over time (Collins et al., 2000). As mentioned above, the inability to extract the entire object, means that frame differencing needs to be augmented by another method so that the whole object can be extracted. In this case frame differencing acts as a marker which provides some boundary co-ordinates of foreground objects.

3.3.2 Background subtraction

Another method of extracting foreground objects is using background subtraction. If the background is static, the background image can be estimated from the first few frames of the video sequence using mean or median calculations. However the majority of applications have dynamic backgrounds which change over time mainly due to environmental changes (sun, wind, clouds, etc.). Therefore in addition to initially estimating the background, a scheme is required to update the background over time, e.g. by adding a fraction of current frame intensity to the existing background intensity while decaying the background at the same time (Eq. 3.3). The constant α determines how quickly the background

will be updated and should depend on the dynamics of the scene.

$$B_{k+1}(x,y) = \alpha B_k(x,y) + (1-\alpha) I_k(x,y) \tag{3.3}$$

The current frame, I_k, can then be subtracted from the background, B_k, and the absolute difference is thresholded to produce foreground objects.

$$|I_k(x,y) - B_k(x,y)| > T_k(x,y) \tag{3.4}$$

This method works well when objects are always moving through the scene. However problems arise when objects become stationary as they will eventually become part of the background. Alternatively objects which were stationary at the beginning of the sequence, may start to move which leaves holes in the background which are later detected as foreground objects. Therefore a more sophisticated way of maintaining the background is required.

3.3.3 Hybrid methods

Hybrid methods combine several different motion detection methods to provide background management and extraction of foreground objects. This subsection describes the two methods which have influenced the work undertaken in this thesis but it also briefly mentions other work for completeness.

The Video Surveillance and Monitoring (VSAM) Project

The report written by Collins et al. (2000), as part of the VSAM project, provides a comprehensive motion segmentation strategy that was applied to surveillance of people and cars in parking areas. This system combines background subtraction with three frame differencing to provide an effective way of detecting moving objects. Equation 3.3 is modified to update a background pixel only if the pixel has been deemed as non-moving. This update takes into account the existence of both background pixels and foreground pixels. If a pixel is deemed as moving, i.e. as part of the thresholded frame differencing result, then the previous background pixel is used without any changes (Eq 3.5). This scheme allows the background to evolve over time and maintain accurate detection rates.

$$B_{k+1}(x) = \begin{cases} \alpha B_k(x) + (1-\alpha) I_k(x) & x \text{ is a non-moving pixel} \\ B_k(x) & x \text{ is a moving pixel} \end{cases} \tag{3.5}$$

Collins et al. (2000) also mention an adaptive way of calculating a threshold $T_{k+1}(x)$ for each pixel x. Furthermore they provide a layered detection scheme which deals with objects stopping and with overlapping objects.

Fast Video Segmentation

The second system of interest was proposed by Chien et al. (2004). This background management scheme was intended for use in hardware based, real-time, content-based MPEG-4 encoding. The aim of the algorithm is to create the Initial Object Mask (IOM), which represents all foreground objects detected in the image frame. Because objects can be stationary, it is important that the algorithm deals with objects that have stopped, and objects which began to move during the sequence. Initially the algorithm relies on a frame difference (FD) between two frames to detect areas of the image frame which are in motion. This frame difference image is then thresholded to create a Frame Difference Mask (FDM).

$$FD_k(x,y) = |I_k(x,y) - I_{k-1}(x,y)| \tag{3.6}$$

$$FDM_k(x,y) = \begin{cases} 1 & \text{if } FD \geq Th \\ 0 & \text{if } FD < Th \end{cases} \tag{3.7}$$

where $I_k(x,y)$ and $I_{k-1}(x,y)$ is the intensity of a pixel at time k and $k-1$ respectively, FD is a binary frame difference image, and FDM is a binary frame difference mask. Chien et al. (2004) also offer a scheme for determining an adaptive threshold Th automatically. The information from frame differencing is then used to produce a Stationary Index (SI) and this in turn is used to produce the background (BG). SI represents how infrequently the pixels change. Higher values of SI mean that pixels in a range have remained static and are therefore part of the background. Background pixels are updated with frame pixels when SI values reach a certain threshold, otherwise "old" background pixels are used. The initial background is usually the first frame in the image or a black image (all pixels with value 0).

$$SI_k(x,y) = \begin{cases} SI_{k-1}(x,y) + 1 & \text{if } FDM_k(x,y) = 0 \\ 0 & \text{if } FDM_k(x,y) = 1 \end{cases} \tag{3.8}$$

$$BG_k(x,y) = \begin{cases} I_k(x,y) & \text{if } SI_k(x,y) = Fth \\ BG_{k-1}(x,y) & \text{otherwise} \end{cases} \tag{3.9}$$

where Fth is an image frame threshold which represents how quickly the algorithm responds to background changes. A low value of Fth means that background will be estimated quickly but it will also change frequently. A higher value means that it will take longer to establish the background initially but once established it will adopt changes slowly based on motion of foreground objects. The parameter Fth is a design parameter which influences the detection of moving objects which are stopping, or stationary objects which commence motion.

Once the background image is created, a background difference (BD) is calculated in conjunction with the current image frame. BD is then thresholded to generate the background difference mask (BDM). This mask represents foreground objects which have been successfully detected as a result of background subtraction.

$$BD_k(x,y) = |I_k(x,y) - BG_k(x,y)| \tag{3.10}$$

$$BDM_k(x,y) = \begin{cases} 1 & \text{if } BD \geq Th \\ 0 & \text{if } BD < Th \end{cases} \tag{3.11}$$

To establish the Initial Object Mask (IOM), first a background indicator (BI) needs to be calculated, which indicates areas where background has been successfully established. For those areas which do not have a reliable background, frame difference mask (FDM) provides information about foreground objects.

$$BI_k(x,y) = \begin{cases} 1 & \text{if } SI_k(x,y) = Fth \\ BI_{k-1}(x,y) & \text{otherwise} \end{cases} \tag{3.12}$$

$$IOM_k(x,y) = \begin{cases} BDM_k(x,y) & \text{if } BI_k(x,y) = 1 \\ FDM_k(x,y) & \text{otherwise} \end{cases} \tag{3.13}$$

Finally a post-processing operation ensures that the stationary index of a pixel (SI) is reset to 0 if the pixel's Initial Object Mask is 1. This ensures that if a foreground object stops it does not get incorporated into the background.

$$SI_k(x,y) = 0 \text{ if } IOM_k(x,y) = 1 \tag{3.14}$$

This scheme deals successfully with various situations where the foreground object becomes stationary, or the background becomes uncovered as a result of an object moving. Chien et al. (2004) further enhanced this baseline system with a shadow detection scheme, an adaptive threshold and a global motion compensation to deal with camera movement.

3.4 Camera Stabilisation

An underwater camera in a sea cage is in constant motion due to several factors: the movement of water currents, the movement of fish causing water disturbances and fish bumping into the camera or the camera cable. This movement has impact on motion segmentation methods (Section 3.3) and it increases the error in the estimation process as explained later in Section 5.6. While camera stabilisation is not a primary concern of this thesis, an initial investigation was carried

out to determine the feasibility of using this feature. The stabilisation algorithm investigated deals with cameras mounted on mobile platforms (Cai and Walker, 2008). The aim of the algorithm is to identify motion jitter in two Local Motion Vectors (LMV) - vertical and horizontal. LMVs are created by estimating optical flow (Cai and Walker (2008) used the Lucas-Kanade method). LMVs are sorted (independently for the horizontal and vertical) and estimated camera motion (CM) is calculated as:

$$p(t) = \arg\min_{k} \{LMV^{v}_{k+\delta}(t) - LMV^{v}_{k}(t)\} \tag{3.15}$$

$$CM^{v}(t) = LMV^{v}_{(p(t)+0.5\delta)}(t) \tag{3.16}$$

where $CM^{v}(t)$ is the vertical camera motion at time t, $p(t)$ minimises the difference between two local motions, k is the index of LVM and δ is a design parameter set to 5-20% of the LVM length. The same calculations are carried out for horizontal camera motion CM^{h}. This approach to calculating the estimated camera motion avoids the need for the selection of a number of bins to calculate a histogram of motion vectors, which can be problematic. Camera motion (CM) is then used to calculate accumulated camera motion (ACM) and smoothed accumulated motion (SAM):

$$ACM(t) = \sum_{i=1}^{t} CM(t) \tag{3.17}$$

$$SAM(t) = \alpha SAM(t-1) + (1-\alpha)ACM(t) \tag{3.18}$$

where SAM is a first-order IIR Filter and α is a design parameter weighing the influence of previous smoothed accumulated motion and current accumulated camera motion (in range 0.95 and 0.98). Note that $ACM(t) = \{ACM^{v}(t), ACM^{h}(t)\}$ and $SAM(t) = \{SAM^{v}(t), SAM^{h}(t)\}$ in the above equations but h and v indices have been dropped for clarity. These two measures are then used to calculated accumulated jitter (AJ), which can be used to provide offset to the original image.

$$AJ(t) = \beta AJ(t-1) + ACM(t) - SAM(t) \tag{3.19}$$

where β is a design parameter which controls the influence of estimation errors for long video sequences (in range 0.90-0.98).

3.5 Summary

A segmentation stage plays a very important role in many computer vision systems, as poor segmentation causes incorrect data flow through to the next stage

of a system. It is important to realise that each application can require a different segmentation method with appropriate parameters, and different pre-processing techniques may be used prior to segmentation. While using a sequence of images may assist in the segmentation process by adding an extra, temporal dimension, care needs to be taken that the algorithm chosen performs adequately for a given application. Real-time applications require fast methods possibly at the expense of accuracy, while applications that require accuracy may be less concerned with speed of execution. This thesis deals with water-based environments with the camera below or above the water, various visibility conditions and different times of day. The segmentation process here focuses on speed, in order to facilitate real-time operation. In the system presented here, once objects have been extracted from image frames, they need to be tracked, so that positional and identification data can be recorded. The next chapter discusses the issue of tracking multiple objects found through segmentation of images from video sequences.

CHAPTER 4

TARGET TRACKING AND DATA ASSOCIATION

4.1 Introduction

Once apparent objects in individual frames have been segmented they need to be tracked from frame to frame to eliminate false apparent objects, provide positional data and help distinguish one object from another. Target tracking methods can enable the estimation of current positions of tracked objects based on their current and previous states and acquired measurements.

The aim of this chapter is to introduce the target tracking concepts, which are to be used in methodology chapters. Section 4.2 describes two algorithms used for tracking of targets: the Kalman Filter and the Particle Filter (and variations on these methods). The Kalman Filter has an application in tracking of fish in sea cages since the motion model of fish in the field of view of the camera can be assumed to be linear. The Particle Filter is suitable for a non-linear motion model and can be applied to fish swimming in a tank, where fish are tracked for extended periods of time, as they manoeuvre and interact with each other.

Section 4.3 extends the concept of tracking to situations with multiple targets, where there is a need to associate arriving measurements to existing target estimates. In both cages and tanks there is a number of fish being tracked at the same time. At each time step in the video sequence a new set of measurements arrive that need to be matched to existing fish tracks. This section explains methods used for association of measurements to existing tracks and elimination of unlikely combinations, and the computational complexity involved in this.

Finally Section 4.4 describes a method which can be utilised when large numbers of fish in cages make it impossible to detect and track individual fish. Such a method may provide an alternative (or complementary) set of data about behaviour of fish in a sea cage.

4.2 State Estimation of Dynamic Systems

A Stochastic Dynamic System describes the temporal evolution of a process which is subject to random noise. The dynamic system is represented by a state space which is a set of all possible states the system can take, expressed in terms of state variables (e.g. position, velocity, etc.). The dynamic system also describes rules on how the system evolves its state over time. In practice, the state of a system is generally not known but can be estimated through observation of measurements. An estimation process uses measurements and previous knowledge about the estimated state to estimate the current state and possibly generate predictions of future states.

4.2.1 Kalman Filter

The Kalman filter is a mathematical process that provides an efficient computational means to estimate the state of a process by recursion (Welch and Bishop, 1995) in the Bayesian framework. It was invented by Rudolf Kalman (1960) and has been widely used, most notably in engineering applications, such as aircraft and missile guidance, radar tracking, sonar ranging and computer vision. The key assumptions of the Kalman filter are that the system dynamics are linear and the process and measurement noise is Gaussian. This allows the expression of the posterior density of the state in terms of means and covariances. What follows is a description of the Kalman Filter based on the tutorial by Welch and Bishop (2001).

The Kalman Filter estimates the state of a dynamic system x_k, described by a linear stochastic difference equation as follows:

$$x_k = Ax_{k-1} + Bu_k + w_k, \tag{4.1}$$

with measurement z_k that is

$$z_k = Hx_k + v_k \tag{4.2}$$

where

A is a state transition matrix, representing the dynamics of the model

B is a control matrix, governing external control inputs

u_k is a control input vector,

w_k is process noise assumed to be Gaussian, $p(w) \sim N(0, Q)$ - w_k is sampled from a normal distribution with zero mean and covariance Q,

H is a measurement matrix, representing the relationship between the state and the measurement

v_k is measurement noise assumed to be Gaussian, $p(v) \sim N(0, R)$ - v_k is sampled from a normal distribution with zero mean and covariance R.

The filter parameters (A, B, H, Q, R) are supplied by the user and depend on the nature of the system observed. It is possible for these parameters to change with time if the dynamics of the system require this.

The filter propagates and updates the state estimate $\hat{x}_k$ and the estimated covariance P_k of the estimate and produces the posterior density $p(x_k|Z^k)$, where $p(x_k|Z^k) = N(x_k; \hat{x}_{k|k}, P_{k|k})$ and $Z^k = z_1, ..., z_{k-1}, z_k$ is the set of all measurements. Notation $N(x; m, P)$ is a Gaussian density with argument x, mean m and covariance P, while notation $\hat{x}_{k|k}$ is *a posteriori* state estimate at time k given observations up to and including time k and notation $P_{k|k}$ is *a posteriori* error covariance matrix.

The two stage, recursive nature of the filter means that data points can be processed sequentially as they arrive, not just in batches (Fig. 4.1). This makes it ideal for real-time applications.

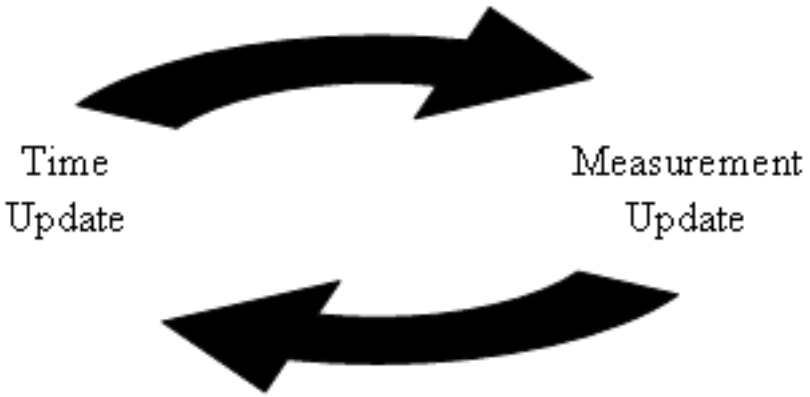

Figure 4.1: Two stages of the Kalman Filter providing a recursive solution able to process data sequentially.

The first stage is called the *time update*. In this stage the state and covariance error from the previous time step are used to predict *a priori* estimates (marked with $^-$) for the current time step.

$$\hat{x}_k^- = A\hat{x}_{k-1} + Bu_k \tag{4.3}$$

$$P_k^- = AP_{k-1}A^T + Q \tag{4.4}$$

The second stage is called the *measurement update*. This stage uses measurements to calculate the Kalman Gain and correct/update the *a priori* estimates to produce *a posteriori* estimates.

$$K_k = P_k^- H^T (H P_k^- H^T + R)^{-1} \tag{4.5}$$

$$\hat{x}_k = \hat{x}_k^- + K_k(z_k - H\hat{x}_k^-) \tag{4.6}$$

$$P_k = (I - K_k H) P_k^- \tag{4.7}$$

This two stage operation continues each time step, as new measurements arrive. If no measurements are available for a given time step then only the time update is carried out. It is important to note that the *time update* increases the covariance error (due to process noise) while the *measurement update* decreases the error based on measurements. For more detailed mathematical explanation of the Kalman filter refer to Welch and Bishop (1995).

In the literature many variations of the Kalman filter have been used in video-based tracking. To track people in videos with non-stationary backgrounds, a Kalman filter has been combined with a Pseudo-2D Hidden Markov Model (Breit and Rigoll, 2001). Another method of tracking people used a Structural Kalman Filter capable of tracking different parts of a person and establishing a relationship between these parts (Jang et al., 2002). This was set-up to deal with partial occlusions, where only parts of the body are being tracked. A different method used a target's colour as a feature and used an adaptive Kalman filter to track people through occlusions based on tracking of occlusion rate (Weng et al., 2006).

The Kalman filter is based on the assumption of a linear system with Gaussian noise. This is a major limitation when trying to model movement of humans and animals as they can change their motion erratically, making the motion model non-linear. Several improvements to the basic Kalman filter have been made in order to deal with possible non-linearity of models.

4.2.2 Kalman Filter Variations

Multiple Models Approach

One of the variations is to consider different motion models that the tracked object may use. For example, a fighter jet can fly in a straight path or it can manoeuvre. The Kalman Filter can be designed to switch between different models by calculating the probability $p_j(k)$ that a given model μ_j is the right model at the time and incorporating this probability as a weight into the calculation of a

posteriori state $\hat{x}_k$ and error covariance P_k (Welch and Bishop, 2001).

$$p_j(k) = \frac{f(z_k|\mu_j)}{\sum_{h=1}^{r} f(z_k|\mu_h)}, \tag{4.8}$$

where r is the number of possible models, and $f(z_k|\mu_j)$ and $f(z_k|\mu_h)$ are the likelihoods of measurement z_k given models μ_j and μ_h respectively.

Extended Kalman Filter

The Extended Kalman Filter (EKF) attempts to deal with non-linear systems by linearising the predicted state and measurement equations using the Jacobian matrices of their respective partial derivatives. One of the main drawbacks of the Extended Kalman Filter is that for non-linear processes, the estimation is not optimal and it can diverge if the process is too non-linear and cannot be modelled adequately. As the linearisation process propagates the mean and covariance of the Gaussian distribution, this distribution may become inconsistent in the statistical sense if the process is heavily non-linear. In addition, the calculation of the Jacobian matrix is a computationally intensive task for more complex models.

Unscented Kalman Filter

A more recent improvement on the Extended Kalman Filter, aimed at dealing with highly non-linear systems, is the Unscented Kalman Filter (UKF), which uses an "unscented transform" (Julier and Uhlmann, 1997). Rather than using a Jacobian matrix to linearise the process, the unscented transform uses a set of points chosen to represent the Gaussian distribution and these points are propagated using the non-linear function. At each time step, the mean and covariance of the estimate are accurately reconstructed from these points and used in the prediction and update stages of the Kalman Filter. The advantage of this filter is that not only does it provide improved estimates for highly non-linear systems but it also avoids the necessity of calculating of the Jacobian matrix. In computer vision, Stenger et al. (2001) used the UKF for tracking of hand movements. This sample based approach leads to another, independently developed, sample-based estimation method called the Particle Filter.

4.2.3 Particle Filter

The Particle Filter originates from a statistical method called Sequential Monte Carlo (SMC) estimation proposed in the 1950's where the "particles" are randomly generated samples of the data. Originally SMC estimation remained largely neglected because computational capabilities at the time made these methods impractical. The concept was "re-discovered" for target tracking purposes by Gordon et al. (1993) who proposed a bootstrap filter (another name for the Particle Filter) based on the Sequential Importance Sampling (SIS) method, with an additional resampling step. With increased computational power, particle filters have become an active research area in the last decade or so.

In a Particle Filter the state evolves in a similar way to Eq. 4.1 but possible non-linearity of the system can be taken into account. The state x_k is expressed as

$$x_k = f_{k-1}(x_{k-1}, w_k), \tag{4.9}$$

where f_{k-1} is a possibly non-linear function of state x_{k-1} and w_k is process noise, assumed to be Gaussian with known probability density function (pdf). For simplicity of presentation, the control parameter u_k from Eq. 4.1 is assumed here not to be utilised. The measurement z_k is expressed as

$$z_k = h_k(x_k, v_k) \tag{4.10}$$

where h_k is a possibly non-linear function of state x_k and v_k is the measurement noise, also assumed to be Gaussian with known pdf.

Following the concept of recursive Bayesian estimation, the Prediction stage is given using the Chapman-Kolmogoroff equation:.

$$p(x_k|Z_{k-1}) = \int p(x_k|x_{k-1})p(x_{k-1}|Z_{k-1})dx_{k-1} \tag{4.11}$$

where $p(x_k|Z_{k-1})$ is the predicted density, $p(x_k|x_{k-1})$ is the transitional density which evolves the state from one time step to the next and $p(x_{k-1}|Z_{k-1})$ is the posterior density at time $k-1$. $Z_k = \{z_i, i = 1, ..., k\}$ is a set of all possible measurements up to and including time k.

The update stage is derived from Bayes' rule:

$$p(x_k|Z_k) = \frac{p(z_k|x_k)p(x_k|Z_{k-1})}{p(z_k|Z_{k-1})} \tag{4.12}$$

where $p(z_k|x_k)$ is the observation density based on the new measurement (also known as the measurement likelihood function), $p(z_k|Z_{k-1})$ is a normalising constant expressed as

$$p(z_k|Z_{k-1}) = \int p(z_k|x_k)p(x_k|Z_{k-1})dx_k \tag{4.13}$$

In practice, the normalising constant can be ignored and the result is proportional to the product of the likelihood function and the predicted density (Ristic et al., 2004; Czyz et al., 2005).

$$p(x_k|Z_k) \propto p(z_k|x_k)p(x_k|Z_{k-1}) \tag{4.14}$$

While the Kalman Filter provides an optimal solution to Bayesian estimation, it can only be applied to Gaussian cases. Suboptimal approximations can be derived using the EKF and UKF but these still attempt to approximate Gaussian distributions (Orderud, 2005). Rather than expressing distributions in terms of the mean and covariance, the Particle Filter uses random samples (Monte Carlo sampling) to provide an approximation to Bayesian estimation. These samples are also known as particles hence the name of the filter. This use of sampling places no restriction on the posterior pdf and allows the handling of highly non-linear models with distributions which cannot be fully described using a mean and covariance. Given enough samples, the approximation of the pdf can be very accurate.

One of the main disadvantages of particle filters is that they can be computationally expensive (Orderud, 2005). This is especially true when dealing with state vectors with many dimensions, because the number of particles required increases significantly in order to provide satisfactory performance. This is known as the "curse of dimensionality" (Bellman, 1957; Daum and Huang, 2003), where complexity increases exponentially with the number of dimensions. The following paragraphs will describe how particles are generated.

Sequential Importance Sampling (SIS)

The principle behind the Particle Filter is that it propagates a set of N support points (particles) and associated weights, $\{X_k^i, w_k^i\}_{i=1}^N$, characterising the joint posterior density $p(X_k|Z_k)$, where $\{X_k^i, i = 1, ..., N\}$ represents a set of support points, $\{w_k^i, i = 1, ..., N\}$ represents a set of weights normalised such that $\sum_{i=1}^N w_k^i = 1$, and $X_k = \{x_j, j = 0, ..., k\}$ represents a set of all states up to time k. The joint posterior density can be expressed as an approximation of weights and support points:

$$p(X_k|Z_k) \approx \sum_{i=1}^{N} w_k^i \delta(X_k - X_k^i) \tag{4.15}$$

where δ is the Dirac delta function and each weight is calculated as follows:

$$w_k^i \propto \frac{p(X_k^i|Z_k)}{q(X_k^i|Z_k)} \tag{4.16}$$

where $p(X_k^i|Z_k)$ is the density from which we want to generate samples (but are unable to) and $q(X_k^i|Z_k)$ is a density from which we can generate samples and this density is similar to $p(X_k^i|Z_k)$. The pdf $q(X_k^i|Z_k)$ is called the *importance* or *proposal density*. Equation 4.16 is based on the theory of importance sampling, which is derived from Monte Carlo integration as described by Ristic et al. (2004)(p. 35-37) and Doucet et al. (2000).

Further transformation of $p(X_k|Z_k)$ yields Equation 4.17, where weights are modified based on the previous state x_{k-1} and measurement z_k.

$$w_k^i \propto w_{k-1}^i \frac{p(z_k|x_k^i)p(x_k^i|x_{k-1}^i)}{q(x_k^i|x_{k-1}^i, z_k)} \tag{4.17}$$

In this equation, $q(x_k^i|x_{k-1}^i, z_k)$ is the importance density, $p(z_k|x_k^i)$ is the likelihood function and $p(x_k^i|x_{k-1}^i)$ is the state evolution (known as the *transitional density* or *transitional prior*).

The new posterior density $p(x_k|Z_k)$ is approximated using the updated weights and the set of propagated support points (Ristic et al., 2004).

$$p(x_k|Z_k) \approx \sum_{i=1}^{N} w_k^i \delta(x_k - x_k^i) \tag{4.18}$$

Unfortunately, the basic particle filter suffers from what is known as a degeneracy problem. It has been shown by Doucet et al. (2000) that the variance of important weights increases over time. This means that after a certain number of steps all but one particle will have negligible weights. One of the ways to decrease this degeneracy is by choosing a good importance density. However choosing the optimal importance density is not straightforward, therefore suboptimal solutions are more practical. As the most popular suboptimal choice, Arulampalam et al. (2002) and Ristic et al. (2004) suggest using the transitional prior:

$$q(x_k^i|x_{k-1}^i, z_k) = p(x_k^i|x_{k-1}^i) \tag{4.19}$$

Substituting Eq. 4.19 into Eq. 4.17 produces a new simplified weight update equation:

$$w_k^i \propto w_{k-1}^i p(z_k|x_k^i) \tag{4.20}$$

While using the transitional prior may decrease degeneration it is not likely to eliminate it. A resampling method called Sampling Importance Resampling (SIR) or the bootstrap filter (Gordon et al., 1993) was proposed to deal with this issue.

Sampling Importance Resampling (SIR)

Resampling is performed when the effective number size, N_{eff}, falls below a certain threshold N_{th} (Ristic et al., 2004), where N_{eff} is estimated with:

$$\hat{N}_{eff} = \frac{1}{\sum_{i=1}^{N} (w_k^i)^2} < N_{th} \tag{4.21}$$

the resampling stage is used to eliminate particles with low weights and to multiply particles with high weights. This however introduces a sample impoverishment problem where high weight particles are selected many times and the sample set contains many repeated particles. The problem can be fixed by performing Gaussian, random *jittering* of particles after resampling, during the prediction stage at the next time step (Gordon et al. (1993) called this procedure *roughening*).

4.2.4 Colour Particle Filter

The colour particle filter is one of the tracking algorithms used in this thesis. This section provides an overview of the filter operation and further expands the concept to multiple target estimation.

The Particle Filter and its variations have been applied in tracking of objects in video sequences. One of the earliest methods was the CONDENSATION algorithm (CONditional DENSity PropagATION) (Isard, 1998). The algorithm is a non-linear Particle Filter which uses shape contours to form a state vector. Another use of the Particle Filter in the context of video originates from the track-before-detect (TBD) concept. The track-before-detect idea allows the system to detect stealthy targets which, from the sensor point of view, tend to blend into the background. Typical sensor processing involves thresholding which aims at eliminating noise before tracking and data association is performed. This means that targets with low detection profiles are likely to remain undetected in this scenario. The TBD concept works on unthresholded data, and by considering several scans of data, it detects patterns which are not random noise and therefore possible targets. However the problem with early TBD algorithms was that they were batch methods, prohibiting or penalising deviations from straight-line motion which were computationally intensive. These algorithms were based on the Hough transform, dynamic programming and maximum likelihood estimation (Ristic et al., 2004). Salmond and Birch (2001) proposed a TBD algorithm based on the Particle Filter and the concept was applied successfully in the computer vision field. The main Particle Filer technique used in computer vision uses colour via a coloured target template. The measurement model is based on a randomly

selected area of an image which is compared with the template to determine if this area represents the target or not. The following subsection describes the comparison operation.

Measurement Model

The state space model represents an area of the image. The shape of this area can be rectangular, elliptical or more complex depending on application requirements. The state vector for each particle can therefore include the centroid of the area, the width and height (Czyz et al., 2005). Scale and velocity components may also be included (Pérez et al., 2002).

The measurement model is built using a histogram based on the Hue Saturation Value (HSV) colour space (Pérez et al., 2002), HSV often deals better with illumination variation than the commonly used RGB colour space. The concept originates from the mean-shift tracker by Comaniciu and Meer (2002). The idea behind using a colour histogram is that the target becomes invariant to shape deformations. However if the background is of a similar colour to the target, problems may arise with detection of true targets.

As with any histogram, the method needs to determine a number of bins which will be required to represent colour. The number of bins in the histogram is $N = N_h N_s + N_v$, where N_h, N_s, and N_v are the number of bins for each component of the HSV colour space. A pixel at position u can be represented as the transpose of its HSV components, $y(u) = [h(u), s(u), v(u)]^T$. Each HSV component can be allocated to its own numbered "bin" and the bin representation of the colour vector $y(u)$ denoted as $[b_h(u), b_s(u), b_v(u)]^T$. The overall bin number, $b(u)$, for pixel $y(u)$ is defined as

$$b(u) = \begin{cases} b_s(u)N_h + b_h(u) & \text{if } s(u) \geq 0.1 \text{ and } v(u) \geq 0.2 \\ b_v(u) + N_h N_s & \text{otherwise} \end{cases} \tag{4.22}$$

This equation denotes that the hue information is only reliable when the saturation component is above 0.1 and value component is above 0.2 (Cai, 2005). At other times only the value component is used for bin calculations.

The histogram is calculated over the region $R(x_k)$, defined by the state vector x_k, at time k and can be denoted as $Q(x_k) = \{q(n; x_k)\}_{n=1,\ldots,N}$, where $q(n; x_k)$ is given by

$$q(n; x_k) = C \sum_{u \in R(x_k)} \delta[b(u) - n] \tag{4.23}$$

where δ is the Kronecker delta function, C is a normalisation constant, u is any pixel within the region $R(x_k)$ and $\sum_{n=1}^{N} q(n; x_k) = 1$. The reference histogram,

$q^*(n; x_0)$, of the colour target template can then be compared with the histogram of the candidate region defined by x_k using the Bhattacharyya coefficient (Cai, 2005). The distance metric, D, between candidate region x_k and template region x_0, is defined as

$$D(x_k, x_0) = \left(1 - \sum_{n=1}^{N} \left[q\left(n; x_k\right) q^*\left(n; x_0\right)\right]^{\frac{1}{2}}\right)^{\frac{1}{2}} \tag{4.24}$$

This metric is used in the calculation of the likelihood function (Eq. 4.20):

$$p(z_k|x_k) \propto \frac{1}{\sqrt{2\pi\sigma}} e^{-\frac{1}{2\sigma^2} D_k^2} \tag{4.25}$$

where σ is a design parameter representing the standard deviation of a Gaussian density (Czyz et al., 2007).

The template matching can be further enhanced by incorporating the image's background information. Given that the background image is available, the Bhattacharyya distance between the template histogram and the candidate region in the background image is given by

$$D^B(x_k^B, x_0) = \left(1 - \sum_{n=1}^{N} \left[q^B\left(n; x_k\right) q^*\left(n; x_0\right)\right]^{\frac{1}{2}}\right)^{\frac{1}{2}} \tag{4.26}$$

and the likelihood function in Eq. 4.25 becomes to

$$p(z_k|x_k) \propto \frac{1}{\sqrt{2\pi\sigma}} e^{-\frac{1}{2\sigma^2}\left((D_k)^2 - \left(D_k^B\right)^2\right)} \tag{4.27}$$

Multiple Targets

When dealing with multiple targets, standard particle filters tend to converge to a single mode of the posterior distribution and end up tracking just one target. To avoid this, a scheme is required that can maintain multiple modes - one for each target. If the number of targets is known, the method used by Czyz et al. (2007) can be applied, in which an existence variable E_k denotes the number of targets in a current frame.

The existence variable can be defined as $E \in \mathbb{E} = \{0, 1, ..., M\}$, where M is the maximum expected number of targets. It evolves using a Markov chain and can be described by a transitional probability matrix (TPM) $\Pi = [\pi_{ij}]$, where

$$\pi_{ij} = Pr\{E_k = j | E_{k-1} = i\}, \quad (i, j \in \mathbb{E}) \tag{4.28}$$

is the probability of transition from i at time $k-1$ to j at time k (Czyz et al., 2007). The TPM for two targets ($M = 2$) can be described as:

$$\Pi = \begin{bmatrix} (1-P_b) & P_b & 0 \\ P_d & (1-P_d-P_m) & P_m \\ 0 & P_r & (1-P_r) \end{bmatrix} \tag{4.29}$$

where P_b and P_d are probabilities of target "birth" and "death" respectively, and P_m and P_r are probabilities that the number of targets will multiply or reduce respectively.

The multi-target state vector for each particle n can then be redefined as

$$y_k^n = [E_k^n, x_{1,k}^n, ..., x_{E_k^n,k}^n]^T \qquad (n = 1, ..., N) \tag{4.30}$$

where N is the number of particles, E_k^n is the variable denoting the number of targets in the state vector, and $x_{i,k}^n$ is the state vector for each target, where $i = 1, ..., E_k^n$. Therefore the state vector y_k can have a variable length depending on the value of E_k:

$$y_k = \begin{cases} E_k & \text{if } E_k = 0, \\ [x_{1,k}^T E_k]^T & \text{if } E_k = 1, \\ [x_{1,k}^T x_{2,k}^T E_k]^T & \text{if } E_k = 2, \\ \vdots & \vdots \\ [x_{1,k}^T ... x_{M,k}^T E_k]^T & \text{if } E_k = M, \end{cases} \tag{4.31}$$

The likelihood for each particle n is derived from Eq. 4.27 but needs to incorporate E_k:

$$L_k^n(E_k^n) = exp\left\{ -\frac{1}{2\sigma^2} \sum_{i=1}^{E_k^n} \left[\left(D_{i,k}^n\right)^2 - \left(D_{i,k}^{n,B}\right)^2 \right] \right\} \tag{4.32}$$

Importance weights can then be calculated based on the likelihood and E_k:

$$\tilde{w}_k^n = \begin{cases} 1 & if\ E_k^n = 0, \\ L_k^n(E_k^n) & if\ E_k^n > 0. \end{cases} \tag{4.33}$$

Czyz et al. (2007) further describes how the state vector for each particle changes based on transitions of the existence variable. They additionally suggest that to stop tracking of multiple objects on the same image region, a condition be applied that if the Euclidean distance between two target state vectors is too close, the corresponding weight will be reset to zero, ($\tilde{w}_k^n = 0$ if $(x_{j,k}^n - x_{i,k}^n)^2 < R^2$, where

R^2 is a design parameter). Pseudo code of the colour particle filter is shown in Table A.1 and further details regarding the implementation will be discussed in Chapter 7. The probability, Pr of number of targets detected in this work is

$$Pr(E_k = m|Z_k) = \frac{1}{N}\sum_{n=1}^{N}\delta(E_k^n, m) \tag{4.34}$$

where $m = 1...M$.

The estimate of state, $\hat{x}_i$ for $i = 1...\hat{m}$ is

$$\hat{x}_{i,k|k} = \frac{\sum_{n=1}^{N} x_{i,k}^n \delta(E_k^n, i))}{\sum_{n=1}^{N}\delta(E_k^n, i)} \tag{4.35}$$

4.2.5 Joint Multi-target Probability Density

The importance density based on the transitional prior (a.k.a the kinematic prior) does not use the actual measurements to propose new particles. The Joint Multi-target Probability Density (JMPD) particle filter version has been proposed by Kreucher et al. (2005) to enhance the kinematic prior by incorporating measurements into proposal. They proposed two methods: Independent Partition (IP) and Coupled Partition (CP), and combined them to form the Adaptive Partition (AP) method (referring to Eq. 4.31, a "partition" is a state vector $x_{i,k}^n$, which represents a target i).

The Independent Partition method is effective when targets are well separated. It assumes that partitions within each state vector are ordered, e.g. partition 1 of particle 1 ($x_{1,k}^1$) and partition 1 of particle 2 ($x_{1,k}^2$) represent the same target, and partition 2 of particle 1 ($x_{2,k}^1$) and partition 2 of particle 2 ($x_{2,k}^2$) represent the second target. Then for a partition t, each particle p has its t^{th} partitions proposed using the kinematic prior (evolution of state) and the respective weights are calculated based on measurements. The weights are normalised and then the t^{th} partition of each particle is sampled with replacement based on the distribution of weights. Because there is a bias which prefers certain particles for a partition, this bias, $b_{p,t}$ is retained for the calculation of the global likelihood. Pseudo code in Table A.2 in Appendix A describes the steps of the Independent Partition method.

When targets are close together, the Independent Partition method is no longer effective, but the Coupled Partition method can be used. For each partition t, R possible realisations of particle p are proposed based on the kinematic prior. These realisations are then weighted using measurements, and weights are

normalised. One of the realisations is selected by sampling based on the distribution of weights. Again this introduces a bias, which is incorporated into the global likelihood. This process is repeated for all particles within partition t. Pseudo code in Table A.3 in Appendix A describes the steps of the Coupled Partition method. The CP method increases the computational cost per particle but tracking performance increases, therefore fewer particles are required.

The Adaptive Partition method combines the above mentioned methods and decides which one should be used, based on the Euclidean distance between partitions. If the distance between partitions is greater than a threshold the IP method is applied, otherwise CP method is used. This means that the computationally more intensive CP method is only used when required. Pseudo code in Table A.4 in Appendix A describes how these schemes are chosen.

The Independent Partition scheme requires that partitions are ordered within each particle. This makes multi-target estimates invariant to permutations of partitions within particles. A sorting operation is required at each time step to ensure that particles have their partitions sorted. This is carried out using the K-means algorithm. The following pseudocode describes the K-means algorithm to sort partitions (Kreucher et al., 2005).

1. Initialise with π = current ordering of partitions
2. Calculate weighted mean of each target partition $t = 1...T_p$, $\bar{X}_t(\pi) = \sum_{p=1}^{N} w_p X_{p,\pi_p(t)}$
3. For each particle p, permute the particle (update π_p) to yield $\pi_p \leftarrow \arg\min_{\pi_p} \sum_{t=1}^{T_p} \left(X_{p,\pi_p(t)} - \bar{X}_t(\pi_p)\right)^2$
4. If no particles have changed permutation from π, quit
   Otherwise set $\pi = (\pi_1, ..., \pi_p, ..., \pi_N)$ and go to 2

The computational burden of the sorting scheme is light since most of the partitions which are not coupled have already been sorted. Those partitions which are coupled are nearly ordered because the sorting occurs at every time step. Therefore a single iteration of the algorithm is usually enough to resort the remaining particles.

4.3 Data Association

When tracking a target in clutter, many measurements may be present at each time step. A tracking system needs to decide which measurement should be as-

Table 4.1: More common data association techniques.

Single-scan methods
Nearest Neighbour (NN)
Global Nearest Neighbour (GNN)
(Joint) Probabilistic Data Association (PDA/JPDA)
Multi-scan methods
Multiple Hypothesis Tracking (MHT)
Multi-dimensional Assignment (MDA)
Mixture reduction data association
many others...

signed to the tracked object. Data association compares all (or a subset of) combinations of measurements and the predicted estimate of the track and decides which combination is the most likely. When dealing with multiple targets, in addition to noisy measurements, an ambiguity may exist regarding which measurements should be allocated to which track estimates. Also a multi-target tracking system may need to deal with new tracks and the data association method can then be used to create tentative tracks. More targets and a greater level of noise increase the number of possible combinations and it becomes difficult to find a good solution.

A first step is elimination of the most unlikely measurements; this is covered in subsection 4.3.1. Once achieved, an association method assigns the remaining measurements to tracks. There are two main types of data association techniques: single-scan and multi-scan (Table 4.1). Single-scan techniques use only measurements and predicted estimates at a single time step, k, to solve the assignment problem. Multi-scan techniques use measurements from multiple time steps before a decision is made as to which measurement originated from which target. Multi-scan techniques are used in more complex tracking environments where single-scan techniques can not provide satisfactory results. However these methods are computationally intensive and require additional management. Two data association techniques are presented in this section: a single scan technique called Global Nearest Neighbour (GNN) in subsection 4.3.2 and a multi-scan technique called Multidimensional Assignment (MDA) in subsection 4.3.3. These two methods use combinatorial optimisation algorithms to solve the problem of data association.

4.3.1 Validation Gate

A validation gate around the target can be used to eliminate unlikely measurements. This allows the data association method to ignore the most unlikely combinations, increasing both the computational efficiency and accuracy. Measurements which are generated by noise and outside the validation gate are excluded at this stage, but any noisy measurements within the validation gate of a track are considered by the data association method.

In the case of the Kalman Filter, an ellipsoidal gate is formed around the predicted measurement $\hat{z}_k$

$$\hat{z}_k = H\hat{x}_k^- \tag{4.36}$$

where $\hat{x}_k^-$ has been calculated during the *time update* stage of the Kalman Filter (Eq. 4.3). For each measurement z_k, the measurement innovation (or residual) v_k and its covariance S_k are calculated.

$$v_k = z_k - \hat{z}_k \tag{4.37}$$

$$S_k = HP_kH^T + R \tag{4.38}$$

Then the normalised distance (squared) can be calculated and compared with gate threshold γ. The gate threshold can be obtained from a χ^2 table based on degrees of freedom (number of variables in the state vector) and the p value:

$$d^2 = v^T S^{-1} v \leq \gamma \tag{4.39}$$

If, for a given measurement, the normalised distance is outside the gate threshold then this measurement will be excluded from data association. Gating can significantly reduce the number of combinations that need to be considered especially when targets are well separated.

Other gating arrangements exist, such as a simple rectangular gates around the track position and more elaborate gates, like $d^2 = v^T S^{-1} v + ln(|S|)$, where the $ln(|S|)$ term penalises tracks with greater uncertainty (Blackman and Popoli, 1999).

4.3.2 Global Nearest Neighbour (GNN)

Global Nearest Neighbour is a simple, single-scan method to detect multiple targets in clutter (noise). The problem is formulated so that it can be solved using Munkres's assignment algorithm (Munkres, 1957). Other algorithms for this assignment problem exist and Blackman and Popoli (1999) argue that an auction algorithm is more efficient than Munkres' algorithm.

The first step is to create an assignment matrix which will show Mahalanobis or Euclidean distance between observations and tracks. For each track, only those measurements which fall within the validation gate will be included. Observations outside the validation gate will be given a very high value, so that they are never picked by the algorithm. Table 4.2 shows an example of an assignment matrix (with X denoting values outside of the validation gate). For this matrix, the following assignments will be selected: O1 to T4, O2 to T1, O4 to T2, O5 to T3 (total cost of assignment is 47) and O3 initiates a new track.

Table 4.2: Assignment Matrix for GNN algorithm - distances with stars minimise the total cost of assignment (Ristic, 2007).

	T1	T2	T3	T4
O1	10	5	8	9*
O2	7*	x	20	x
O3	x	21	x	x
O4	x	15*	17	x
O5	x	x	16*	22

4.3.3 Multidimensional Assignment Problem (MDA)

Multi-dimensional Assignment extends the 2D assignment problem to more dimensions, therefore providing more data to accomplish better association but at the same time making the optimisation problem much more difficult. While the two dimensional assignment problems can be solved optimally using efficient algorithms, for higher dimensional problems, optimal solutions are difficult to obtain. However, there are methods which provide appropriate sub-optimal solutions. The best know method, developed specifically for target tracking is the use of Lagrangian relaxation to solve a binary integer programming problem (Poore et al., 1993). The basic principle behind Lagrangian relaxation is that a K-dimensional problem is reduced to a $K-1$ dimensional problem. This continues recursively until a 2-dimensional problem is reached, at which point an optimal solution can be found. A recovery procedure is then run which recovers each dimension in turn by updating Lagrangian multipliers. The Lagrangian relaxation method originates from branch and bound techniques to solve binary integer programming problems. Lagrangian relaxation is fast (therefore suitable for real-time tracking) and bounds can be reasonably tight if Lagrangian multipliers are carefully chosen. Indeed one of the most critical aspects of MDA is how to select and adjust Lagrangian multipliers to obtain solutions quickly (Blackman

and Popoli, 1999). Another relaxation method which can be applied in branch and bound method is called Linear Programming (LP) relaxation. Hillier and Lieberman (2010) argue that LP relaxation provides an appropriate compromise between speed and tightness of bounds.

4.3.4 Other Data Association Methods

Several methods have been proposed in the Bayesian framework. Probabilistic Data Association for a single target proposes several hypotheses that each measurement came from the target and an alternate hypothesis that none of the measurements belong to the target (Bar-Shalom and Tse, 1975). Probabilities for all hypotheses are calculated and combined, and the result is incorporated into the Kalman Filter to produce a new estimate. A multi-target version of PDA method is Joint Probabilistic Data Association (JPAD), where probabilities are calculated for all measurements and all tracks, and then combined. While (J)PDA methods are designed to deal with a moderate level of noise and number of targets, a method designed to deal with a high level of noise and large number of targets is Multiple Hypothesis Tracking (MHT) (Reid, 1979; Cox and Hingorani, 1996). Unlike JPDA, which combines hypotheses, MHT defers the association decision and propagates hypotheses to the next time step (Blackman and Popoli, 1999). This way it is possible to resolve uncertainty as new measurements arrive. The more measurements from different time steps, the better the decision made by MHT. Because MHT generates an exhaustive number of hypotheses (the hypothesis tree grows exponentially), additional methods have been developed to prune unlikely hypotheses, combine similar hypotheses together and cluster tracks which are close together and deal with them separately from other tracks. MHT method has high computational requirements and is likely to be used in military or civilian radars, where the requirement is to track hundreds of targets and the required computational power is available. MHT methods often serve as benchmark methods in terms of ability to track large number of targets in noisy environments. Bar-Shalom and Li (1995) provide details of JPDA and MHT theory and implementation, while Blackman and Popoli (1999) also provide a good overview of JPDA, MHT, GNN and MDA methods and discuss other less known advanced methods.

4.4 Global Motion Patterns

When tracking of individual targets is not possible due to a large volume of possible targets (e.g. a crowd of people at a train station), it may still be feasible

to look at the overall motion pattern of these targets. The basic idea is to extract some motion information from a sequence of images and compare that sequence with a prior sequence or even a template. This can be achieved using the motion flow fields method, which originates from the need to track motion patterns of crowds in malls, shopping centres and marathons (Hu et al., 2008).

Motion flow fields method uses a dense optical flow to extract flow vectors for M frames. The optical flow procedure generates a large number of vectors, many of which can be attributed to noise. The noise is removed by thresholding with all vectors below the threshold are set to zero. The resulting flow vectors are combined into a Point Flow Field (Ali and Shah, 2008). The Point Flow Field for point i is defined as $Z_i = (X_i, V_i)$, where $X = (x_i, y_i)$ represents location of the point and $V_i = (v_x, v_y)$ represents velocity components of the motion. V_i is the mean of optical flows calculated from M frames, which means the Point Flow Field contains combined motion information about a number of frames and additionally, it has an effect of smoothing out the camera motion. To decrease the number of vectors from thousands to hundreds, Hu et al. (2008) used the Gaussian ART algorithm (Williamson, 1996). This achieves a decrease in the number of flow vectors without affecting the geometric structure of the flow field.

Once the Point Flow Field is established, a sink seeking process is carried out to determine motion tracks within the field. For each flow field vector Z_i, the sink seeking process is defined by a series of points $\widetilde{Z}_{i,t} = (\widetilde{X}_{i,t}, \widetilde{V}_{i,t})$, where $t = 1, 2, ...$ The process was initialised with $\widetilde{Z}_{i,1} = Z_i$ and the points for $t > 1$ are defined by:

$$\widetilde{X}_{i,t} = \widetilde{X}_{i,t-1} + \widetilde{V}_{i,t-1} \tag{4.40}$$

$$\widetilde{V}_{i,t} = \frac{\sum_{n \in Neighbour(\widetilde{X}_{i,t})} V_n W_{t,n}}{\sum_{n \in Neighbour(\widetilde{X}_{i,t})} W_{t,n}} \tag{4.41}$$

The weights $W_{t,n}$ are calculated using kernel based estimation similar to the mean shift approach (Comaniciu and Meer, 2002) and are defined by:

$$W_{t,n} = exp\left(-\left\|\frac{\widetilde{V}_{i,t-1} - V_n}{h}\right\|^2\right) \tag{4.42}$$

where h is the bandwidth of the kernel. This process continues until a stopping condition is satisfied. The stopping condition can be the amount of progress made from the last point. If the algorithm stalls and makes no progress, it is terminated. An additional stopping condition is when the point moves outside the Point Flow Field.

The next step of this process is to cluster sinks together and create super tracks. Clusters are initialised with an empty set. A candidate sink $Z_i^* =$

(X_i^*, V_i^*), which is part of path P^{Z_i} is matched with each cluster C_k. If a match is found then the sink is added to the cluster, otherwise a new cluster is formed. Within each cluster the candidate sink is compared with all sinks within the cluster using three measures: i) distance between sinks, ii) similarity between directions (cosine similarity) and iii) Hausdorff distance between sink paths (Hu et al., 2008). These metrics are be defined by:

$$\text{i) } D_x(Z_I^*, C_k) = max_{Z_j^* \in C_k} \left\| X_i^* - X_j^* \right\| \tag{4.43}$$

$$\text{ii) } D_v(Z_I^*, C_k) = min_{Z_j^* \in C_k} \frac{< V_i^*, V_j^* >}{\|V_i^*\| \|V_j^*\|} \tag{4.44}$$

$$\text{iii) } D_p(Z_I^*, C_k) = max_{Z_j^* \in C_k} \text{HausdorffDist}(P_{Z_i^*}, P_{Z_j^*}) \tag{4.45}$$

Finally, these three metrics are combined together to determine which cluster is the closest, $idx = max(\frac{1}{D_x}\frac{1}{D_p}D_v)$, where idx is the index of the cluster.

4.5 Summary

The choice of a tracking and data association method depends on the application. In practice, the approach is to first select the simplest method possible and determine if that method performs in a satisfactory manner. The Kalman filter is a very popular and effective tracking method but is restricted to linear systems, though with careful design, the basic KF filter can deal with slight deviations from linearity. For more non-linear cases, the Unscented Kalman Filter is recommended in preference to the Extended Kalman Filter. The Particle Filter can deal with non-linear systems through sample approximation. However Particle Filters have their own difficulties regarding performance (due to the number of particles required to successfully approximate distributions), the choice of importance density and multi-target tracking. However the ability to deal with unpredictable motion patterns is appealing when tracking fish in tanks, and colour based Particle Filters may be able to detect fish as they try to adapt to tank surroundings.

In data association, the Global Nearest Neighbour is the preferred method when dealing with a small number of targets. However fish interactions in tanks cause frequent occlusions which take several time steps to resolve. This might warrant the use of more advanced methods like Multidimensional Assignment.

This thesis looks to apply tracking concepts in the aquaculture context in the following methodology chapters. In sea cages (Chapter 5) there will be lots of targets but they only need to be tracked for short periods of time, just enough to extract velocity data from the tracker, and the emphasis will be on real-time

performance of the system, so the tracking system must fit into this requirement. In tanks there are two tracking objectives. The first is to track fish when possible to determine their positions and velocities (Chapter 8). The second (far more difficult to achieve) objective is to track fish for long periods of time, with correct identification at all times and without an error (Chapter 7).

CHAPTER 5

ESTIMATING FISH MOVEMENT IN SEA CAGES

5.1 Introduction

The previous chapter reviewed concepts behind tracking of targets in cluttered backgrounds. The aim of this chapter is to describe the development of a computer vision system to track fish in commercial sea cages. In the following two chapters the research focus is on observing large groups of fish in sea cages, in order to interpret fish behaviours based on their movement.

The task of the tracking system is to detect as many fish as possible from the video file and calculate an aggregate velocity profile for the whole population. Individual descriptors of the profile such as the mean and standard deviation of speed and direction, are then used to identify patterns in fish behaviour over time. The system consists of three major stages: the segmentation stage, the tracking and data association stage, and the data logging and display stage. The system has been designed using MATLAB® /SIMULINK® software, a tool used to model dynamic systems which uses block based design instead of a usual programming interface. In addition, some of the functions were written in the C programming language to increase the computational speed of the system.

Figure 5.1 shows the SIMULINK® model of the tracking system and this chapter explains the computational steps used to extract fish sub-images from video sequences, manage fish tracks and calculate the above mentioned descriptors of the velocity profile. Section 5.2 describes details of image segmentation and object extraction with several segmentation methods covered. Section 5.3 introduces the implementation of the tracking methods and association of multiple measurements to multiple tracked fish. The system also has a target management module to create, maintain and delete targets (Section 5.4) and a module to generate velocity statistics from each sampling period (Section 5.5). The accuracy of the system is discussed in Section 5.6.

Another important factor is the movement of the camera and Section 5.7 deals briefly with the issue of camera stabilisation. Section 5.8 describes how optical flow can be utilised to detect changes in movement patterns when individual fish cannot be detected and tracked.

5.2 Image and Video Segmentation

Segmentation of video frames into binary images is the first step of the tracking system and is used to extract measurements from image frames. Segmentation, when used, is a very important stage in image processing as it determines which features can be extracted from the image, impacting later stages of processing. When tracking objects using video, good segmentation produces better object measurements which can then be fed into the tracking system. The importance of segmentation is further highlighted in Section 5.6 where the accuracy of the system is investigated.

Five segmentation methods are evaluated: global thresholding, adaptive (local) thresholding, edge detection, background subtraction by computing median over time, background subtraction by using mean background estimation. The first three methods work on individual frames while background subtraction methods require a sequence of frames.

5.2.1 Global Thresholding

Global thresholding used a histogram equalisation procedure followed by thresholding using Otsu's (Otsu, 1979) method as explained in Subsection 3.2.2. The histogram was created using 64 bins. It was noticed that the default threshold provided by Otsu's method was inadequate and it was multiplied by 0.25 (determined empirically) to produce better results. The requirement for such significant adjustment may be due to the fact that Otsu's method works best on bimodal histograms and underwater images used during this research were in general not bimodal.

The method had the advantage of simplicity and hence the processing speed, and it was observed that the average speed of processing was 35 fps. It produced acceptable results when the density of fish was low by detecting 5-15 sample fish per minute. This number was the lowest of the methods tried and this method often could not detect whole shapes of fish. The computational cost was low which made this method suitable for real-time deployment.

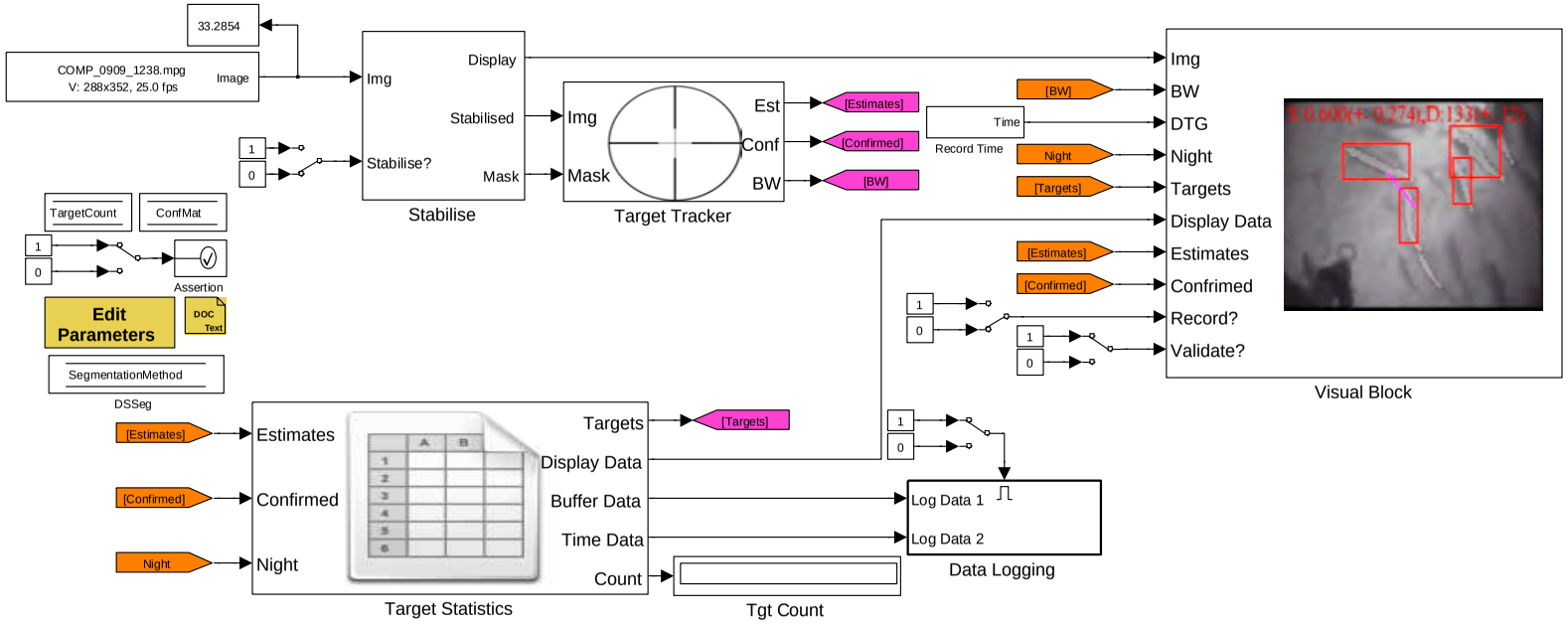

Figure 5.1: Simulink based tracking system to analyse fish movement in aquaculture sea cages. Frames per second is shown at the top left of the model (33.2854 fps).

5.2.2 Adaptive (Local) Thresholding

Adaptive thresholding, also explained in Subsection 3.2.2, produces on average 40-70 samples per minute but at a lower frame rate than global thresholding (22 fps). The higher computational cost is due to the application of the median filter which has an execution speed dependent on the size of the neighbourhood. The quality of fish shapes extracted using adaptive thresholding was better during the day because the method dealt better with various illumination changes within an image frame. Night time recordings produced lower quality samples because the orientation of the light was sideways relative to the camera.

5.2.3 Edge Detection

When dealing with small fish, the thresholding methods often failed to detect any shapes and the overall outcome was a low detection rate. To improve the detection rates of small fish, edge based segmentation techniques were examined. The edge segmentation proved to be superior in terms of number of detections in a given period. While it did not always pick up whole shapes of fish, it was successful at segmenting the length of the fish even if the middle of the fish was not segmented completely. (Extraction of the length of the fish was the main objective of the segmentation process because this measurement was used in the calculation of speed in body lengths per second.) Two edge detection methods were investigated: Sobel and Canny. While producing similar outcomes, Sobel was computationally faster so it was the preferred method.

5.2.4 Median Background Estimation

Median background estimation method estimates the background by computing the median image using 50 frames. The current frame is then subtracted from the background and the absolute difference is thresholded. This method is effective when the fish density is lower, the size of the fish is smaller and fish tend to be further away from the camera. These conditions allow for the background to be successfully estimated and motion segmentation can yield a reasonable number of fish for the tracking system. The main problem with this method is movement of the camera which invalidates the current background quickly. This creates false measurements, which may be tracked if they persist for a significant period of time. The method can be reset to restart the background estimation process to help minimise the effects of camera movement on background estimation but this will not eliminate these effects completely. Also frequent resets require additional

computational resources (mainly due to median calculations) and during this time the frame rate slows down significantly.

5.2.5 Mean Background Estimation

Mean background estimation method estimates the background using the running mean over all frames processed to that point by the system. This simple method was chosen as a comparison to the median method. It provides similar segmentation capability and suffers the same problems due to the camera movement. However it avoids the computation of median and it is therefore more computationally efficient.

5.2.6 Day/Night Detection

Special consideration was given to recordings which included both day and night footage (LL-photoperiod manipulation) because light sources and therefore backgrounds were different (natural light from above during the day, artificial light positioned sideways during the night). A simple indicator was developed to automatically distinguish night from day:

$$\text{Day/Night Indicator} = \begin{cases} \text{night time} & \text{if } m_k > 0 \\ \text{day time} & \text{if } m_k <= 0 \end{cases} \tag{5.1}$$

where m_k is a variable which increments or decrements based on another variable s which describes the relationship between mean and variance calculated for each image frame. Both variables are calculated using the following equations:

$$m_k = \begin{cases} m_{k-1} + 1 & \text{if } s = 0 \\ m_{k-1} - 1 & \text{if } s = 1 \end{cases} \tag{5.2}$$

$$\begin{aligned} s = (\bar{x} < M_{high} \text{ AND } \sigma^2 < V_{high}) \\ \text{OR } \bar{x} < M_{low} \text{ OR } \sigma^2 < V_{low} \end{aligned} \tag{5.3}$$

where M_{high} and M_{low} are high and low thresholds for mean (0.525 and 0.4 respectively). V_{high} and V_{low} are high and low thresholds for variance (0.035 and 0.025 respectively). These values have been determined empirically for optimal differentiation between night and day.

The variable m_k increments or decrements over time but can never exceed the transition threshold (set to 15,000 frames or 10 minutes at 25 frames/second).

This metric allows a switch between two segmentation methods: one for day-time recordings (Adaptive Thresholding) and one for night-time recordings (Median Background Estimation). Calculation of the night time metric can be disabled if only day time footage is being analysed.

5.2.7 Object Extraction

Once the binary image is created, shape features are extracted using SIMULINK's *Blob Analysis* block. Prior to this step, thick borders are drawn around all edges of the image (with the *Blob Analysis* block set to ignore objects touching the borders of the image). This is to prevent detection when fish are appearing or disappearing from the field of view. During this time fish shapes are increasing or decreasing rapidly in size and this may affect the final tracking estimates. The *Blob Analysis* block is set to extract up to 20 shapes and outputs the following data for each: centroid co-ordinates, bounding box size, major and minor axis length, orientation, eccentricity (defined as the ratio of the distance between the foci of the ellipse and its major axis length (Mathworks, 2009)), number of extracted shapes and a binary image of extracted shapes. From the tracking perspective, the centroid co-ordinates are the most important because they determine the velocity of fish movement. However other variables play a role in the data association by influencing the value of the validation gate prior to association.

5.3 Tracking and Data Association

The tracking system, as shown in Fig 5.2, is based on the basic Kalman Filter described in Subsection 4.2.1 which assumes a linear motion model and Gaussian noise. While the motion of fish in sea cages is not linear but curvilinear, the assumption of linearity generally holds while fish are in the field of view of the camera. At times when this assumption does not hold, the system will lose the track and report the last estimate. Due to the averaging nature of the system, the effect of these estimates is minimised.

5.3.1 Kalman Filter

The Kalman filter is supplied as a block by Simulink's Signal Processing Blockset. The block has been setup to track up to 10 targets at a time. This restriction has been placed mainly to decrease the computational load. Because the *Blob*

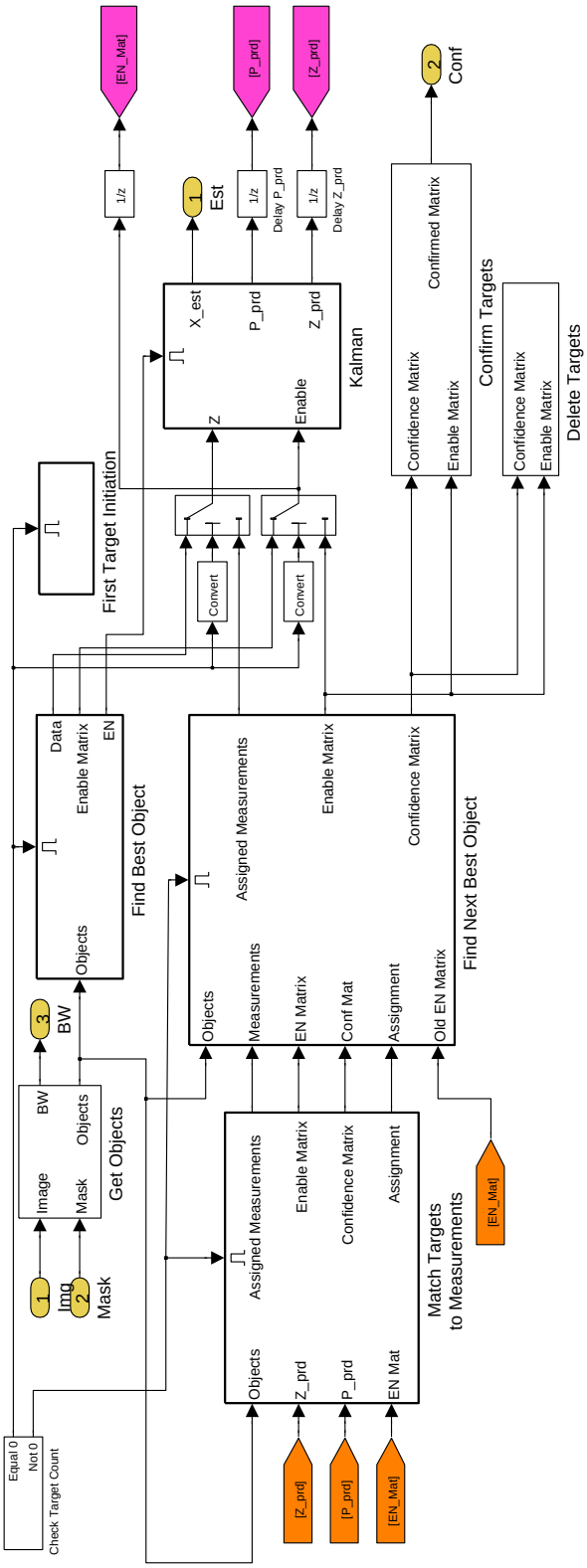

Figure 5.2: Target tracking module.

Analysis block detects 20 possible objects, Section 5.4.1 describes how these objects are selected to accommodate the limitation in the Kalman filter block.

Each target is tracked by a separate filter bank. These banks are enabled or disabled via the Enable Vector (Section 5.4.1). Each state vector x contains location, kinematic and descriptive information about the target that will help to differentiate it from other targets during data association. The state is defined as $x = \begin{bmatrix} r & c & \dot{r} & \dot{c} & h & w & o & e & a1 & a2 \end{bmatrix}^T$ where r and c are row and column co-ordinates of the object's centroid (in pixels), $\dot{r}$ and $\dot{c}$ are velocity components (in pixels/frame), h and w are row and column sizes of the bounding box (in pixels), o is orientation with respect to x-axis (columns) (in degrees), e is eccentricity of the object, $a1$ and $a2$ are lengths of major and minor axes respectively (in pixels). The measurement vector z is defined in a similar way but without the velocity components which are calculated through the State Transition Matrix: $z = \begin{bmatrix} r & c & h & w & o & e & a1 & a2 \end{bmatrix}^T$.

The initial estimated state of the system x_0 is set to zero for all values and the initial estimated error covariance P_0 is set to the identity matrix with a gain $100 * I_{10}$. To calculate the Kalman filter equations from Subsection 4.2.1, the following matrices have been defined:

State transition matrix:

$$A = \begin{bmatrix} 1 & 0 & 1 & 0 & 0 & 0 & 0 & 0 & 0 & 0 \\ 0 & 1 & 0 & 1 & 0 & 0 & 0 & 0 & 0 & 0 \\ 0 & 0 & 1 & 0 & 0 & 0 & 0 & 0 & 0 & 0 \\ 0 & 0 & 0 & 1 & 0 & 0 & 0 & 0 & 0 & 0 \\ 0 & 0 & 0 & 0 & 1 & 0 & 0 & 0 & 0 & 0 \\ 0 & 0 & 0 & 0 & 0 & 1 & 0 & 0 & 0 & 0 \\ 0 & 0 & 0 & 0 & 0 & 0 & 1 & 0 & 0 & 0 \\ 0 & 0 & 0 & 0 & 0 & 0 & 0 & 1 & 0 & 0 \\ 0 & 0 & 0 & 0 & 0 & 0 & 0 & 0 & 1 & 0 \\ 0 & 0 & 0 & 0 & 0 & 0 & 0 & 0 & 0 & 1 \end{bmatrix}$$

Measurement matrix:

$$H = \begin{bmatrix} 1 & 0 & 0 & 0 & 0 & 0 & 0 & 0 & 0 & 0 \\ 0 & 1 & 0 & 0 & 0 & 0 & 0 & 0 & 0 & 0 \\ 0 & 0 & 0 & 0 & 1 & 0 & 0 & 0 & 0 & 0 \\ 0 & 0 & 0 & 0 & 0 & 1 & 0 & 0 & 0 & 0 \\ 0 & 0 & 0 & 0 & 0 & 0 & 1 & 0 & 0 & 0 \\ 0 & 0 & 0 & 0 & 0 & 0 & 0 & 1 & 0 & 0 \\ 0 & 0 & 0 & 0 & 0 & 0 & 0 & 0 & 1 & 0 \\ 0 & 0 & 0 & 0 & 0 & 0 & 0 & 0 & 0 & 1 \end{bmatrix}$$

Measurement noise covariance:

$$R = \begin{bmatrix} .75 & 0 & 0 & 0 & 0 & 0 & 0 & 0 \\ 0 & .75 & 0 & 0 & 0 & 0 & 0 & 0 \\ 0 & 0 & 10 & 0 & 0 & 0 & 0 & 0 \\ 0 & 0 & 0 & 10 & 0 & 0 & 0 & 0 \\ 0 & 0 & 0 & 0 & 10 & 0 & 0 & 0 \\ 0 & 0 & 0 & 0 & 0 & 10 & 0 & 0 \\ 0 & 0 & 0 & 0 & 0 & 0 & 10 & 0 \\ 0 & 0 & 0 & 0 & 0 & 0 & 0 & 10 \end{bmatrix}$$

Process noise covariance:

$$Q = \begin{bmatrix} 2 & 0 & 0 & 0 & 0 & 0 & 0 & 0 & 0 & 0 \\ 0 & 2 & 0 & 0 & 0 & 0 & 0 & 0 & 0 & 0 \\ 0 & 0 & .75 & 0 & 0 & 0 & 0 & 0 & 0 & 0 \\ 0 & 0 & 0 & .75 & 0 & 0 & 0 & 0 & 0 & 0 \\ 0 & 0 & 0 & 0 & 2 & 0 & 0 & 0 & 0 & 0 \\ 0 & 0 & 0 & 0 & 0 & 2 & 0 & 0 & 0 & 0 \\ 0 & 0 & 0 & 0 & 0 & 0 & 2 & 0 & 0 & 0 \\ 0 & 0 & 0 & 0 & 0 & 0 & 0 & 2 & 0 & 0 \\ 0 & 0 & 0 & 0 & 0 & 0 & 0 & 0 & 2 & 0 \\ 0 & 0 & 0 & 0 & 0 & 0 & 0 & 0 & 0 & 2 \end{bmatrix}$$

The first four values of the state vector x represent the motion of the tracked fish $(r, c, \dot{r}, \dot{c})$. From the velocity components, $\dot{r}$ and $\dot{c}$, the swimming speed

and direction can be extracted. The remaining values are auxiliary and their existence within the Kalman filter is for the averaging purposes. They are however used during the validation gate calculation where they help to determine if the newly acquired measurement falls within the validation gate of the tracked fish. The selection of the covariance matrices for measurement and process noises was through experimentation. One principle applied was that the Kalman Filter needed to "weight" the process model more than measurements - it assumed that measurement would be noisy but the process was stable.

5.3.2 Data Association

The system uses the GNN method for data association, which utilises Munkres' algorithm (Munkres, 1957) to associate multiple measurements to multiple tracks. The original Munkres C++ code was written by Buehren (2009) and rewritten to make it suitable for integration with Simulink. The validation gate has been implemented and it is calculated using normalised distance squared (Eq 4.39), which is also used as the cost of assignment value by the Munkres algorithm. The threshold for the gate is $\chi^2 = 21.67$ as taken from the chi-square table ($df = 9$ and $P = 0.01$). All distances above this value will fail the gating test and be set to infinity; these values are ignored during the assignment process.

Once the association is carried out, the system creates two matrices: the Measurement Matrix and the Enable Vector. The Measurement Matrix provides ordered measurement vectors to the Kalman Filter banks, while the Enable Vector specifies which Kalman Filter bank should be enabled. At the same time the Confidence Matrix is also incremented for existing targets. This matrix is used by the system to detect for how many time steps a particular target has been tracked. Targets with longer tracking times will be more reliable and are more likely to be included in statistical calculations, as explained in Section 5.5.

5.4 Target management

5.4.1 Target selection

If the track list is empty the system initialises the list with the most suitable object. To extract the most suitable object for analysis, the system compares the eccentricity value of each object with a threshold value ($E_{th} = 0.95$). Objects with higher eccentricity values have longitudinal shapes and are more likely to be fish. Other metrics such as ratio of major axis to minor axis could also be

considered.

The system creates at most one track at each time step. Subsequent tracks are selected similarly to the first one using the eccentricity comparison. The system examines the segmented objects, ignores the ones already tracked and selects the next best object that can be tracked (if any exist). It adds a feature vector for this object to the measurement matrix and passes the data to the Kalman Filter. The Enable Vector is also updated to enable an additional Kalman Filter bank. The newly enabled Kalman Filter bank will start estimating a new track in addition to the other enabled banks.

5.4.2 Target confirmation

For target confirmation, the system uses an integer-based Confidence Vector (CFV) and a binary-based Confirmed Vector (CV), both of length N, where N is the maximum number of targets that can be tracked. Each time a successful measurement to target association is carried out, CFV is incremented for the given target index. Once a target has been tracked for 8 consecutive frames, CV is updated from 0 to 1 for that target index.

$$CV(n) = \begin{cases} 1, & if\ CFV(n) > 8 \\ 0, & otherwise \end{cases} , n = 1...N \tag{5.4}$$

The Confirmed Vector (CV) is used to decide whether the data should be displayed or not. The system also detects transitions from 1 to 0, to capture the last measurement for each target. This last measurement is logged by the system and used in statistical calculations, as explained in Section 5.5.

5.4.3 Target deletion

If the Enable Vector entry at index n is changed from 1 to 0, it signifies that the the target n is no longer tracked. Both the Confidence Vector (CFV) and Confirmed Vector (CV) at index n are reset from 1 to 0. This transition will be picked up and the last measurement for the target will be recorded in the buffer (a delay block ensures that these measurements are available once the transition is detected). Target data will be recorded only if $CV(n) = 1$. If $CV(n) = 0$, this means the system was unable to track the target long enough and no data are recorded. This approach ensures that noisy measurements are not detected as valid tracks and that tracks used in statistical calculation are of sufficient quality.

5.5 Target Statistics

Target statistics are generated at the end of each time step, with bounding boxes for tracked objects created for display purposes. Two methods have been used for the calculation of statistical data: a buffer-based method and a time-based method. Both methods calculate the mean and the standard deviation of speed and direction of tracks but differ in these statistics calculation methods.

5.5.1 Buffer-based approach

The buffer-based method was developed initially and is not currently used to generate data for analysis. However its output is used in the video display block to show how fast fish are moving and in which direction. The method uses a first-in-first-out (FIFO) buffer of a certain length. The buffer is filled with tracking data, and once full, calculates statistical data (mean and standard deviation). When a new entry arrives, the oldest entry in the buffer is removed and statistics are recalculated. This approach provides a smoothing window and the influence of each track depends on the length of the buffer. A short length buffer indicates that each data point has a high impact, therefore statistics generated are more likely to be noisy but also more reflective of what actually happens in the cage within a short period of time. A long length buffer indicates that each data point has a low impact, statistics will be less noisy but cover a longer time span. The buffer effectively acts as a smoothing filter and its length determines how much smoothing is done. Because the number of tracks detected in any given period varies there may be situations where the buffer fills up quickly when numerous tracks are available or slowly when few tracks are available. This makes it difficult to determine the optimal length of the buffer and also makes it difficult to relate to a time span. For that reason the time-based method of calculating descriptive statistics was developed.

5.5.2 Time-based approach

The time-based method samples data points at regular time intervals (30 seconds). There is no limit on the number of samples tracked in a given period (no buffer), therefore statistics obtained are reflective of what actually happened during the period in question. A further weakness of the implementation of the buffer-based method is that it failed to take into account that the directional data are circular in nature. Batschelet (1981) provides a detailed discussion of circular statistics and provides equations for calculating the mean and (a form

Table 5.1: SQL database table for sea cage data

Column	Data Type	Descrption
testrun	int	ID of the analysis run
sampletime	datetime	Date/time of the sample
spix	decimal(9, 4)	Speed (pixels/s)
dir	decimal(9, 4)	Direction (deg)
spixstdev	decimal(9, 4)	Speed std dev (pixels/s)
dirstdev	decimal(9, 4)	Direction std dev (deg)
spbl	decimal(9, 4)	Speed (body lengths/s)
spblstdev	decimal(9, 4)	Speed std dev (body lengths/s)
totaltgts	int	Number of targets so far for this analysis run
tgts	smallint	Number of targets in this sample
night	smallint	Is night recording? (0 - NO, 1 - YES)
feeding	tinyint	Sample during feeding? (0 - NO, 1 - YES)
mealpercent	decimal(3, 2)	Percentage of daily food intake (%)
temp	decimal(4, 2)	Temperature (C)
visibility	decimal(2, 1)	Visibility (m)
salinity	decimal(3, 1)	Salinity (ppt@4m) - parts per thousand
do	decimal(3, 1)	Dissolved oxygen (mg/l)
dosat	decimal(3, 2)	Dissolved oxygen saturation (%)
tide	decimal(9, 8)	Tide Level (1 - high, 0 - low)
spixse	calculated	Speed standard error (pixels/s)
dirse	calculated	Direction standard error (deg)
spblse	calculated	Speed standard error (body lengths/s)
mealid	int	which meal of the day
invalid	tinyint	Is the sample invalid? (0 - NO, 1 - YES)
tideslope	smallint	Tide slope (1 - rising, -1 - falling)

of) standard deviation of circular data, used in the time based approach.

5.5.3 Data Storage

Calculated statistics are stored in an internal array within MATLAB. Once the analysis of the video file is finished all data are saved to the SQL Server (Microsoft SQL Server 2005 Express Edition).

5.5.4 Data Display

The data accumulated for display purposes includes: grey-scale image frame, segmented binary image, target co-ordinates, direction/speed line co-ordinates. The binary image is overlaid on the image frame to highlight regions which were segmented by the system. Target co-ordinates are used to draw red rectangles around each valid target. These targets are then used in averaging calculations. A direction/speed line uses orientation to show in which direction fish are travelling in relation to the camera, and length to show speed in pixels per second.

5.6 Accuracy of the System

The system described in this chapter was developed to model fish behaviour in sea cages through estimation of fish swimming speed and direction. The accuracy of the system can be compared with manual observations in terms of individual fish and the fish population.

The first approach is to look at individual fish and compare the automated speed and direction estimation of the system with manual analysis. This will determine if estimates are accurate but more importantly it will provide the error between manual and automated estimation. If the system can produce 20-80 samples per minute during daylight hours, then this can amount to over 8000 samples daily. Any individual inaccuracies will be averaged and it may be possible to calculate an average error of estimation. The system design focused on detection of changes in swimming speed and direction rather than providing very accurate estimates, but knowing the error of estimation allows the results to be adjusted to provide more accurate adjusted estimates. This approach is investigated in this section.

The second approach is to examine whether the system estimates the movement of the whole population of fish, given that the camera is positioned properly (at a right depth and location in the cage), and if the system discriminates between fast or slow fish or fish closer or further from the camera. This issue has not be covered in depth in the thesis but casual observations of the working system have shown that the detection is improved by proximity of fish to the camera. Due to the turbidity of the water, fish further from the camera are blurry and the segmentation process may not differentiate these fish from the background. Another concern may be that the system has a bias in regards to fish that swim faster or slower. Casual observations have not revealed any bias but further studies will be required to ensure that the system acquires unbiased samples from the field of view of the camera.

5.6.1 Recording Details

The test recording used here to check the accuracy of the system was a 7 hour recording of the daily routine on the 13^{th} of March 2008. The recording started at 7:55am and the camera was at a depth of 8 meters. No environmental or feeding data were available for this recording but tidal information was available from the Australian Bureau of Meteorology (BOM).

5.6.2 Accuracy Test

Five randomly selected 5 minute videos were extracted from the test recording. From each video, 20 random samples of automatically tracked fish were extracted (a total of 100 samples). For random video sequence selection, the MATLAB random number generator was used. For sample selection, a virtual die was used from http://www.random.org. When the result was 6, the sample was analysed, otherwise it was ignored. For each selected sample, only the last five frames were examined. Manual length measurements were made from the head to the tail of the fish using the MATLAB measurement tool. Length was recorded for each frame and the average of five frames was used as the final length. Speed measurements were usually carried out by determining the location of the tip of fish's head in each frame. There were times when fish manoeuvres caused the head to move in a different direction to the centre of the mass. In this case pectoral fins were used as points of reference for speed measurements. Having coordinates of the same point in five frames, row and column inter frame differences in displacement were calculated. These differences were then used to calculate inter frame velocity. The final velocity was calculated based on the difference between the first and the last frame. Inter frame velocities were compared with the final velocity to eliminate erroneous data entry and help evaluate fish motion and camera motion. Unusual fish motion and severe camera motion could cause high error of estimation. The final velocity was broken down into speed and direction components and these values were matched against the last automated estimate from the Kalman Filter.

Differences between automated and manual results were calculated. To avoid the influence of outliers, median and inter-quartile range (IQR) were used as preferred descriptive statistics (Table 5.2).

The system provided a sufficiently accurate estimation of direction (Fig. 5.3i), as any difference within 60° meant that fish were travelling in a generally similar direction within the field of view of the camera (median = 14°, IQR = 20°). Higher variations in direction could be due to camera movement.

Table 5.2: Descriptive statistics of differences between automated and manual estimations. Median and inter-quartile range (IQR) were used to reduce the influence of outliers.

	Median	IQR
Direction difference (deg)	14	20
Length difference (pixels)	-3	14
Speed difference (pixels/s)	-8	17
Speed difference (bodylengths/s)	-0.1	0.39

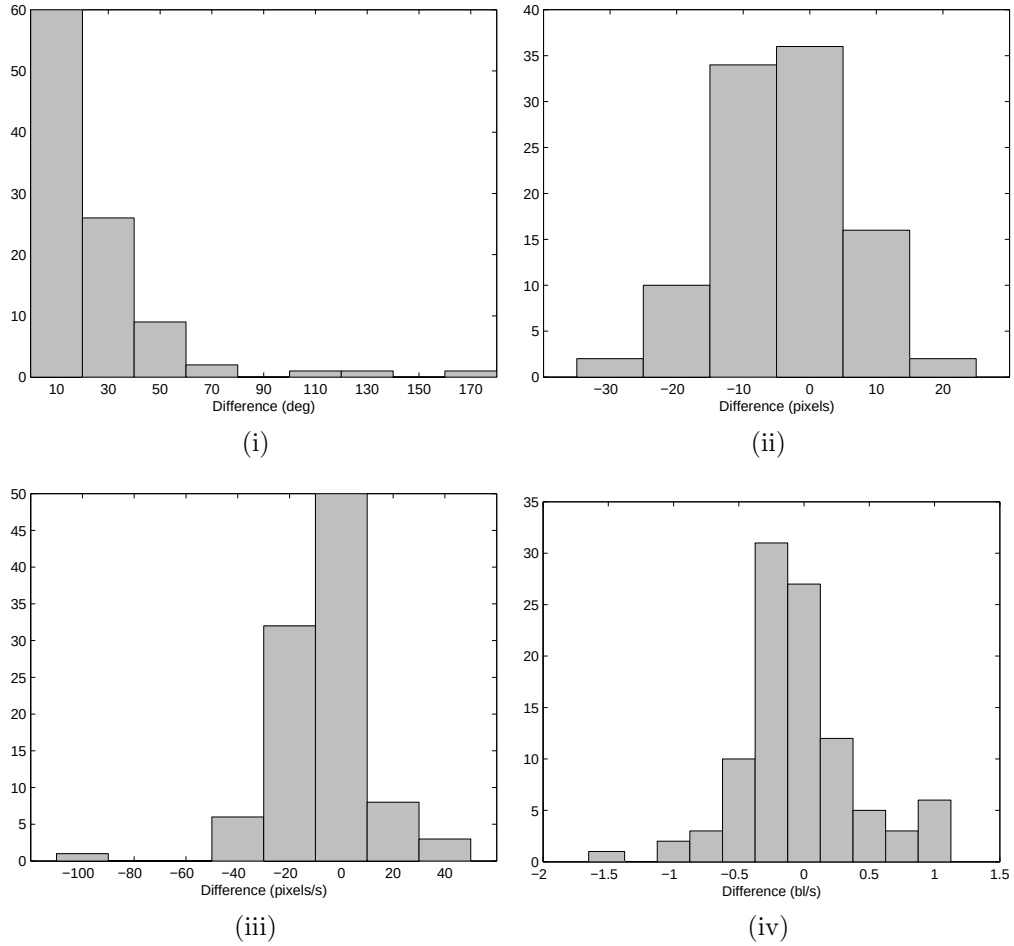

Figure 5.3: Histograms of differences between manual estimates and automated estimates. (i) Direction, (ii) Length, (iii) Speed in pixels/second, (iv) Speed in body lengths/second.

Estimation of fish length was the most difficult measurement to perform accurately due to imperfections in the segmentation process (Fig. 5.3ii). The system often extracted only a portion of fish shape, underestimating the length of fish (median = -3 pixels, IQR = 14 pixels). The Kalman Filter was designed to assign less significance to these measurements and therefore there was less opportunity for these poor measurements to affect the final estimate. A substantial number of automated length estimates (20%) were higher than their manual counterparts due to the system detecting multiple fish as one while the manual analysis would correctly identify only one fish.

Speed in pixels per second tended to be underestimated by the system in comparison with manual estimation (median = -8 pixels/s, IQR = 17 pixels/s) (Fig. 5.3iii). This could be due to manual estimates being taken only during the last 5 frames before the track was lost, while the automated system may have tracked the fish for much longer prior to the comparison. Another reason is that during the analysis, the motion of the camera may have affected the estimate. Because only the last 5 frames were manually analysed, the camera movement could have occurred then or earlier in the automated tracking. The automated tracking would deal at that time with the camera movement by smoothing the estimate (using the Kalman Filter). The manual analysis did not attempt any smoothing.

The speed in body lengths per second was being used to standardise the measurement, given that no attempt has been made to detect the distance of a tracked fish from the camera. Because this measurement is a combination of speed in pix/s and the length, the error of estimation can be compounded as seem in Fig. 5.4. However the median difference of $-0.1bl/s$ is satisfactory for the purpose of this system (Fig. 5.3iv). Table 5.3 indicates other possible sources of error within the system. Of these, the two most important are the segmentation process and camera movement. Improvements in the segmentation process may decrease the errors in length estimation and increase the duration of tracking. The camera movement can at times have a significant effect on the estimation process. Looking at this problem frame by frame, the tracked fish may appear to be moving forwards in the first few frames while in the following frames, due to the camera movement, it will appear to move backwards. The estimation process will attempt to account for this error to a degree but it can nevertheless have difficulty in determining the correct direction of movement and provide incorrect estimates. However the use of validation gates (see Section 4.3.1), especially when motion of the camera is severe, means that the track will be terminated rather than continue to produce poor estimates.

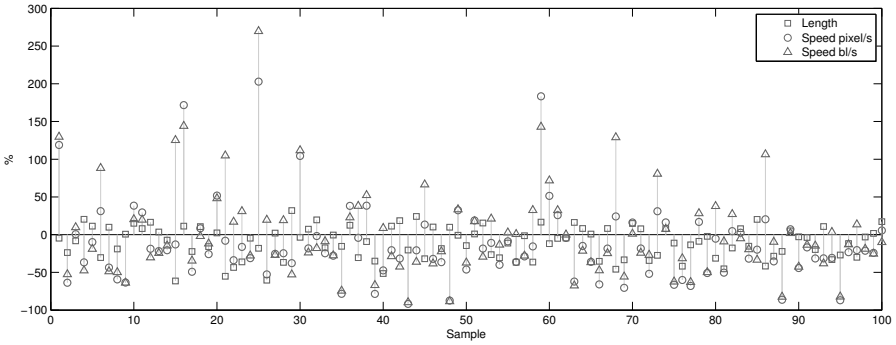

Figure 5.4: Influence of length and speed errors, for each sample, on the body lengths per second errors.

Table 5.3: Source of errors within the tracking system.

System errors	**Problem domain errors**
Segmentation	Natural variability in fish movement
Data association	Camera movement
Estimation errors	Variability in environmental conditions
	Human interference

5.7 Camera Stabilisation

The stabilisation algorithm is based on work by Cai and Walker (2008) described in Section 3.4. Local Motion Vectors (LMVs) are created by estimating optical flow using the Lucas-Kanade method available in SIMULINK (Mathworks, 2009). The following value of parameters have been used: $\delta = 20\%$ of the LVM array size, $\alpha = 0.95$, and $\beta = 0.8$. The β parameter was lower than the range suggested by Cai and Walker (2008) perhaps due to additional rotational motion of the camera which was not accounted for in this stabilisation method. More recent work by Cai and Walker (2009) addresses this issue but has not been part of this research. Section 9.4 (Further Work) will discuss possible improvements to the algorithm mentioned in this section.

5.8 Global Motion Patterns

There are situations where tracking of individual fish may not be possible at all in sea cages. This is most likely to occur when fish are larger, the density is higher and fish swim close to the camera. Also night time recordings, while using

artificial light, produce poor segmentation results and therefore poor tracking performance. However it would still be desirable to detect changes in fish behaviour. Rather than attempting to track individual fish as described throughout this chapter, an alternative approach may be to look at spatio-temporal changes between a sequence of image frames, taking images as a whole rather than extracting objects of interest.

To achieve this motion flow fields can be used (Hu et al., 2008) as described in Section 4.4. Rather than using Gaussian ART algorithm (Williamson, 1996) to decrease the number of motion vectors in the Point Flow Field, a simpler, yet effective method has been used. The original flow field was a matrix the size of the image frame - 160x120 (19200 motion vectors). Through nearest neighbour interpolation this matrix was resized to 20x15 (300 motion vectors) (Fig. 5.5i) and this is followed by creation of sink paths based on motion vectors. Figure 5.5ii demonstrates how the sink seeking processes traverses through points using the kernel based estimation. Once the sink seeking process is complete, supertracks are generated through sink clustering. Empirically, if $D_x \leq 17$, and $D_v \geq 0.75$ and $D_p \leq 17$ (calculated using Eq. 4.43, 4.44, and 4.45) then the sink is assigned to the cluster, otherwise a new cluster is created. Figure 5.6ii shows five supertracks created as a result of clustering of sinks shown in Figure 5.6i.

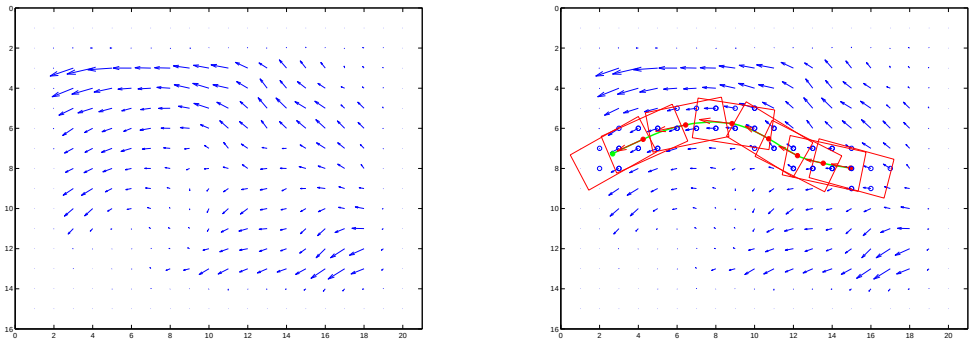

(i) (ii)

Figure 5.5: Generation of sink paths: (i) Point Flow Field and (ii) the sink seeking process.

Supertracks from one sequence of images can be compared with another sequence. This can be used to detect changes between consecutive sequences and the degree of change. Hu et al. (2008) provide metrics to perform supertrack matching and this could be used to detect differences in fish movement.

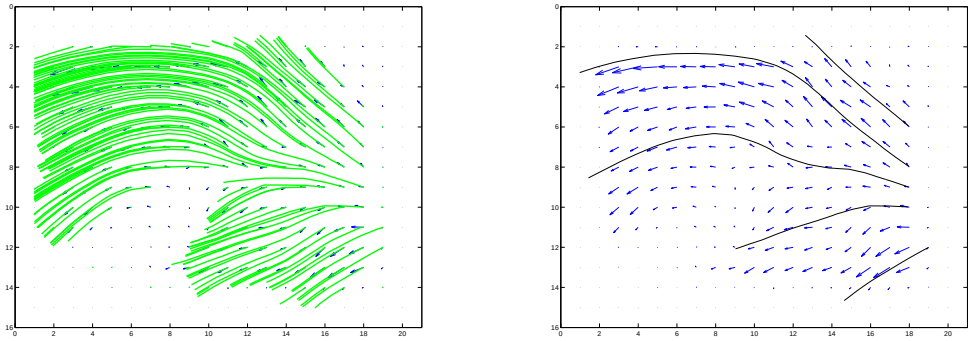

(i) (ii)

Figure 5.6: Generation of supertracks: (i) sink paths within the field and (ii) the result of sink clustering: supertracks. Short sink paths are discarded as they are likely to originate from points on the edge of the field.

5.9 Summary

The system described in this chapter allows tracking of individual fish within a sea cage for short periods of time. Using a number of fish tracks, an average speed and direction can be calculated for a given sampling period. Estimations of these tracks contain natural variation of fish movement as well as errors resulting from the tracking system. Only preliminary work has been performed to investigate how these system errors can be mitigated, especially the movement of the camera. Further improvements in the area of segmentation and camera stabilisation are required to increase the accuracy of the system. Despite these issues, the system provides useful data on fish movement in sea cages of similar quality to the manual observation but on continuous basis, providing a superior outcome comparing to any current video based method of observation. The next chapter presents several experiments, which provide some insight into how the system could be utilised in a real-time, commercial setting, and what sort of output is expected from it.

CHAPTER 6

ANALYSIS OF FISH BEHAVIOUR IN SEA CAGES

6.1 Introduction

Video technology is used in aquaculture to observe fish behaviour during feeding (Ang and Petrell, 1998), at different times of day (Kadri et al., 1991), and in different seasons (Smith et al., 1993). Currently it is not possible to sample fish behaviours continuously due to the tedious and intensive nature of video analysis. To facilitate continuous analysis, a computer tracking system was investigated in Chapter 5 to automatically analyses fish movement in sea cages from the underwater video. The system was designed with commercial operations in mind and it was important to test its viability on a commercial aquaculture site.

The aim of this chapter is to demonstrate the results obtained from the tracking system described in the previous chapter and analyse results in the aquaculture context. The chapter examines specific variations in swimming speed and direction within days and between days, aligns data with environmental variables and provide an interpretation of the data in this context. This interpretation is used to validate that the system can produce meaningful data for both aquaculture researchers and commercial aquaculture operators.

6.2 Materials and Methods

The chapter describes four experiments. All experiments examine swimming speed and direction changes of Atlantic salmon but in different contexts. Experiment 1 was a short term recording in order to generate pilot data used to examine the initial potential of the system in detecting differences in swimming speed and direction (in relation to the camera orientation) within days and between days. This experiment was followed by a longer recording sequence to

examine between day differences (Experiment 2). An outbreak of Ameobic Gill Disease (AGD) on the farm meant that the original objective of Experiment 2 could not be achieved, therefore the focus shifted to examination of the differences before and after fresh water bathing, which was carried out once AGD was identified by farmers. Experiment 3 was designed to answer a specific question - the time required for young smolts, transferred from a freshwater hatchery, to acclimatise to a sea cage. From previous experience, farm operators estimated that it would take around three to four weeks for the fish to settle into a schooling pattern. The purpose of this experiment was to independently confirm operator interpretations through the use of the automated tracking system. The initial recording was carried out and analysed in 2009. This recording was replicated again in 2010 to investigate if swimming patterns observed in the first recording would appear again.

In all recordings tidal times were only as obtained from the Australian Bureau of Meteorology (BOM) since equipment to measure the water current was not available on site. Tidal values have been represented by an interpolation between the high and low tide (as supplied by BOM). The low tide has been given a value of zero, while the high tide has been given a value of one. Values between tides are a real numbers between 0 and 1 with flood tide values being expressed as positive numbers (0 to 1), while ebb tide is expressed as s negative value (-1 to 0). In early 2011 there was an opportunity to use a water current meter to measure the strength and direction of the current simultaneous with the recording of fish behaviour (Experiment 4). This experiment provided an opportunity to measure the water current directly and compare it with the tidal times obtained from BOM and also compare measurement directly with the swimming speed and direction obtained by the tracking system. Examination of these two relationships allows validation of the findings in earlier experiments in terms of how tides may influence swimming speed and direction of fish.

All experiments have been carried out at Van Diemen Aquaculture Pty Ltd in the Tamar River, Rowella, Tasmania, Australia in 25m x 25m square cages (Fig. 6.1 and 6.2). The site has some unusual features which may specifically influence fish behaviour: strong currents (including tidal currents), comparatively high temperatures for salmon farming due to its geographical location and easy access to cages from the shore leading to increased human activity.

6.2.1 Experiment 1 - Influence of tidal cycle on fish movement

The objective of this experiment was to evaluate the ability of the tracking system to detect changes in swimming speed and direction, and to observe variations in

Figure 6.1: Van Diemen Aquaculture farm in relation to the Tamar River (oriented North). Image courtesy of Google Earth (2003).

swimming speed and direction between days. A total of 27,294 Atlantic salmon (*Salmo salar*) with a mean individual weight of 1.05kg, estimated biomass of 28,576kg at an average density of 5.2 kg/m^3 were monitored in the sea cage (number 12) for 6 days on 10-15 April 2008. All video recordings started at 06:30h and finished at 18:30h (12 hours) with the exception of 15 April when the recording inadvertently ceased after 4.5 hours. While environmental data were not available, tidal times were available and recorded (See Appendix Section B.1), as supplied by Australian Bureau of Meteorology (BOM) for the farm area. Feeding times were also recorded (See Appendix Section B.1). The video camera was positioned at a depth of 6 metres facing upward connected to a laptop with TV tuner. Figure 6.1 the position of the farm in relation to the river and river currents, including layout of the farm in 2003 and Figure 6.2 shows the current layout of the farm (2010-2011). Video data were analysed using the adaptive threshold segmentation method (See Section 5.2.2), which produced 7,250 records, each record representing 30 seconds of data.

The analysis of data included plotting swimming direction as Cartesian and polar graphs. Cartesian graphs show the relationship between the swimming direction and the tidal cycle. Polar graphs denote time as a radius of the circle (with midnight (00:00h) in the middle of the circle and 20:00h on the outer edges) and plot the directional data in a circular form. This approach demonstrates the daily variations in direction but in relation to the camera rather than in relation

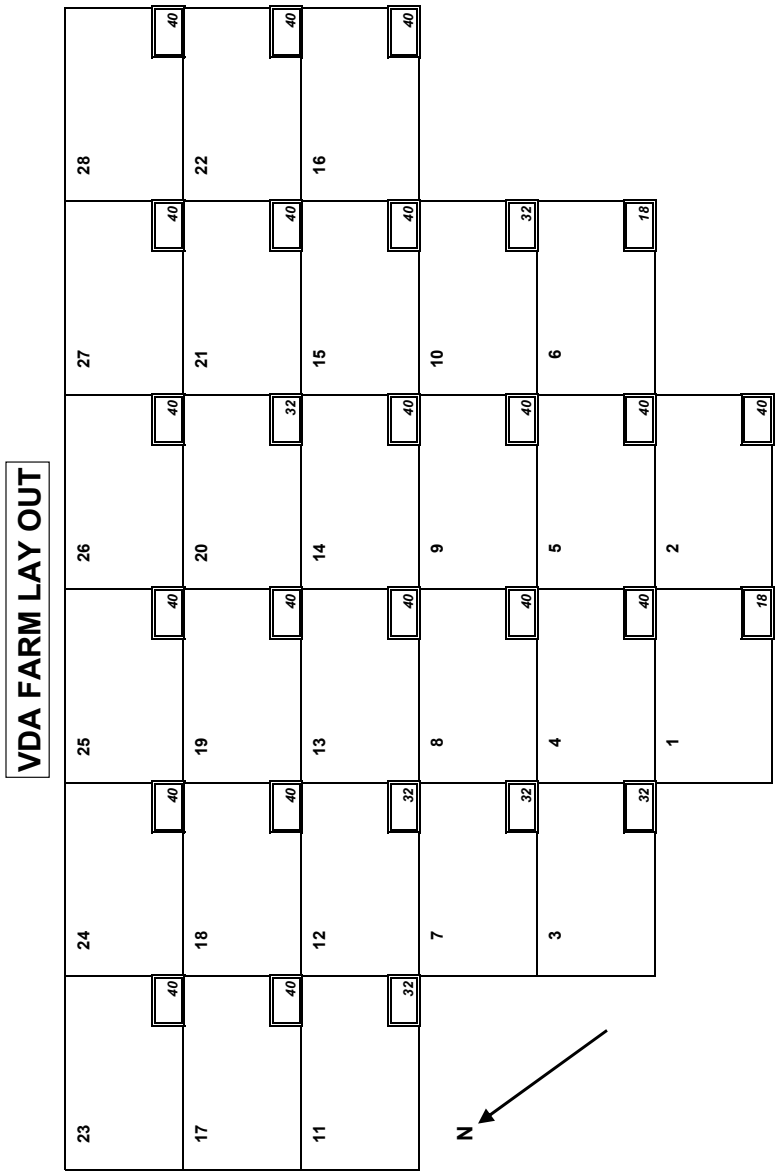

Figure 6.2: Current farm layout at Van Diemen Aquaculture. The number in the top left of each cage is the cage number, the number in the bottom right denotes the mesh size. Upstream direction is south-east.

to the cage. The speed has been plotted in Cartesian co-ordinates to allow for visual analysis against the tidal cycle.

Changes in speed in the middle of ebb and flood tides have been calculated using MATLAB graphs. The absolute speed difference was manually calculated between observed peaks and the absolute tide level recorded at the top of the more prominent peak.

6.2.2 Experiment 2 - Daily swimming profile in the summer during an outbreak of AGD

The initial objective was to simply observe daily routine during high summer temperatures. In the course of recording Amoebic Gill Disease (AGD) was detected and freshwater bathing was required, providing an opportunity to observe differences before and after freshwater bathing. This experiment observed the daily swimming profile of salmon in cage #1 during the summer of 2009 with the mean weight increasing from 556g to 666g from the start to the end of the recording period of 24 days (21 Jan - 19 Feb 2009). Feeding times, tidal times (low and high tide) and some environmental data were recorded (see Section B.2 in Appendix B). Initial recordings (21-25 Jan) started at 05:30h and finished at 21:00h. Later recordings (26 Jan - 19 Feb) started at 06:30h and finished at 20:30h. There was a 15 minute gap in the middle of the day (12:45h to 13:00h) because the recording software could not fit the whole day within a single video file and this gap was required to conclude the morning recording and reset the system for the afternoon recording. Freshwater bathing was carried out between 2-6 Feb. In total, the video analysis system produced 34,422 records using the adaptive threshold method as described in Subsection 5.2.2.

The analysis of speed used Cartesian graphs analogous to graphs used in Experiment 1.

6.2.3 Experiment 3 - Smolt behaviour post-transfer from hatchery to sea cage

The aim of this experiment was to record the behaviour of out of season salmon smolts for 40 days, after fish arrived from the freshwater hatchery and were transferred directly into a sea cage. On 21 April 2009, ca. 68,000 fish were transported by road tanker from Sevrup Fisheries hatchery at Cressy, Tasmania and directly transferred to cage #3 at Van Diemen Aquaculture. The mean weight of fish, provided by farm operators, increased from 149g (68,135 fish, density 3.6 kg/m^3)

to 234g (67,998 fish, density 5.7 kg/m^3) from the start to the end of the recording period of 40 days from (22 Apr - 31 May 2009). Feeding times and daily feeding percentages were recorded and each meal constituted ca. 20% of the daily feeding ration. The feeding data have been tabulated in Appendix Section B.3. Tidal data (times of high and low tides) were as provided by Australian Bureau of Meteorology (BOM) for farm location, however no information about the strength of the current was available (Appendix Section B.3). Environmental variables (temperature, dissolved oxygen and visibility) were provided by farm operators and recorded as am/pm measurements in the database daily (Appendix Section B.3).

Days not recorded were usually maintenance days which were required to offload recordings on the laptop (with limited hard drive capacity) to a mobile hard drive. At the time it was not expected that a loss of a few days would affect the outcomes of the experiment. The initial set of recordings (9 days) started on 22 April at 06:15h and finished at 18:00h (30 April). As the daily light phase shortened, further recordings (19 days) were started at 06:45h and finished at 17:45h (1-20 May). The last set of recordings (10 days) started at 07:00h and finished at 17:30h (21-31 May).

The segmentation of video data was carried out using the edge detection algorithm (as described in Subsection 5.2.3) due to the small size of fish. This provided an acceptable number of samples to calculate averages. Around 11% of captured records (a total of 46,380 records) were excluded due to various technical problems encountered during recording.

In order to identify relationships within the data set, Pearson's correlation test has been performed on several response variables (Table 6.1). The data set for this analysis was truncated to dates from the 11th of May (inclusive) until the end of recordings. Days before 11th of May were non-schooling behaviour days and therefore it would be difficult to look at patterns given that fish were still settling down. In addition 20th of May was excluded from the analysis because net cleaning was carried out in the cage as well as surrounding cages disrupting normal swimming patterns for the whole day. In total there were 19,382 samples available from the 16 days included in the analysis.

The analysis of data involved the use of polar graphs to plot the swimming direction over time for each day, similar to the graphs used in Experiment 1. This was done to clearly demonstrate how swimming direction was used to detect the difference in non-schooling and schooling behaviour. Cartesian graphs were used for swimming speed and direction to highlight the relationship with the tidal cycle.

Oriented fish shapes is another method of visualising differences between non-schooling and schooling behaviours where samples recorded are represented as fish

Table 6.1: Response variables for the smolt dataset.

Response variables	**Description**
spblsmooth	Speed in body length/second
spblchange	Rate of change in speed
spblstdevsmooth	Std Dev of speed in body lengths/second
spblstdevchange	Rate of change in Std Dev of speed
dirchange	Rate of change in direction
dirstdevsmooth	Std Dev of direction
dirstdevchange	Rate of change in Std Dev of direction

shapes, each with its own orientation. Each sample's orientation represents an average direction of all tracks detected in a 30 second interval. Fish shapes are arranged from bottom left and are filled upwards in columns.

A further recording was carried out in 2010 (26 April to 16 July). The cage was stocked from the Sevrup Fisheries hatchery on 22 April 2010 with 69,994 O^+ smolts with an initial mean weight of 134g (biomass of 9,557kg and density 3.4kgm^{-1}).

6.2.4 Experiment 4 - Relation between water current flow, tides and fish movement

In February/March of 2011, Van Diemen Aquaculture temporarily installed a water current meter (Model 106 Lightweight Current Meter, Valeport Ltd, UK) to examine water currents around the farm. The farm operators also took video recordings for several days during this time on a cage in position 10 (as shown in Figure 6.2). The camera was placed halfway between the centre of the cage and the south-eastern edge of the cage to enable the observation of the circular movement of the fish school and the water current meter was placed several meters under the camera. The aim of the experiment was to compare current flow measurements recorded by the meter with data received from Australian Bureau of Meteorology (BOM) and to analyse swimming speed and direction of fish in combination with current flow measurements. Water current measurements were carried out between 26 February 2011 and 15 March 2011. The period of video recordings was shorter, between 26 February and 7 March. In total 12,456 sample periods were extracted of which 12,123 were valid with an average of 45 tracks per sample period. Tide times were extracted from http://www.willyweather.com.au for location Sidmouth (based BOM data) in addition to data from the water current meter. Each data entry generated by the tracking system was matched

to its corresponding water current measurement and tide times, and entered into the SQL server database.

Analysis involved plotting water current measurements against the tide values interpolated from BOM data. In addition swimming speed and direction were plotted in Cartesian co-ordinates against water current measurements to examine the relationship between fish behaviour and tidal currents.

6.3 Results

6.3.1 Experiment 1 - Influence of tidal cycle on fish movement

Direction

Figure 6.3 shows Cartesian and polar plots of swimming direction with interpolated tide lines. Fish direction changed suddenly by over 100° during low tide on most of the monitored days. This pattern occurred at a regular advancing time on consecutive days - 09:12h, 10:03h, 11:02h, 11:55 h, 12:38h on 10, 11, 12, 13, 14 of April respectively (recording had stopped before the low tide on the 15^{th}). The average difference between days was 51.5 minutes, which corresponds very closely with the daily tidal shift. The standard deviation of direction did not change significantly during this time, indicating that fish changed swimming direction uniformly as a group and continued their schooling.

Speed

Figure 6.4 presents the swimming speed of fish with interpolated tide lines. Table 6.2 presents changes in speed in the middle of ebb tide. There was no obvious influence of low or high tide on the swimming speed of fish. However a change in speed by an average of ∼0.9bl/s was observed in the middle of the ebb tide (Table 6.2). This was not visible for 12 April because of a shortened recording due to technical problems. A less prominent pattern occurred during the middle of the rising tide, with a mean change of ∼0.5bl/s (Table 6.3).

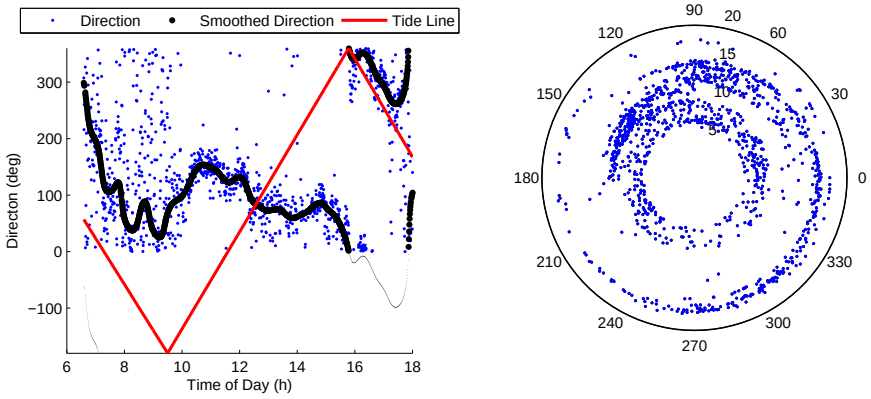

(i) 10th April

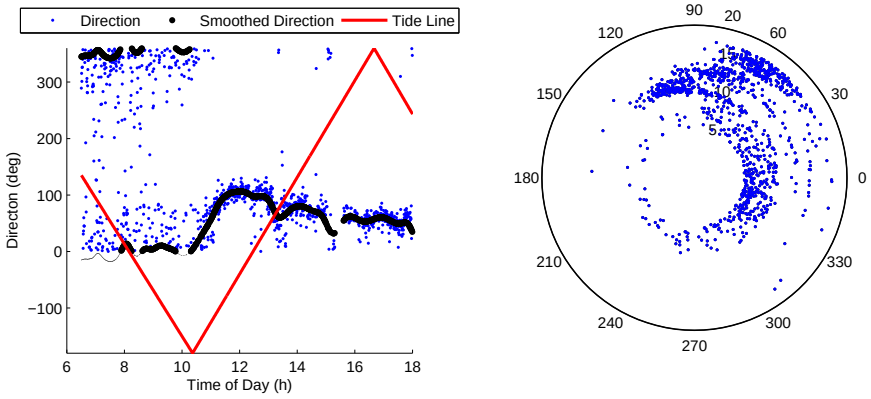

(ii) 11th April

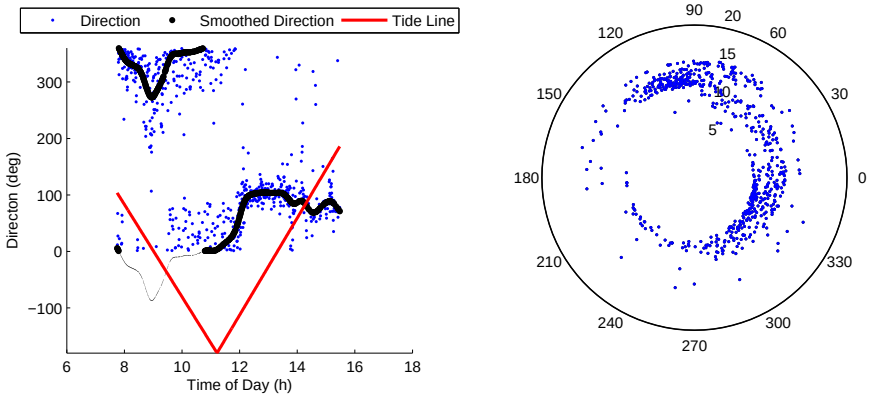

(iii) 12th April

Figure 6.3: Direction during 10-15 April 2008 in Cartesian and polar coordinates. Red lines represent interpolated tide values between low and hight tide (bottom of the graph) and high tide (top of the graph).

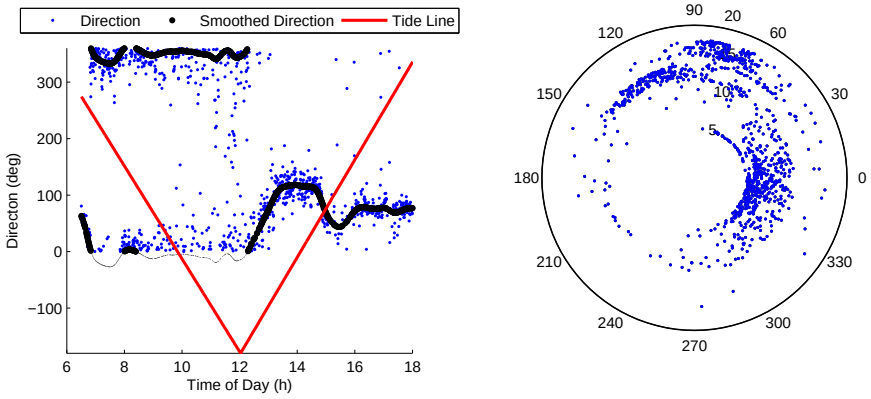

(iv) 13th April

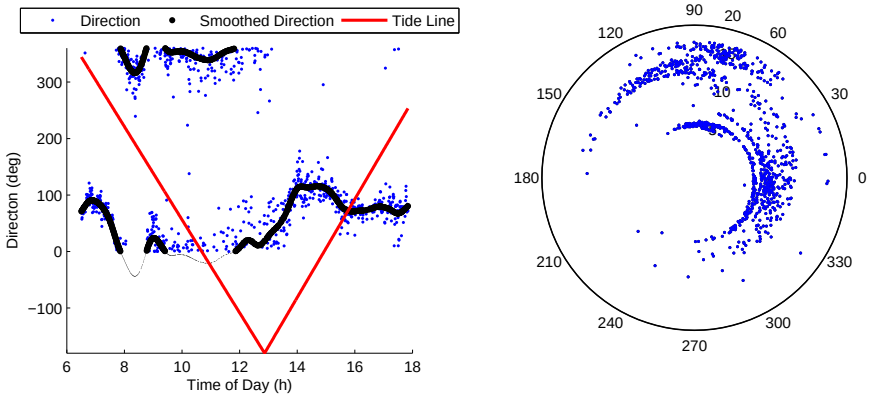

(v) 14th April

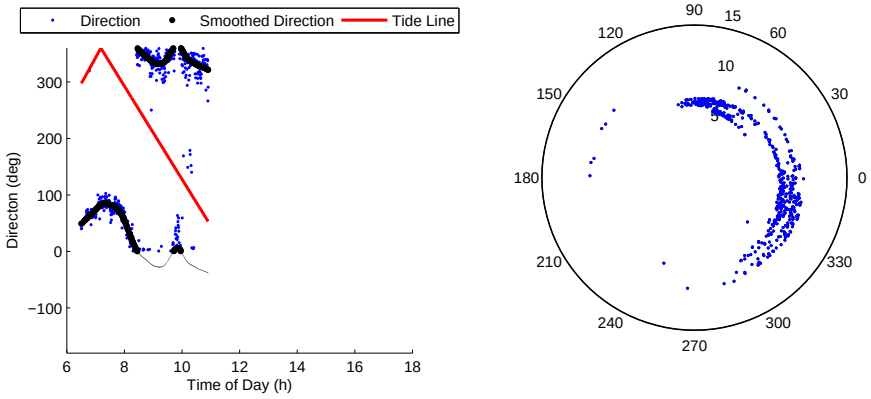

(vi) 15th April

Figure 6.3: (Cont.) The polar graph shows how direction varied throughout the day with radius being the time of day and data points being swimming direction at a given time.

Table 6.2: Change in swimming speed observed in the middle of the ebb tide (Low tide is indicated as 0 and high tide as 1).

Day	**Time**	**Speed diff (bl/s)**	**Tide level**
10 April	17:25	0.67	0.72
11 April	6:56	0.77	0.51
12 April	N/A	N/A	N/A
13 April	8:12	1.06	0.57
14 April	9:06	1.04	0.57
15 April	9:57	1.15	0.57

Table 6.3: Change in swimming speed observed in the middle of the rising tide (Low tide is indicated as 0 and high tide as 1).

Day	**Time**	**Speed diff (bl/s)**	**Tide level**
10 April	14:13	0.59	0.76
11 April	15:13	0.53	0.78
12 April	15:09	0.43	0.63
13 April	16:12	0.47	0.67
14 April	16:38	0.77	0.61
15 April	N/A	N/A	N/A

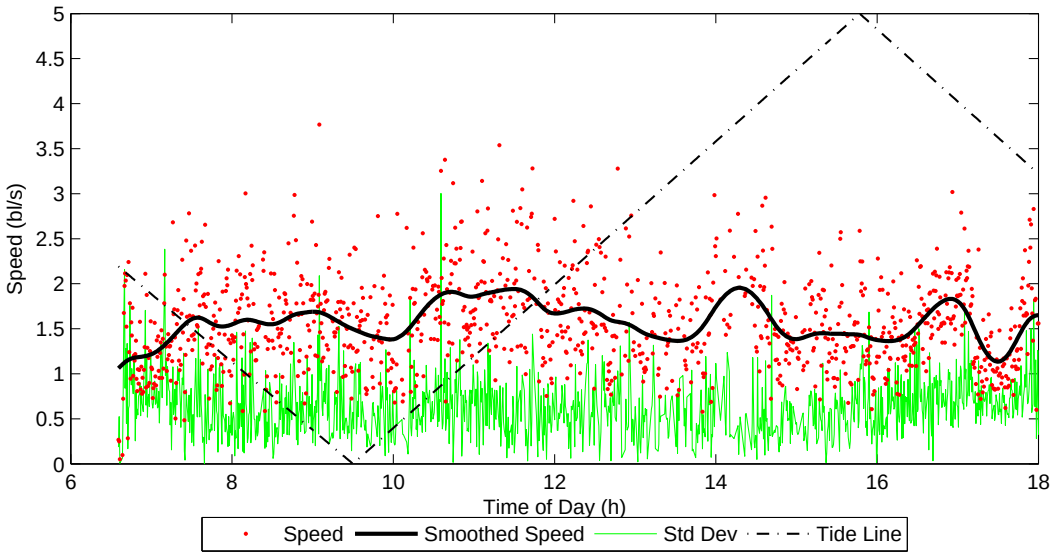

(i) 10th April

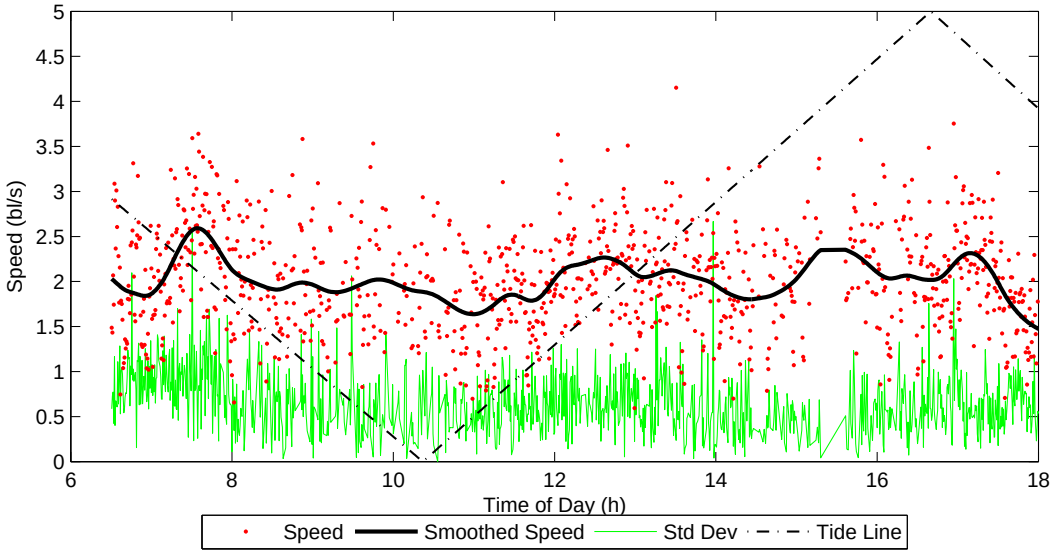

(ii) 11th April

Figure 6.4: Speed during 10-15 April 2008. Broken lines represent interpolated tide values between low tide (bottom of the graph) and high tide (top of the graph). Speed data are sampled every 30s.

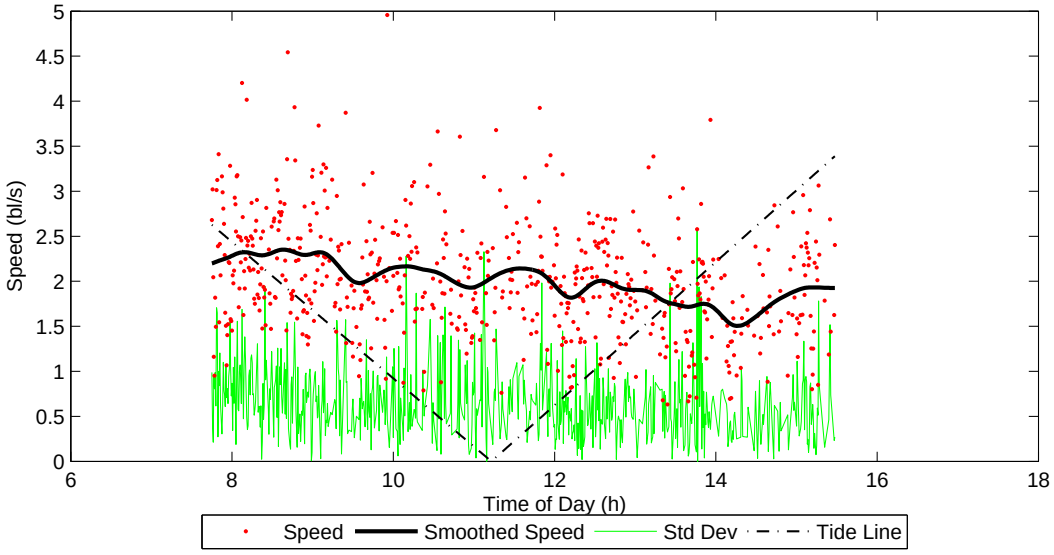

(iii) 12th April

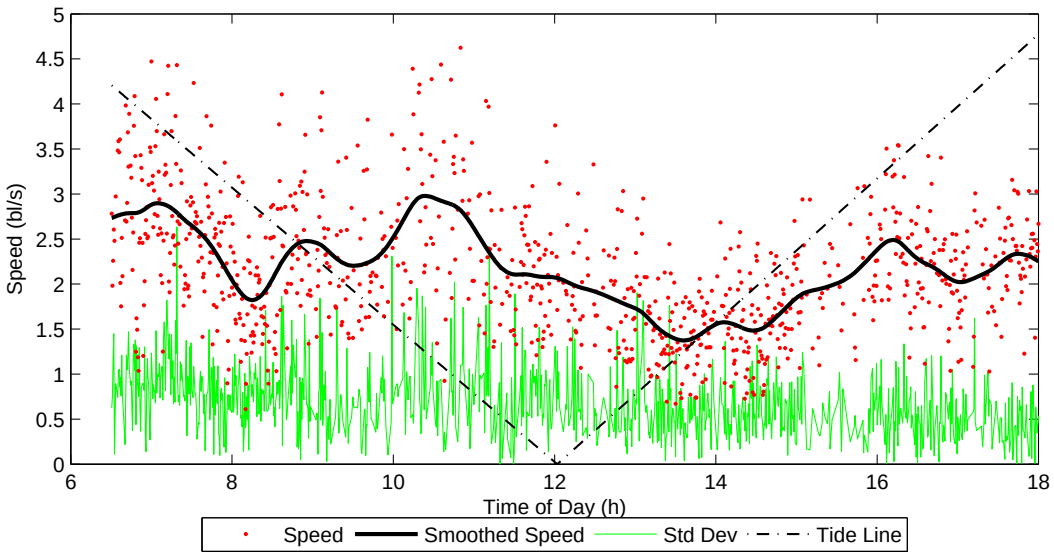

(iv) 13th April

Figure 6.4: Continued.

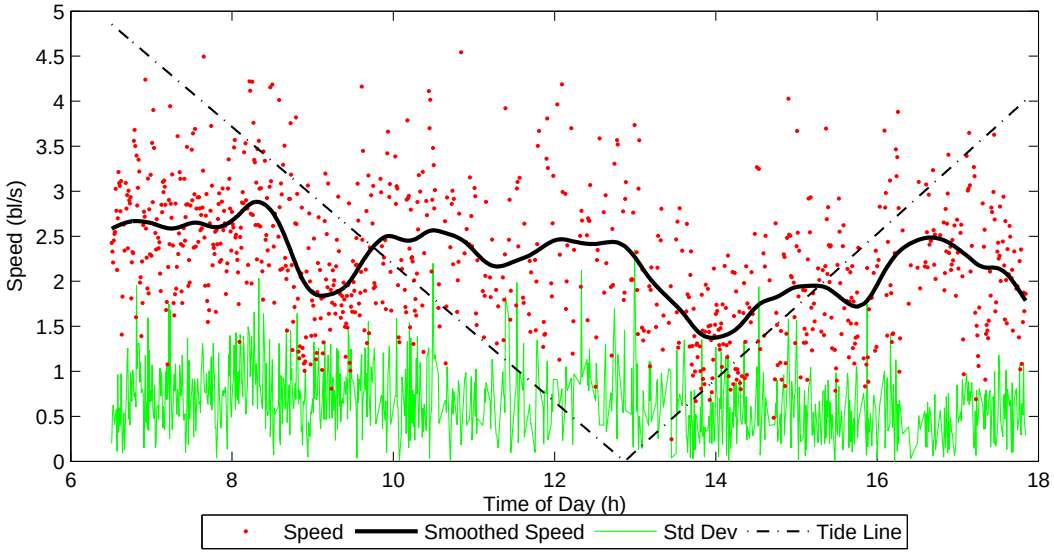

(v) 14th April

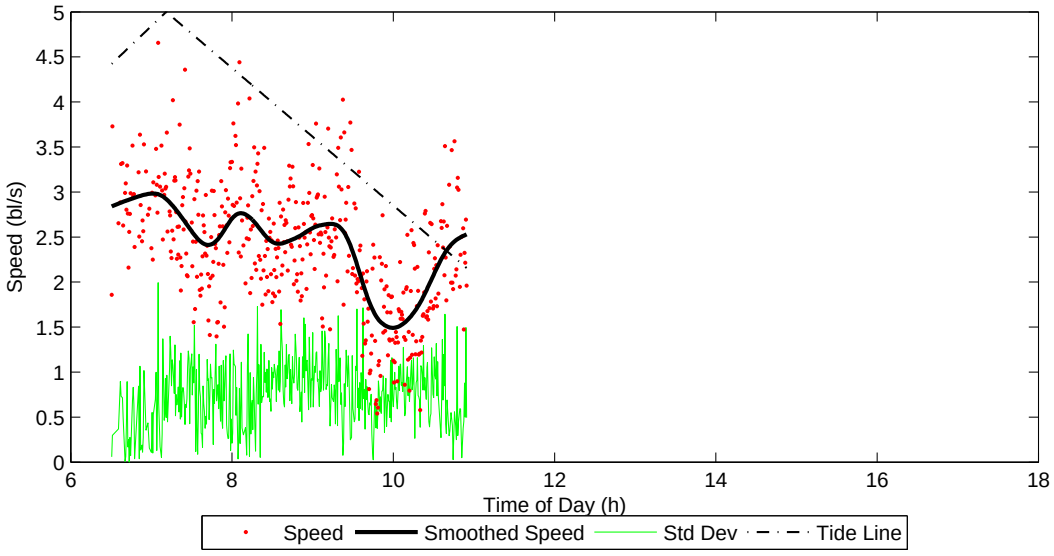

(vi) 15th April

Figure 6.4: Continued.

6.3.2 Experiment 2 - Daily swimming profile in the summer during an outbreak of Amoebic gill disease (AGD)

Swimming speeds were analysed before bathing (21 Jan to 1 Feb) and after bathing (7-15 Feb) as illustrated in Figure 6.5 with AGD detected on 28 January. This figure shows gaps in data and also there are several days that have not been recorded or had to be discarded due to the poor camera orientation. Three days (21 Jan, 1 Feb, and 15 Feb) were selected from the dataset, which were complete and judging from the available data, likely to be representative of neighbouring days (Figure 6.6). On 21 January swimming speed was ranged between 1.5bl/s and 2.0bl/s throughout the day with no major deviations regardless of time of day or feeding times. On 1 February the swimming speed was ca. 2.0bl/s in the morning and over 5 hours it dropped to ca. 1.0bl/s. For the remainder of the day swimming speed was maintained at just below 1.5 bl/s. There were some significant differences in environmental conditions between these two days (Table B.5). The temperature was higher on the 1 February by ca. 2.1°C in the morning and 1.3°C in the afternoon. There was also a decrease in dissolved oxygen by 0.7mg/l (morning) and 0.6mg/l (afternoon) as well as a decrease in D.O. saturation by 4% (morning) and 10% (afternoon). The final day, 15 February, depicts fish behaviour at the end of the recording period, over a week after bathing. The speed throughout most of the day remains below 1.0bl/s with little variation. Of the three days, the dissolved oxygen was lowest on the 1 February increasing slightly by 15 February. The temperature was also highest on the 1 February, but had only slightly decreased by 15 February. Visibility throughout the data set was low and of the three days it was lowest on 15 February (the lowest visibility for the whole data set was on 12 February). The general trend was that the swimming speed decreased after bathing amid variations in environmental variables.

The average low-to-high amplitude of the tide (peak-to-peak) was investigated during the three days before bathing (30, 31 Jan and 1 Feb) and the three days after bathing (13-15 Feb). The difference between average amplitudes (2.26m and 2.72m respectively) was 0.45m.

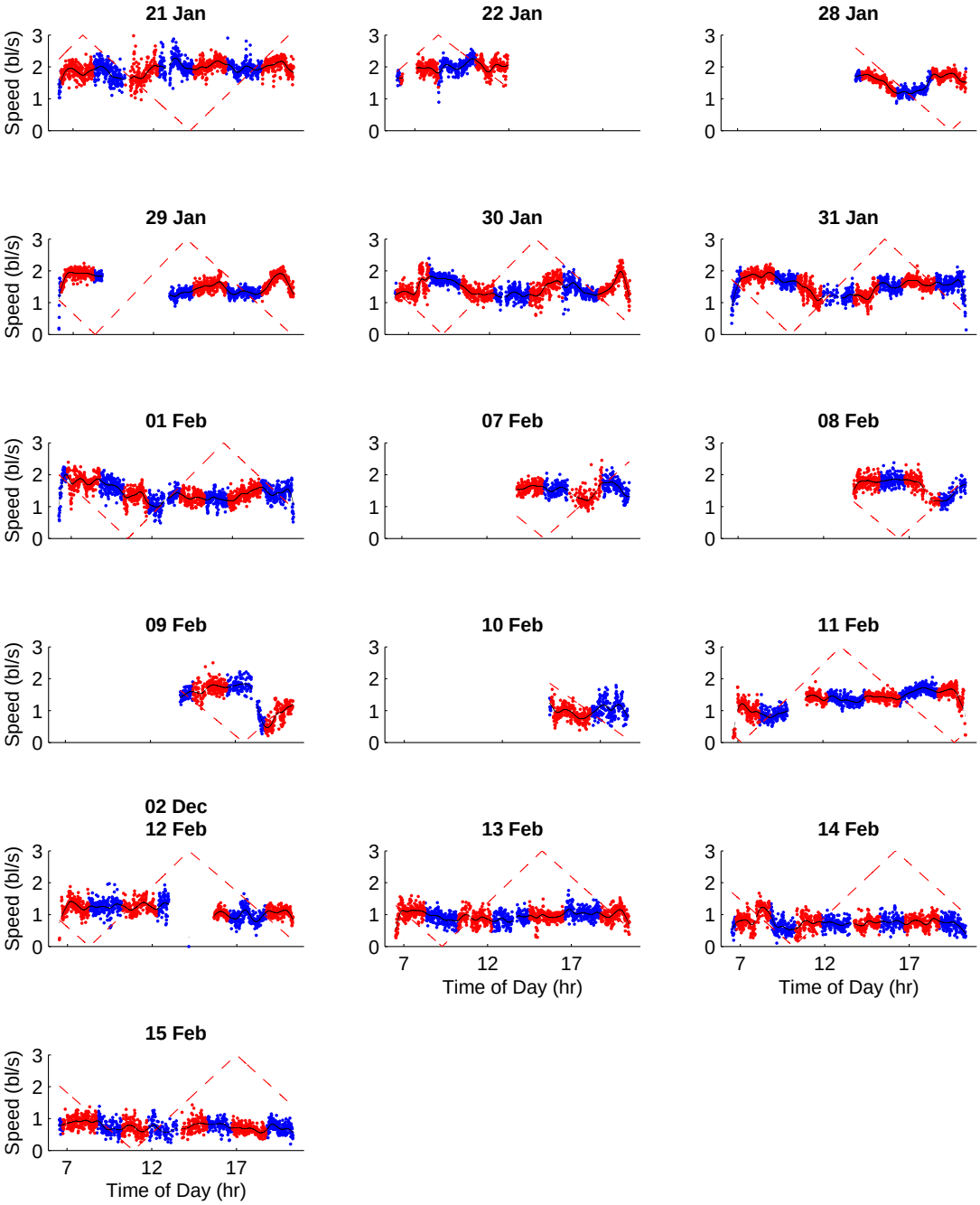

Figure 6.5: Swimming speed before bathing (21 Jan - 1 Feb) and after bathing (7-15 Feb). Red data points represent speed during feeding, blue during non feeding times. Red broken line represents the tide value (low tide at the bottom, high tide at the top).

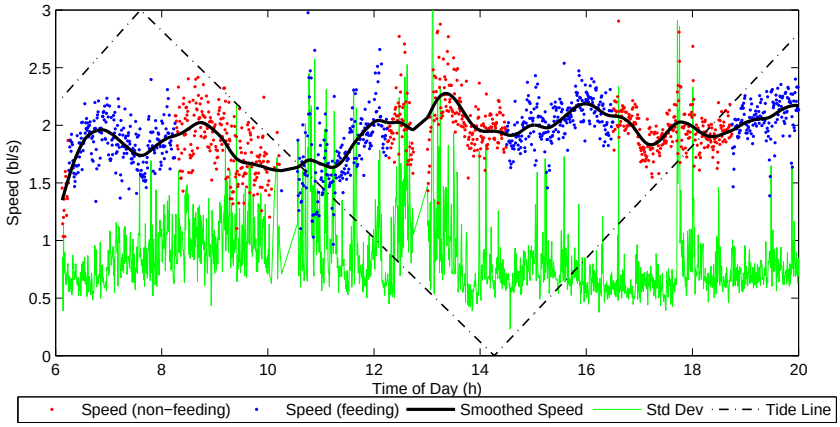

(i) 21 Jan

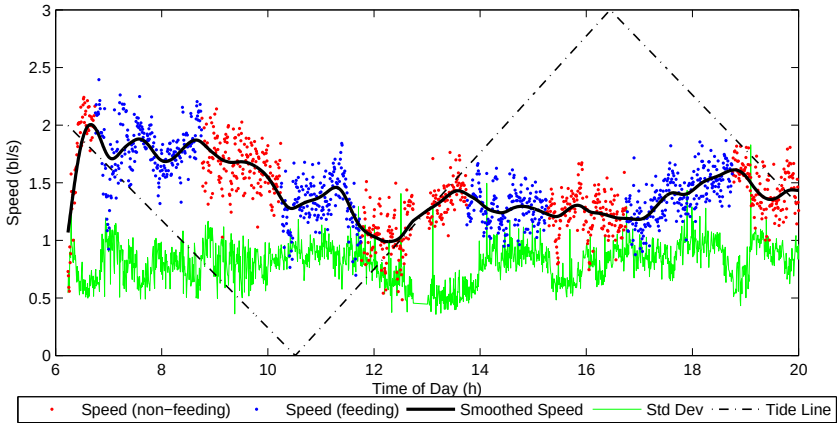

(ii) 1 Feb

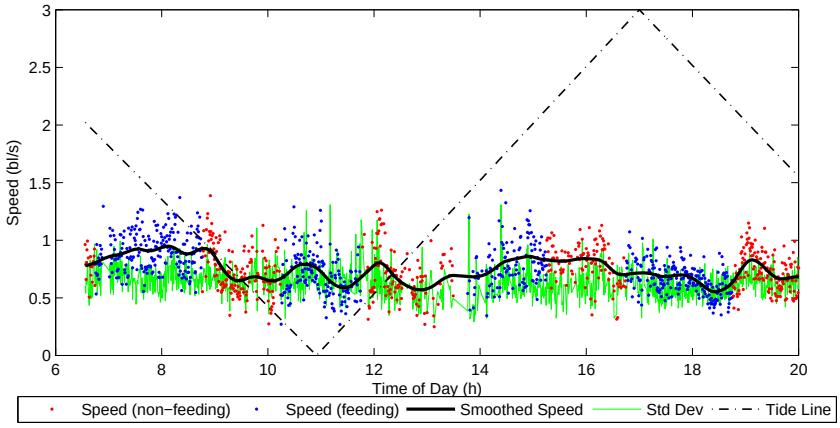

(iii) 15 Feb

Figure 6.6: Three days selected from the dataset: (i) beginning of the recording, (ii) prior to bathing, (iii) end of the recording (after bathing). Swimming speed on 15 Feb is lower and less variable than the other two days.

Table 6.4: Low-to-high tide amplitude (occurring twice a day) before and after bathing. Three days on each side of bathing have been selected for comparison.

Low-to-high tide amplitude (metres)			
Before Bathing	Average: **2.26**	After Bathing	Average: **2.72**
30-Jan (1)	2.05	13-Feb (1)	2.75
30-Jan (2)	2.26	13-Feb (2)	2.73
31-Jan (1)	2.26	14-Feb (1)	2.87
31-Jan (2)	2.29	14-Feb (2)	2.62
1-Feb (1)	2.44	15-Feb (1)	2.90
1-Feb (2)	2.29	15-Feb (2)	2.46

6.3.3 Experiment 3 - Smolt behaviour post-transfer from hatchery to sea cage

Relationship between speed and standard deviation of direction

Due to a large number of samples, most correlations are statistically significant but only several have strongly significant correlations. The data were assumed to be normally distributed given the large sample size (Central Limit Theorem) and this permits the use of Pearson's correlation test as opposed to Spearman's rank correlation test (Lumley et al., 2002). The only relationship discussed is the strong, negative correlation (Pearson's $r = -0.74, df 18831, p < 0.001$) between swimming speed and standard deviation of direction and it suggests that when fish are swimming slowly they tend to travel in many different directions (in relation to the camera) (Figure 6.7). When fish swim fast, they tend to all swim in the same direction. This relationship was confirmed via manual observation of video footage - when fish were swimming slowly there was generally a breakdown in schooling behaviour; when they were swimming faster, a larger proportion of fish conformed to the schooling behaviour and they swam in the same direction.

Detection of Schooling Behaviour

For days from 23 April until 9 May swimming direction is very variable covering the whole circle throughout the day. This indicates a lack of schooling pattern but some attempts at schooling can be noticed on the morning of 2, 3 and 4 May. There were not data recorded for 10 May due to technical failure. This was a critical delineation day because more defined schooling behaviour starts from 11 May onwards and this is reflected by a much smaller variability in direction. A noticeable exception is 20 May when net cleaning was carried out. First an

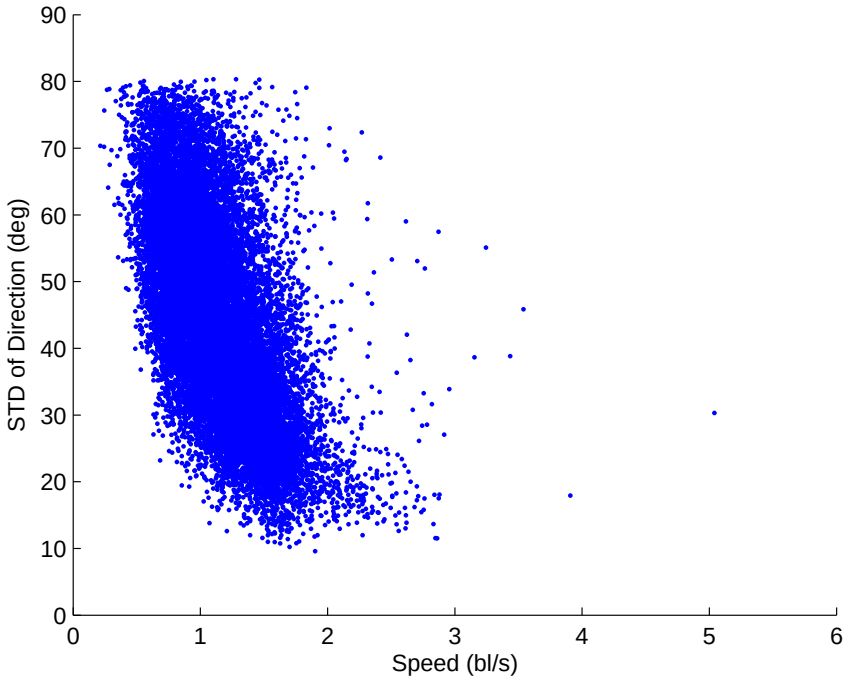

Figure 6.7: Scatter plot of speed vs standard deviation of direction.

adjacent cage was cleaned from around 09:20h and this was followed by cage cleaning on this particular cage at 12:05h. Cleaning ceased at around 13:15h and resumed again at 14:10h until 15:00h. It appears that fish continued to be unsettled for the remainder of the day. This finding was confirmed by manual observation from farm operators.

Data obtained from recordings carried out in 2010 reveal a similar pattern of behaviour (shown in Figure 6.9) when the schooling behaviour became more defined after 4 weeks. It was also observed that full Moon was on 9 May 2009 and 27 May 2010, near the supposed transition from non-schooling to schooling and new Moon was observed on 25 Apr 2009 and 14 May 2010. In addition the 2010 data set had an additional full Moon on 28 Apr 2010. A technical failure caused a gap in recording between 24-29 May during which fish transitioned from non-schooling to schooling behaviour. This failure was not identified and rectified until 30 May. From 23 June video was recorded at night time in addition to day-time because farm operators deployed underwater lights on the cage. The night time recording was carried out to provide a continuity in recording between day and night.

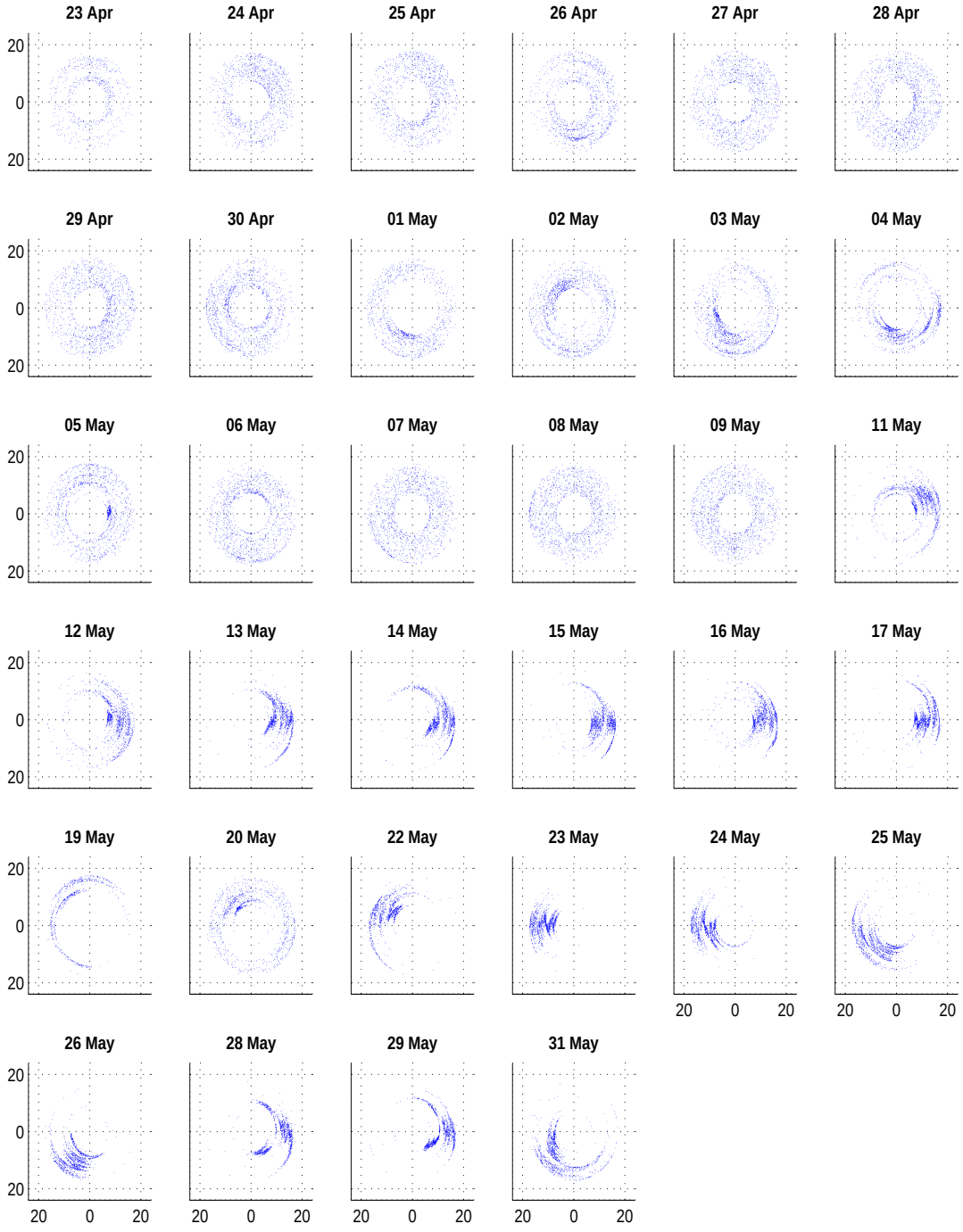

Figure 6.8: Variations is swimming direction for each day in 2009 dataset. XY-axes signify time as a radius of each polar plot (midnight in the middle of each plot, 20:00h on the outside). Each direction data sample is plotted in polar co-ordinates against the sample time.

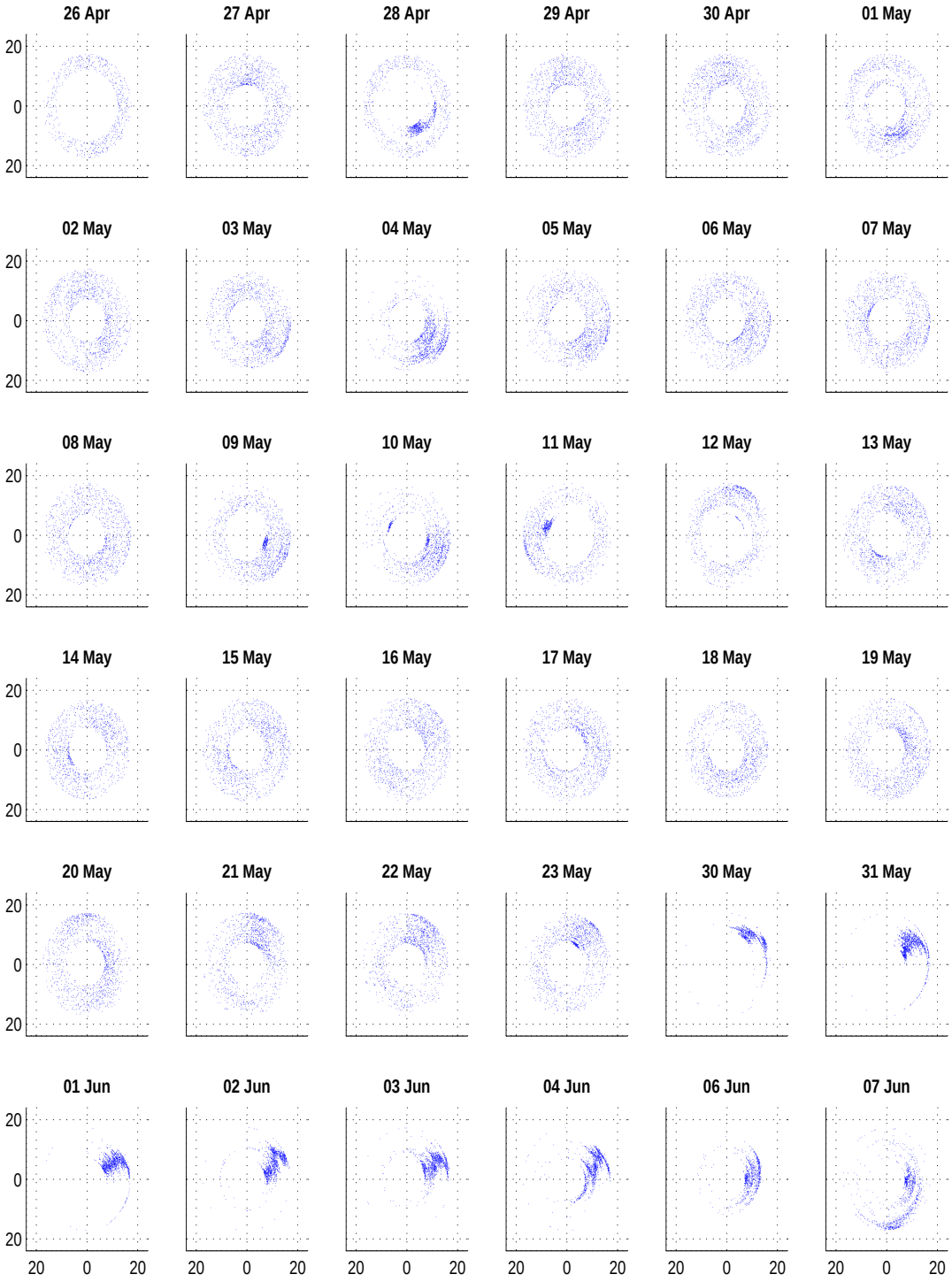

Figure 6.9: Variations is swimming direction in 2010 dataset (for explanation of polar plots see Figure 6.8).

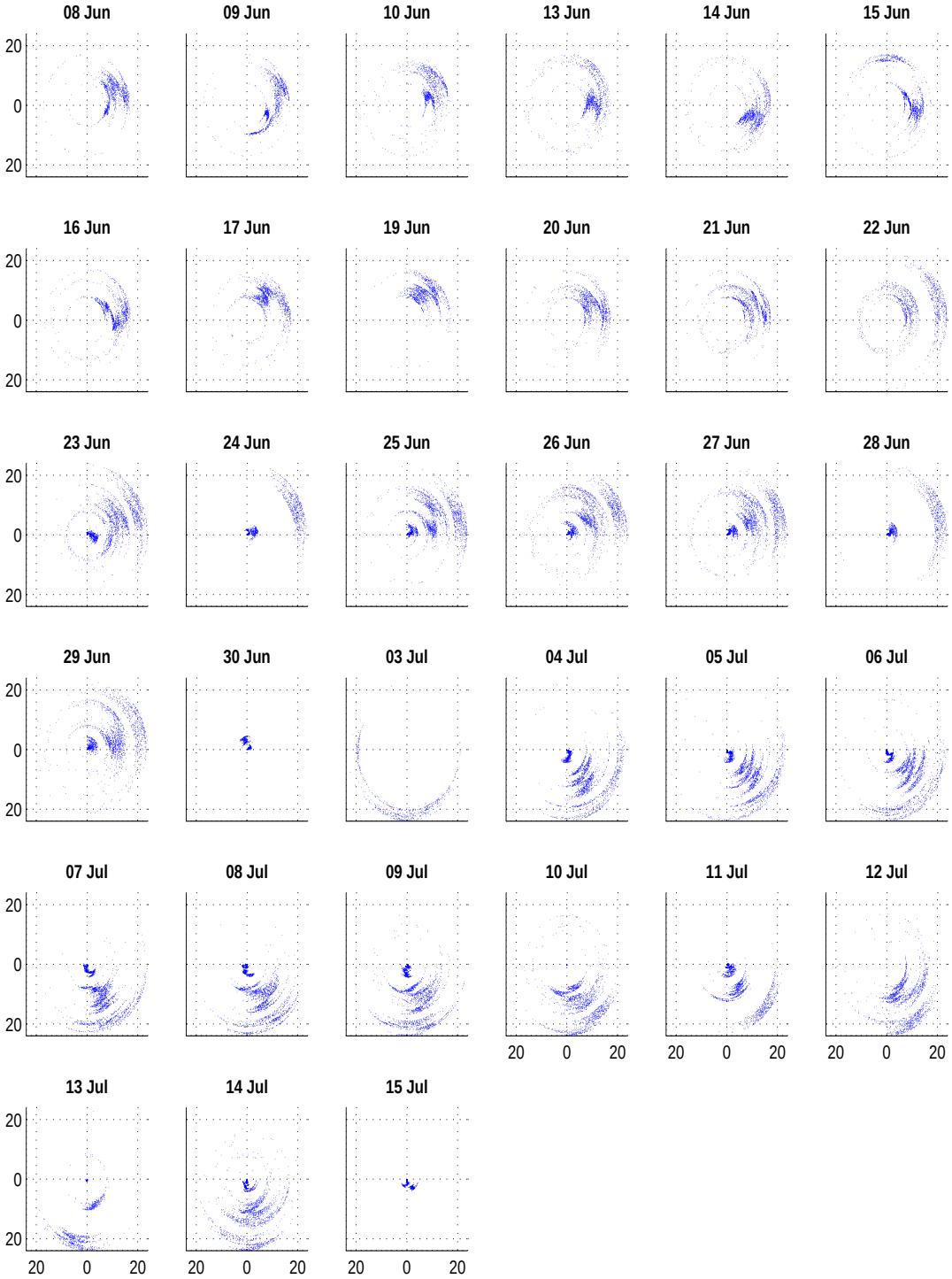

Figure 6.9: Continued.

Oriented fish shapes graph demonstrates a clear difference between the two days - 28 April, before schooling commenced and 28 May, after schooling commenced (Figure 6.10). On the 28 April fish were disorganised, changing direction frequently, while on the 28 May there is more orderly movement with directional changes occurring in an orderly fashion. Red fish shapes represent samples during feeding periods and blue fish shapes represent samples during non-feeding periods.

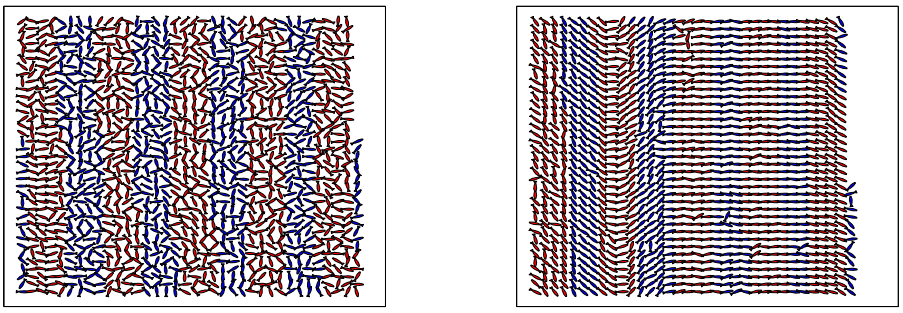

(i) (ii)

Figure 6.10: Visualisation of differences in direction between non-schooling behaviour on 28 April (i) and schooling behaviour on 28 May (ii). Red fish represent feeding periods, blue fish non-feeding periods.

The difference between non-schooling and schooling behaviour can be detected by examining the standard deviation of daily direction samples to determine if the mean of these daily standard deviations for days between 23 April and 9 May is the same as the mean of daily standard deviations for days between 11 May and 31 May (Figure 6.11).

The mean of the daily standard deviations of daily direction samples was significantly different between non-schooling and schooling days (two sample t-test: $t_{32} = -8.00, p < 0.001$) given variances are equal (F-test: $F_{16,16} = 1.34, p = 0.564$). The mean daily standard deviation of daily direction samples for days when schooling behaviour was not established, was 2.3 times greater than when schooling behaviour was evident (Figure 6.12).

The mean of daily speeds in body lengths per second (Figure 6.13) was significantly different between non-schooling and schooling days ($t_{32} = 3.71, p < 0.01$) given the variances were not significantly different ($F_{16,16} = 1.45, p = 0.467$). The mean of daily speeds when schooling behaviour was established was 20% higher than when schooling behaviour was not evident (Figure 6.14).

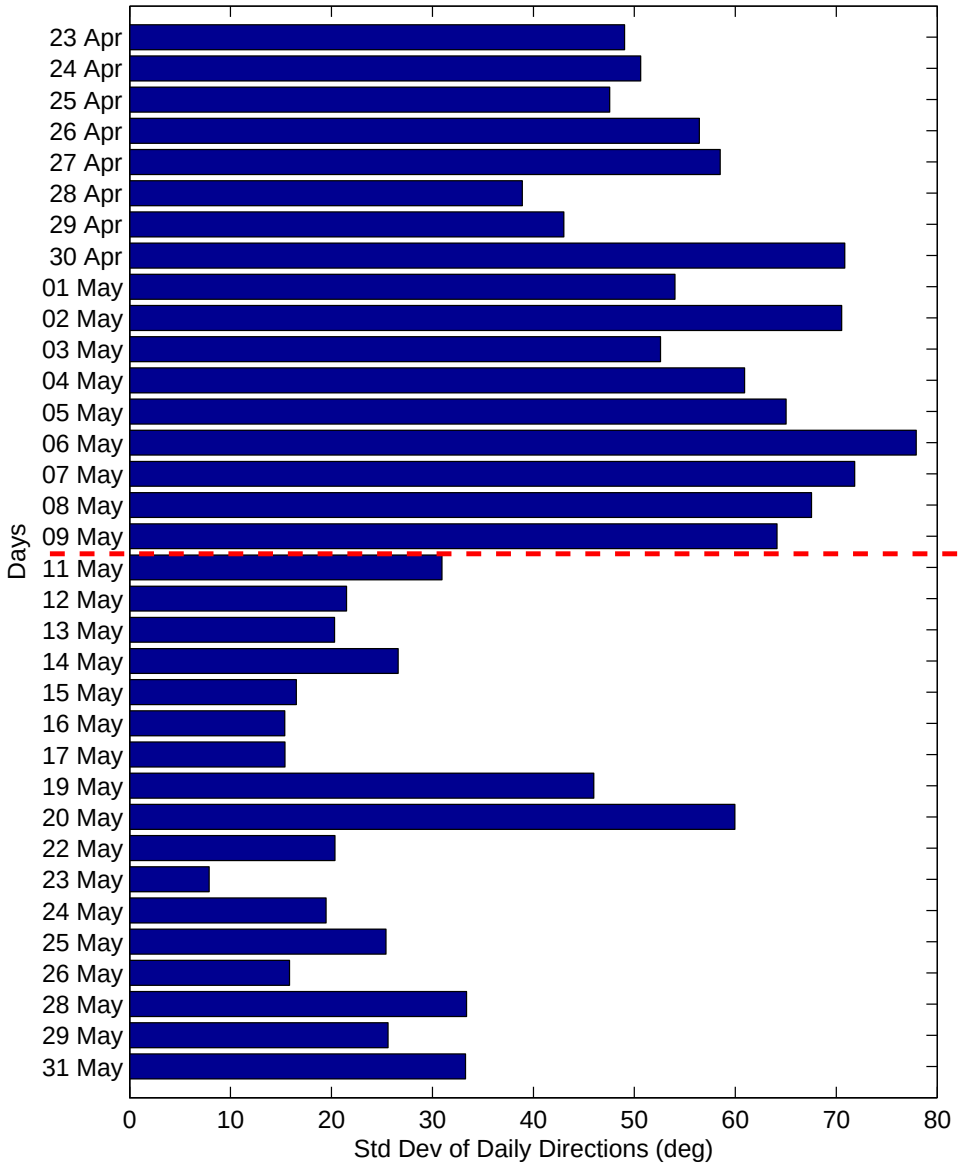

Figure 6.11: Standard deviations of daily direction samples for 2009 dataset. Broken red line denotes when the schooling behaviour has commenced. 19 May represents a partial recording of only several hours, while on 20 May fish were disturbed due to cage cleaning.

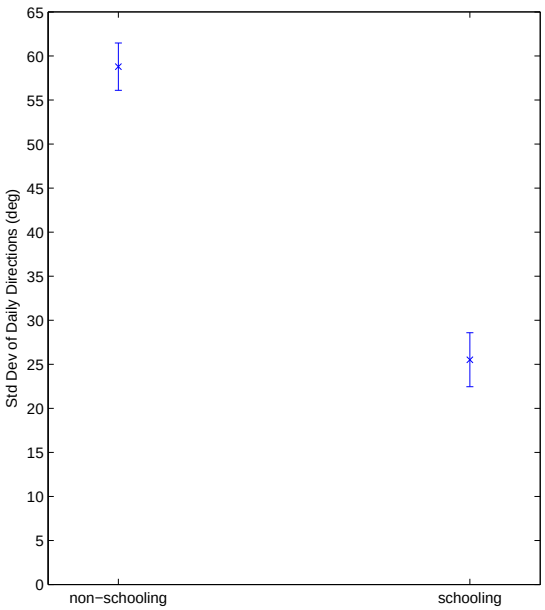

Figure 6.12: Mean of daily standard deviations of direction samples with SE for non-schooling and schooling behaviour.

Influence of tides on swimming direction

This subsection will investigate the influence of tides on swimming direction and speed of fish during the 2009 experiment. Because the actual current measurement was not available, low and high tide times were taken from the BOM web site.

Figure 6.15 shows swimming directions for all days within the dataset with tide lines included (red broken line). Days prior to May 11 have been ignored in this investigation because fish have not settled into their schooling behaviour, therefore it would be difficult to look for tide related patterns. However days from May 11 show a pattern about 1 hour after low tide, where direction suddenly changes by about 90° (similar to results obtained in Section 6.3.1). The standard deviation of direction also changes after low tide (between 25° to 75°). The exceptions to this are 15 and 16 May where standard deviation remains high well before low tide and subsequently does not change after low tide. The operator log revealed that weather conditions were rough on 15 May and after the initial good feeding response in the morning, fish swam at depth in the cage to feed and remained deep throughout the day. On the 16 May, the feeding response was good initially before slowing. During the 09:15h meal, fish started at the surface before swimming at depth and feeding response was poorer later in the day.

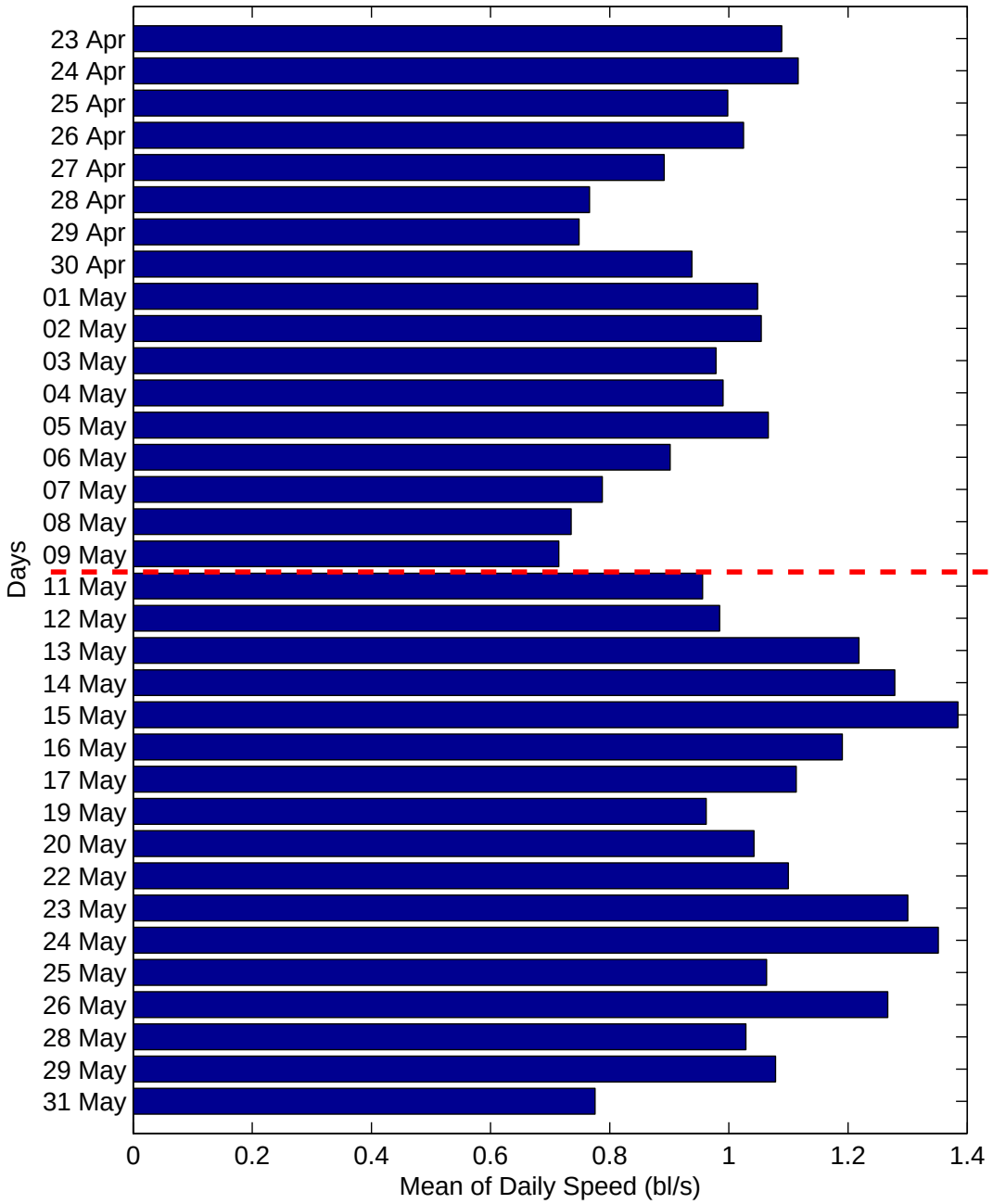

Figure 6.13: Daily means of speed for 2009 dataset. The broken red line denotes when the schooling behaviour commenced.

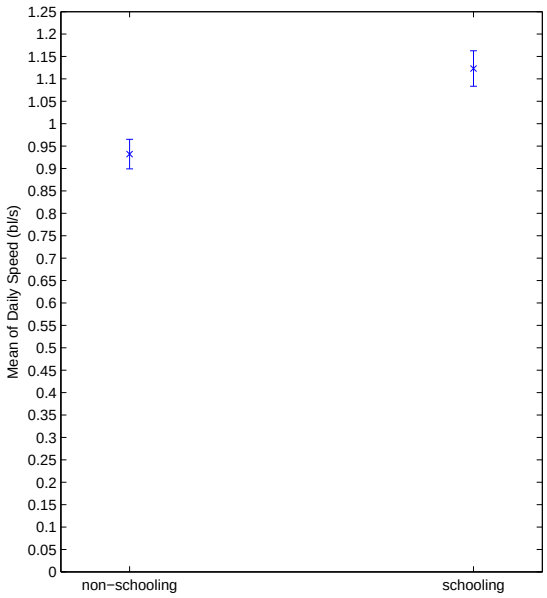

Figure 6.14: Averages of daily mean of speed with SE for non-schooling and schooling behaviour. Means are statistically significantly different from each other.

Comparing days before and after 15-16 May, it appears that feeding responses were depressed during 15 and 16 May. It is possible that rough weather might be the cause and fish were disturbed more throughout both days.

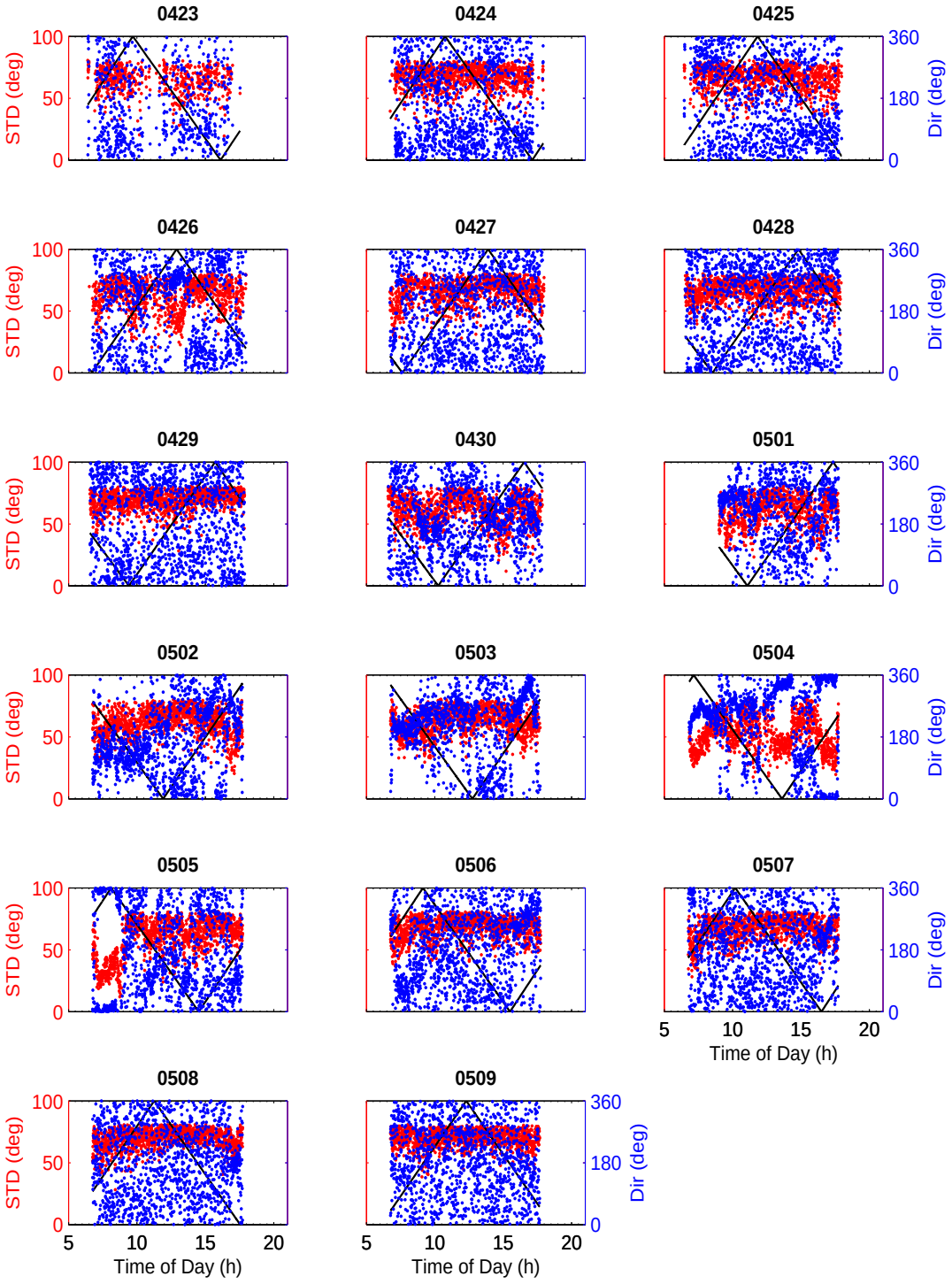

Figure 6.15: Direction (blue) and standard deviation (red) of direction in relation to tides (black line).

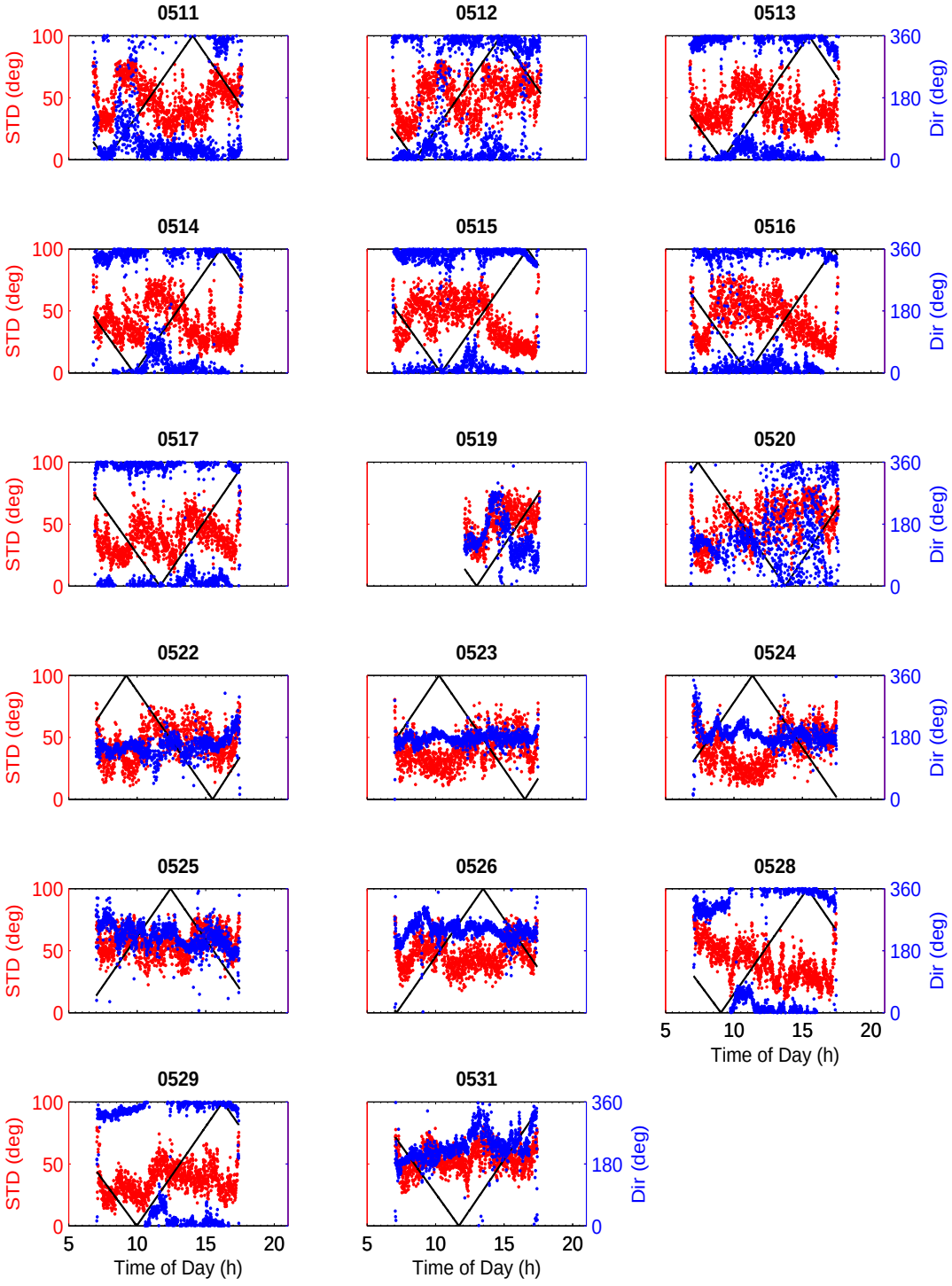

Figure 6.15: Continued.

Influence of tides on swimming speed

A similar pattern related to tides has emerged for swimming speed. During low tide, the speed increased by about 1 bl/s (different to results obtained in Subsection 6.3.1 where speed changes were in the middle of the ebb and rising tides). This increase in speed was not evident on every day partly because there was no low tide during the recording period. However this increase was also noticed prior to commencement of schooling behaviour. Figure 6.16 shows swimming speed for each day in relation to tides (red broken line). Feeding time data points are shown as red, while non-feeding ones are blue. The increase in speed at or around low tide is visible in the following days: 28-30 April, 2, 3, 5, 11-15, 17, 19, 20, 23, 26, 28, 29, 31 May. This behaviour does not appear or is difficult to detect on 23, 24, 26, 27 April, 1, 4, 6, 7, 16, 22 May. The remaining days do not have a low tide within their recording period. Plotting speed versus tide value reveals increase in speed at low tide (tide value of 0) and at high tide (tide value of 1 when flood tide or -1 when ebb tide) (Figure 6.17).

There was an unusual increase in speed in the afternoon on 15 and 16 May beginning from 13:00h at 0.8 bl/s and continuing to increase throughout the remainder of the day to a speed of 2.5 bl/s. Indeed manual examination of the footage for both days shows an observable increase in speed at the end of the day comparing to the time around 13:00h.

Relationship between speed and time of day, and feeding

Plotting of speed versus time of day reveals a visible increase at the beginning and end of the day (Figure 6.18). Plotting of speed versus feeding/non-feeding box plot does not reveal any observable difference (Figure 6.19).

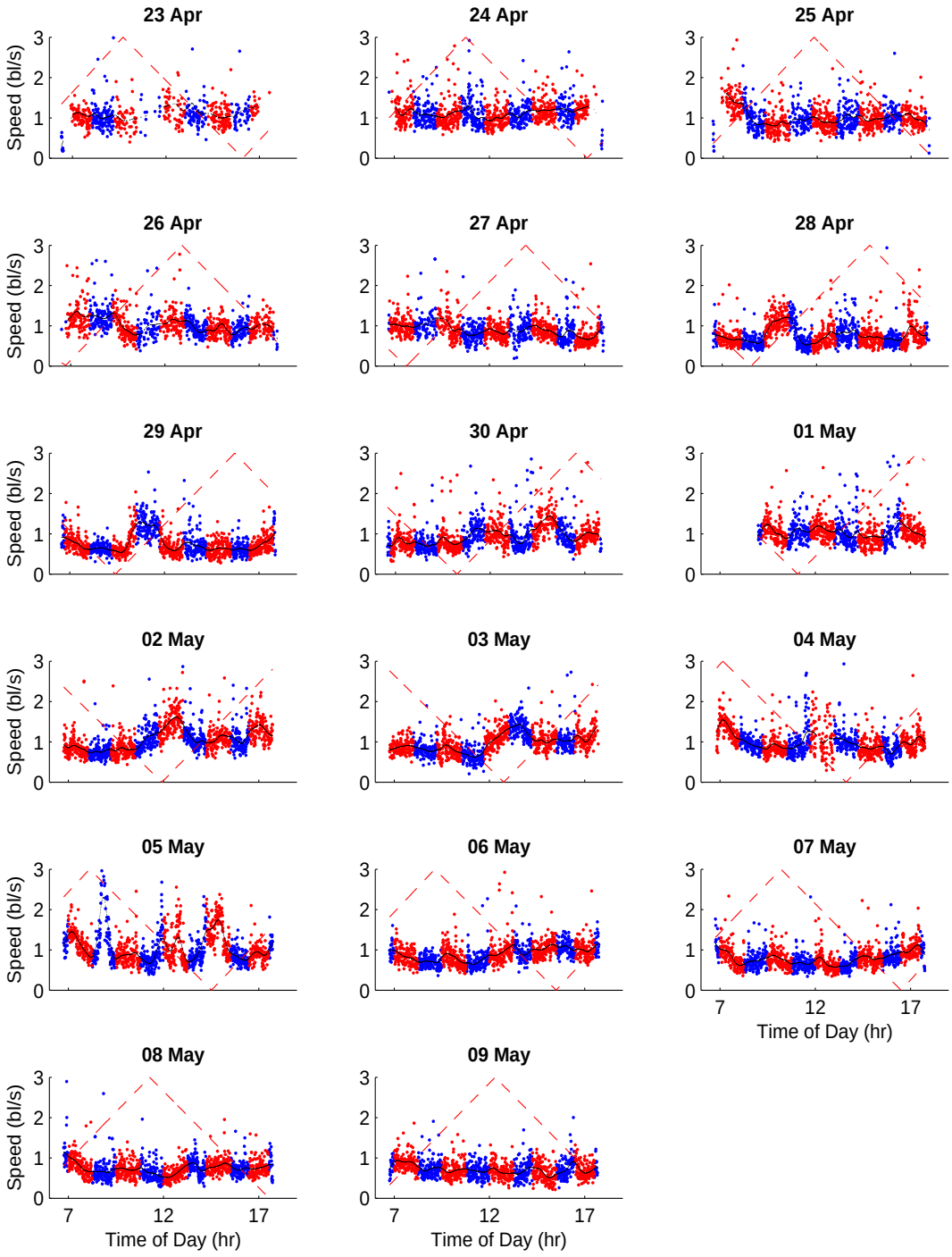

Figure 6.16: Swimming speed in relation to tides (red broken line). Red points represent fish during feeding times. Blue points represent fish during non-feeding times.

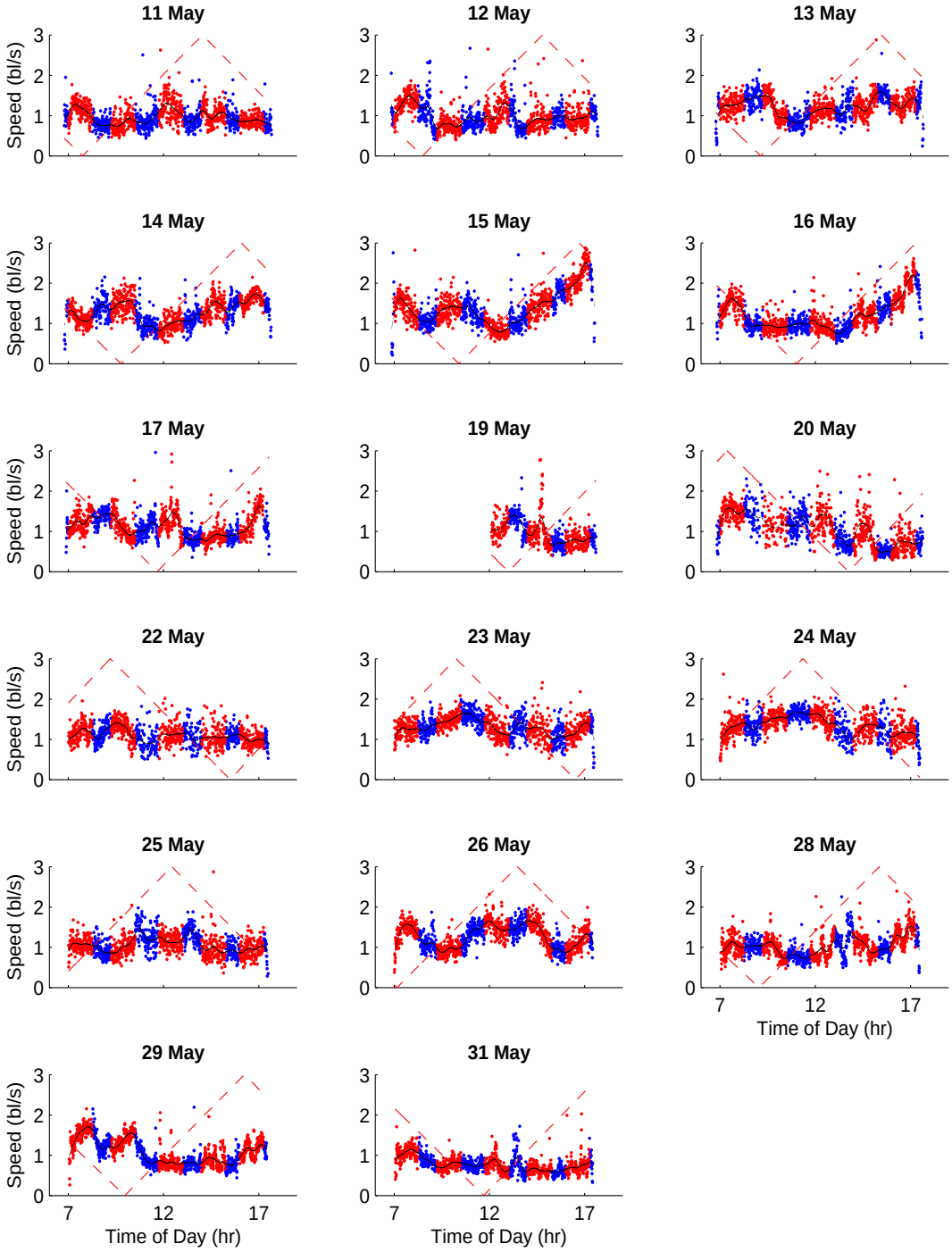

Figure 6.16: Continued.

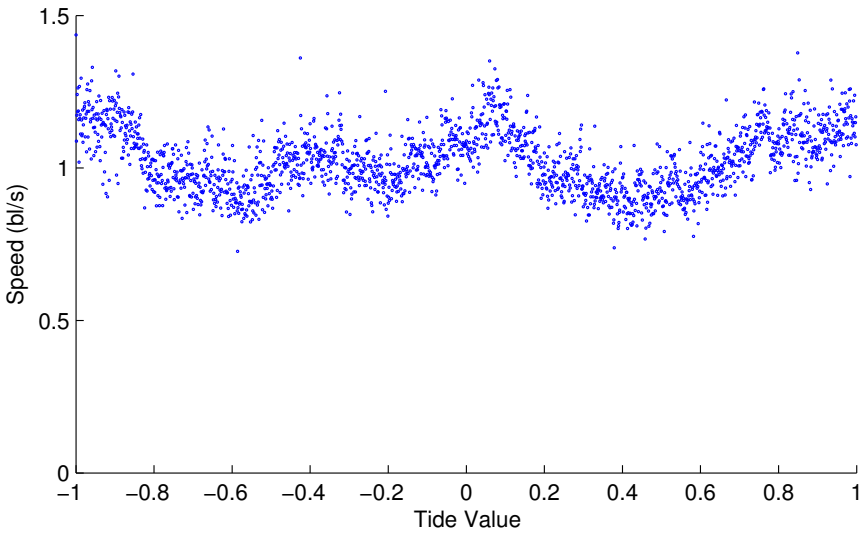

Figure 6.17: Average Speed per Tide Value for 2009 dataset. Tide value represents low tide (0) and high tide (flood = 1, ebb = -1). There is a visible increase in speed at Low tide and high tide, and less prominent increase in the middle of ebb tide.

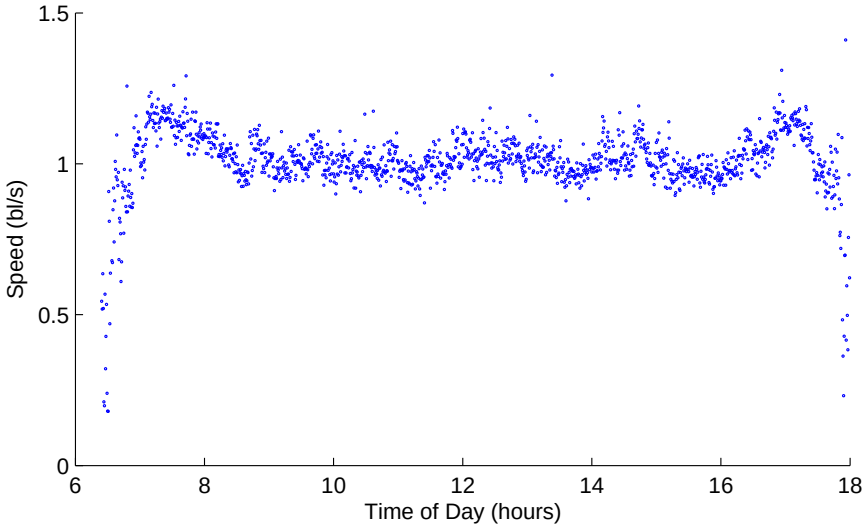

Figure 6.18: Average Speed vs Time of Day for 2009 data set. There is a visible ramp up in speed in the morning and slow down in the evening.

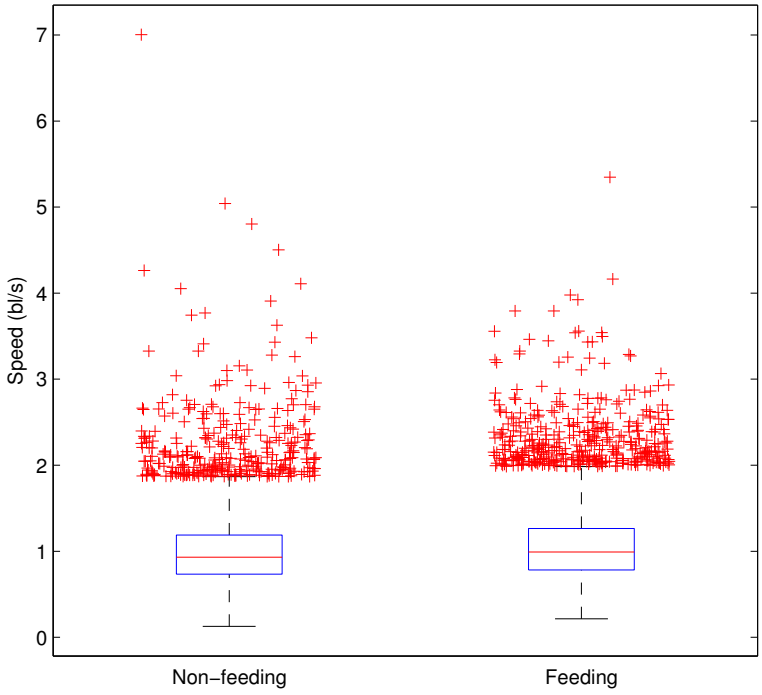

Figure 6.19: Speed vs Feeding/Non-feeding for 2009 dataset.

6.3.4 Experiment 4 - Relation between water current flow, tides and fish movement

Relationship between water current data and tide values

The availability of the water current meter allowed for a direct comparison of tidal times from BOM (similar to ones used in earlier experiments) against the actual tide flow and direction readings. Although these data do not prove actual low/high tide times on the farm versus BOM times, they provide an opportunity to describe the pattern of currents around the subjective Low/High tides over an extended period to profile daily changes in current relative to tide height and lunar cycle and compare measured current to recorded fish behaviour (speed and direction).

There was an observable pattern of change in water current direction and the tide value (Figure 6.20). The current direction generally changed about 1 hour after low or high tide. This "delay" could be caused by the difference between Sidmouth and the location of the farm (Sidmouth is located ca. 6.5km up river) and the adjustment required. However BOM records suggest that there is a 1

hour 18 minutes delay between Low Head (near the mouth of the river) and Launceston around 60km upriver. This might suggest that delay might be due to the size of the farm and local current condition around the farm rather than time difference from the reference point at Sidmouth. Farm managers mentioned that a recent farm expansion created an "island effect", where currents move around or across the farm, creating different current conditions in different cages (especially outer cages). It could also be due to the time required to change direction after "top" and "bottom" of the tide.

The water current flow varies between days (Figure 6.21). Initially (26 Feb - 1 Mar) water current is highly variable throughout the day. From 2 March the current flow just prior to high tide decreases significantly. The current meter actually reported several zero values between 2-7 Mar. It is unlikely that the flow of current would actually be zero for a period of 3-4 hours, but the value must have been below 0.03 m/s, the lower range limit for the device. It is important to note that a new Moon occurred on 4 March and the high tide height at 12:26h was 2.8m while neighbouring low tides were 1.1m (06:36h) and 0.9m (19:03h), a peak-to-peak amplitude of 1.7m and 1.9m respectively. In comparison the height of the high tide 27 Feb at 08:03h was 3.3m with neighbouring low tides being 0.8m (02:13h) and 0.4m (14:39h), a peak-to-peak amplitude of 2.5m and 2.9m respectively. These lower amplitudes on 4th March may have caused low flow values on the 4 March as well as days between 2-7 March. Table 6.5 summarises Moon states as a percentage of full Moon and tide amplitudes for all days in the data set. Figure 6.22 provides another view of the current flow for the entire data set, with flow displayed as an average hourly. Clearly, values in the middle of the bar graph (between 3-7 Mar) are lower than the remaining data.

Another comparison of water flow is carried out with the tide value (Figure 6.23). The tide value refers to values between 0 (low tide) and ± 1 (high tide), where tide times have been taken from meteorological data and values in between have been linearly interpolated. Positive values refer to a flood tide, while negative values refer to an ebb tide. Figure 6.23 shows the differences in water current flow between flood and ebb tide. As expected water current flow is generally higher during the outgoing tide due to the additional influence of the river current.

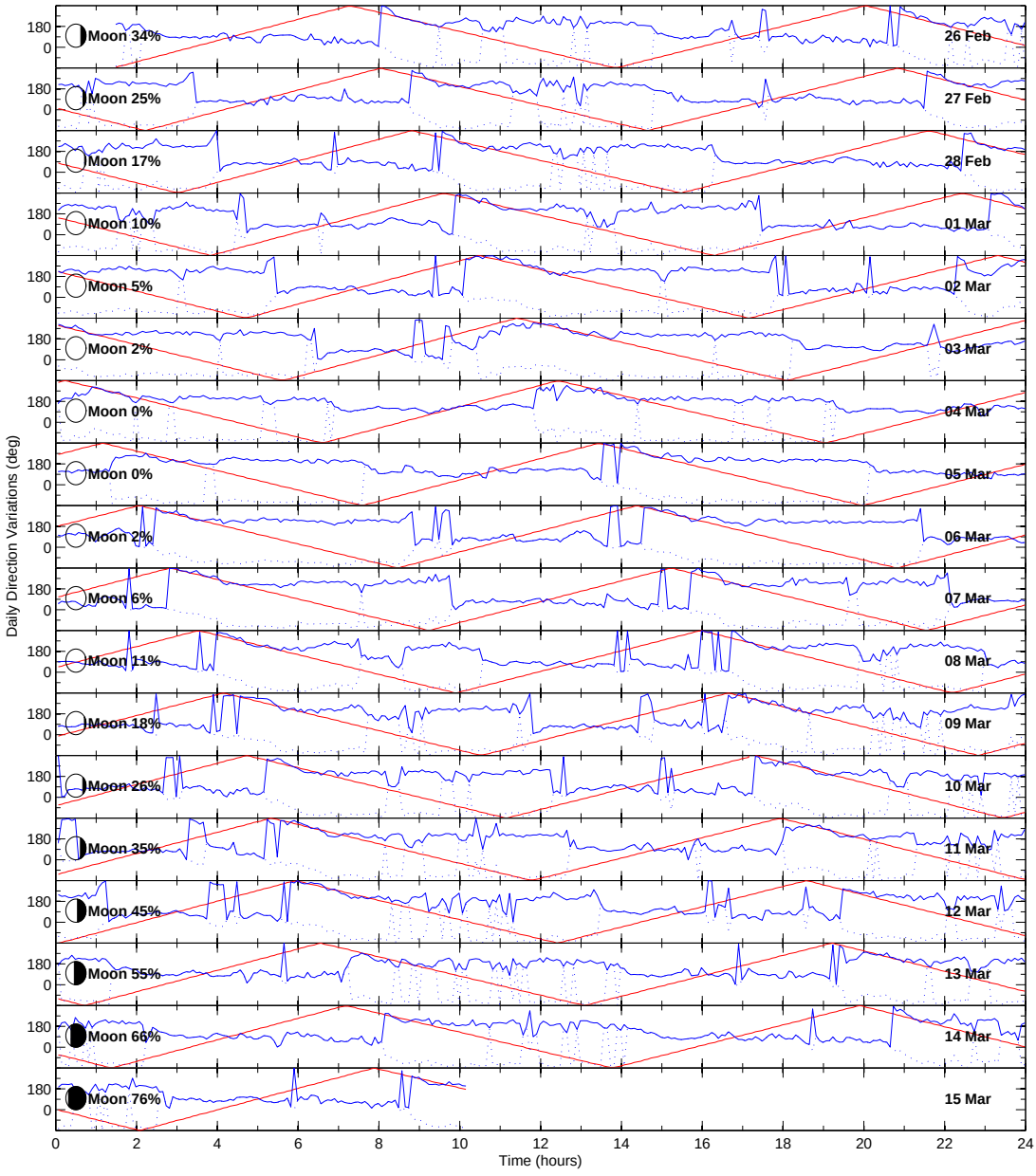

Figure 6.20: Water current direction (blue) as measurement by the meter and tide value (red) as reported for Sidmouth, Tasmania. The current direction is more variable on the incoming tide than outgoing. Upstream direction is at around 135°.

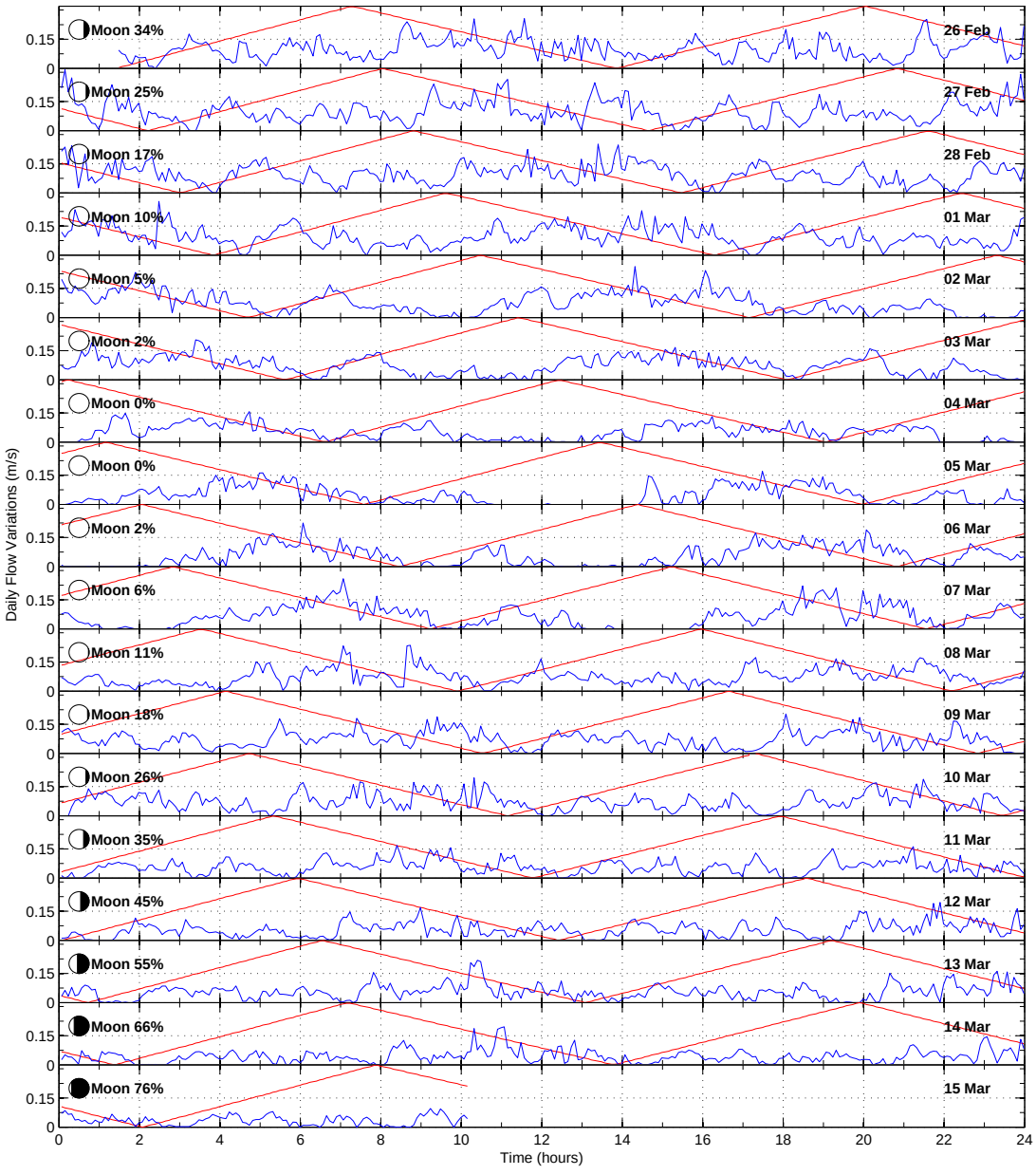

Figure 6.21: Water current flow magnitude (blue) as measurement by the meter and tide value (red) as reported for Sidmouth, Tasmania. The current flow is more variable on outgoing tide and on days around 4 March, the incoming tide shows minimal current flow.

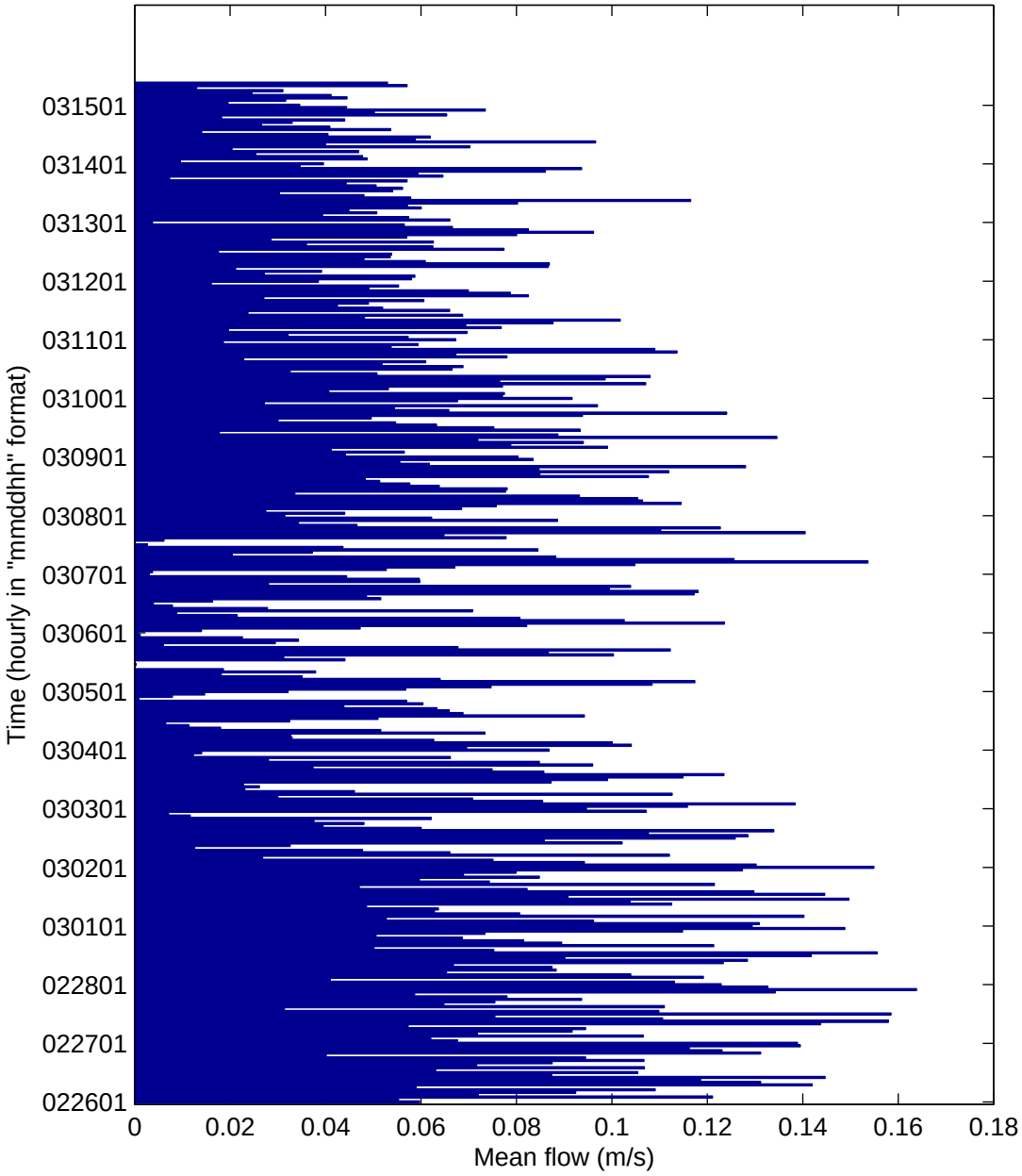

Figure 6.22: Average flow per hour measured by the current meter.

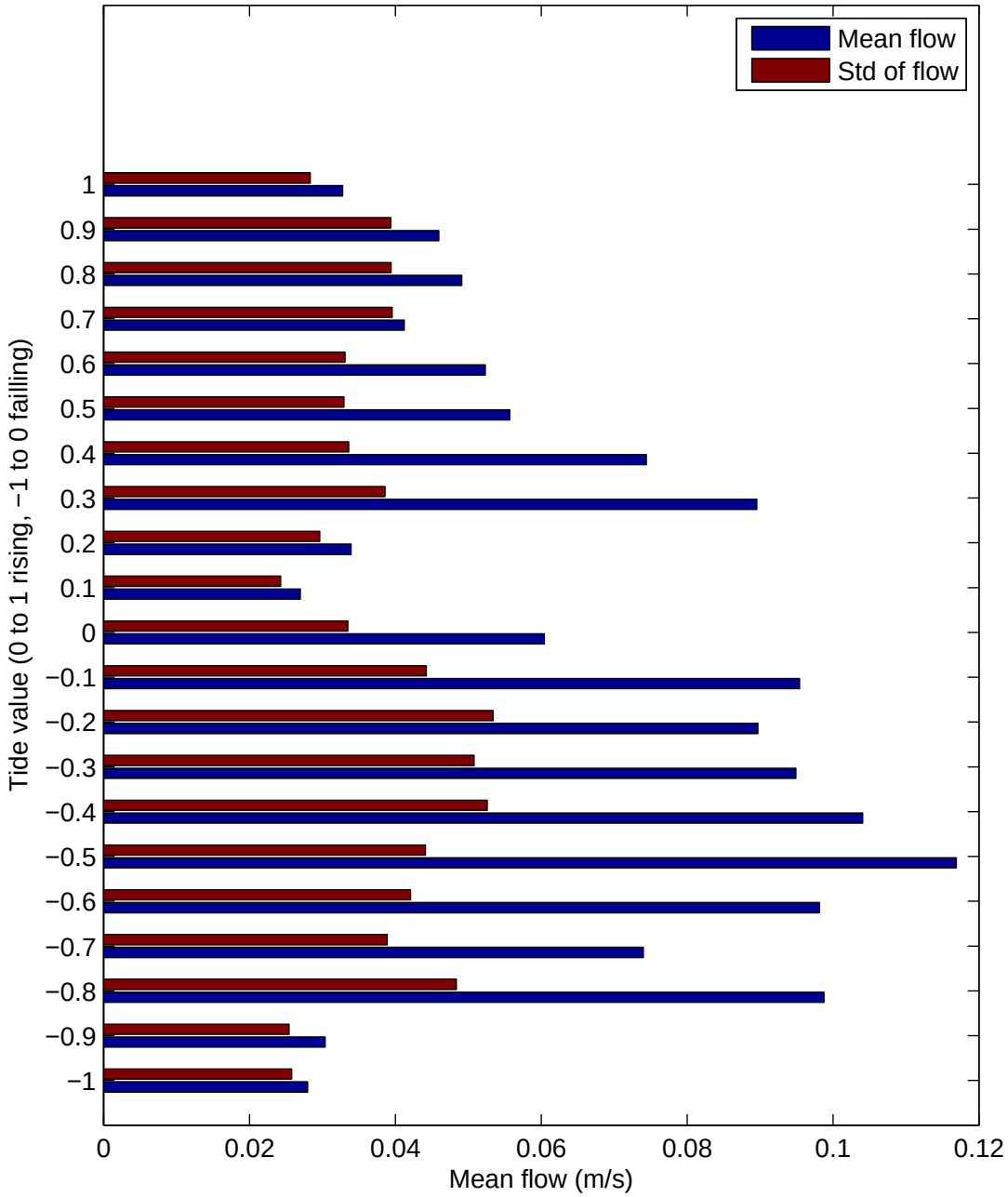

Figure 6.23: Average flow per tide value. Positive tide values (0 to 1) are for flood tide, negative tide values (-1 to 0) are for ebb tide. 0 represents low tide, ± 1 represent high tide. The flow is stronger on the ebb tide.

Table 6.5: Moon phase percentage and tide amplitude during Experiment 4.

		Tide Amplitude (m)			
Date	Moon (%)	Low/High	High/Low	Low/High	High/Low
26-Feb-11	34	2.7	3.2	3	2.4
27-Feb-11	25	2.5	2.9	2.7	2.2
28-Feb-11	17	2.3	2.7	2.5	2
1-Mar-11	10	2.1	2.5	2.3	1.8
2-Mar-11	5	1.9	2.3	2.2	1.8
3-Mar-11	2	1.8	2.1	2	
4-Mar-11	0	1.7	1.9	1.9	1.7
5-Mar-11	0	1.7	1.9	1.9	1.7
6-Mar-11	2	1.8	1.9	2	1.8
7-Mar-11	6	2	2	2.1	2
8-Mar-11	11	2.1	2	2.1	2.2
9-Mar-11	18	2.3	2.1	2.2	2.3
10-Mar-11	26	2.4	2.2	2.2	2.4
11-Mar-11	35	2.5	2.2		2.5
12-Mar-11	45	2.5	2.1	2.2	2.5
13-Mar-11	55	2.5	2.1	2.2	2.6
14-Mar-11	66	2.6	2.1	2.2	2.7
15-Mar-11	76	2.6	2.1	2.2	2.7

Relationship between water current data and swimming speed, and direction

As the direction of current changed after the high tide, the fish swimming speed also changed (Figure 6.24). This change could be characterised as a short increase in speed followed but a sudden decrease in speed by around 0.5 bl/s. This change became less prominent on 5 March and non existent on 7 March.

The relationship of swimming speed to the water current flow is different to relationship of swimming speed to the water current direction (Figure 6.25). Within each day, it appears that generally when water current flow is high, the swimming speed is lower and when the water current flow is low, the swimming speed is high. This is especially apparent in the first four days of the data set (26, 27, 28 Feb and 1 Mar), less evident during days 2-6 Mar and non-existent during 7 Mar.

When the current changes direction at low or high tide, the swimming direction of fish also changes (Figure 6.26). It is important to note that the swimming direction of fish is relative to the orientation of the camera and no attempt has been made to ensure that this orientation remains constant. As it was difficult

to maintain a constant camera orientation, it was not possible to examine the relationship between the fish swimming direction and current direction. The water current direction is the actual direction as provided by the current flow meter.

There is no relationship between the swimming direction and the water current flow (Figure 6.27). However it appears that lower flow values on days 4-7 March result in more gradual changes in direction.

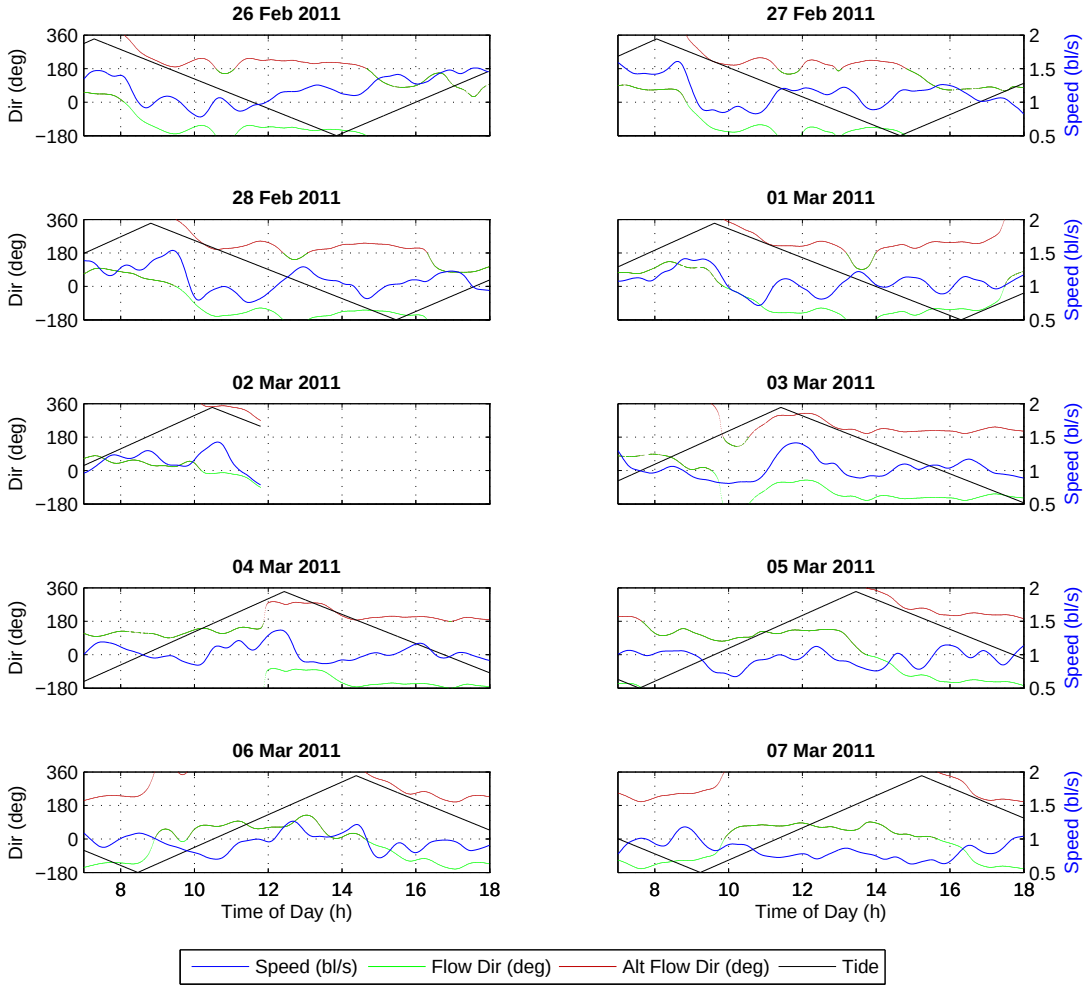

Figure 6.24: Swimming speed and current direction. All data presented have been smoothed using moving average.

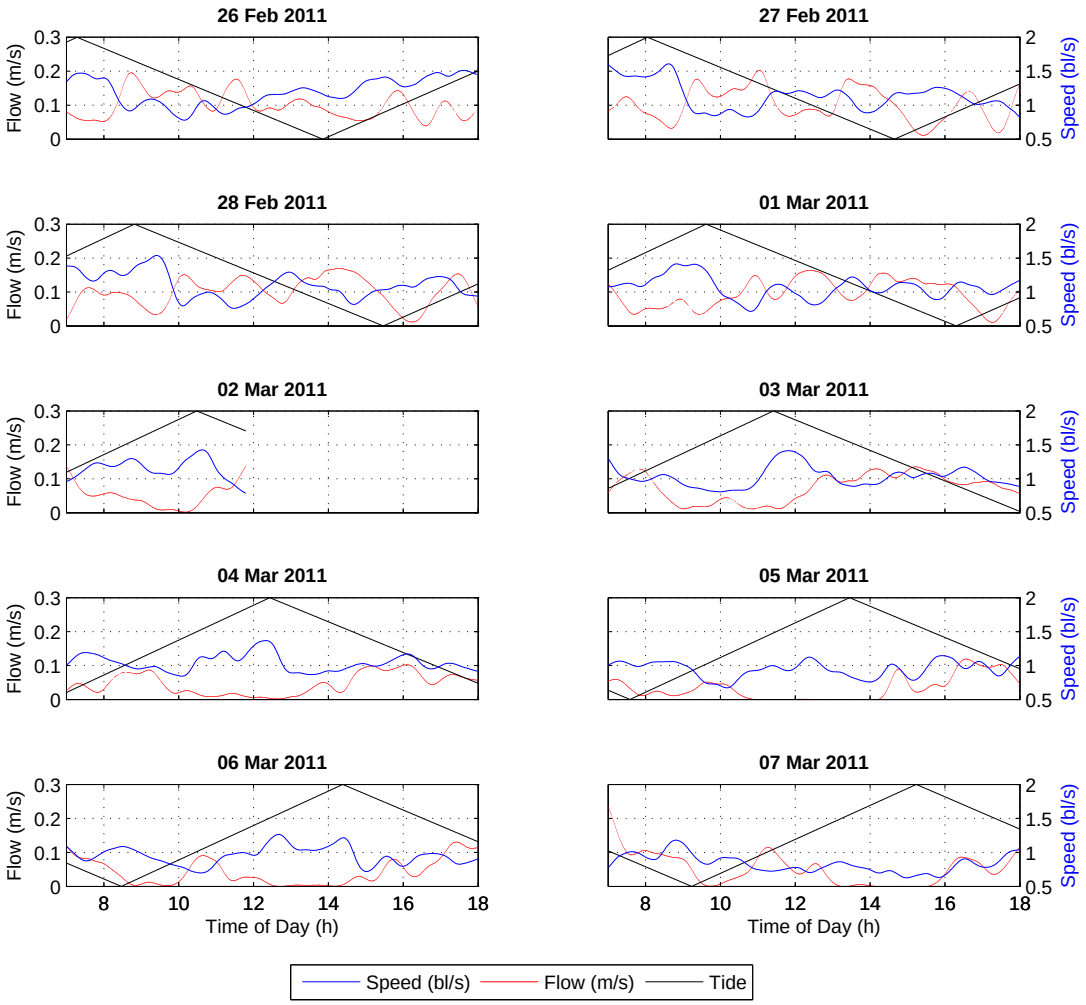

Figure 6.25: Swimming speed and current flow. All data presented have been smoothed using moving average.

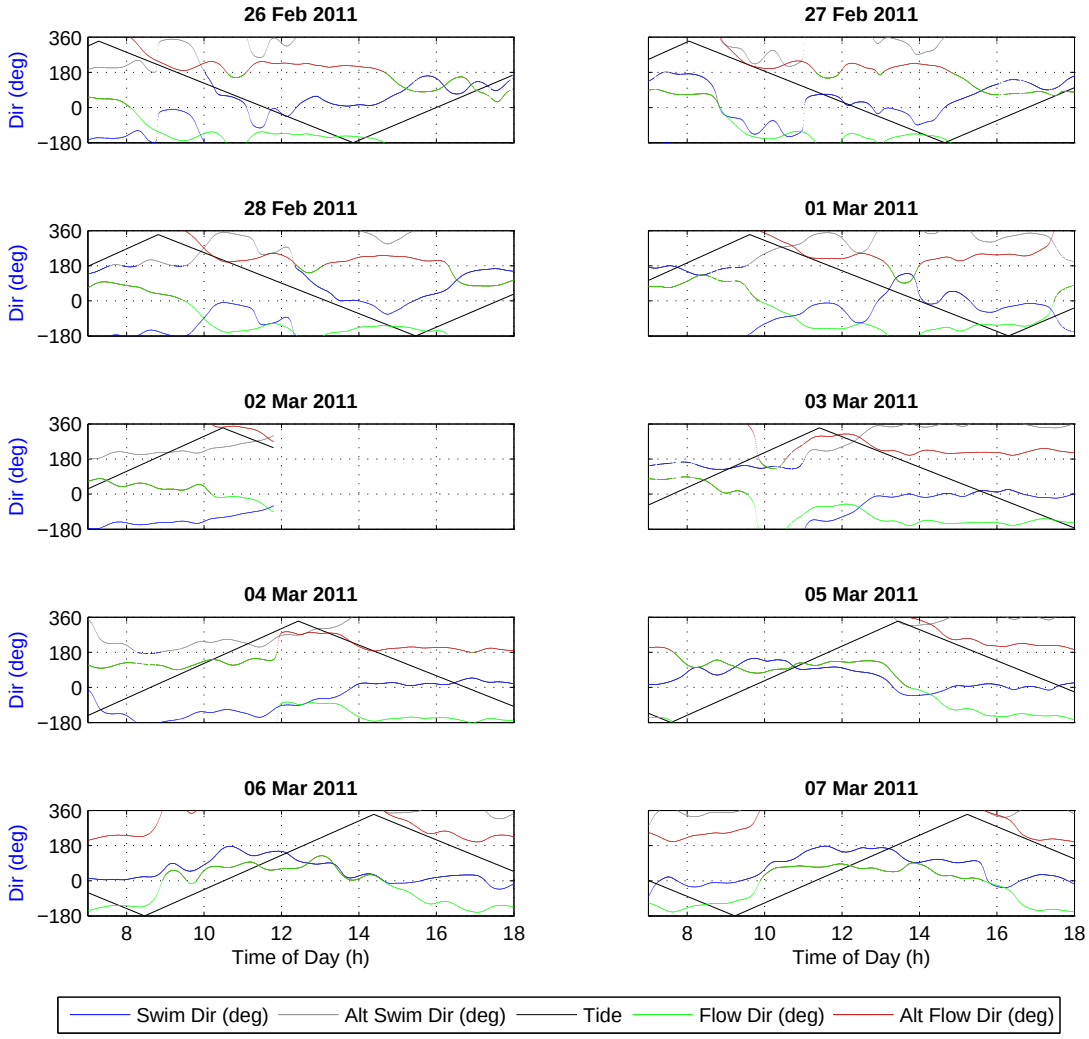

Figure 6.26: Swimming direction and current direction. All data presented have been smoothed using moving average.

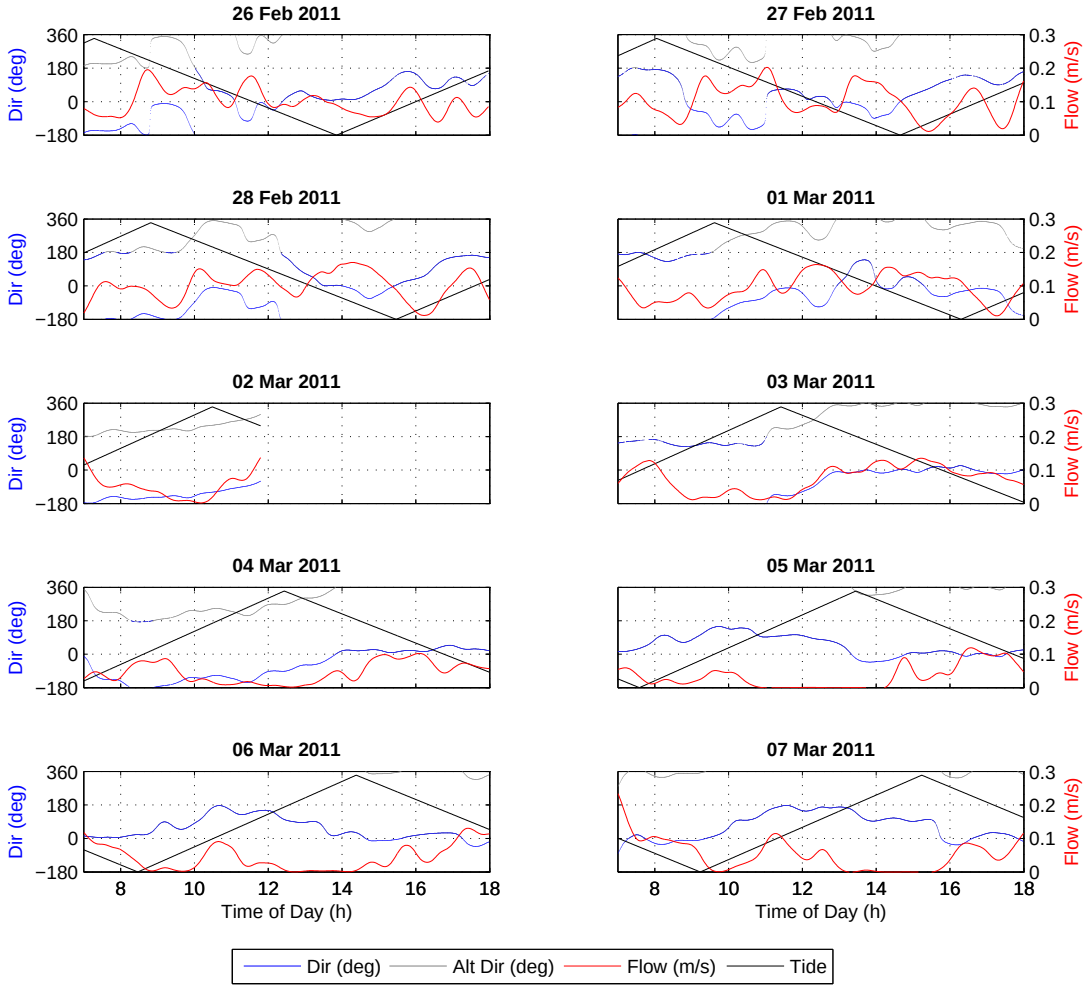

Figure 6.27: Swimming direction and current flow. All data presented have been smoothed using moving average.

6.4 Discussion

A general observation from all experiments is that variability in swimming speed and direction, detected by the system, may be a result of several influences: time of the day, tides, feeding/non-feeding times, temperature, dissolved oxygen, turbidity. Not all of these influences were observed or recorded but perhaps the most obvious one was the influence of tides and associated river currents. Similar observations were made by farm operators that fish were influenced by currents at different stages of the tidal cycle and some management practices like feeding times had to accommodate changes in fish behaviour.

One factor which may influence the results of these experiments is the depth of the camera. A camera close to the surface (<4m) is likely to capture feeding behaviours, therefore the system might detect increases in speed during feeding times. A camera located deeper (4-8m) is likely to capture a wider range of fish movement. This may involve feeding at lower depths but may not capture accurately near-surface activity (the increase in speed may therefore be undetected). One obvious modification to the system would be to use multiple cameras at various depths (4m and 6m for example). This would provide a better picture of what is happening with the whole population in the cage.

All experiments experienced difficulties where no data could be gathered. This was due to technical problems with hardware, a need to rotate recordings because of limited hard drive space, power outages and equipment maintenance (e.g. camera cleaning by farm personnel). However the purpose of these experiments was to demonstrate that the system is capable of detecting changes in swimming speed and direction and that some meaning can be attributed to the changes. Technical challenges experienced during these experiments will be addressed in further research and are a component of conducting research on commercial farms.

6.4.1 Experiment 1 - Influence of tides on fish movement

Experiment 1 was the initial preliminary experiment and it showed that there is variation in speed and direction of fish movement within days and between days (Kadri et al., 1991; Dempster et al., 2008). Data have shown several interesting areas where direction or speed changes with a regularity corresponding closely with a tidal cycle which shifts every day by around 50 minutes. It appears that the fish in cage #12 adjusted their behaviour according to tidal changes in the Tamar River (farm operators reported that effects of tides vary from cage to cage). Change in swimming direction at low tide suggests that the change in

direction of the current, "encourages" fish to alter their direction of swimming but their schooling behaviour continues. The change starts at low tide gradually, and is completed about 1 hour after low tide.

Changes in speed are less prominent and as they occur in the middle of the ebb and rising tides are even more difficult to explain with only tide times available and not the actual current strength and direction. While the tide lines in Figures 6.3 and 6.4 represent a linear interpolation between high tide and low tide, and vice versa, the actual changes in current would be expected to be non-linear as show in Experiment 4. It is possible that there is a significant interaction between the tidal currents and the river current in the middle of each tide in this particular cage. Because these events occurred with the regularity of a tidal cycle it is likely that they occurred independently of the feeding times, when the swimming speed is expected to be higher. It is possible that some of the variation could be attributed to feeding when the tidal event overlapped the feeding time.

This experiment suggested an influence of tidal currents on the swimming speed and direction of fish while a study by Kadri et al. (1991) found that the time of day had greater influence than the tidal cycle despite strong currents reported near cages. While the actual current measurements were not available, high and low tide times were available and data in between were interpolated to provide some form of a measure. It is evident that longer experiments (of several lunar cycles) would be required to determine influences of tides and availability of actual current measurements may help explain changes observed.

6.4.2 Experiment 2 - Daily swimming profile in the summer during outbreak of AGD

The presence of AGD and freshwater bathing during Experiment 2 presented a unique opportunity to observe swimming speeds before and after bathing. Results suggest that fish behaviour on the 21 January was usual evidenced by higher speed and variability of speed also encountered earlier in Experiment 1 but environmental conditions were already deteriorating. By contrast fish behaviour on the 1 February may be indicative of poor health of fish. It is quite possible that fish were more active in the morning after more favourable night conditions but by afternoon they were more affected by the environmental conditions through the day. However no evidence exists to support such hypothesis. It was also observed that swimming speed on days 12 to 15 Feb was lower and had less variation throughout the day. This may be attributed to lower visibility during these days in addition to low dissolved oxygen levels and high temperatures.

An interesting aspect of this data set is how little variation there was on

days 13-15 Feb, especially when comparing these days to an example three days prior to bathing (30, 31 Jan and 1 Feb). The data obtained from the Bureau of Meteorology show that the average peak-to-peak amplitude between high and low tide was lower by 0.45m on the former days. This suggests that the difference in amplitude of the tide is the driving factor behind the difference in fish behaviour rather than other environmental variables like dissolved oxygen or temperature. A similar situation has been observed in Experiment 4, where during low current flows, the variability in swimming speed was low and and the speed was also lower.

Due to technical problems there were some gaps in the recording of data. This happened because at times, the underwater camera was not positioned correctly and was facing sideways rather than upwards. For this reason, estimates generated by the tracking system were incorrect and had to be excluded from the data set. Also, there were some technical issues with the actual recording process and several days were not recorded. Because of the gaps in data it is difficult to make definitive conclusions regarding the results of this data set.

6.4.3 Experiment 3 - Smolt behaviour after transfer from hatchery to sea cage

Experiment 3 confirmed what was already known by operators at Van Diemen Aquaculture (VDA) that salmon smolts in this cage took 3-4 weeks post transfer to settle into schooling behaviour. However farm operators believed that this change was gradual as opposed to sudden. The reason for this opinion might be that operators observe fish during feeding times and sometimes they observe schooling behaviour. This was confirmed by the tracking system and Figure 6.8 shows brief moments of schooling on 1, 3, 4 and 5 May especially in the morning (during the morning feeding event). Once feeding was finished and fish were no longer being observed by operators, the tracking system continued to monitor fish and data shows that schooling behaviour ceased (until it was properly established on 11 May). This difference of opinion does not in any way discredit the automated tracking system proposed. It demonstrates that a continuous analysis can provide much more data than operator observations and changes between non-schooling and schooling behaviour are clearly detected when analysing swimming direction of fish.

There was also a difference in swimming speed between non-schooling and schooling periods of 0.2bl/s. While this difference may seem to be quite small, swimming speeds in this experiment varied between 0.3bl/s and 2.5bl/s (median of 0.9bl/s) and in literature it has been reported that daily speeds vary between

0.2bl/s and 1.9bl/s (Oppedal et al., 2011). Therefore the increase in speed by around 0.2bl/s is about 9% of the range observed in this experiment and 12% of the range reported by Oppedal et al. (2011).

Fish also responded to tidal changes during Experiment 3. The influence of tides has been well known at the VDA site as operators often change feeding schedules to avoid feeding at high or low tide. Changes in direction and speed detected by the system may explain why fish do not feed well during low tide. Changes in the swimming direction were similar to those observed in Experiment 1 (Subsection 6.3.1). Given that cages and fish sizes were different between the two experiments, this suggest some commonality in the influence of current on fish regardless of position on the farm or the fish size. However the pattern related to changes in speed was different between the two experiments suggesting that cages might be exposed to slightly different conditions depending on their location within the farm. These results seem to concur with what has been observed on the farm by operators in that while all cages are affected by tidal current, there are variations due to the distance from the middle of the river and position on the farm.

An interesting observation was that around the transition from non-schooling to schooling behaviour there was a full Moon in both 2009 and 2010 datasets. This may raise a hypothesis that full Moon, directly or most likely indirectly, may trigger a behaviour change in Atlantic salmon smolts which causes the commencement of the schooling behaviour. Previous studies have found an influence of Moon phase on Pacific salmon smolts (DeVries et al., 2004), masu and amago salmon smolts (Yamauchi et al., 1984), and Atlantic salmon smolts (Hvidsten et al., 1995), and these influences have been linked to thyroxine levels (Yamauchi et al., 1984). Further research could reveal if the change observed during this experiment is triggered by the light during full Moon, association with a tidal cycle or a physiological change. Furthermore there may be an optimal time at which smolts can be transferred from the freshwater hatchery to a sea cage, so that the period of non-schooling behaviour is minimised, which is desirable from the fish management point of view. While there are insufficient data to confirm such a hypothesis, it was interesting to note that smolts recorded in 2009 were transferred to a sea cage around the new Moon (25 Apr 2009) and took around 18 days to commence the schooling behaviour, while smolts recorded in 2010 were transferred around the full Moon (28 Apr 2010) and took between 28 and 35 days to commence the schooling behaviour - almost twice as long.

There were no observable patterns suggesting that speed during feeding times was higher than during non-feeding times (Figure 6.19) or that speed during morning and evening phases is higher than during the midday phase (Figure 6.18),

although some points on the graph did suggest it was higher at the end of the day. This was in contrast to Kadri et al. (1991) who observed that fish swim faster in the morning and evening during a continuous feeding regime. Kadri et al. (1991) also determined the influence of tides to be not statistically significant, i.e. they found that time of day was the key factor affecting swimming speed. It is possible that the unusual location of the VDA farm on a river with strong tidal currents means that tides have a greater influence on fish than time of day. It was expected that fish would increase their speed during feeding but no clear visual pattern appeared to confirm this. Feeding patterns are also dependent on seasons. Blyth et al. (1999) analysed feeding responses during four seasons and observed that there were no clear feeding peaks during autumn (the season of this recording). Smith et al. (1993) also observed differences between seasons but did not see the patterns reported by Kadri et al. (1991). It is also likely that the feeding regime of five meals per day used at VDA negated some of the effects reported in literature. A high number of feeding events in a day may have decreased the need for fish to increase swimming speed in search of or response to food. Similar findings were reported by Andrew et al. (2002) when comparing a normal feeding regime with a demand feeding regime. Fish fed on demand were reported to have lower speeds during feeding than the control group using a normal feeding regime. While it is still possible that there was an increase in speed during feeding, it is likely to be more subtle and the effects of tides and time of day meant that it was difficult to detect feeding patterns in this experiment. Another factor could be the size of the fish, with the feeding patterns of smolts being different to larger fish (Noble et al., 2007).

There was an increase in speed on 15 and 16 May from 0.8bl/s at 13:00h to 2.5bl/s by the end of the day (17:00h). If this type of behaviour was observed in many more days, the swimming profile would be similar to the one observed by Kadri et al. (1991). However that was not found to be the case, with the increase in speed on those days likely to be caused by weather conditions, as reported in the operator log. Fish were feeding poorly earlier in the day, therefore they may have increased their activity to compensate for this and increased food intake in anticipation of night-time.

6.4.4 Experiment 4 - Relation between water current flow, tides and fish movement

Experiment 4 demonstrated that the use of tide times and then the association between time and current pattern in earlier experiments, without knowing the actual strength and direction of the current, was valid, in that a clear correspon-

dence exists between these two at the Van Diemen Aquaculture site, though there is a time offset. However it would be advantageous to measure the water current strength and direction in further studies as this could explain variations in the swimming speed. Combined with other variables and events on the farm it may be possible to explain the usual swimming speeds and behaviour which occur in a particular sea cage. This could create a 'baseline' behavioural profile and be used to detect unusual behaviours.

The lunar cycle has a significant influence on tidal amplitudes and associated current flows. The strength of the water current during days around the new Moon (4 March) were much lower than 26 Feb - 1 Mar. Low flows caused less variation in swimming speed and more gradual changes in direction during high or low tide. This may imply that during days with low current flows, for example 7 Mar, the main factor affecting the swimming speed of fish is their own energy output. During days with higher water flows, for example 27 Feb, the fish seemed to increase speed (relative to the fixed camera) when the flow is lower and decrease speed when the flow is higher. This might imply that energy expenditure is actually the same throughout these changes, i.e. fish do not try to increase their energy output when the water flow is high to maintain the same speed. The swimming direction changed during high or low tide but low current flow made this change much smoother and less prominent, while during higher current flows this change was much more abrupt and noticeable. These changes in swimming speed and direction in relation to the water current flow might suggest that fish try to maintain their schooling behaviour regardless of the water flow conditions.

6.5 Summary

This chapter described experiments which were undertaken to confirm the tracking system's ability to track fish accurately and to detect changes in fish behaviour. These experiments demonstrated that the swimming direction or, more importantly, standard deviation of the swimming direction for each sample period, provides a good indication of how uniform the movement of fish is in a sea cage. Given there is a correlation between the speed and the standard deviation of direction, a combination of these two variables could be used to detect unusual behaviours in sea cages. This knowledge could potentially be used to detect predator attacks, where the schooling behaviour may be disrupted, with fish individually reacting to the predator, or that fish will flee as a school which would result in a sudden change of direction but steady standard deviation. In addition swimming speed is likely to increase suddenly. If these and other behaviours can be observed it would be possible to define behavioural signatures to

form the basis of an alarm system. Determining signatures of usual behaviours would also be beneficial, as any deviation from these patterns could be used to alert farm operators.

Feeding patterns were difficult to observe from this analysis. One aspect that becomes apparent from the literature review and the inconclusive results of experiments in this chapter is that fish behaviour during feeding is dependent on many factors. The site, seasons, environmental conditions, day length, time of day, and tides all play a role. The system proposed in this thesis may be a valuable tool in determining how these factors interact and affect fish behaviour.

The next two chapters examine tracking systems developed for use in tanks. The focus shifts from observing large groups of fish to observing individuals (Chapter 7) and small groups (Chapter 8).

CHAPTER 7

TRACKING INDIVIDUAL FISH IN TANKS

7.1 Introduction

Aquaculture researchers are often interested in tracking individual fish in small tanks to investigate their interactions, aggressive behaviours (Hedenskog et al., 2002), spatial distribution (Bégout Anras and Lagardère, 2004) and feeding behaviours (Brännäs and Alanärä, 1993; Alanärä et al., 2001; Covès et al., 2006). The analysis of video is usually manual and hence limited in duration. The use of colour tags aids in visual identification of individuals. Fish can also be tracked using acoustics (Conti et al., 2006), including use of acoustic tags (Bégout Anras and Lagardère, 2004). However the use of tags may affect the physical attributes of fish and requires handling, which can stress fish and affect the behaviour (Baras and Lagardère, 1995). It is desirable to have a way of tracking fish, without using tags, and with minimal human effort and no handling of fish.

The previous two chapters pertained to tracking fish in commercial sea cages when large numbers of fish are involved and hence tracking any single fish can only happen for short periods of time. This chapter describes a technique (based on video technology) to track two fish in a tank, without tagging. The aim of this chapter is to track multiple fish in a tank for long periods of time with the ability to uniquely identify fish at all times. Such an approach can provide researchers with a method of identification of interactions between unique fish, their movement patterns and their habits within the tank. The chapter describes the tracking system researched to track two fish in a tank. Section 7.2 outlines computational aspects of the system, from detecting fish using motion segmentation, to tracking multiple fish through occlusions and various manoeuvres without loosing their identifications. The results in Section 7.3 demonstrate the tracking outcomes from two video sequences of two fish swimming in a tank, which contain a number of interactions between two fish. The discussion (Sec-

tion 7.4) focuses on the viability of this technique to track fish in the context of aquaculture research and identify challenges faced during the implementation of this approach.

7.2 Materials and Methods

The tracking technique is based on a modified Particle Filter with additional data association carried out to attempt to identify fish uniquely. It combines several existing computer vision methods to create a unique multi-target tracking system. This section will describe the methods used in the detection, tracking and identification of multiple fish in a tank with the purpose of long term tracking and unique identification.

7.2.1 Background Estimation and Motion Segmentation

Segmentation plays an important role in computer vision systems as it allows foreground objects (in this case fish) to be detected and distinguished from background areas (in this case the tank) in the presence of noise (Chapter 3). The motion segmentation in this tracking system is used to find regions where fish might be located, rather than being used to detect fish for the purpose of tracking. New particles used with the Particle Filter can then be randomly seeded in these candidate regions rather than randomly throughout the whole image frame. While the estimated background is used in motion segmentation, it is also utilised by the particle filter in the calculation of importance weights.

The system described in this chapter performs segmentation using a three-frame differencing method (Collins et al., 2000) combined with adaptive background subtraction (Chien et al., 2004). Details of these methods have been presented in Chapter 3 and the following section will focus on applying the methods in the specific context of the experiment.

As described in Subsection 3.3.3, a Stationary Index (SI) matrix describes which pixels are stationary and which are in motion (Eq. 3.8 from Chapter 3). The index for each pixel increments each time the corresponding index within FDM is deemed as stationary. The Stationary Index is then used to determine the background (Eq. 3.9 from Chapter 3) using the threshold $Fth = 10$ frames. This value was selected experimentally to provide fast background updates and to provide good stability once the background is established, while avoiding the appearance of background artefacts caused by motion of the fish. Both background and the current image frame are treated as RGB images (three dimensions) and

the Stationary Index is required for each colour dimension. This is achieved by applying an SI matrix to each dimension of the background image. Estimating the background as a colour image allows for it to be used in the calculation of the likelihood for the Colour Particle Filter.

The next step in the segmentation process is to generate an Initial Object Mask (IOM) using Eq. 3.13 from Chapter 3. The Initial Object Mask is further refined by removing any objects which are outside the research tank and by removing small objects using morphological operations. The final step in the procedure is to modify the Stationary Index based on the IOM using Eq. 3.14 from Chapter 3. The object mask used in this adjustment of SI is dilated to enlarge the detected objects preventing the inclusion of outlines of fish shapes into the background. The Initial Object Mask can now be used to improve the seeding of particles.

7.2.2 Colour Particle Filter

The tracking system is based on a particle filter using colour target templates to calculate the importance weights (Czyz et al., 2007) discussed in Section 4.2.4. The system uses the state vector $x = [r, c, h, w, rv, cv]$, where r and c are target centroid co-ordinates, h and w describe the size of the bounding box around the target, and rv and cv represent components of the velocity vector. The following pseudo-code describes a single time step of the particle filter specific to the problem in this chapter. The remainder of this section will focus on details of individual steps.

The algorithm assumes that the number of targets is known and uses the existence variable, E, to determine how many targets are being represented within each particle. At the beginning of each iteration (Table 7.1) the existence variable determines if a particular particle will increase or decrease the number of targets it represents, or if the number of targets will remain unchanged.

In Step 1, the Transition Probability Matrix (TPM), Π is used to evolve the existence variable from one time step to the next using Equation 4.29, where the probability of target "birth", $P_b = 0.95$, the probability of target "death", $P_d = 0.05$, the probability that the number of targets will increase, $P_m = 0.15$ and the probability that the number of targets will decrease, $P_r = 0.30$. Empirical selection of these parameters gives the system an ability to quickly detect new targets and should a loss of track occur, they can be removed from the tracking system quickly. The transition of existence variable, E, is determined by the regime transition algorithm of Ristic et al. (2004) shown in Table A.5 in

Table 7.1: Colour Particle Filter Pseudo-Code.

1. Transitions of E_{k-1} variable
   (a) $\left[\left\{E_k^n\right\}_{n=1}^N\right] = \textbf{ETrans}\left[\left\{E_{k-1}^n\right\}_{n=1}^N, \Pi\right]$
2. Extract objects, L from Initial Object Mask
3. Get current frame, I_k and background, BG_k and convert from RGB to HSV colour space
4. FOR each partition $t = 1..T_{max}$
   (a) $d(t) = min_{j \neq t} \|\hat{x}_t - \hat{x}_j\|$
   (b) IF $d(t) > \tau$ OR number of current targets, $T_{curr} \leq 1$
      i. Propose partition t using **Independent Partition** method
      ii. Set method used for the partition $m(t) = 0$
   (c) ELSE
      i. Propose partition t using **Coupled Partition** method
      ii. Set method used for the partition $m(t) = 1$
5. Extract colour histograms for current frame and background for all particles
6. IF all partitions are independent
   (a) FOR $n = 1...N$
      i. Calculate **Importance Weights** but add a penalty if the Euclidean distance between state vectors within a particle is small
      ii. $counter = 0$

   ELSE
   (a) IF $counter < 3$
      i. FOR $n = 1...N$
      Calculate **Importance Weights**
   (b) ELSE
      i. FOR $n = 1...N$
      Calculate **Importance Weights** but add a penalty if the Euclidean distance between state vectors within a particle is small
   (c) increment *counter*
7. Normalise weights with biases included
8. Resample
9. Sort Partitions
10. Get number of targets t_{curr} and estimate positions $\hat{x}_1 ... \hat{x}_{t_{curr}}$
11. Perform data association

Appendix A, where s is the size of Π matrix ($s \times s$) and u is randomly chosen to be 0 or 1. Note the C/C++ use of 0 bound indexing in the algorithm, while MATLAB indices start with 1.

Steps 2 and 3 use the results of the motion segmentation described in Section 7.2.1. The Initial Object Mask is used to obtain the centroid co-ordinates and bounding box dimensions of segmented objects and these parameters are used to seed 50% of new particles. This changes the distribution of particle seeding scheme to be non-uniform due to these specific regions and therefore improves the rate at which targets are detected or re-detected (after a loss of track). The current image frame and the background image are converted from RGB to HSV colour space to allow histogram comparisons (Pérez et al., 2002) when calculating importance weights.

In Step 4 each partition is examined and the minimum distance between target estimates is used to determine whether the Independent Partition scheme or the Coupled Partition scheme should be used. The threshold (τ) is set at average fish size in pixels multiplied by 0.75. If the minimum distance is greater than this value or there is only one target or no target has been detected, then the Independent Partition scheme is used, otherwise the Coupled Partition scheme is used. A flag $m(t)$ for each partition is set to indicate which scheme is used. Also biases are created for both partition schemes (see Appendix A for the pseudo code of partition methods) which will be used in normalising weights in Step 8.

Step 5 extracts all colour histograms for all particles and all state vectors within these particles. Histograms are of the current image frame and of the current background image (retrieved in Step 2) which are both in HSV colour format. This allows the use of the measurement model due to Pérez et al. (2002), described in Subsection 4.2.4.

Step 6 uses the likelihood function to generate importance weights (further details will be given in Subsection 7.2.2). In Step 7 weights are normalised with the addition of biases generated in Step 4 and this is followed by the resampling step (Step 8). The resampling step is carried out using systematic resampling code from Doucet and Freitas (1998). Partitions of particles are sorted in Step 9 (as described in Subsection 4.2.5). Target estimates are calculated in Step 10 after the number of targets tracked has been determined.

The final step, Step 11, involves assigning current target estimates to appropriate target tracks. This can be carried out using Global Nearest Neighbour or Multidimensional Assignment algorithms, as specified in Subsection 7.2.3.

The following subsections describe additional details of the above mentioned steps.

Target Template

The target template used by the tracking system to identify likely targets can be extracted either manually or automatically. The manual method involves selecting 20 template images of fish in the video to be analysed in various areas of the tank. The automated method uses motion segmentation information contained in the Initial Object Mask (as described in Section 7.2.1) and Kalman filter tracking to extract the required number of template images. The Kalman filter in this case is used to ensure that noisy results of segmentation are not mistaken for valid objects. The assumption here is that valid objects will persist from frame to frame while noisy objects will occur only sporadically, therefore the Kalman filter will ignore them. Template images are selected randomly throughout the tracking process, based on bounding boxes of tracked targets. Once all template images have been extracted, a colour histogram is created for each image. The template colour histogram is created by averaging individual histograms.

Particle seeding and physical constraints

The standard particle filter algorithm uses random particle seeding, however additional knowledge about the problem space can be used to seed particles in specific areas to maximise the efficiency of the filter. In the case of this particle filter tracking system, data provided by the Initial Object Mask can be used to seed particles around segmented objects. To maintain sufficient variation in particle seeding, only 50% of particles are seeded specifically around segmented objects. The remaining particles are seeded uniformly.

Another advantage of the particle filter is that physical constraints can be incorporated into the system. Particles generated or propagated by the system can be inspected to determine if they fall within or outside the tank. When particle coordinates fall outside the tank, the particle is sampled again. This process is repeated up to a maximum of 10 times at which point the state vector for this particle will be removed.

Target Detection

The multi-target capability of the particle filter is governed by a pair of existence variables (E^n_{k-1}, E^n_k). If $E^n_{k-1} = E^n_k$ then all state vectors within the particle are propagated using the transitional prior $x^n_{i,k} \sim p(x_k|x^n_{i,k-1})$. If $E^n_{k-1} < E^n_k$, this means that the number of targets within a particle has increased. Existing state vectors are drawn using the transitional prior and the new state vector is drawn randomly as per Subsection 7.2.2. If the number of targets within a particle

has decreased, $E^n_{k-1} > E^n_k$, the system randomly selects E^n_k state vectors and propagates them using the transitional prior. The remaining state vectors are ignored. This scheme allows for constant detection of new targets (up to the maximum number of known targets) and also allows deletion of targets which seem to have disappeared from the scan area (e.g. due to the noise of water reflections).

Adaptive Partition

The Adaptive Partition method (Step 4 in the pseudo code) was implemented to better deal with the multi-modal nature of the particle filter when tracking multiple targets. It also aims to decrease the number of particles required and to utilise the kinematic motion of tracked objects to propagate particle states. Using this scheme the system has been found to be able to track two targets using 350 particles. This subsection will describe the implementation details of both partition schemes and the partition sorting algorithm.

The Independent Partition method is activated when targets are well separated and propagation of particle states within each target partition can be done independently. For each target partition a set of particles (the original set) are sampled based on particles from the previous time step (using kinematic motion model $p(X^k_{p,t}|X^{k-1}_{p,t})$ as shown in Table A.2). Colour histograms based on these new particles are then extracted to be used in the calculation of importance weights. Both the current image frame and the background image are used in the extraction of histograms. The normalised weights are then used to generate a random set of indices based on a distribution of these weights using sampling with replacement. This set of indices is then used to generate the final set of particles from the original set mentioned above. In addition a bias weight is returned for each particle which is used in the calculation of the normalised weights (Step 7 in Table 7.1).

The Coupled Partition method is activated when targets are close or overlapping. Its main objective is to use the kinematic motion model to propagate each particle separately. For each particle within each target partition t, R random proposals are generated based on the kinematic motion model, with $R = 5$ (Table A.3). Next, colour histograms are generated for the current frame and background image in the area specified by each realisation of R. This is used to calculate weights for each of the R proposals. The distribution of normalised weights is then used to generate a single random index j. This index defines which of the R proposals will be selected. A bias weight is returned based on the weight of the R proposal with index j.

Calculating Importance Weights

The likelihood functions which calculate importance weights are different for the independent partition and coupled partition methods. For the coupled partition the likelihood function follows Eq. 4.32 from Chapter 4 which sums distance differences (from background) of target state vectors within the particle. Distances are calculated using Eq. 4.24 from Chapter 4. For the independent partition, $L_k^n(E_k^n)$ in Eq. 4.32 from Chapter 4 is multiplied by a factor based on the minimum squared distance between target state vectors within a particle to produce a modified likelihood $\bar{L}_k^n(E_k^n)$.

$$\bar{L}_k^n(E_k^n) = L_k^n(E_k^n) * exp\left\{-\alpha * \frac{1}{min\,(d_n^2)}\right\} \tag{7.1}$$

where $\alpha = 1000$ is a design parameter (chosen experimentally) and d_n^2 is a vector of squared Euclidean distances between centroids of target state vectors within particle n (calculated in pixels). This modified likelihood penalises particles which have their state vectors close to each other in Euclidean space. This approach, having large α, ensures that particles which have state vectors further away from each other are weighted more favourably, therefore preventing the filter from converging onto a single target and activating the coupled partition method prematurely. Weights are assigned according to variable E_k^n using Equation 4.33 from Chapter 4.

Calculating Estimates

In order to determine the number of targets, $\hat{m}_k$, that are currently tracked by the system, the following formula is used:

$$\hat{m}_k = \underset{m=0,1,\ldots,M}{\arg\max}\ (P_m) \tag{7.2}$$

$$\text{where } P_m = \frac{1}{N}\sum_{n=1}^{N}\delta(E_k^n, m), \quad \delta(i,j) = \begin{cases} 1, & \text{if } i \neq j \\ 0, & \text{if } i = j \end{cases}$$

N is the number of particles, M is the maximum number of targets, P_m is the probability that the number of targets is m and δ is Kronecker delta function (Czyz et al., 2007).

Because of the use of the adaptive partition scheme to optimise the particle filter, estimates are calculated based on different partitions (Kreucher et al.,

2005). First a variable $\tilde{I}_p(i)$ is calculated which indicates if particle p has a partition corresponding to target i:

$$\tilde{I}_p(i) = \begin{cases} 1 & \text{if partition } i \text{ exists in particle } p \\ 0 & \text{otherwise} \end{cases} \tag{7.3}$$

Then weights are calculated using $\tilde{I}_p(i)$ multiplied by the weight of the particle obtained in Subsection 7.2.2. New weights are normalised by the sum of all $\tilde{I}$ multiplied by respective weights.

$$\hat{w}_p = \frac{w_p \tilde{I}_p(i)}{\sum_{l=1}^{N} \tilde{I}_l(i) w_l} \tag{7.4}$$

The estimate and covariance of the state of target i is given by:

$$\hat{X}(i) = E[X(i)] = \sum_{p=1}^{N} \hat{w}_p X_{p,i} \tag{7.5}$$

$$\hat{\Lambda}(i) = \sum_{p=1}^{N} \hat{w}_p (X_{p,i} - \hat{X}(i))(X_{p,i} - \hat{X}(i))' \tag{7.6}$$

where $X_p = [x_{p,1}, x_{p,2}, ..., x_{p,i}]$ is a particle p containing state vectors for i targets.

7.2.3 Data association

In this system data association is not incorporated into the particle filter. Rather it is used to associate calculated estimates in the current time step with target estimates from previous time steps. Two methods have been examined, the first one being the single scan Global Nearest Neighbour method, the second one being the multi scan Multidimensional Assignment method.

Global Nearest Neighbour

The GNN method uses an assignment matrix to list costs of all possible assignments between tracks and measurements. The cost is calculated using a squared Euclidean distance measure, d^2. The measure involves (measured in pixels) the centroid coordinates r, c, the size of the bounding box h, w and velocity components rv, cv of tracks and measurements:

$$\begin{aligned} d^2 = &(r_{track} - r_{meas})^2 + (c_{track} - c_{meas})^2 + \\ &\alpha * \left((h_{track} - h_{meas})^2 + (w_{track} - w_{meas})^2\right) + \\ &\beta * \left((rv_{track} - rv_{meas})^2 + (cv_{track} - cv_{meas})^2\right) \end{aligned} \tag{7.7}$$

where $\alpha = 0.1$ is a parameter used to decrease the influence of the bounding box on the value of d^2, and $\beta = 10$ is a parameter used to increase the influence of track motion (velocity) on the value of d^2.

The assignment matrix is then used in Munkres' algorithm (1957) (MATLAB implementation provided by Ristic (1998)) to minimise the cost of assignment and return valid associations. The implementation also keeps the history of track estimates from previous time steps and updates the velocity of the current track with the average velocity of several previous time steps. This allows smoothing of the current velocity component, but still allows detection of changes in fish manoeuvres. For any unallocated measurements, a new track is created, but only if the current number of tracks is less than the maximum number of expected targets (the assumption is that the number of targets in the problem area is known).

Multidimensional Assignment

The Multidimensional Assignment method uses a branch-and-bound algorithm based on linear programming to solve the underlying binary integer programming problem. While this method may appear excessive for tracking two fish, the original intention was to expand the tracking problem to 3-5 fish. The algorithm utilises the LP-relaxation technique to find an optimal solution instead of Lagrangian relaxation. The function in MATLAB used for this purpose is `bintprog` and it attempts to solve a problem of the form:

$$\min_x f^T x \text{ such that } \begin{cases} A \cdot x \leq b, \\ Aeq \cdot x = beq, \\ x \text{ is binary vector} \end{cases} \tag{7.8}$$

where f, b, and beq are vectors, A and Aeq are matrices, and x is a solution vector which can only have values of 0 or 1 (Mathworks, 2009). Only equality $Aeq \cdot x = beq$ is of interest in the assignment problem and the inequality $A \cdot x \leq b$ is irrelevant.

Six scans of data are used to determine the measurement to track association at each time step. This allows the reversal of previous association decisions, should newly arrived measurements allow for a better association solution. First a number of measurements in each time step is determined and a matrix outlining all possible combinations of assignments is created. Next the track score vector (f in Eq. 7.8) is created using the assignment matrix and data from the current timestep. The track score vector contains an entry for each combination in the assignment matrix and utilises Euclidean distance of each track's centroid and

velocity components to every other track to calculate the cost of the particular combination. However more complex track score based on likelihood ratio can also be used (Blackman and Popoli, 1999).

$$cost_{i,j} = \sqrt{(r_i - r_j)^2 + (c_i - c_j)^2 + (rv_i - rv_j)^2 + (cv_i - cv_j)^2} \tag{7.9}$$

$$trackscore_i = -\frac{1}{\sum_{j=1}^{L} cost_{i,j}} \tag{7.10}$$

where $i, j = 1...L$, L represents the number of all possible combinations.

The result of `bintprog` is a vector x which represents a feasible solution as 1 and all other entries are 0. This result vector is used as an index to the combination matrix which provides the optimal assignment of measurements to tracks.

7.2.4 Video Recording in Tanks

Two video sequences were recorded of two rainbow trout in a 1m diameter circular tank (250L). A short acclimatisation period was undertaken in order to settle the fish after transfer from the holding tank. The recordings were undertaken during periods of higher fish activity, so that the system could be tested against the dynamic movement of fish.

7.2.5 Compilation and Display of Data

Data from experiments were formatted in various forms to deal with multimedia and paper based presentations of data. An output video was produced marking each fish with a unique ID. For paper based reports, each fish was represented as a x-y graph of locations, each location point corresponding to a different, sequential time step.

7.3 Results

Two track sequences each involving two fish are represented in the results. The first sequence shows fish interactions and loss of tracks while the second sequence shows fish manoeuvres (turns and accelerations).

7.3.1 Sequence 1

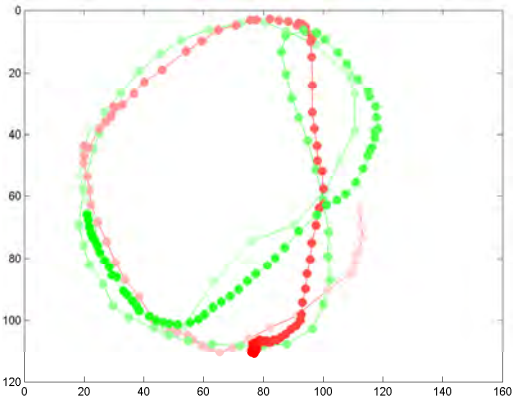

(i) Ground truth

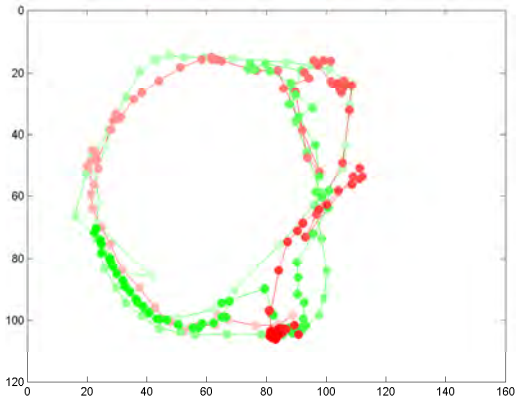

(ii) GNN data association

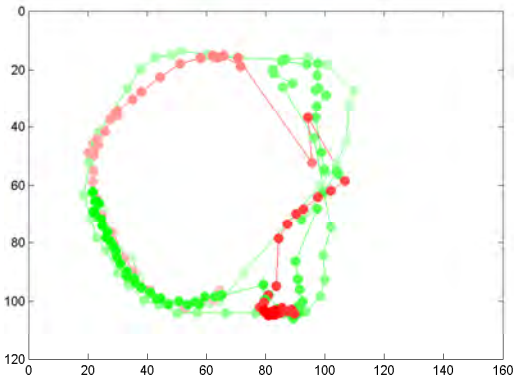

(iii) MDA data association

Figure 7.1: Tracking results for Sequence 1 comparing GNN and MDA data association methods. Strength of the colour determines the temporal order. Lighter points are at the beginning of the sequence, darker points are at the end of the sequence. Ground truth was acquired through manual annotation of video at each time step.

The whole of Sequence 1 is shown in Figure 7.1i. While it is much easier to view results of these experiments using video and animations, the data have

been transformed to allow for temporal interpretation of data on paper. To allow this, points have been marked with different colours to distinguish different fish. Points have also been made lighter in colour at the beginning of the sequence and darker at the end of the sequence. This gives a better temporal comprehension of fish motions and interactions. Within this sequence, there are three interactions which will be investigated below. They involve an avoidance manoeuvre, an overlap of two fish moving in opposite directions, and a complex manoeuvre which involves change of direction, speed and illustrates loss of tracking due to reflections. The video sequence was analysed using both GNN (Fig. 7.1ii)and MDA (Fig. 7.1iii).

Tracking Performance

Tracking performance was examined for the MDA data association method. The system used Eq. 4.34 from Chapter 4 to calculate the probability that zero, one or two targets have been detected by the system (Figure 7.2). The system immediately detects the first target and after about 10 time steps the second target is detected. After about 50 time steps, light reflections, water movement, and proximity of both fish to each other cause a loss of one track. Once both fish re-emerged from occlusions they are re-acquired by the system. The figure shows that the system is capable of rapidly acquiring tracks as they appear. Similarly should problems occur in tracking a target, the system responds quickly to the loss of the track.

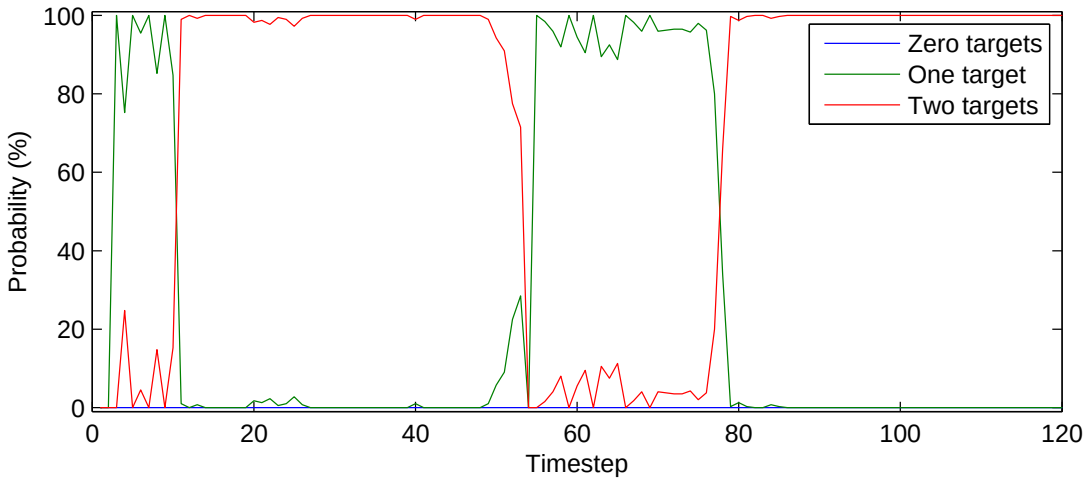

Figure 7.2: Probability of detecting zero, one or two targets during Sequence 1.

By estimating the variance of the system at each step, it is possible to examine

how certain the system is regarding its estimates (Figure 7.3). The initial high variance for Fish 2 around time step 20 occurs when a track for Fish 2 is first acquired. The next increase in variation occurs at around time step 50 when both fish are close to each other and severe light reflections occur, preventing successful tracking. The system recovers its confidence in track Fish 1 until uncertainty increases again as Fish 2 is re-acquired at time step 80. Some minor uncertainty occurs between time steps 90 and 100, after which time the system tracks both fish with high confidence.

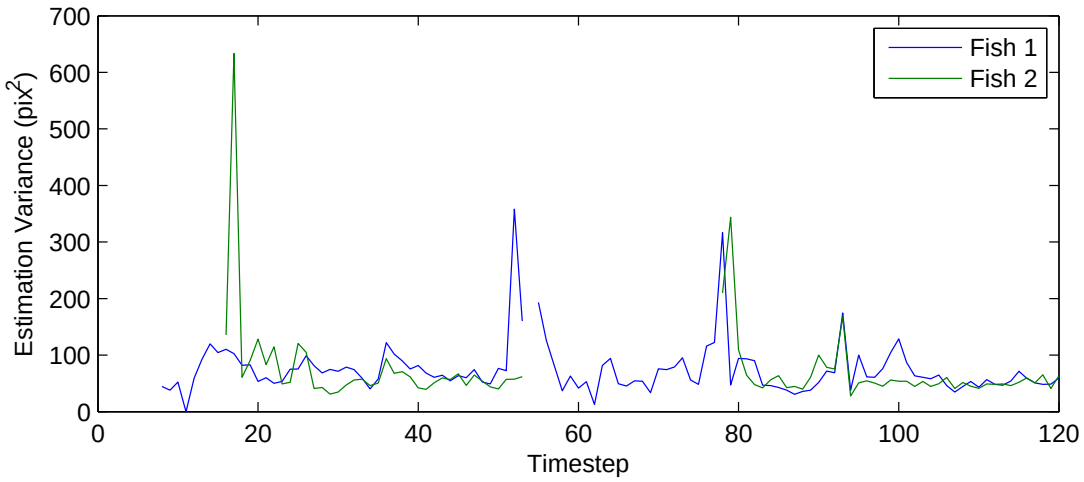

Figure 7.3: Certainty about the accuracy of position estimates is expressed by calculating the estimation variance. Lower variance is better.

The difference between the ground truth and the results from the tracking system varies throughout the sequence and depends largely on the proximity of fish to each other (Figure 7.4). Both fish are tracked correctly until around time step 50, where loss of tracks occur. At this stage Fish 1 is still tracked correctly but the track for Fish 2 is lost and the comparison is made against the last known location. When both fish are re-acquired by the tracking system after time step 80, track swapping causes the error between the ground truth and the tracking results to become high. This eventually decreases around time step 90 when the MDA method correctly assigns both fish. The system performs well for the remainder of the sequence (distance to ground truth is below 10 pixels).

Avoidance Manoeuvre

This subsection describes a short avoidance manoeuvre carried out at time step 1-20. The ground truth, determined by manual annotation of video, shows the

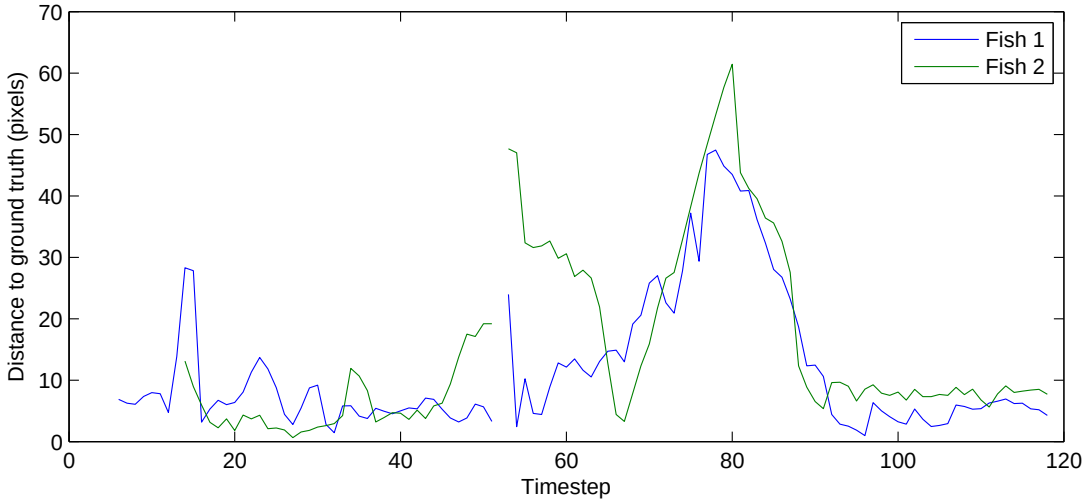

Figure 7.4: Error distance between the ground truth and the tracking system.

interaction between fish (Figure 7.5i) as they approach each other from opposite sides of the tank (left and right) towards the lower part of the tank. The Red fish continues along the wall from right to left while the Green fish takes an evasive manoeuvre towards the centre of the tank and then continues to the top right of the tank. The distance between individual points in the ground truth figure indicates that the fish move at different speeds as the manoeuvre occurs. The Green fish moves quickly towards the top of the tank, while the Red fish continues at its original speed.

For both data association methods in Fig. 7.5, the Red fish has been detected later due to the fish being obstructed by a pipe and the tracking system not detecting it early. Increasing the number of particles would improve the initial detection rate. The MDA method picks up the Red fish later because it needs 6 time-steps to determine if the target tracked is genuine. Both methods perform data association correctly.

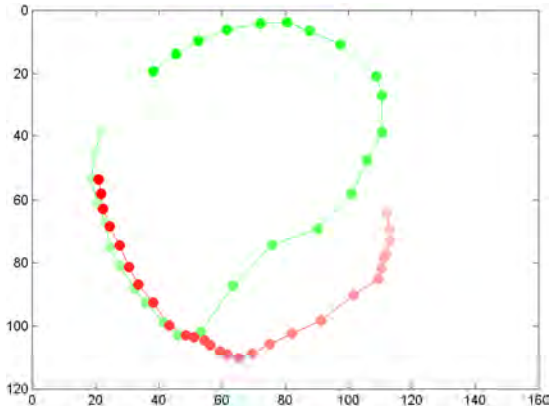

(i) Ground truth

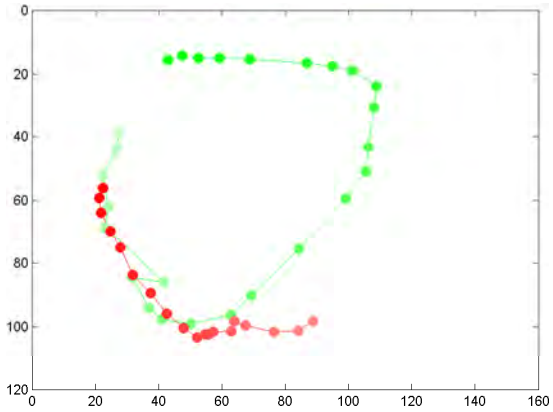

(ii) GNN data association

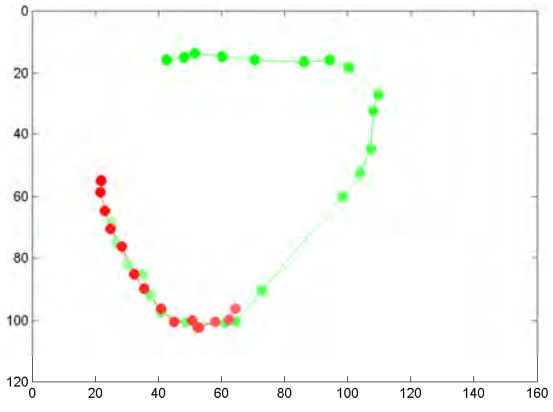

(iii) MDA data association

Figure 7.5: Avoidance Manoeuvre in Sequence 1 (Timestep 1-20).

Fish Passing By Manoeuvre

The passing by manoeuvre occurs at time step 25-45. The ground truth shows that The Green fish arrives from the top of the tank, while the Red fish arrives from the bottom of the tank (Figure 7.6i). They bypass each other on the left wall of the tank, Green going down, Red going up relative to the orientation of the plot. Both fish do not exhibit any accelerations; they simply move past each other (one above the other).

Both data association methods show a similar result. As the swimming directions of both fish are different and their speeds relatively steady, no major problems with data association are experienced.

Complex Manoeuvres

Complex manoeuvres are carried out at time step 50-100. The ground truth shows a complex manoeuvre carried out by the Green fish (Figure 7.7). Both fish travel to the top of the plot (Green from the bottom, Red from the left). The Green fish turns around and both fish then begin to travel downwards in relation to the plot. In relation to the tank, Green fish swims alongside the wall of the tank initially, Red fish close to the middle of the tank. Both fish reach the bottom in relation to the plot and they slow down. In relation to the tank both fish are near the wall of the tank.

This sequence involves a severe loss of tracking. When the Green fish turns around at the top in relation to the plot, the water surface is disturbed and reflections cause loss of track for one of the fish. While GNN data association attempts to track both fish whenever tracking permits, MDA data association does not track the Red fish until it has been reacquired correctly. Both methods re-assign fish correctly but GNN method swaps a single track estimate between the two targets until it is able to recover completely. MDA delays its assignment for the Red fish until enough information is available. It was observed that there has not been much difference in detection performance between GNN and MDA. Both methods tracked poorly when fish tracks were lost for prolonged periods and although MDA offers multiple scans of data before a decision is made it did not perform any better than GNN. Perhaps the only advantage of MDA is that the multi-scan capability allows the method to reverse its decisions as more data arrive. The GNN method on the other hand would be much faster due to fewer computations required.

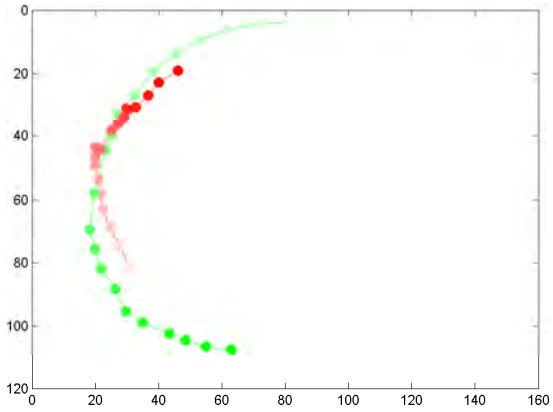

(i) Ground truth

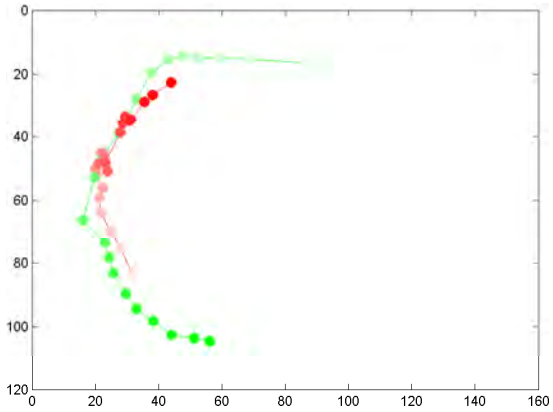

(ii) GNN data association

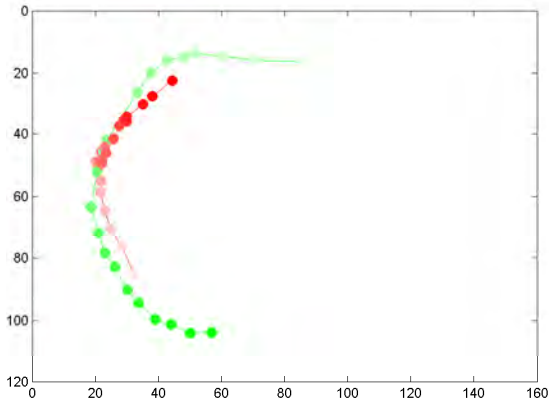

(iii) MDA data association

Figure 7.6: Fish Passing By Manoeuvre in Sequence 1 (Timestep 25-45).

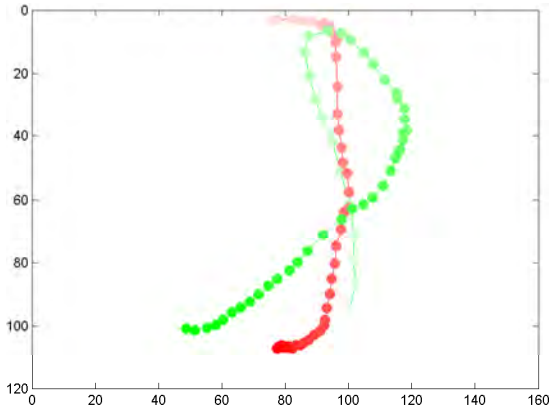

(i) Ground truth

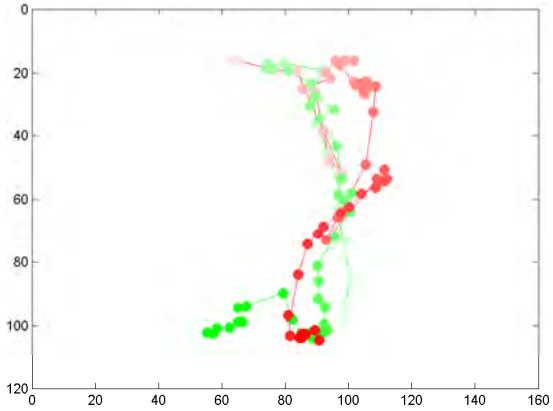

(ii) GNN data association

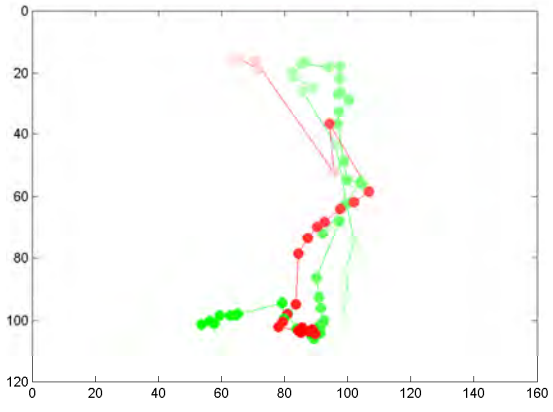

(iii) MDA data association

Figure 7.7: Complex manoeuvres in Sequence 1 (Timestep 50-100).

7.3.2 Sequence 2

The second sequence demonstrates manoeuvrability of fish and the system's ability to track these manoeuvres. The sequence is shown in Figure 7.8 and points lighter in colour are at the beginning of the sequence while darker points are towards the end of the sequence. There are two main interactions in the sequence: the first being a manoeuvre and change of speed by the Green fish, the second one being a circular movement by the Red fish along the sides of the tank while the Green fish is stationary. Only MDA data association has been considered in this sequence as differences between GNN and MDA have been addressed in Sequence 1.

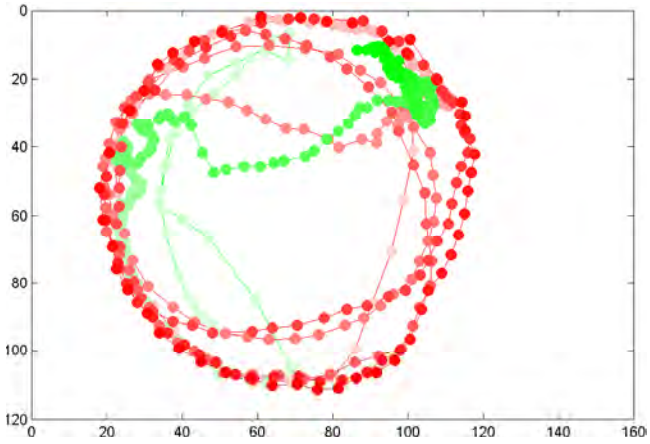

(i) Ground truth

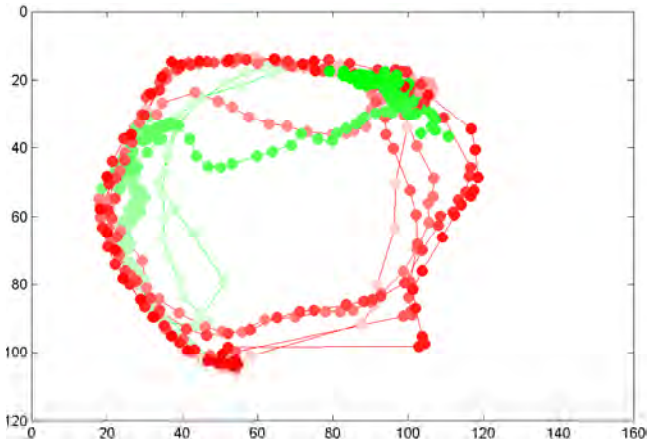

(ii) MDA data association

Figure 7.8: Tracking results for Sequence 2. Strength of the colour determines the temporal order. Lighter points are at the beginning of the sequence, darker points are at the end of the sequence.

Complex Manoeuvres

This manoeuvre starts with the Green fish swimming from the bottom of the image to the top of the image, towards the Red fish (Fig. 7.9). When the Green fish reaches the top of the image, there is an interaction with the Red fish (the Green fish touches the tail of the Red fish). The Green fish turns around and both fish begin to travel to the bottom of the image. As Red fish reaches the bottom and starts to move towards the left side of the image along the wall of the tank, the Green fish suddenly accelerates, performs a turn and starts following the Red fish.

The tracking system copes well with the sudden change of direction by the Green fish, as the Particle filter can deal with non-linear motion. The filter also deals with acceleration of the Green fish but activation of the Coupled Partition component generates inaccuracy in tracking. The system recovers and correctly associates both targets at the end of the sequence.

Passing a Stationary Fish

This case looks at the Red fish swimming around the tank while the Green fish is stationary. In Figure 7.10, the Red fish begins its circling motion from the top right of the image, approaches the stationary Green fish and then continues along the wall of the tank downwards and to the right hand side of the image. The sequence continues in Figure 7.11 where the Red fish goes past the Green fish for the second time. The Green fish remains essentially still; its slight motion is mainly to maintain its station in relation to the current.

The system has no trouble tracking both fish while the Green fish is stationary and the Red fish is moving and passing the Green fish. There is a loss of track in Figure 7.11ii but the tracking filter recovers without issues.

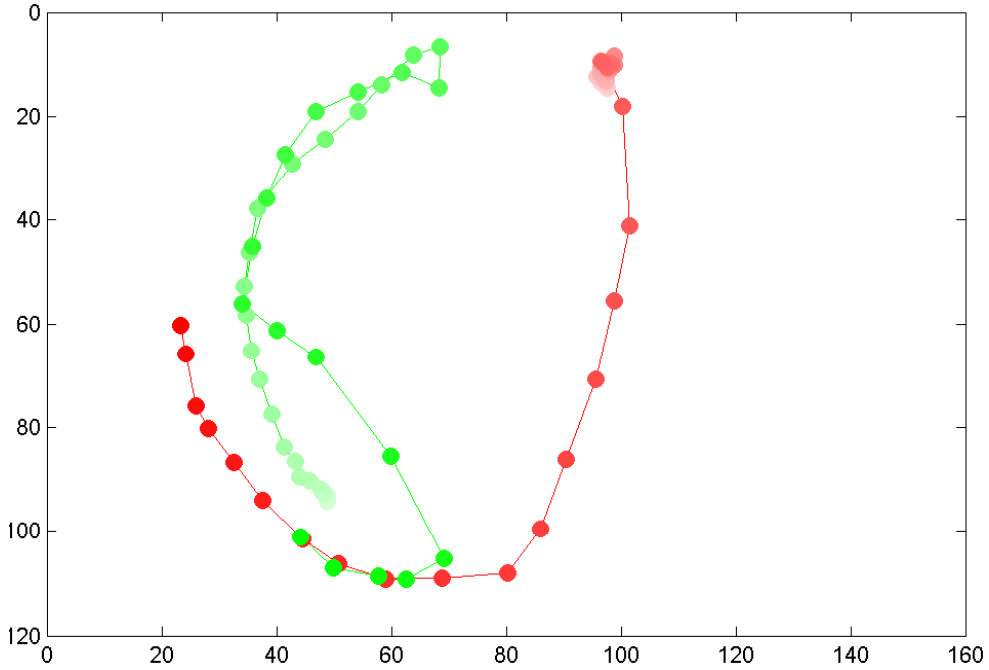

(i) Ground truth

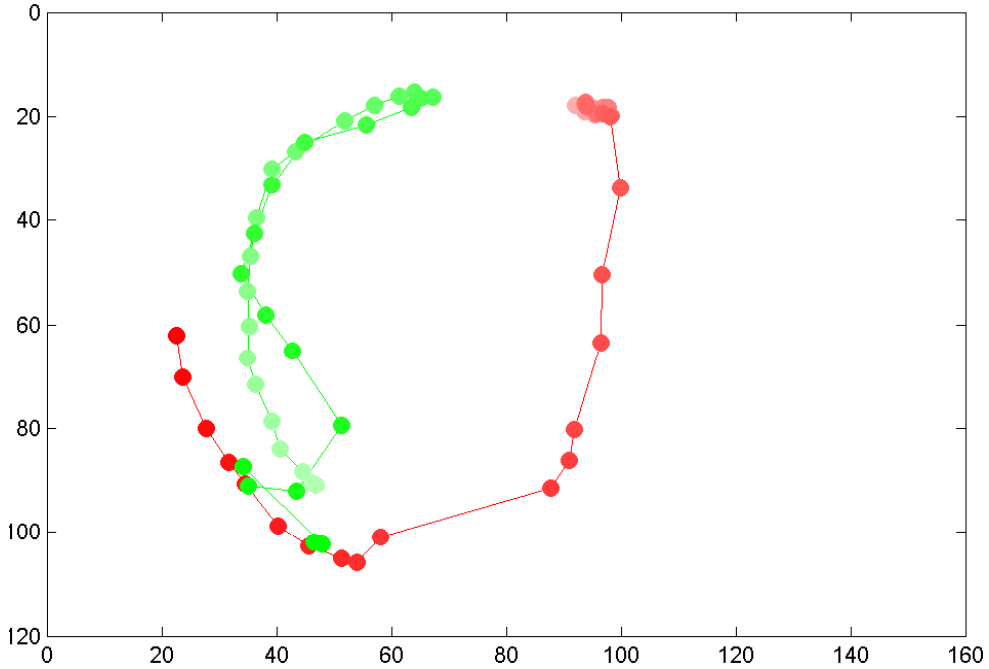

(ii) MDA data association

Figure 7.9: Complex manoeuvres in Sequence 2.

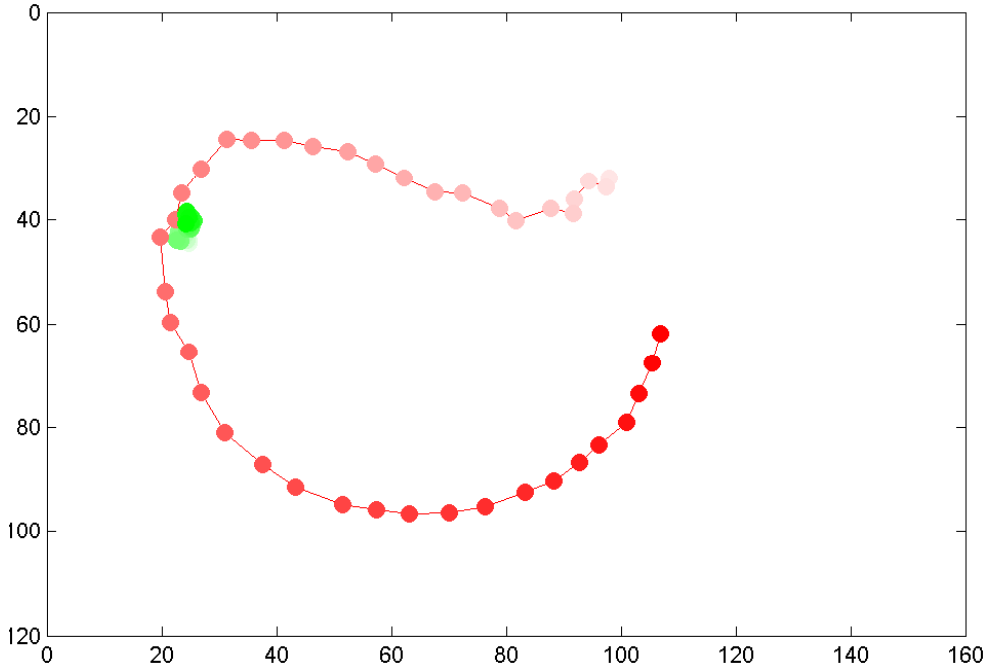

(i) Ground truth

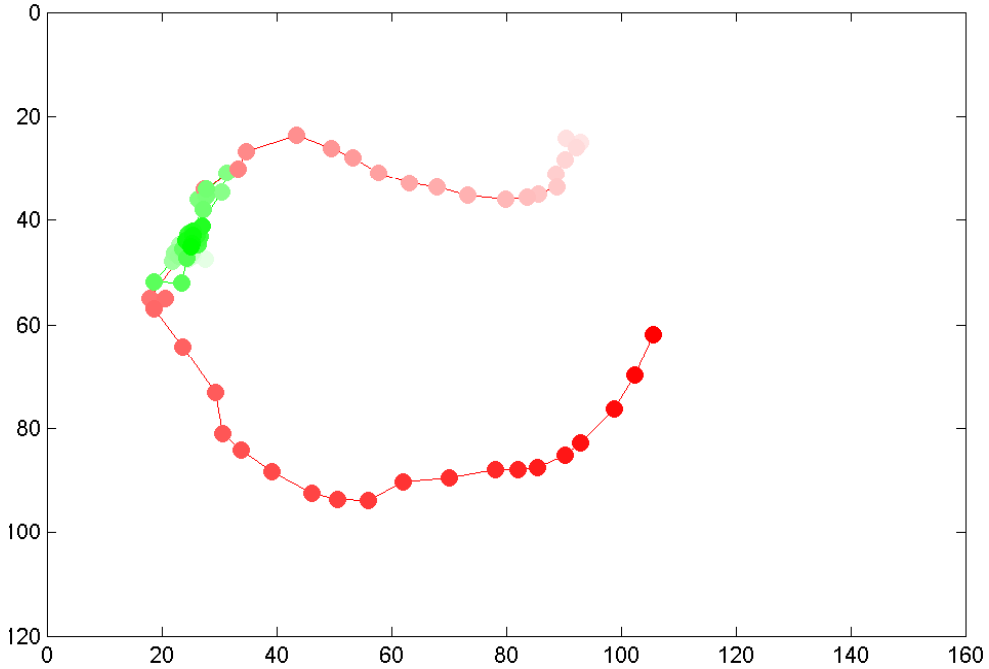

(ii) MDA data association

Figure 7.10: Swimming past a stationary fish first time in Sequence 2.

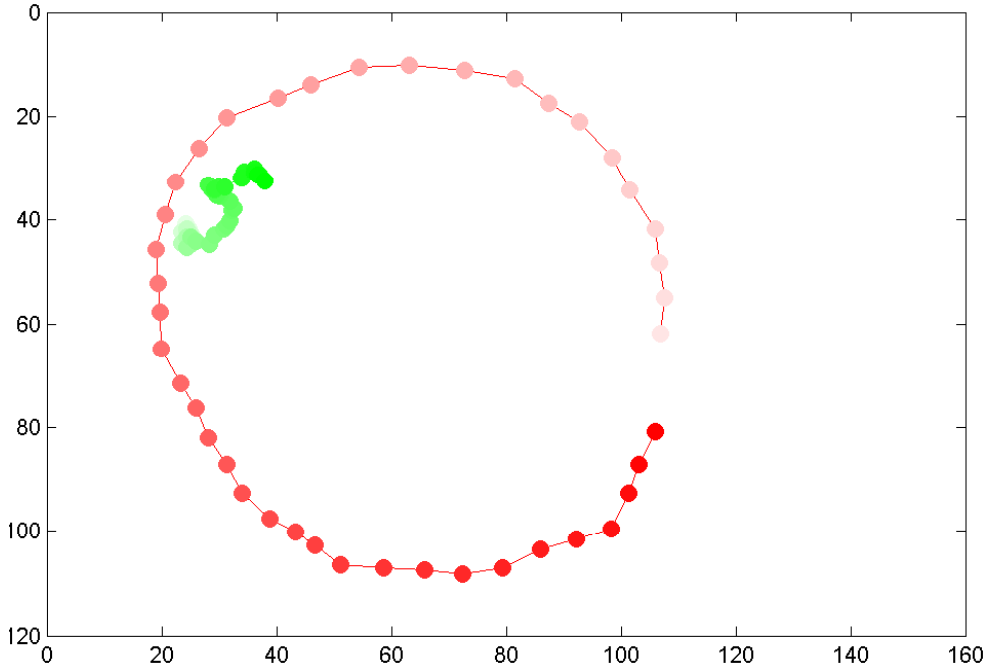

(i) Ground truth

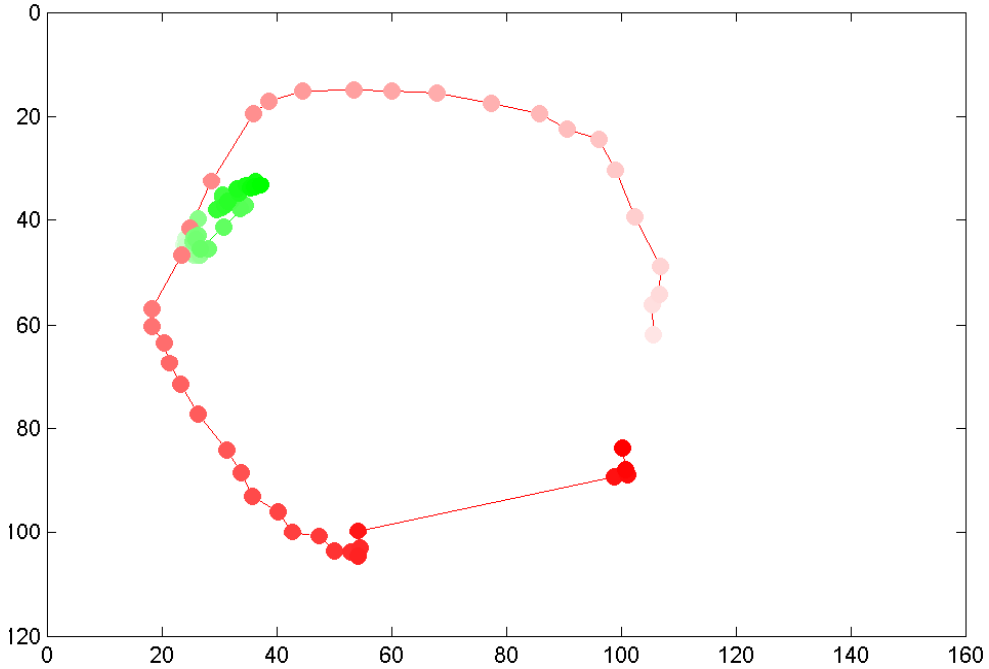

(ii) MDA data association

Figure 7.11: Swimming past a stationary fish second time in Sequence 2.

7.4 Discussion

The use of a target template within the tracking system has the advantage that it utilises the prior knowledge about possible targets, and the use of histograms makes the template shape invariant. The disadvantage of this method is that the template has to be created (manually or automatically) with particular regard to different levels of illuminations within a tank. Making illumination levels even throughout the tank is desirable but not always possible. Therefore experimental design can impact on the ability to detect fish in a tank. Estimating the background can improve tracking but again care needs to be taken during experimental design to reduce the number of reflections through appropriate positioning of lights. An ideal recording setup would involve a wide lens camera in the middle of the tank just under the surface looking down. This would eliminate the surface movement (and thus reflections).

The results in Section 7.3 demonstrate the ability of the particle filter is in tracking multiple targets, at least in short video sequences. It can track fish during unpredictable movement and change of direction. The data association works successfully when fish pass each other without major changes in speed or direction. However, it is questionable if the filter could maintain its correct data association in longer video sequences. Once an error has been made it would be impossible for the system to recover from it. Therefore an additional correction mechanism would be required which would periodically ensure that fish have correct identifications. One way would be to tag fish using RFID technology. RFID tags are very small and therefore their impact on fish might be minimal. The technology would allow a system to receive periodic readings as fish approach the scanner and readjust identifications if necessary. While using tagging to complement video may be successful, the purpose of this research was to remove the need for tagging fish. Therefore an alternative might be for the tracking system to identify unique features of each fish. This may only be possible with a high-resolution camera used to take periodic shots of fish in order to identify them.

The performance of the coupled partition scheme is also questionable as at times the filter tends to converge into a single mode. It works well when targets move with constant speed and opposite direction but when they manoeuvre while the coupled partition is active this scheme performs poorly. For that reason step 6 and 7 of the pseudo-code, in section 7.2.2, contains a counter variable which is used to allow only 3 iterations of the original coupled partition scheme. After that the importance weight calculation includes distance between partitions favouring those further away from each other. This generally prevents the filter from converging into a single mode and enabling it to remain multi-modal.

Further improvements to the system could involve the use of elliptical particles or the use of multiple bounding boxes to describe each fish. This second possibility could be used to track movements of the body and the tail of each fish.

The next chapter examines the possibility of tracking a slightly larger group of fish in a tank with focus on group dynamics rather than individual behaviours.

CHAPTER 8

TRACKING A SMALL GROUP OF FISH IN TANKS

8.1 Introduction

The tracking system described in Chapter 7 attempted to track two fish in a tank while always being able to uniquely identify both fish. This proved a difficult task to achieve without invasive methods, including tagging. Another approach to tracking of fish in tanks is to track individual fish as part of a group without unique identification. Instead of observing individual behaviours, the focus is on the group behaviour. This chapter will examine if it is possible to track a small number of fish in a tank for the purpose of identifying group behaviours.

The aim of the chapter is to determine what type of data the tracking system can produce and demonstrate how these data could be used in experiments which require observations of different groups of fish in tanks. Its suitability in feeding experiments will be examined. Similarly the system could also be used in disease challenge experiments to observe differences between diseased fish and a control group.

8.2 Materials and Methods

This chapter examines behaviours of a group of 10 fish (rainbow trout) in a tank and how they interacted as a group in relation to a demand feeder, generating daily activity patterns. While individuals were being tracked, there was no attempt made to uniquely identify them. Instead the spatio-temporal activity of fish was examined: preferred areas of occupation, activity at different times of the day, and feeding vs non-feeding activities. The experiment was set up to test the computer vision techniques rather than trying to answer a specific aquaculture question. It was important to find out which parameters of fish behaviour could

be detected by the tracking system. Daily graphs of average swimming speed, distance of fish from the feeding area and location from the centre of the tank are presented in Appendix C.

8.2.1 Experiment Set-up

The aim of the experiment was to observe fish activity on video in a tank, then to analyse this activity using the fish tracking system and correlate it with feeder activations. Thirty fish (mean weight 25.6g) were transferred to three 1m diameter circular tanks (10/tank) connected to a water recirculation system. A demand feeder was installed on each tank and controlled by a Programmable Logic Controller (PLC) from SoftPLC Pty. Ltd. via Supervisory Control and Data Acquisition (SCADA) software from Citect Pty. Ltd. The objective was for naive fish to learn to pull a red coloured bead (2 cm below surface) and be able to feed on demand (the feed was 2mm pellets from Skretting Pty Ltd, Cambridge, Tasmania). Each activation was logged to a text file using Chronolab software with a time-stamp to the closest minute.

Fish were exposed to the photoperiod cycle of 12:12 LD. Lights were turned on at 07:00h and turned off at 19:00h. All lights in the room including those above tanks were set up to turn on/off simultaneously but there was a variation in the light timer which turned the light on 4-8 minutes past 07:00h.

The experiment started on 27 January 2010 and concluded on 2 March 2010 (35 days). On 19 February the access to food was restricted to between 08:00h and 09:00h. Fish were still able to activate the feeder and activations were logged during feed time and outside delivery time. The purpose of measuring outside feeding time was to observe changes in fish behaviour in relation to feeding and in relation to activations. Technical problems and time constraints prevented continuation of this experiment past 2 March 2010, which was before fish had adapted to this new feeding regime.

Video recordings were carried out on one of the tanks, the other two serving as replicates for the feeding system. Lights positioned above the tank provided adequate lighting while minimising reflections for the video recording. The other two tanks were set up with similar light conditions. The video camera used was a 120^o lens camera with a SONY CCD sensor. The wide angle of the lens allowed the camera to be positioned relatively close to the tank surface to minimise water surface reflections.

8.2.2 Tracking System

The tracking system used in this analysis evolved from the sea cage tracking system described in Chapter 5. Minor modifications to the sea cage tracking system were carried out to ensure that the location of each fish detected could be logged. The system calculated the swimming speed of individual fish. To provide a speed estimate, the system tracked a fish for 10 frames or longer, providing a reliable instantaneous velocity calculation. The resulting position and speed data were logged to the SQL database for further analysis. Additional modifications to the segmentation module was used, in that each image frame was contrast-adjusted prior to the application of an adaptive thresholding, to account for specific light conditions around the recorded tank.

Four methods of displaying the results are used. Actograms are used to report activations of the demand feeder and speed aggregated over hourly periods of time. A series of heat maps are used to describe the spatial distribution of fish over time. Each heat map is an activity pattern over a 30 minute period giving a total of 24 heat maps per day. Standard xy-plots demonstrate changes in speed and distance from the feeding area over time (similar to plots in Chapter 6). The last method of display is a polar graph representing the mean direction of fish location from the centre of the tank (similar to plots in Chapter 6).

8.3 Results

The movement of fish was analysed against three variables: i) speed of swimming, ii) distance and direction from the feeding location (bead), and iii) distance and direction from a central point in the tank. In addition a single day, 24 February 2010, was analysed in more detail to identify events that occurred on this day and how they influenced fish behaviour presented as typical data to show diurnal variations in fish behaviour.

8.3.1 Feeder Activation Patterns

Figure 8.1 shows actogram of demand feeder activations between 27 Jan and 27 Feb on 12:12 LD cycle. Figure 8.2 shows a colour coded actogram of the same data. There was a small number of random activations during the first c. 6 days (Fig. 8.1 and 8.2). Feeder activations increased after 6 days and appeared to maintain some consistency by day 19. The activity between 14-20 Feb (7 days) indicates that fish had a preference to feed in the morning, with low activity

during most of the day followed by a slight increase in the evening. Higher activity patterns on 20 Feb could be related to the implementation of a restricted ration regime (food released only in the morning) with fish possibly testing the feeder for release of food. Fish also responded strongly to the period of three days of fasting between 21 and 23 Feb (due to equipment failure) with increased activity on the mornings of 24 and 25 Feb.

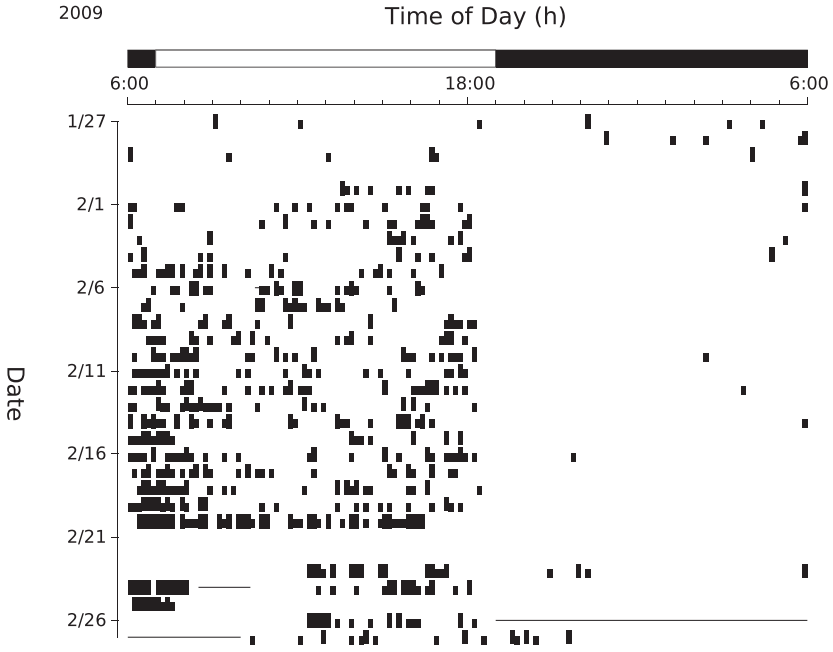

Figure 8.1: Classic actogram of demand feeder activations of 12:12 LD cycle between (27 Jan and 27 Feb).

8.3.2 Speed

Speed was expressed in pixels per second (shown in the Fig. 8.3 as multi-coloured scale and for each day in Fig. C.1) and no visible patterns were observed in relation to feeder activations. One possible exception was 15-19 of February where the speed was higher in the morning (between 07:00h and 10:00h), slightly lower for the reminder that day followed by an increase in the evening. Also the number and frequency of activations was higher in the morning. The restriction on feeding time from 20 February onwards had mixed effects on swimming speed. On 20 February while the number of activations throughout the day was higher the swimming speed was not greatly affected by the lack of food during these activations. However, technical problems during the next three days meant the

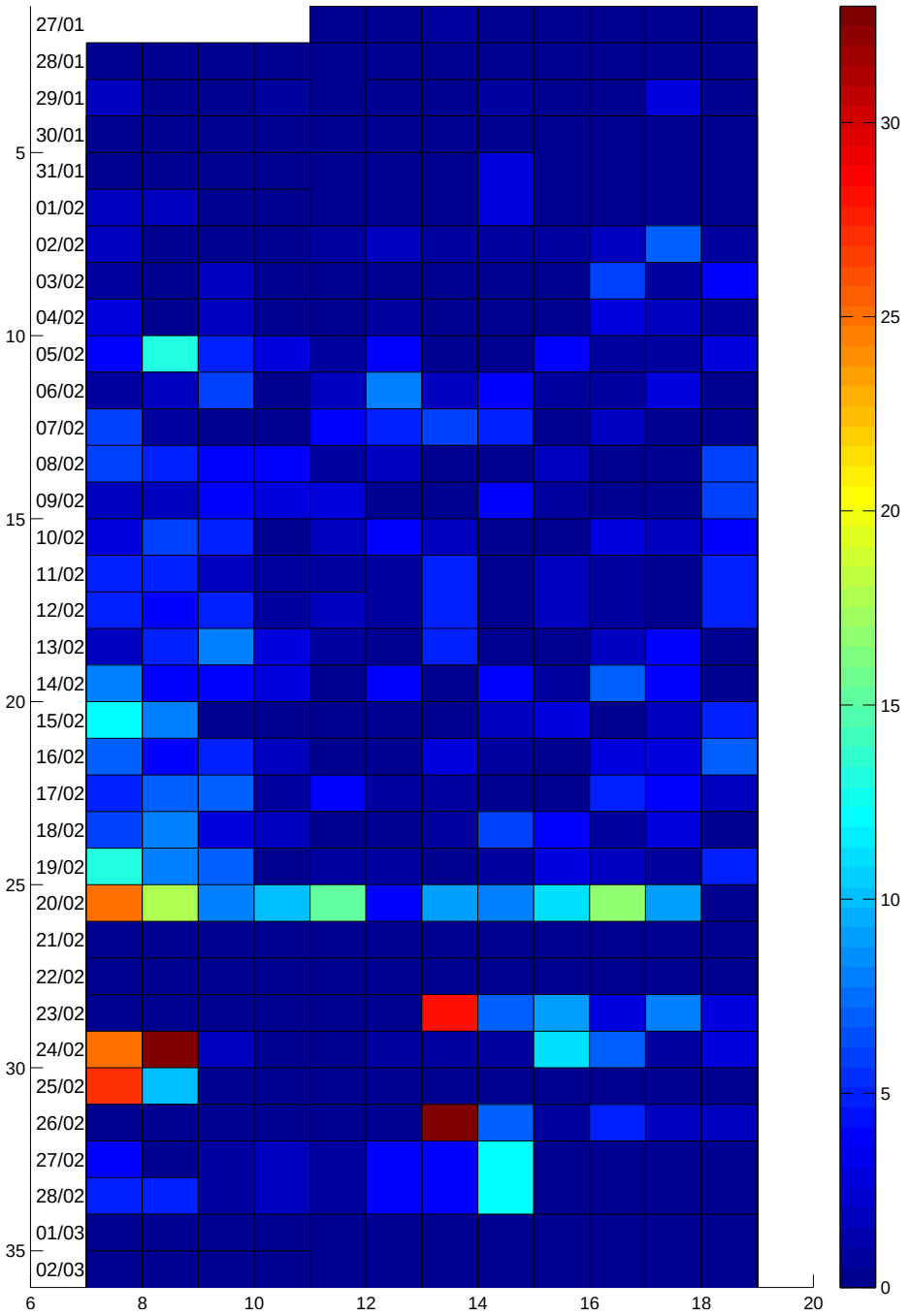

Figure 8.2: Coloured actogram of demand feeder activations throughout day time hours of the LD cycle (07:00h - 19:00h). The colour scale represents the number of activations.

feed control system was not functioning properly until it was restored on 23 February at 13:00h. The next day the swimming speed increased significantly during the feeding period between 08:00h and 09:00h as fish were attempting to compensate for missed feeding. Once fish reached apparent satiation after 09:00h, they only resumed activations later in the afternoon and the speed remained lower throughout the day. The speed also increased on the following day between 08:00h and 09:00h even though activations had commenced from 07:00h.

8.3.3 Distance From the Feeding Area

The distance of fish from the feeding area (bead location) was used to examine the relationship between activations of the demand feeder and therefore feeding, and locations of fish within the tank (Fig. C.2). It was expected that upon activation most fish would approach the feeding area and either congregate in this area searching for food or depart and make another approach. Three measures were used to examine this hypothesis: median distance, inter-quartile range and range from the feeding area for a given time sample.

The median distance was used in preference to the mean in order to detect where the majority of fish were and avoid the effects of an outlier fish which might have been at a distance from the feeding area. Similarly the inter-quartile range was used in preference to the standard deviation to avoid the influence of outliers. The range is a measure between the minimum and maximum and it would help identify extremes in fish positioning.

No consistent pattern between the distance to the feeding area and activations was found (Figure C.2 in Appendix C). The distance measure was not reflective of feeding times but it did vary with time.

A high variation in the median distance was observed on 28 January. Manual observations revealed that some fish had a preferred position in relation to the current flow (Fig. C.2ii). While initially agonistic behaviours occurred in various parts of the tank, later these behaviours changed in the afternoon with fish mainly located around the inflow area showing agonistic behaviours towards each other as observed manually.

8.3.4 Direction

The direction from the centre shows fish positioning preferences throughout the day (Figure C.3). While initially the positioning was random, after only three days fish chose an area in front of the water inlet (between 300^o and 60^o) as their

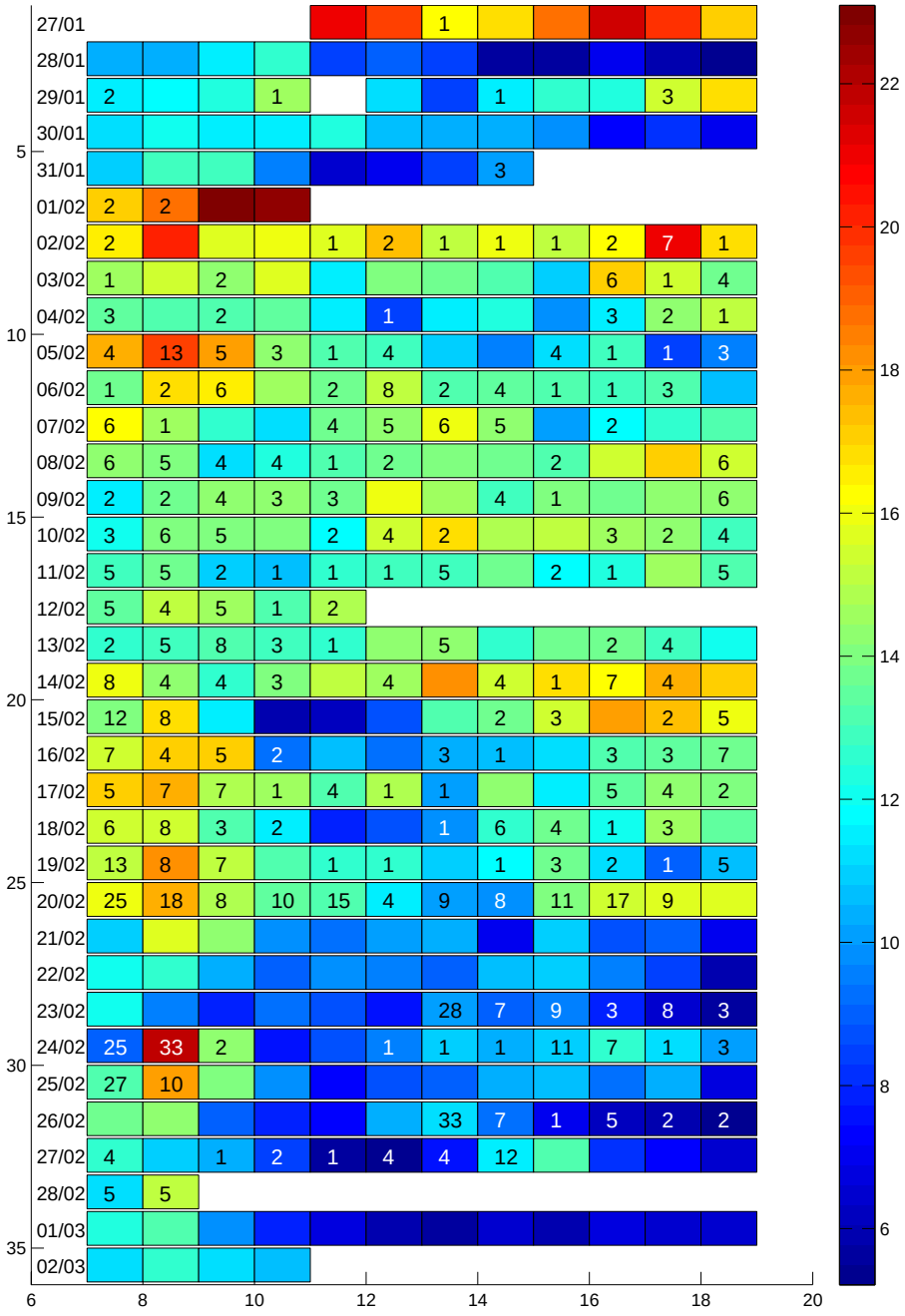

Figure 8.3: Actogram of swimming speed (07:00h - 19:00h). Each rectangle represents one hour of activity and is coloured according to the scale on the right which shows speed in pixels per second. Demand feeder activations are shown as numbers for each time period. White areas show loss of swimming speed data. From 19 Jan feed availability was restricted between 08:00h and 09:00h.

preferred position. Initial feeder activations did not affect the position of fish but over time activations brought fish into the feeding area (between 210^o and 300^o). Similar observations were made by Bégout Anras and Lagardère (2004), where fish preferred to occupy the feeding area and water inlet. This is evident from 8 February onwards. On 20 February the demand feeder was changed to restricted feeding. While the number of activations was high throughout the day, the direction of fish from the centre was similar to 15-17 and 19 February. However technical problems which affected the feeder also caused a change in fish behaviour. Direction samples were scattered throughout the day on 21-23 February when the feeder was non-operational, returning to a previous pattern on 24 February when feed became available in the morning.

8.3.5 Single Day Analysis

This subsection will provide a more detailed analysis of a single day - 24 February. This day was selected because technical difficulties with the demand feeder during previous days meant that fish had not been fed for 3 days. Their response on this particular day was therefore noticeable both in terms of speed variation and distribution of fish, and was probably associated with compensatory feeding or feeding following food deprivation.

Distribution of fish varied little throughout the day except during the morning (Fig. 8.4). During the first 30 minute block, fish activity occurred throughout the tank, while they activated the demand feeder expecting food (Fig. 8.4i). During the second 30 minute period the activity decreased, the number of activations decreased, and fish were separated from each other and were generally stationary (Fig. 8.4ii). This changed once the food became available after 09:00h. The activity increase over the next 60 minutes, as shown in Figures 8.4iii and 8.4iv, corresponded to increased number of activations and increased speed of swimming (Fig. 8.5). Once the demand feeder stopped dispensing the feed, activity decreased and fish distribution was primarily in the area of the water inlet. Sporadic feeder activations resumed after 12:30h with increased frequency between 15:00h and 16:00h but the distribution of fish and their swimming speed did not change noticeably. The distance from the feeding measure revealed only one observable change that could be related to feeding. Shortly after 09:00h the range and inter-quartile range have decreased noticeably for about 30 minutes (Fig. 8.6).

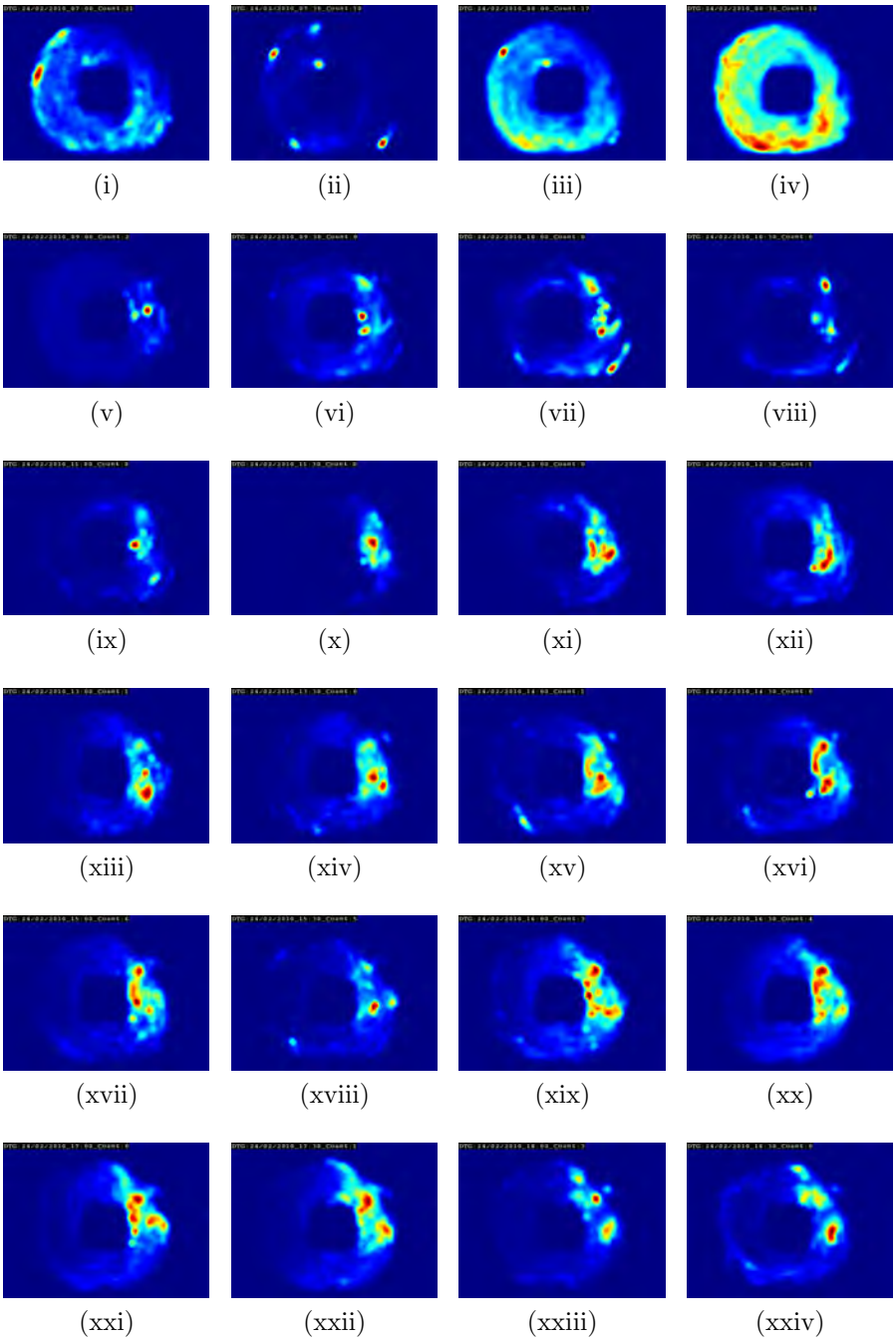

Figure 8.4: Heat maps of activity on 24 Feb 2010 starting from 0700h (each colour image represents 30 min. of activity). Images (iii), (iv) show activity when food from the demand feeder was available. The feeding area is located roughly at the bottom of each image.

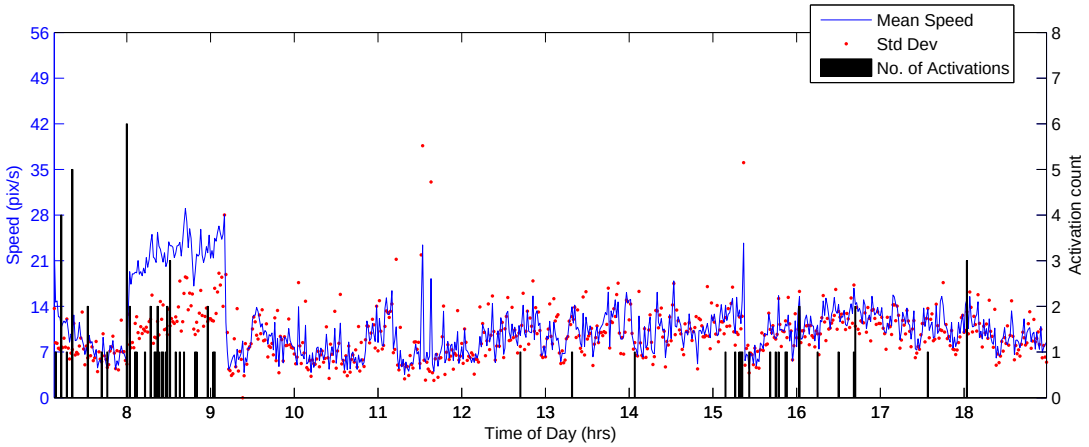

Figure 8.5: Mean swimming speed of 10 fish in a research tank on 24 Feb 2010.

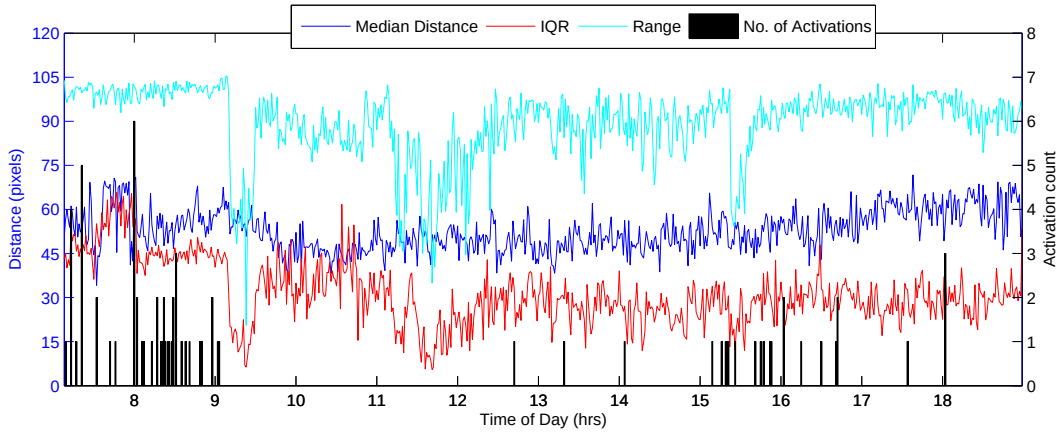

Figure 8.6: Median distance from the feeding area of 10 fish in a research tank on 24 Feb 2010.

8.4 Discussion

It was observed that initially activations of the demand feeder were random but after c. 20 days (from 15 February) fish tended to activate the feeder mainly in the morning. This confirms the observations of other researchers when using the demand feeder approach: trout develop a pattern of feeding in the morning (Bailey and Alanärä, 2006).

There was an expectation that a daily swimming speed pattern would emerge (high in the morning, low during the day, high late in the day). Such a pattern was observed on 15 February only, and on the following days it became less noticeable. Unrestricted access to food meant that fish did not have to compete for food and therefore did not have to increase their speed for longer periods. Short accelerations which occurred during feeding activations might have been smoothed within the 1 minute sampling period. (The one minute sampling period was selected to coincide with the activation sampling period of the demand feeder.) It is possible that some activities of shorter durations were not measured. On 24 February, the swimming speed during the period of feed availability was higher than during the rest of the day. Because of technical difficulties in previous days, fish had not received food for 3 days. When the food did become available between 08:00h and 09:00h, there was increased competition for food and therefore increased speed of swimming. Once food was no longer available, the high activity stopped. On the following day there was also an increase in speed up until 08:30h. After this time, activations ceased and the speed started to decrease. Activity during these two days might suggest that after a 3 days of hunger, the feeding response was stronger (compensatory feeding) than after an overnight fasting. Activity on 24 February was high because of hunger, while on 25 February, the hunger had less effect on fish. Research has shown that restricted rations created anticipation of a meal event from fish after a period of acclimatisation. This experiment was too short in duration to observe this anticipatory behaviour.

This study showed that the fish tracking system can be used in tanks on groups of fish in order to analyse daily movement patterns. While the experiment did not achieve significant aquaculture outcomes due to limitations in the access and equipment, it did demonstrate that differences in fish movement could be detected by the system.

8.5 Summary

Manually observing groups of fish in controlled tanks experiments is a tedious task and usually requires sub-sampling if experiments last for extended periods. The system proposed in this chapter demonstrated that it is possible to automatically track fish and extract useful information from the data gathered. Daily heat maps of activity, combined to run as a video sequence, provided the best visual differentiation between preferred feeding times and other times. However analysis of swimming speed could be improved upon and some suggestions are presented below.

The demand feeder activation counts were sampled at one minute intervals and therefore the swimming activity was sampled at the same interval. It is possible that this sampling rate may have obscured some agonistic activities which were very short in duration. While this system did not have the capability to differentiate between behaviours, it can detect changes of speed and direction associated with it. Decreasing the sampling to 5 or 10 seconds might reveal some instantaneous speed bursts. In addition it may be desirable to identify high speed bursts detected by the system and provide a count for a given period (per minute for example). It has been observed on video that most of the time fish were stationary and only a few fish would accelerate and exhibit agonistic behaviour. An automated count of such behaviour could perhaps show a change in behaviour that could not be observed otherwise (due to the averaging process).

Finally, feeding events usually involved surface activity and tracking of fish is difficult during this time due to multiple reflections associated with turbulent water at the surface. An alternative method is therefore required which will look at changes within an image or a sequence of images.

The next chapter of the thesis summarises findings from the thesis work, explains limitations and problems encountered and suggests paths for further research.

CHAPTER 9

CONCLUSIONS

Currently the analysis of fish behaviour in aquaculture is a manual, tedious process carried out mainly during feeding and for specific reasons. Limited by lack of technology, the analysis relies on sub-sampling at a particular time of day in order to generate meaningful and manageable data sets. The aim of this thesis was to investigate a computer vision based tracking system to analyse fish behaviours automatically and to examine its ability to detect these behaviours in experiments in sea cages and tanks. In sea cages the objective was to track individual fish for short periods of time in order to calculate an average swimming speed and direction. In tanks, the goal was to track individuals on a prolonged basis for the purpose of identifying agonistic behaviours and observing behaviours of small groups of fish.

9.1 Summary of Results

This thesis described research into a computer vision system to automate the analysis of fish behaviour in sea cages and tanks. It demonstrated that the extracted data can be meaningful if paired with environmental data (e.g. current speed, tidal cycle, lunar cycles).

9.1.1 Technology Development

Two tracking systems have been developed to detect and track fish. For sea cages, a system used image and video segmentation to detect fish and the Kalman Filter to track fish through time. To account for multiple targets, the system was enhanced with the Global Nearest Neighbour data association technique. The emphasis in selecting these methods was to keep the computational requirements low to allow for real-time operation.

Visibility in underwater footage and uneven illumination proved to be the

biggest challenges when extracting fish shapes from the background. Several segmentation techniques were investigated, with edge detection being suitable for smaller sized fish and adaptive thresholding used for larger fish. Motion segmentation could prove effective at extraction of objects if the motion of the camera could be accounted for which was not able to be performed. The camera stabilisation issue was briefly mentioned in Section 5.7 but further work will be required to investigate if the increased computational burden will be justified by increasing the number and quality of objects extracted in the framework of real-time operation. The system's strength is that it can extract and track 20-80 fish per minute. Inaccuracies of individual measurements due to the movement of the camera may be offset by the averaging process. For that reason the concept of camera stabilisation was only briefly examined. If the accuracy of the system was to be increased disregarding the computational costs, stabilising the camera through software would be beneficial but would also have to account for rotational motion (Cai and Walker, 2009) in addition to vertical/horizontal motion. Global motion patterns (Section 5.8) may be used to track fish when individuals cannot be successfully extracted from the background and tracked, for example when the density of fish is high. Again the computational expense will need to be considered when exploring real-time operation.

For the tracking of a small number of individuals in tanks, a Particle Filter was used, based on colour template matching. This method improved detection rates and allowed analysis of the manoeuvres carried out by fish. The algorithm was augmented with the Adaptive Partition method (Kreucher et al., 2005) to help minimise the number of particles needed. Two data association methods were examined, Global Nearest Neighbour (GNN) and Multidimensional Assignment (MDA). While it was expected that MDA would perform better during times of severe loss of track, performance of both methods was similar. While the system tracked two fish in the demonstrated sequences, the computational burden and the need to uniquely identify fish at all times may make it infeasible on a larger number of fish. This requirement will need to be explored in further studies of unique fish identification.

Tracking of a group of fish in tank produced better results. Without the need to uniquely identify fish at all times, the tracking system used in sea cages could be modified to suit the tank environment. This reduced the computational burden of the tracking system and allowed for long term recordings. A loss of a single track was not detrimental because the experiment looked at movements of fish as part of a group.

9.1.2 Analysis of Fish Movement in Sea Cages

The system used in sea cages is capable of gathering continuous day-time data of fish swimming speed and direction. The time-stamped dataset combined with environmental and farm related data can be used to detect changes in behaviours.

Experiments carried out demonstrated that the system was able to detect changes in fish movement influenced by environmental changes (in this case variations in tidal cycle). The schooling behaviour of Atlantic salmon smolts changed in relation to low tide. Direction changed by about 100 degrees one hour after the low tide and this change persisted for 1-2 hours. Swimming speed increased by about 1 bl/s during low tide. While it was not possible to measure the current strength during many of these experiments, the measured behaviours shifted daily by an hour which suggests a strong influence of the tide. Experiment 4 in Chapter 6 was the only one to use a water current meter and confirmed a relationship between the current direction and flow and the swimming speed and direction of fish. It also established a relationship between the water current measured by the meter and tide times supplied by the Australian Bureau of Meteorology (BOM). While there was a delay between these measures, this might be attributed to the unique conditions at the farm. Results from Experiment 4 do not change the interpretation of earlier experiments in relation to tides - the one hourly shift in behaviour each day was still observed and this is most likely attributed to the tides. The influence of tides on fish behaviour observed during this research is is in-line with comments made by Van Diemen Aquaculture employees based on their experiences of the local farm conditions.

Interestingly, experiments carried out in sea cages did not detect any observable influences of feeding or time of day on fish activity. In contrast, Kadri et al. (1991) observed that for fish with a mean weight of 1.09 kg, the time of the day has a greater influence than the tide with fish more active in the morning and the evening than during the middle of the day. Similar observations were reported by Blyth et al. (1993). It is important to note that the experiment of Kadri et al. (1991) was carried out in the northern hemisphere summer, while smolts in this thesis were recorded in the southern hemisphere autumn. Therefore the age of fish, time of the year and environmental conditions could explain why swimming speed patterns observed by Kadri et al. (1991) were not detected during the experiments described here. Furthermore Smith et al. (1993) conducted a longer term study (autumn to spring) at the site used by Kadri et al. (1991) and found that daily patterns varied with seasons. They also noted that water clarity and the cloud cover might have influenced results observed by Kadri et al. (1991). Another possibility for results obtained in this thesis is that when smolts were fed 5 times a day, they did not have a need to increase the swimming speed in

search of food and did not have to compete for food. Smith et al. (1993) also suggested that swimming speed may not be a reliable indicator of appetite under some conditions and perhaps that is what has been observed in this experiment.

Differences in behaviour of smolts before and after schooling have clearly been observed in Experiment 3 in Chapter 6. The change from non-schooling behaviour to schooling behaviour was quite sudden, but the exact day of the transition could not be identified due to equipment failure. This sudden change is in contrast to what farm operators perceive. Their perception is that the change is more gradual. This may be because observations are made only during feeding times. Indeed Fig. 6.8 and 6.9 do show some evidence of uniform direction for brief periods during first few weeks. An interesting observation was made that a transition from non-schooling to schooling occurred during or very close to full Moon. If the Moon phase is relevant it raises the possibility that transfer from a hatchery to a sea cage could be planned around Moon phases to minimise the time it takes for fish to commence schooling behaviour, producing a positive effect not only on fish management but possibly on fish welfare. This hypothesis could be investigated in a separate study using the monitoring system developed during this thesis.

9.1.3 Tracking of Fish in Research Tanks

In research tanks the objective of tracking individuals uniquely through long video sequences proved too difficult to achieve. While the system developed is capable of detecting and tracking fish through most interactions, when a data association error is made, the system has no mechanism to recover from it. Section 9.4 will elaborate further on how this may be addressed.

While tracking a group of fish in a tank was generally successful, no clear patterns have emerged in the preliminary experiments carried out. The experiment experienced technical problems with the demand feeder failures making it difficult to interpret results. There was an indication that fish were more active in the morning after several weeks of learning how to activate the demand feeder. The experiment did demonstrate the ability of this system to produce appropriate output for fish activity. Heat maps can be used to observe spatio-temporal changes during experiments and indicate a measure of activity. Swimming speed can be another indication of instantaneous activity patterns. The system may have a useful application in experiments where different groups of fish need to be compared (i.e. disease challenge). The output could be analysed visually or statistically depending on requirements.

9.2 Limitations of Video Analysis in Aquaculture

Several limitations have been observed while using video technology for underwater analysis. While these limitations are also applicable to manual observation, they have even greater impact on the application of computer vision techniques. In addition there are limitations which affect computer vision techniques specifically and they are summarised in Table 9.1. This section will highlight these concerns to give an understanding of challenges involved when designing video based aquaculture experiments.

Table 9.1: Limitations of video technology in marine environment and considerations required when applying computer vision techniques in aquaculture research.

Video Limitations	**Computer Vision Limitations**
Day-time only	Motion of the camera
Turbidity	Uneven illumination
Field of view	Orientation of the camera
Reflections	Density of the fish
	Size of the fish

9.2.1 Video Limitations

Typical video cameras can only be utilised during daylight hours. While light conditions can be controlled in tank experiments, on a farm the daylight period is dependent on the season of the year, so for long experiments the daily length of recordings will vary. The ability of low light cameras to capture footage at night in sea cages is limited to experiments where artificial lights are used so that 24-hour light conditions exist. However, artificial light sources may be positioned differently to the sun in relation to the camera and this means that a computer vision system which can analyse day-time footage may perform poorly on artificially lit night-time footage. Infra-red performs poorly in the underwater imaging due to absorption of infra-red in the water. The most promising alternative which would allow 24-hour coverage is Dual-frequency IDentification SONar (DIDSON) from Sound Metrics Corp. However the price of DIDSON is around 40 times more than a video camera system and so it may not be viable for deployment on aquaculture farms but could be used in aquaculture research if funds were available. DIDSON can also work in high turbidity conditions where visibility for normal cameras decreases significantly but its ability to penetrate a school of fish would need to be investigated.

Field of view is a consideration when employing cameras in aquaculture experiments. Wide lens cameras are commonly used but care is required to ensure that lens distortion will not affect the analysis of the experiments. In sea cages depth also has an impact on the field of view. A camera placed near the surface facing up will not view many fish and those viewed may not accurately represent the overall behaviour of fish in the cage. However if the camera is too deep, the system is likely to track only fish which swim down deep in the water column and again the behaviours detected may not be representative of the wider population. Ideally the camera would be placed somewhere in between to capture a range of behaviours and provide the best generalisation of the population. Multiple cameras could be used at different depths to capture behaviours specific to certain depths, with performance exceeding single camera system.

Reflections are most problematic for analysis in tanks where the camera is placed out of the water, with reflections occurring at the air/water boundary above the tank. It is important to place lights in positions where reflections due to the movement of the water will be minimised, otherwise the analysis, manual or automated, will be difficult. However care needs to be taken because manipulation of light position may alter the normal or accepted rearing conditions.

9.2.2 Computer Vision Limitations

Analysis of underwater video using computer vision techniques has additional limitations. A camera in a sea cage is likely to be in constant motion (however small) due to movement of the water and a cage. More severe movement tends to be caused by fish bumping into the camera or the camera cable. This produces momentary, but severe, movement during which tracking is not possible. While it is possible to ignore this movement if it is not too adverse in time or total movement intensity, camera stabilisation algorithms may have to be applied. One has to consider not only horizontal or vertical motion of the camera but also more complicating rotational motion.

Orientation of the camera can also be important. A direction measurement can be difficult to interpret because relative direction will change if the camera is turned around. Hence it is more informative to use standard deviation of direction to see the tendency of fish movement. But if an experimental set-up could ensure that the camera is always in the same orientation (or that the orientation can be computed), direction could provide additional information about fish movement relative to the layout of the cage, direction of the water current or position of the feeding station.

Density and size of the fish may have an impact on the detection rates. Large

fish at high density may cause two fish to be detected as one and a single fish may obstruct the camera more often (hence placement of the camera is important). Lower density sea cages are likely to provide better tracking results as fish will be more separated from each other. Small fish may render some segmentation techniques ineffective but edge detection can return a reasonable number of samples. At times when fish cannot be tracked due to high density, global motion, described in Section 5.8, could be used to identify motion patterns. This technique could also be complementary to the tracking of fish if it provides additional data about fish movement. However the computational cost of the technique may make it currently unfeasible for real-time operation.

9.3 Significance

The thesis is an important first step to leveraging video technology to enhance aquaculture research and commercial aquaculture operations. The computer vision system presented in this thesis is the first of its kind.

Despite the previously mentioned limitations of the system, it has a potential to aid in farm management as a fish behaviour monitoring tool. Farm operators are familiar with and used to video technology, and the low cost per cage means that it can be widely deployed. The system could be used to identify baseline behaviours in various conditions and could then act as an alarm system if unusual behaviours were detected. This could help protect fish from predator attacks, detect disease outbreaks early and possibly assist in feeding optimisation. In addition, the fish movement could be used as an Operational Welfare Index and when combined with other indices, it could be used by fish welfare researchers to develop an integrated welfare assessment system for use on farms (Oppedal et al., 2011).

The system can become part of aquaculture projects where observation of fish behaviour is required because it offers aquaculture researchers an automated collection of large amounts of fish movement data at a very high sampling rate. Such a capability potentially allows researchers to focus on analysing the movement data rather than spending significant amount of resources on extracting it from video, therefore accelerating the rate of research.

9.4 Further Work

Further research on this topic should focus on improving the detection and tracking in a variety of conditions encountered on commercial farms. The system will need to deal with different fish sizes and densities which may affect the number of tracks obtained per sampling period.

The tracking system may benefit most from the addition of camera stabilisation. Section 5.7 presented a solution to stabilise vertical and horizontal movement though the manual observation of video footage has shown the need for rotational stabilisation (Cai and Walker, 2009). The stabilisation may improve video segmentation as the background subtraction methods will produce improved detection of shapes and fewer false/shadow shapes which were due to camera motion. Segmentation may also be improved by combining several methods together and creating a hybrid method; however care needs to be taken to ensure that the hybrid method is still fast enough to allow real-time operation. Stabilisation may also improve the accuracy of the tracking system as the motion model of fish will be more linear and Kalman Filter will have a smaller estimated covariance. The estimated covariance for each tentative track could also be used to determine if the track should become a confirmed target. Rather than tracking for 8 consecutive frames before the decision is made whether the track is a confirmed target (See Subsection 5.4.2), the use of covariance would allow for a dynamic decision based on a covariance threshold. The threshold would be determined empirically and only tentative tracks below the threshold would become confirmed targets. Similarly, if the covariance of the confirmed target increased above a certain threshold (not necessarily the same threshold as for tentative tracks), the target could be deleted. This would decrease the number of detections per sampling period but the remaining detections would be more accurate.

In the sea cage tracking system, eccentricity has been used as a feature to select candidate shapes. It is a simple measure but may not be the most effective. Another measure which could be added is solidity, which is a ratio between the area of the shape and the convex area of the shape. This method may eliminate shapes which include multiple fish, camera cable or debris in the water. Additionally comparison of texture measures (range, standard deviation or entropy) may be used to distinguish fish shapes from non-fish shapes. However the poor quality of video footage (due to low resolution and particles in the water) may make this approach impractical.

There may also be times when detecting and tracking fish in sea cages will not be possible. Section 5.8 was an initial investigation into Motion Flows, which

could give an indication of motion within a video sequence. Supertracks from neighbouring video sequences could be compared and a change threshold established. It is also possible that events like feeding or predator attacks may produce a unique set of motion patterns and therefore supertrack. This technique could be supplemental to actual tracking of fish and could also be used in video analysis of marine life within the marine science field.

A further long term goal is to produce a stand alone real-time system. Prolonged data gathering would then be possible, and the system could be used to detect behavioural patterns in data. Pattern detection could be used to distinguish usual and unusual fish behaviours and classify these behaviours. Such a system could be used as an alarm system to warn farmers of possible disease outbreaks, predator attacks, changing behaviour due to environmental changes and it could help optimise feeding management.

From the aquaculture research point of view, the transfer of smolts from hatchery to sea cage could be further investigated in relation to lunar cycles, to determine if the full Moon has a role to play in the commencement of smolt schooling behaviour. Because the behaviour of Atlantic salmon is influenced by many variables, long term lunar cycle analysis would be needed while recording other environmental data. These data could be used to identify not only influences of the moon but also examine the effect of different environmental variables, like time of the day, seasons, feeding, temperatures, salinity, visibility and oxygen levels and so on.

In tanks the major issue is that of data association after prolonged loss of tracks and when multiple targets overlap for extended periods. The inability of the data association to recover from an error of association is a major impediment to prolonged tracking. The system could be augmented by using a tagging system (acoustic, PIT or low frequency RFID). While the original objective of this study was to develop a non-invasive system based on video, this was not achieved. However current generation tags are of very small size and are likely to have minimal effect on physical attributes of fish. To maintain the non-invasive principle of fish behaviour analysis in tanks, a high resolution video system could be used. This could provide additional features that could be used to distinguish fish uniquely.

Another improvement to tracking individuals in tanks may be modifications to the particle filter. Rectangular particle vectors could be replaced with ellipsoidal particle vectors. The orientation and eccentricity could play an important role in determining the best particles. Furthermore, Active Shape Models (Cootes and Taylor, 2001) could be used to define the fish shape and possible deformations of the shape. However the state vector would contain more elements and therefore

the number of particles required for effective tracking would need to increase (as per the curse of dimensionality mentioned by Daum and Huang (2003)).

Computer vision systems investigated in this thesis open up new possibilities in terms of acquisition of new knowledge about fish behaviour. For researchers, a continuous observation of fish movement allows analysing a greater amount of data without substantial human effort. Instead the time can be spent on the interpretation of data gathered against multiple environmental variables. For commercial operators, the outcome of this research can act as a tool to aid farm management, provide an alarm system if unusual behaviours are detected and provide real-time monitoring of fish.

Appendices

APPENDIX A

PARTICLE FILTER PSEUDO CODE

Table A.1: **Colour Particle Filter Pseudo Code (Czyz et al., 2007).**

$\left[\{y_k^n\}_{n=1}^N\right] = PF\left[\{y_{k-1}^n\}_{n=1}^N, z_k\right]$
1) Transitions of E_{k-1} variable
$\left[\{E_k^n\}_{n=1}^N\right] = ETrans\left[\{E_{k-1}^n\}_{n=1}^N, \Pi\right]$
2) FOR $n = 1 : N$
a) Based on (E_{k-1}^n, E_k^n) pair, draw at random $x_{1,k}^n, ..., x_{E_k^n,k}^n$
b) Evaluate importance weight $\tilde{w}_k^n$
END FOR
3) Normalise importance weights
a) Calculate total weight: $t = \sum_{n=1}^N \tilde{w}_k^n$
b) FOR $n = 1 : N$
Normalise: $w_k^n = t^{-1}\tilde{w}_k^n$
END FOR
4) Resample:
$\left[\{y_k^n, -, -\}_{n=1}^N\right] = RESAMPLE\left[\{y_k^n, w_k^n\}_{n=1}^N\right]$
5) Compute the output of the PF

Table A.2: **Independent Partition Pseudo Code (Kreucher et al., 2005).**

1) For each partition, $t = 1...T_{max}$,
   a) Propose partition t via Independent Partition Subroutine
2) Compute $w_p^k = w_p^{k-1} \frac{p(z|X_p)}{\prod_{t=1}^{T_p} b_{p,t}}$

Independent Partition Subroutine for Target t:

1) For each particle $p = 1, ..., N$,
   a) Sample $X_{p,t}^* \sim p(X_{p,t}^k | X_{p,t}^{k-1})$
   b) Compute $w_p = p(z|X_{p,t}^*)$
2) Normalise w_p to sum to 1, $w_p \leftarrow w_p / \sum_{i=1}^N w_i$
3) For each particle $p = 1, ..., N$
   a) Sample an index j from the distribution defined by w
   b) Set $X_{p,t} = X_{j,t}^*$
   c) Retain bias of sample, $b_{p,t} = w_j$

Table A.3: **Coupled Partition Pseudo Code (Kreucher et al., 2005).**

1) For each partition, $t = 1...T_{max}$
   a) Propose partition t via Coupled Partition Scheme
2) Compute $w_p^k = w_p^{k-1} * \frac{p(z|X_p)}{\prod_{t=1}^{T_p} b_{p,t}}$

Coupled Partition Subroutine for Target t

1) For each particle $p = 1, ..., N$
   a) For each proposal $r = 1, ..., R$
      i) Sample $X_{p,t}^*(r) \sim p(X_{p,t}^k | X_{p,t}^{k-1})$
      ii) Compute $w_r = p(z|X_{p,t}^*(r))$
   b) Normalise w_r to sum to 1, $w_r \leftarrow w_r / \sum_{i=1}^R w_i$
   c) Sample an index j from the distribution defined by w
   d) Set $X_{p,t} = X_{p,t}^*(j)$
   e) Retain bias of sample, $b_{p,t} = w_j$

Table A.4: **Adaptive Partition Pseudo Code (Kreucher et al., 2005).**

1) For each partition $t = 1 : T_{max}$
   a) $d(t) = min_{j \neq t} \|\hat{x}_t - \hat{x}_j\|$
   b) if $d(t) > \tau$
      Propose partition t using IP method
   c) else
      Propose partition t using CP method
2) For each particle $p = 1, ..., N, w_p^k = w_p^{k-1} * \frac{p(z|X_p)}{\prod_{t=1}^{T_p} b_{p,t}}$

Table A.5: **Regime Transition (Ristic et al., 2004).**

$\left[\{E_k^n\}_{n=1}^N\right] = \mathrm{RT}\ \left[\left\{E_{k-1}^n\right\}_{n=1}^N, \Pi\right]$

FOR $i = 1 : s$
  $c_i(0) = 0$
  FOR $j = 1 : s$
    $c_i(j) = c_i(j-1) + \pi_{ij}$
  END FOR
END FOR
FOR $n = 1 : N$
  Draw $u_n \sim U[0,1]$
  Set $i = E_{k-1}^n$
  $m = 1$
  WHILE $(c_i(m) < u_n)$
    $m = m + 1$
  END WHILE
  Set $E_k^n = m$
END FOR

APPENDIX B

TIDAL, FEEDING AND ENVIRONMENTAL DATA FOR SEA CAGE EXPERIMENTS

B.1 Tide experiment - 10-15 April 2008

Table B.1: Tide times for tide recording.

	Tide			
Date	**High**	**Low**	**High**	**Low**
10-Apr	2:52	9:30	15:47	22:01
11-Apr	3:45	10:22	16:40	22:51
12-Apr	4:37	11:13	17:30	23:41
13-Apr	5:28	12:02	18:17	
14-Apr	6:19	12:52	19:04	0:30
15-Apr	7:11	13:44	19:52	1:20

Table B.2: Meal times for tide recording. Meals were 40%, 20%, 40% of the daily intake respectively.

	Meal Time		
Date	**1**	**2**	**3**
10-Apr	0700-0815	1245-1345	1830-1945
11-Apr	0700-0815	1245-1345	1830-1945
12-Apr	0700-0815	1245-1345	1830-1945
13-Apr	0700-0815	1245-1345	1830-1945
14-Apr	0700-0815	1245-1345	1830-1945
15-Apr	0700-0815	1245-1345	1830-1945

B.2 Freshwater bathing experiment - 21st Jan - 19th Feb 2009

Table B.3: Tide times for freshwater bathing recordings.

	Tide					Tide			
Date	**High**	**Low**	**High**	**Low**	**Date**	**High**	**Low**	**High**	**Low**
21-Jan	7:36	1:46	20:25	14:16	**08-Feb**	9:32	3:45	22:39	16:24
22-Jan	8:15	2:30	21:09	14:59	**09-Feb**	10:39	4:51	23:45	17:30
23-Jan	8:58	3:14	21:57	15:43	**10-Feb**	11:50	6:02		18:38
24-Jan	9:45	4:01	22:48	16:30	**11-Feb**	0:51	7:13	13:03	19:44
25-Jan	10:35	4:52	23:41	17:20	**12-Feb**	1:53	8:18	14:13	20:45
27-Jan	0:32	6:42	12:22	19:03	**13-Feb**	2:50	9:17	15:15	21:40
28-Jan	1:21	7:34	13:14	19:51	**14-Feb**	3:42	10:09	16:11	22:29
29-Jan	2:06	8:22	14:03	20:36	**15-Feb**	4:27	10:55	17:00	23:13
30-Jan	2:47	9:06	14:52	21:19	**16-Feb**	5:09	11:37	17:45	23:54
31-Jan	3:27	9:49	15:40	22:02	**17-Feb**	5:47	12:17	18:27	
01-Feb	4:05	10:31	16:27	22:45	**18-Feb**	6:24	12:56	19:06	0:32
07-Feb	8:30	2:44	21:34	15:22	**19-Feb**	7:00	13:34	19:45	1:11

Table B.4: Meal times for freshwater bathing recordings. Meal percentages were 30%, 20%, 20%, 30% of the daily ration.

	Meal Time			
Date	**1**	**2**	**3**	**4**
21-Jan	0615-0815	1015-1215	1430-1630	1845-2045
22-Jan	0615-0815	1015-1215	1430-1630	1845-2045
23-Jan	0615-0815	1015-1215	1430-1630	1845-2045
24-Jan	0645-0845	1015-1145	1345-1515	1645-1845
25-Jan	0630-0830	1015-1200	1400-1600	
27-Jan	0615-0815	1015-1215	1430-1630	1845-2045
28-Jan	0615-0815	1015-1215	1430-1630	1845-2045
29-Jan	0615-0815	1015-1215	1430-1630	1845-2045
30-Jan	0615-0815	1015-1215	1430-1630	1845-2045
31-Jan	0645-0845	1015-1145	1345-1515	1645-1845
01-Feb	0645-0845	1015-1145	1345-1515	1645-1845
07-Feb	0645-0845	1015-1145	1345-1515	1645-1845
08-Feb	0645-0845	1015-1145	1345-1515	1645-1845
09-Feb	0615-0815	1015-1215	1430-1630	1845-2045
10-Feb	0615-0815	1015-1215	1430-1630	1845-2045
11-Feb	0615-0815	1015-1215	1430-1630	1845-2045
12-Feb	0615-0815	1015-1215	1430-1630	1845-2045
13-Feb	0615-0815	1015-1215	1430-1630	1845-2045
14-Feb	0645-0845	1015-1145	1345-1515	1645-1845
15-Feb	0645-0845	1015-1145	1345-1515	1645-1845
16-Feb	0615-0815	1015-1215	1430-1630	1845-2045
17-Feb	0615-0815	1015-1215	1430-1630	1845-2045
18-Feb	0615-0815	1015-1215	1430-1630	1845-2045
19-Feb	0615-0815	1015-1215	1430-1630	1845-2045

Table B.5: Environmental data for freshwater bathing recordings.

	D.O (mg/l)		D.O. Sat (%)		Visibility (m)		Temp (°C)	
Date	**AM**	**PM**	**AM**	**PM**	**AM**	**PM**	**AM**	**PM**
21-Jan	7.4	7.4	92	98	2.7	2.5	18.3	19
22-Jan	7.2	7.6	91	97	2.8	2.2	18.5	19
23-Jan	6.9	7.3	87	92	2.6	2.8	18.3	18.8
24-Jan	7	8.3	88	105	3	2.7	18.3	18.8
25-Jan	8.1	8.2	103	103	2.8	2.8	18.5	18.7
27-Jan	7.9	8	100	100	2.8	3	18.8	18.8
28-Jan	7.3	7.5	94	96	2.8	3	19	19.4
29-Jan	7	6.9	90	91	2.7	3.5	19.1	19.8
30-Jan	6.5	6.9	85	94	3	3.1	19.6	19.8
31-Jan	6.7	6.8	90	89	2.9	2.4	20	20
01-Feb	6.7	6.8	88	88	2.5	2.8	20.4	20.3
07-Feb	6.9	6.8	90	92	2.6	2.4	20.3	21.1
08-Feb	6.5	6.7	87	89	2.2	2.5	20.7	21
09-Feb	6.36	7	87	91	2.1	2	20.4	20.6
10-Feb	6.7	6.9	88	90	2.2	2.2	20.3	20.6
11-Feb	7	7	91	92	2.5	2.2	20.2	19.9
12-Feb	6.6	6.8	87	87	1.8	1.8	19.9	20.1
13-Feb	6.8	6.9	89	89	2.1	2.2	20	19.8
14-Feb	6.8	7.1	89	89	2.3	2.5	19.6	20
15-Feb	7	7	90	92	2.1	2.4	18.8	20
16-Feb	6.9	7	91	88	2.6	2.4	19.5	19.4
17-Feb	6.8	7	90	91	2.3	2.4	19.6	19.8
18-Feb	7	7.1	90	92	2.9	2.8	19.2	19.7
19-Feb	6.6	7	84	91	2.6	2.4	19.3	19.7

B.3 Smolt experiment - 21st April 2009 - 31th May 2009

Table B.6: Tide times for smolt recordings.

	Tide					Tide			
Date	**High**	**Low**	**High**	**Low**	**Date**	**High**	**Low**	**High**	**Low**
21-Apr			20:27		**12-May**	1:54	8:29	14:47	21:00
22-Apr	8:44	15:11	21:14	2:52	**13-May**	2:35	9:08	15:28	21:37
23-Apr	9:42	16:07	22:05	3:45	**14-May**	3:15	9:46	16:05	22:14
24-Apr	10:45	17:08	23:01	4:43	**15-May**	3:54	10:24	16:42	22:51
25-Apr	11:50	18:11	23:58	5:43	**16-May**	4:33	11:01	17:17	23:29
26-Apr	12:54	19:13		6:42	**17-May**	5:12	11:40	17:52	
27-Apr	0:55	7:38	13:54	20:10	**18-May**	5:53	12:19	18:28	0:08
28-Apr	1:49	8:32	14:49	21:04	**19-May**	6:35	13:00	19:05	0:48
29-Apr	2:44	9:25	15:43	21:55	**20-May**	7:22	13:45	19:45	1:32
30-Apr	3:36	10:15	16:32	22:45	**21-May**	8:14	14:34	20:30	2:20
01-May	4:29	11:05	17:21	23:34	**22-May**	9:12	15:30	21:21	3:13
02-May	5:21	11:55	18:08		**23-May**	10:15	16:31	22:17	4:09
03-May	6:14	12:45	18:55	0:24	**24-May**	11:21	17:36	23:17	5:08
04-May	7:09	13:37	19:44	1:15	**25-May**	12:26	18:41		6:09
05-May	8:07	14:31	20:34	2:10	**26-May**	13:28	19:44	0:18	7:09
06-May	9:08	15:30	21:28	3:07	**27-May**	1:19	8:07	14:27	20:42
07-May	10:12	16:30	22:23	4:06	**28-May**	2:18	9:03	15:22	21:37
08-May	11:16	17:33	23:20	5:06	**29-May**	3:17	9:58	16:15	22:30
09-May	12:18	18:34		6:04	**30-May**	4:15	10:50	17:04	23:23
10-May	0:15	6:58	13:14	19:29	**31-May**	5:12	11:42	17:52	
11-May	1:07	7:45	14:03	20:17	**01-Jun**	6:09	12:32	18:39	0:15

Table B.7: Meal times for smolt recordings. All meals were 20% of the daily intake.

	Meal Time				
Date	**1**	**2**	**3**	**4**	**5**
22-Apr	645-800	915-1030	1145-1300	1415-1530	1630-1745
23-Apr	645-800	915-1030	1145-1300	1415-1530	1630-1745
24-Apr	645-800	915-1030	1145-1300	1415-1530	1630-1745
25-Apr	645-800	915-1030	1145-1300	1415-1530	1630-1745
26-Apr	645-800	915-1030	1145-1300	1415-1530	1630-1745
27-Apr	645-800	915-1030	1145-1300	1415-1530	1630-1745
28-Apr	645-800	915-1030	1145-1300	1415-1530	1630-1745
29-Apr	645-800	915-1030	1145-1300	1415-1530	1630-1745
30-Apr	645-800	915-1030	1145-1300	1415-1530	1630-1745
01-May	645-800	915-1030	1145-1300	1415-1530	1630-1745
02-May	645-800	915-1030	1145-1300	1415-1530	1630-1745
03-May	645-800	915-1030	1145-1300	1415-1530	1630-1745
04-May	645-800	915-1030	1145-1300	1415-1530	1630-1745
05-May	700-815	930-1045	1200-1315	1415-1530	1630-1730
06-May	700-815	930-1045	1200-1315	1415-1530	1630-1730
07-May	700-815	930-1045	1200-1315	1415-1530	1630-1730
08-May	700-815	930-1045	1200-1315	1415-1530	1630-1730
09-May	700-815	930-1045	1200-1315	1415-1530	1630-1730
10-May	700-815	915-1030	1145-1300	1400-1515	1600-1715
11-May	700-815	915-1030	1145-1300	1400-1515	1600-1715
12-May	700-815	915-1030	1145-1300	1400-1515	1600-1715
13-May	700-815	915-1030	1145-1300	1400-1515	1600-1715
14-May	700-815	915-1030	1145-1300	1400-1515	1600-1715
15-May	700-815	915-1030	1145-1300	1400-1515	1600-1715
16-May	700-815	915-1030	1145-1300	1400-1515	1600-1715
17-May	700-815	915-1030	1145-1300	1400-1515	1600-1715
18-May	700-815	915-1030	1145-1300	1400-1515	1600-1715
19-May	700-815	915-1030	1145-1300	1400-1515	1600-1715
20-May	700-815	915-1030	1145-1300	1400-1515	1600-1715
21-May	700-815	915-1030	1145-1300	1400-1515	1600-1715
22-May	700-815	915-1030	1145-1300	1400-1515	1600-1715
23-May	700-815	915-1030	1145-1300	1400-1515	1600-1715
24-May	700-815	915-1030	1145-1300	1400-1515	1600-1715
25-May	700-815	915-1030	1145-1300	1400-1515	1600-1715
26-May	700-815	915-1030	1145-1300	1400-1515	1600-1715
27-May	700-815	915-1030	1145-1300	1400-1515	1600-1715
28-May	700-815	915-1030	1145-1300	1400-1515	1600-1715
29-May	700-815	915-1030	1145-1300	1400-1515	1600-1715
30-May	700-815	915-1030	1145-1300	1400-1515	1600-1715
31-May	700-815	915-1030	1145-1300	1400-1515	1600-1715

Table B.8: Environmental data for smolt recordings.

	D.O (mg/l)		D.O. Sat (%)		Visibility (m)		Temp (°C)	
Date	**AM**	**PM**	**AM**	**PM**	**AM**	**PM**	**AM**	**PM**
22-Apr	7.3	7.3	88	89	4	4	16.2	16.3
23-Apr	7.3	7.2	89	88	3.8	3.7	16.1	16.2
24-Apr	7.3	7.5	88	91	4	3.5	16.2	16.1
25-Apr	7.5	7.5	89	88	3.8	3.7	16	16.1
26-Apr	7.6	7.4	94	90	3.6	3.2	15.9	16
27-Apr	7.2	7.9	85	92	3.8	3.6	15.5	15.4
28-Apr	7.8	7.8	92	92	2.8	2.8	15.1	15.1
29-Apr	7.4	7.8	86	90	2.8	3	14.9	14.9
30-Apr	8	8	91	93	3	3.2	14.5	14.6
01-May	8.2	8.2	93	92	3.2	3	14.5	14.5
02-May	8.1	7.9	93	91	3	3.1	14.4	14.3
03-May	7.5	7.9	85	92	3	2.8	14.3	14.3
04-May	7.6	7.9	87	91	2.6	3.2	14.3	14.3
05-May	7.4	7.6	84	87	3.8	3.4	14.2	14.2
06-May	6.6	7.2	76	84	3.2	3.6	14.1	14.2
07-May	7.5	7.7	87	90	3.2	3.6	14.1	14.2
08-May	7.5	7.8	88	90	4	4.2	13.9	14
09-May	7.7	7.7	89	90	3.8	4	13.9	14.1
10-May	7.4	7.6	85	89	3	3.2	13.8	14
11-May	7.3	7.3	84	85	4	3.8	13.8	14
12-May	7.5	7.5	87	88	3.4	4	13.8	14
13-May	7.8	7.9	85	92	3.2	3.5	13.8	13.9
14-May	7.8	7.6	91	89	4	4	13.7	13.8
15-May	7.8	7.8	89	90	3.2	3	13.6	13.7
16-May	7.7	8.1	89	92	4	4.2	13.4	13.5
17-May	7.6	7.9	87	89	4	3.8	13.2	13.3
18-May	7.8	7.9	89	91	4.4	5	13.1	13.1
19-May	7.9	8.2	89	93	3.4	3.8	13.1	13
20-May	7.8	7.9	89	90	3.4	3.6	12.9	13
21-May	7.9	8.3	93	94	4.6	4.4	13	12.9
22-May	7.5	8.2	86	92	5.2	5.2	13	12.8
23-May	8.1	8.5	85	93	5.1	5.2	12.9	12.9
24-May	7.6	7.9	87	90	5.8	5.4	13.1	13.1
25-May	7.6	7.7	87	88	4.2	5	13	13.4
26-May	8.1	8.3	92	96	3.8	3.8	13.1	13.4
27-May	7.2	8	82	90	3.8	3.8	13	13.5
28-May	8.1	8.3	93	95	2.8	3.2	13	13.2
29-May	8.1	8.4	90	96	3	3.1	12.6	12.9
30-May	7.8	7.7	89	87	3.2	2.8	12.7	12.9
31-May	8	7.9	91	90	3.6	3.6	12.8	12.6

APPENDIX C

SMALL GROUPS IN TANKS GRAPHS

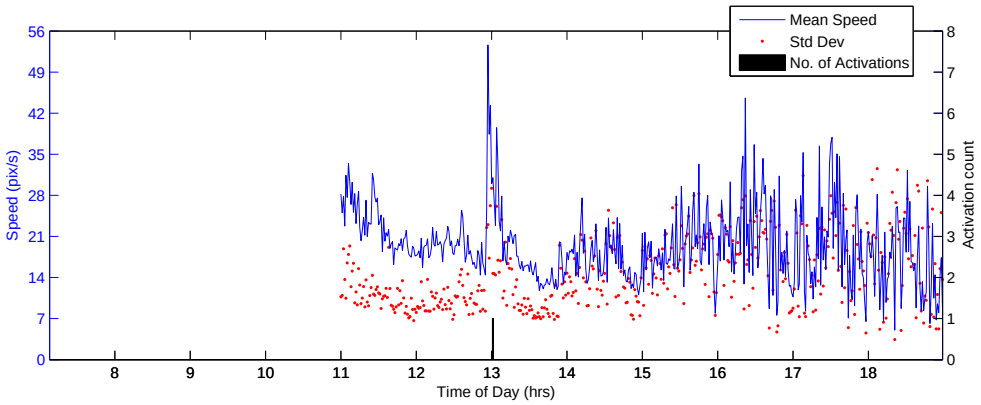

(i) 27 January

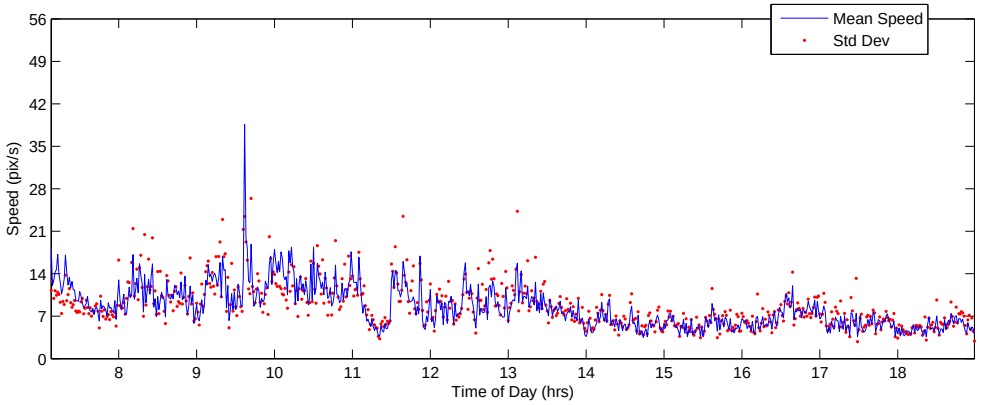

(ii) 28 January

Figure C.1: Average swimming speed from 10 fish in a research tank during 35 days (27 Jan - 2 March 2010).

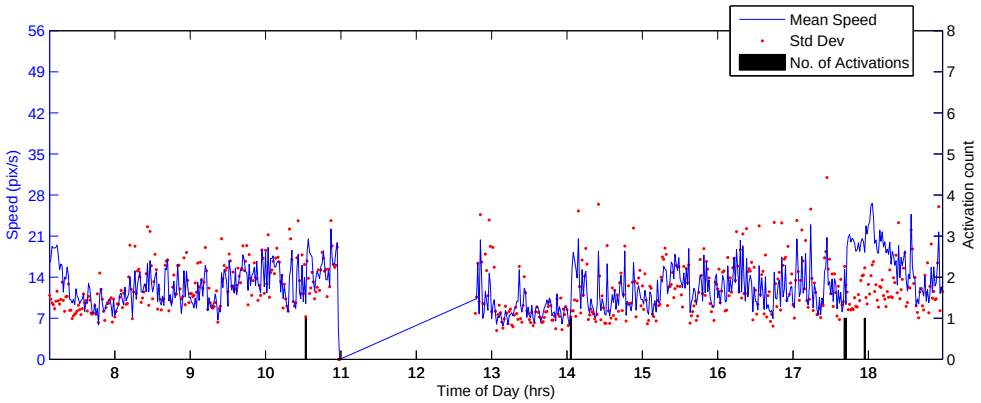

(iii) 29 January

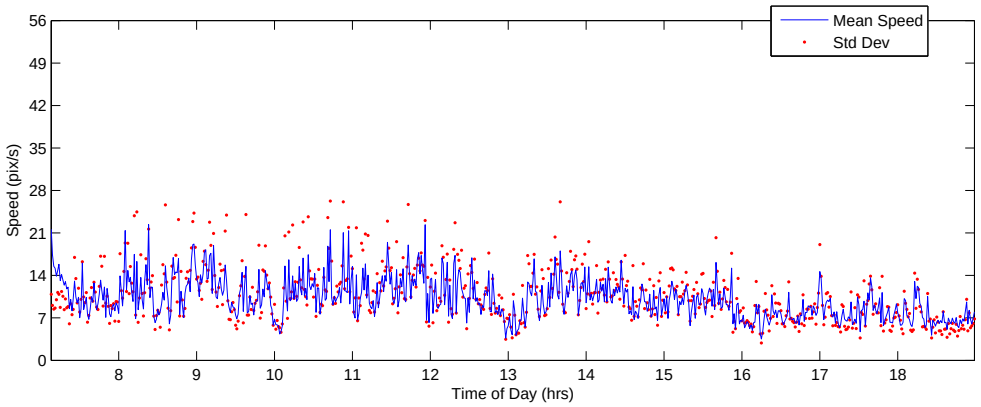

(iv) 30 January

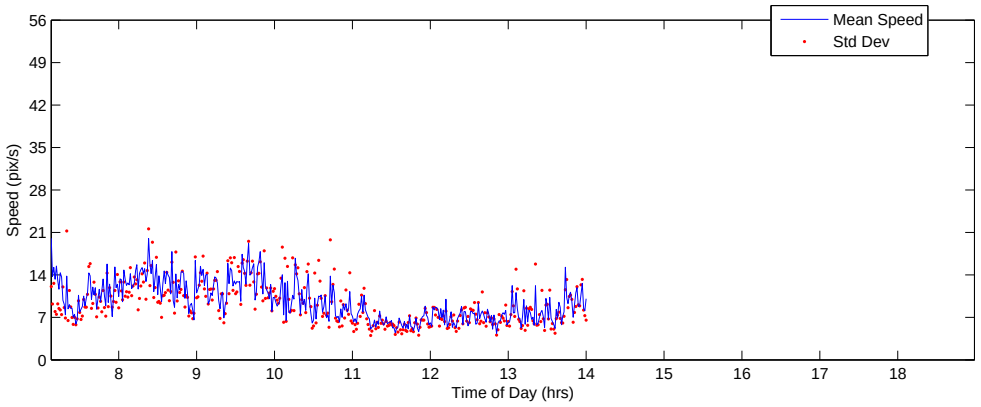

(v) 31 January

Figure C.1: Continued.

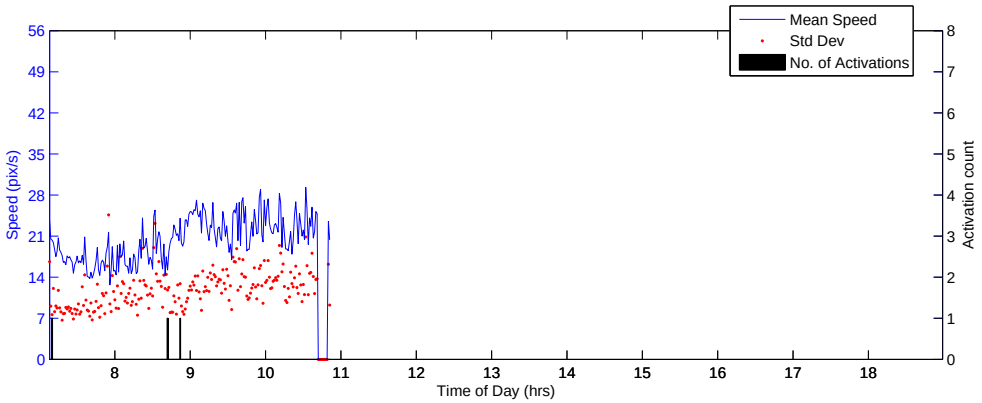

(vi) 1 February

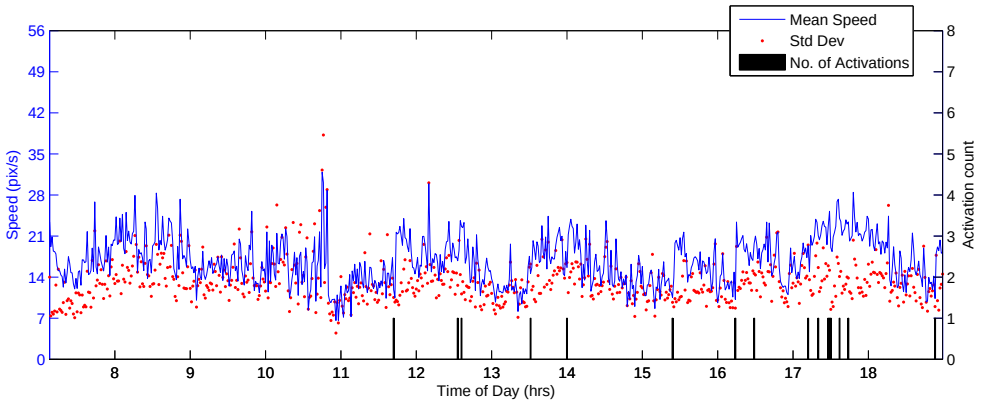

(vii) 2 February

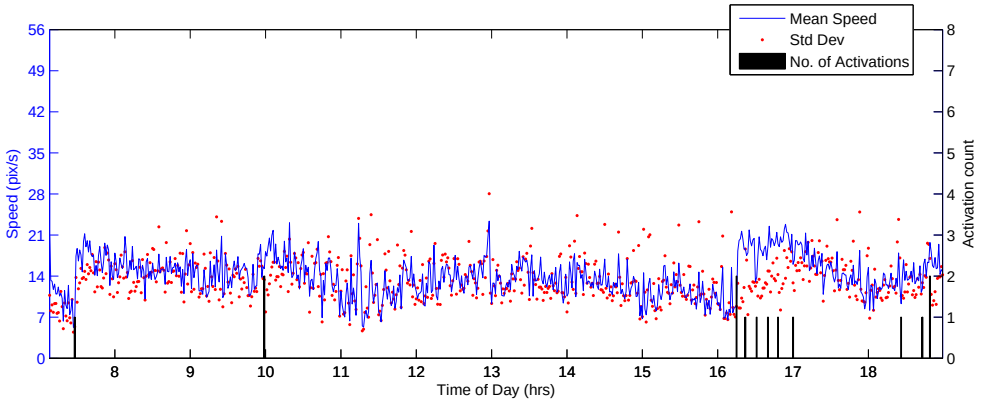

(viii) 3 February

Figure C.1: Continued.

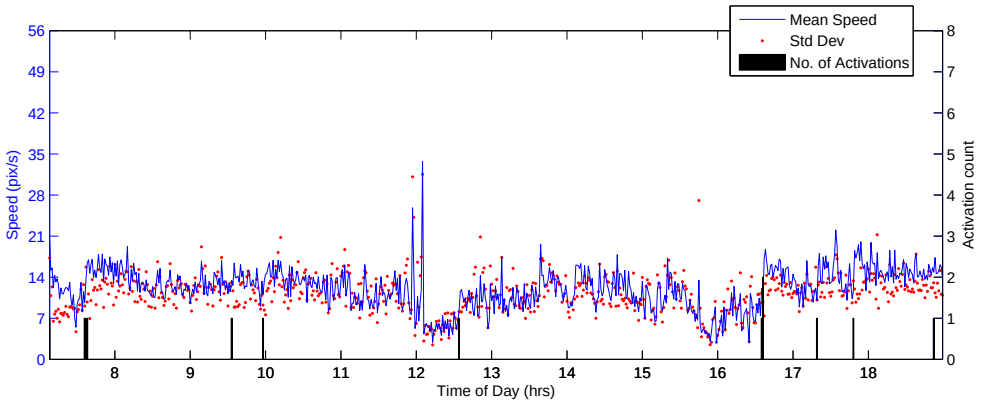

(ix) 4 February

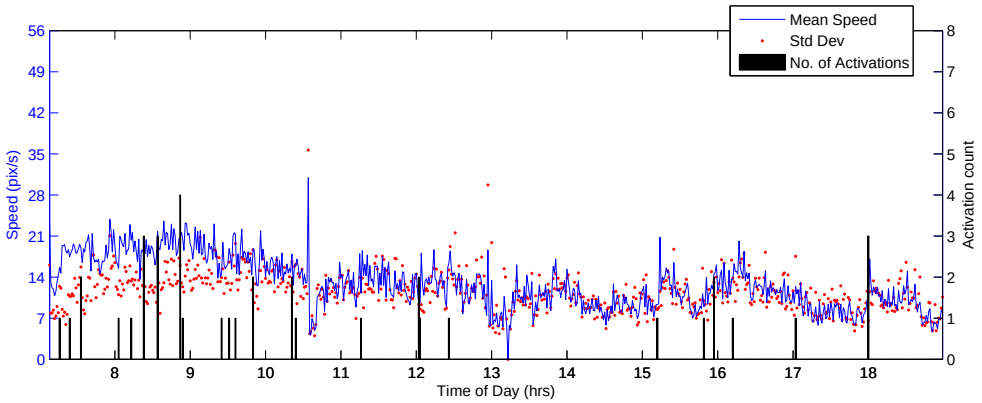

(x) 5 February

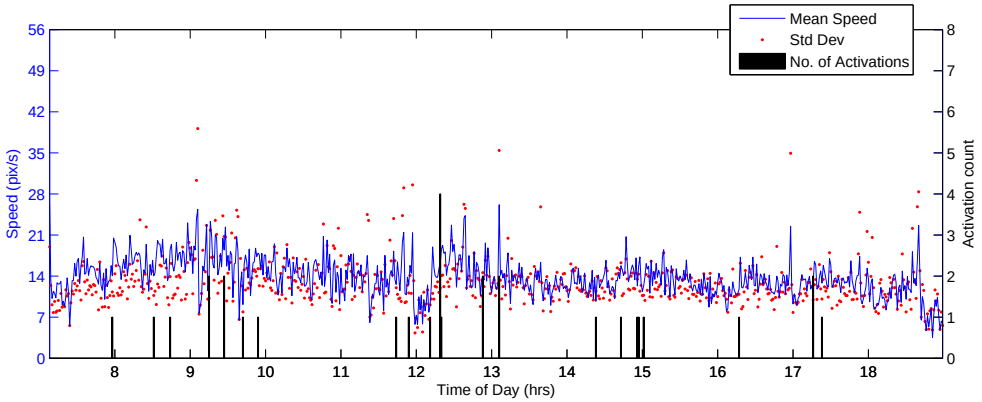

(xi) 6 February

Figure C.1: Continued.

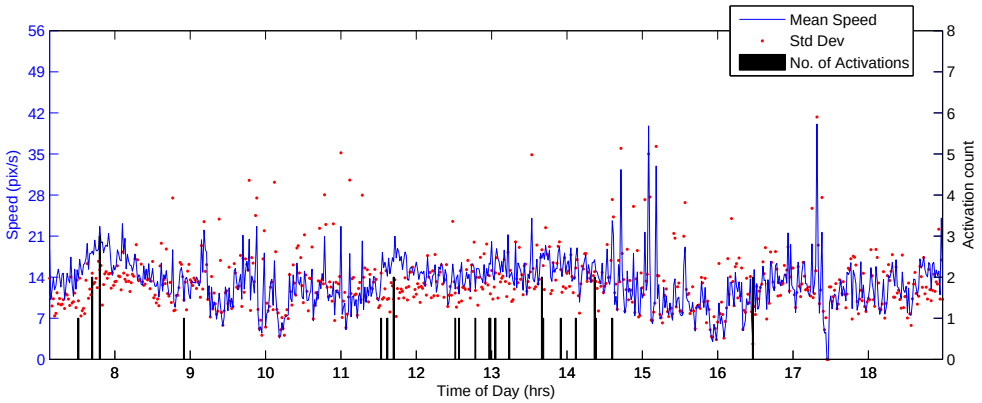

(xii) 7 February

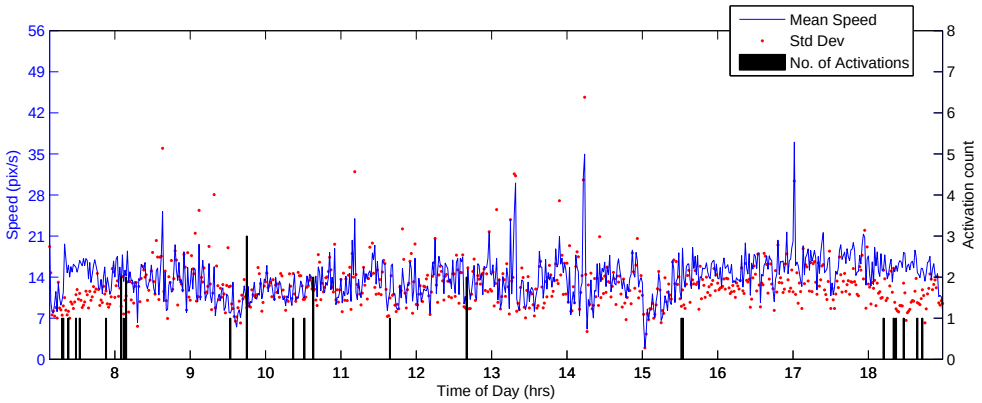

(xiii) 8 February

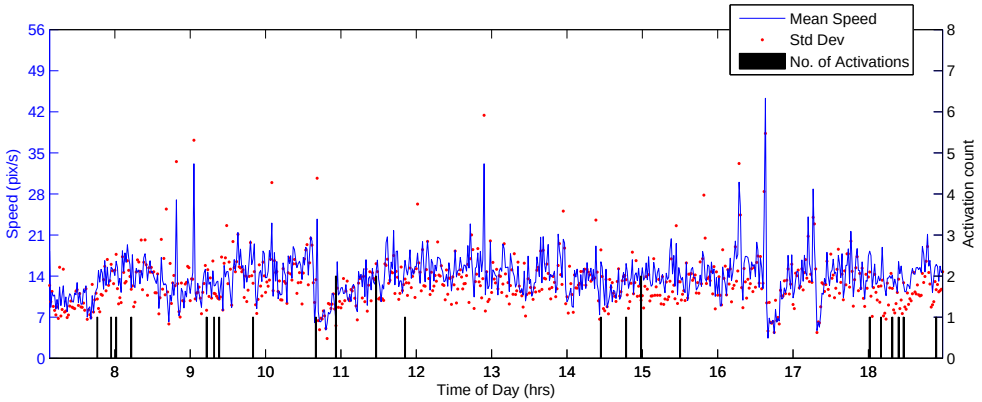

(xiv) 9 February

Figure C.1: Continued.

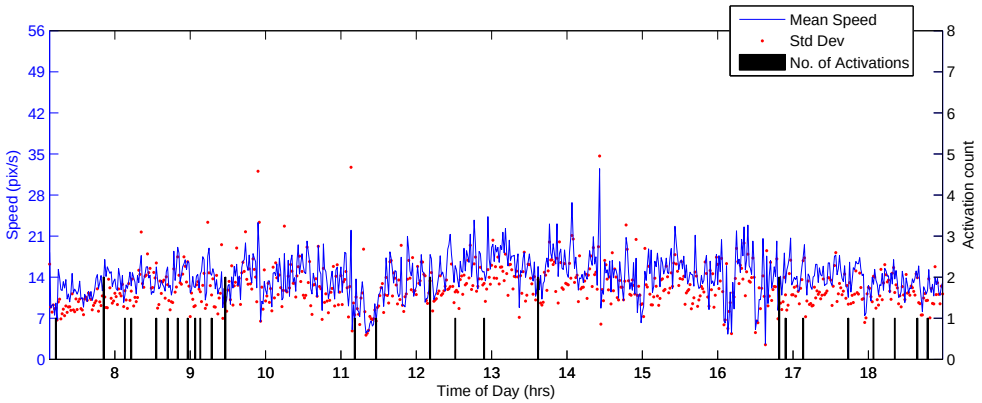

(xv) 10 February

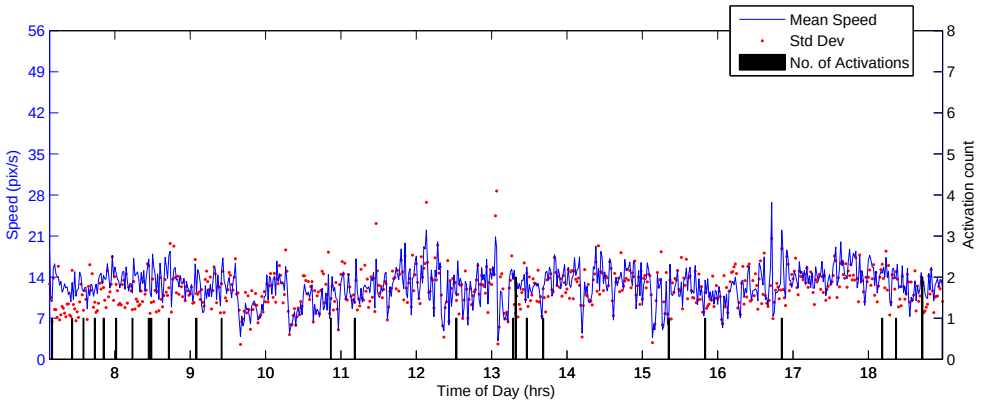

(xvi) 11 February

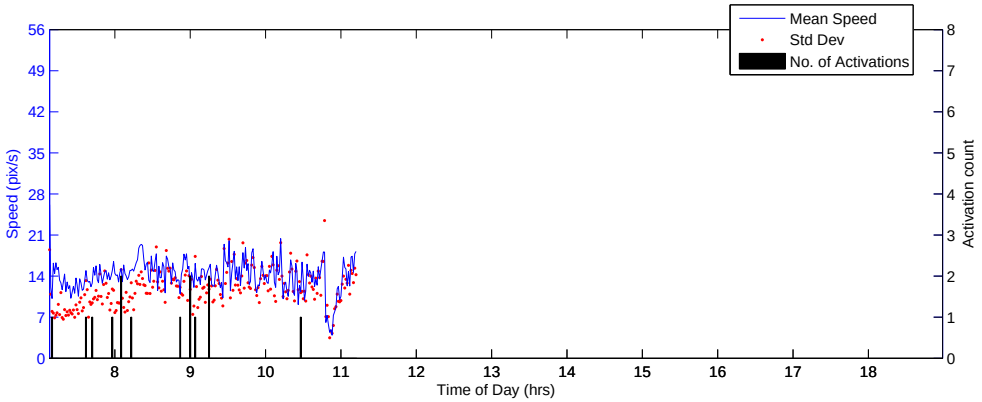

(xvii) 12 February

Figure C.1: Continued.

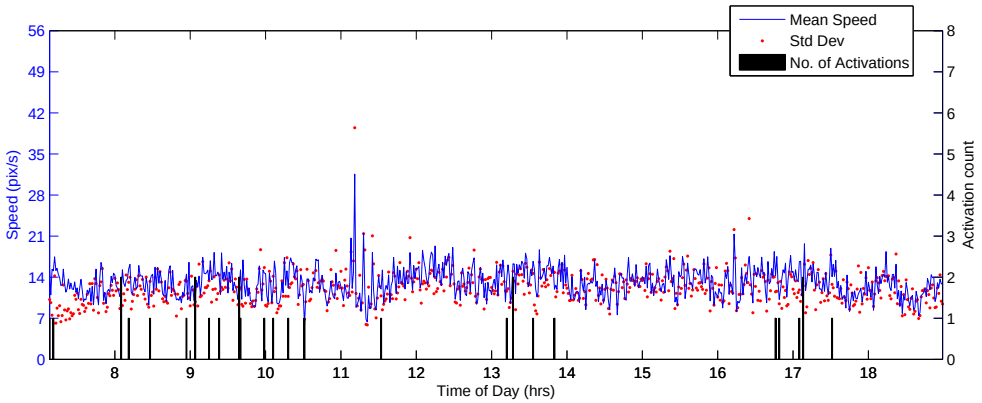

(xviii) 13 February

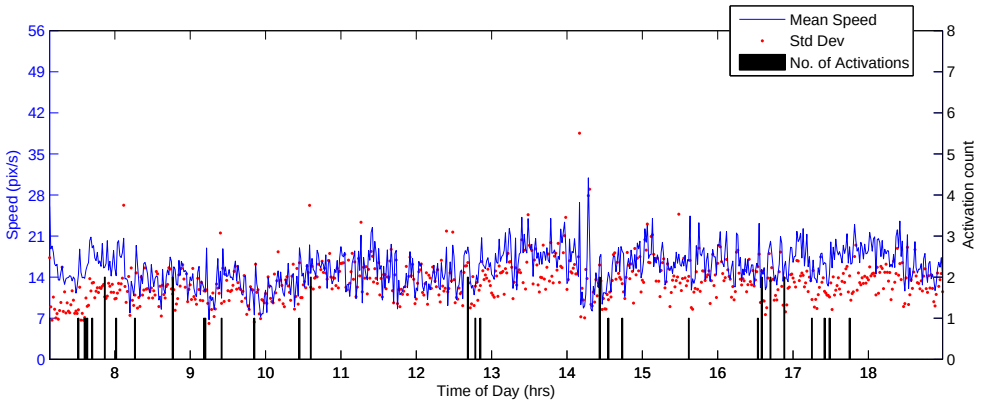

(xix) 14 February

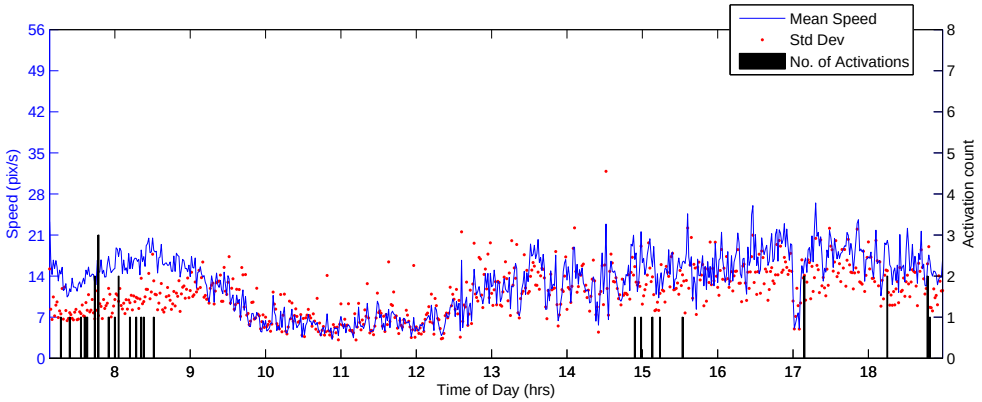

(xx) 15 February

Figure C.1: Continued.

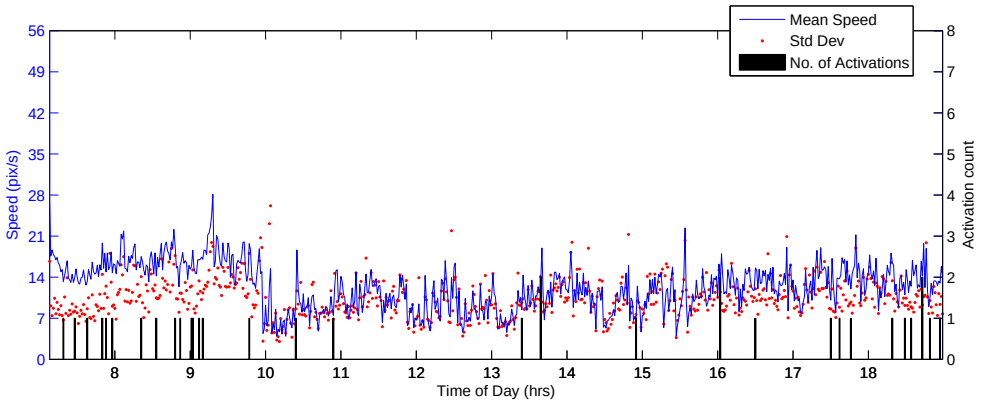

(xxi) 16 February

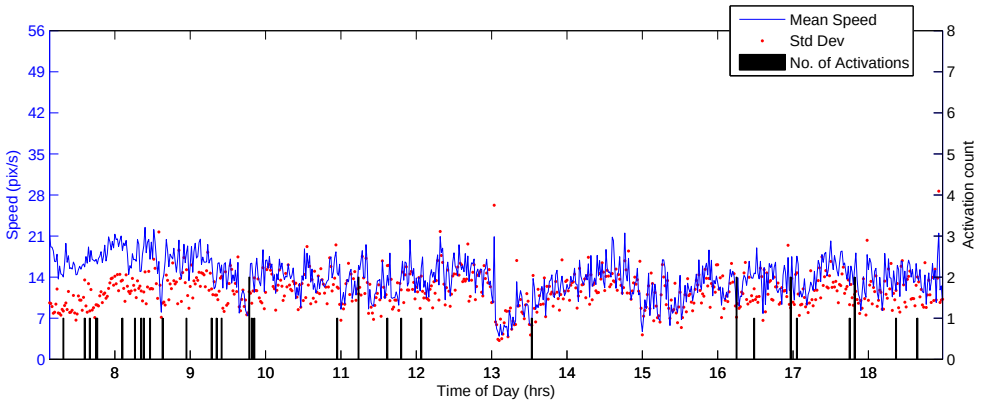

(xxii) 17 February

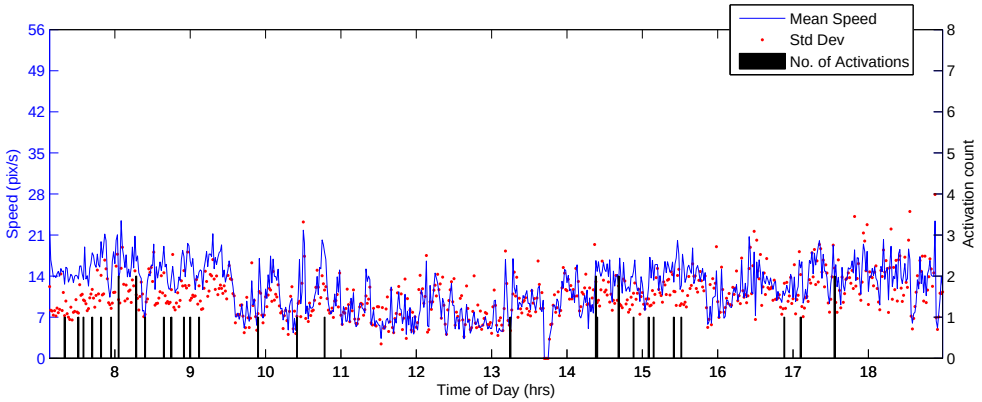

(xxiii) 18 February

Figure C.1: Continued.

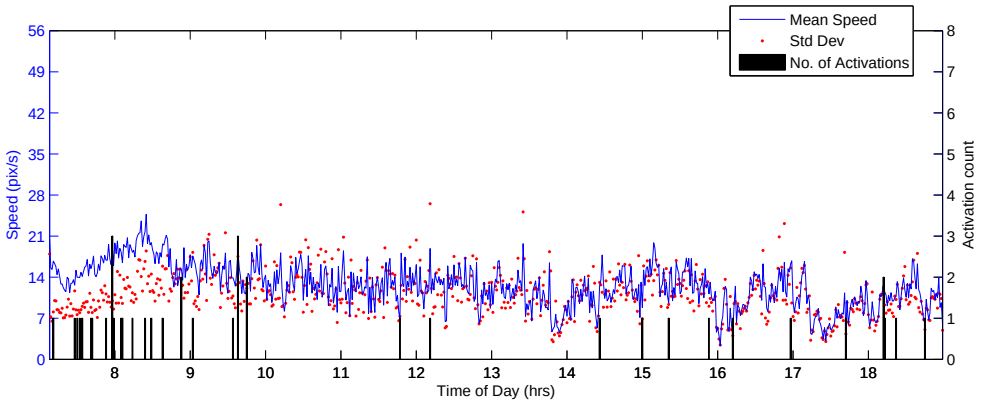

(xxiv) 19 February

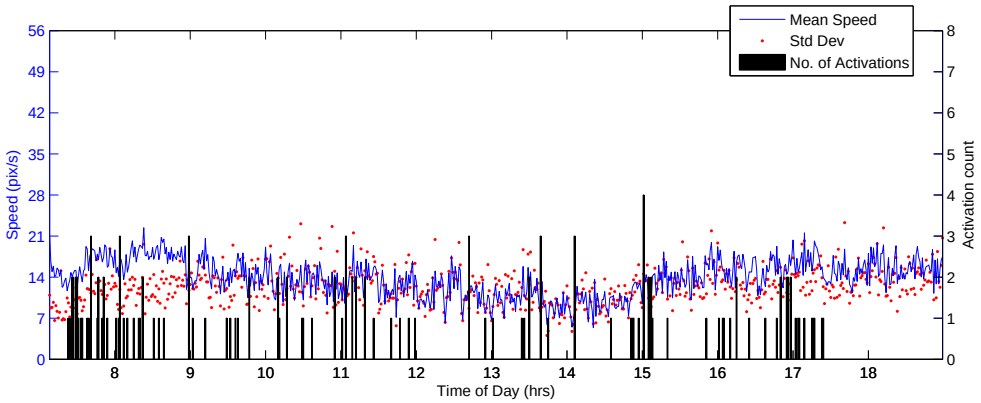

(xxv) 20 February

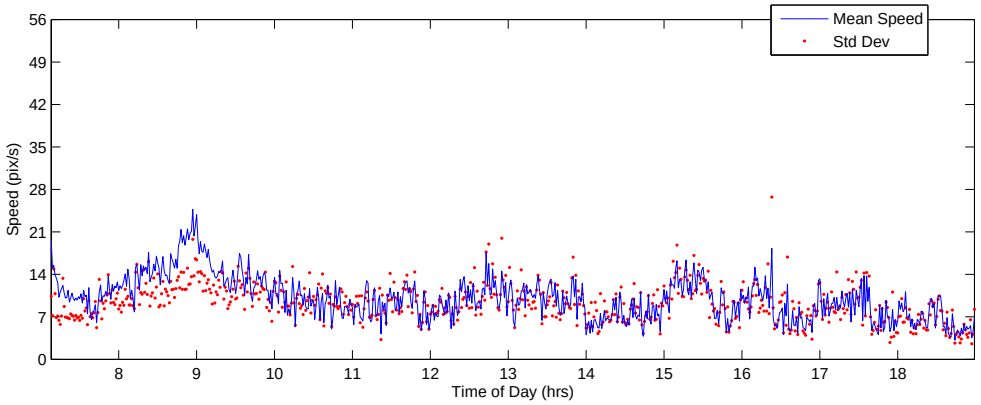

(xxvi) 21 February

Figure C.1: Continued.

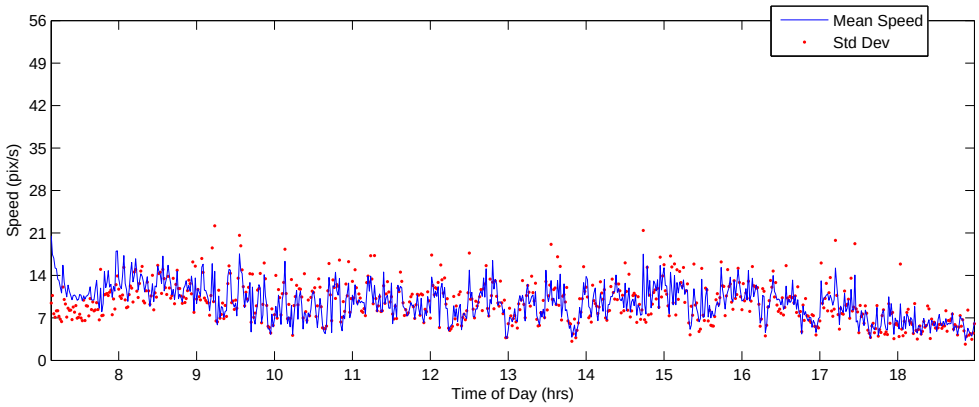

(xxvii) 22 February

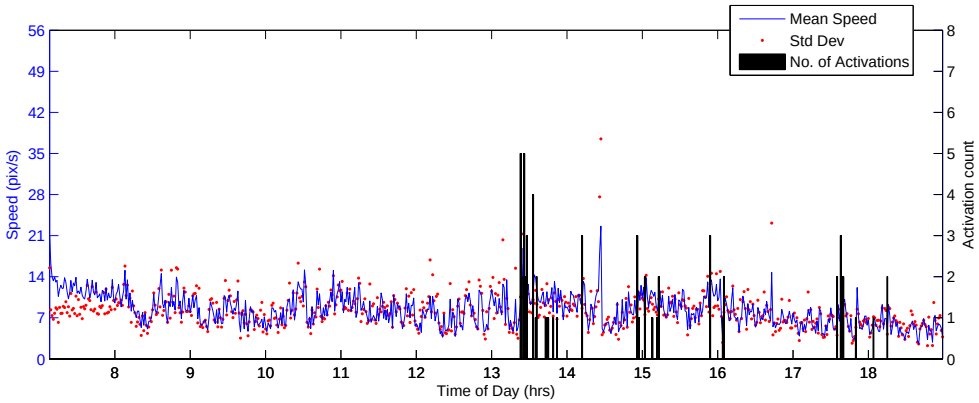

(xxviii) 23 February

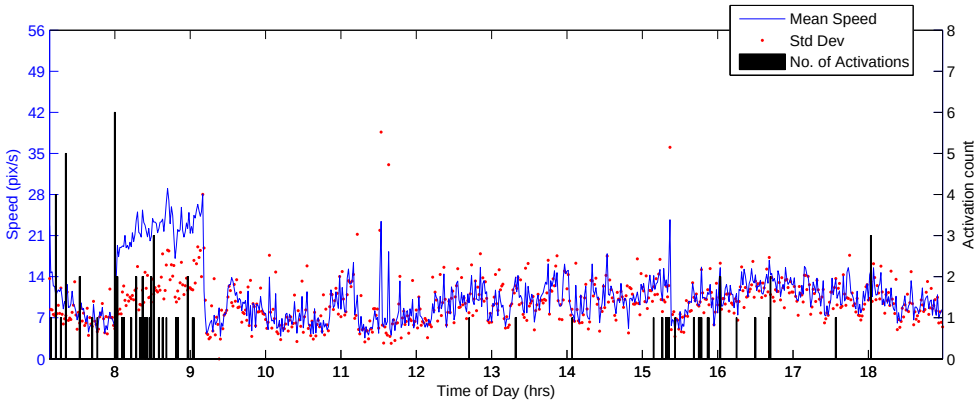

(xxix) 24 February

Figure C.1: Continued.

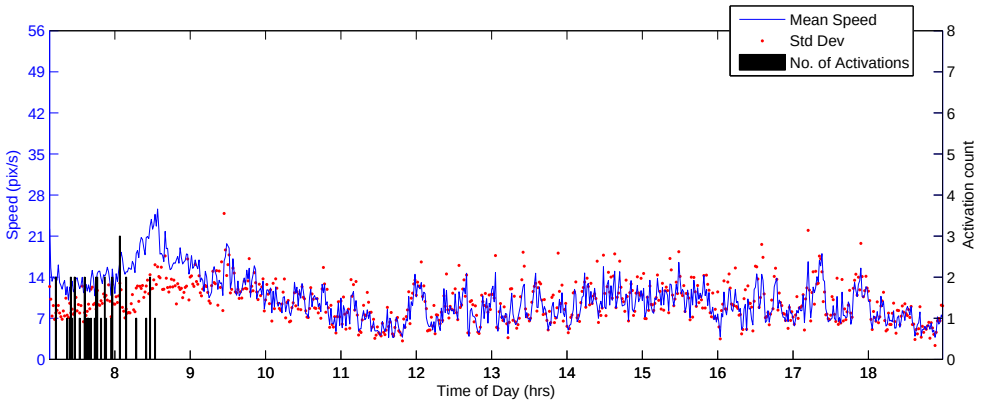

(xxx) 25 February

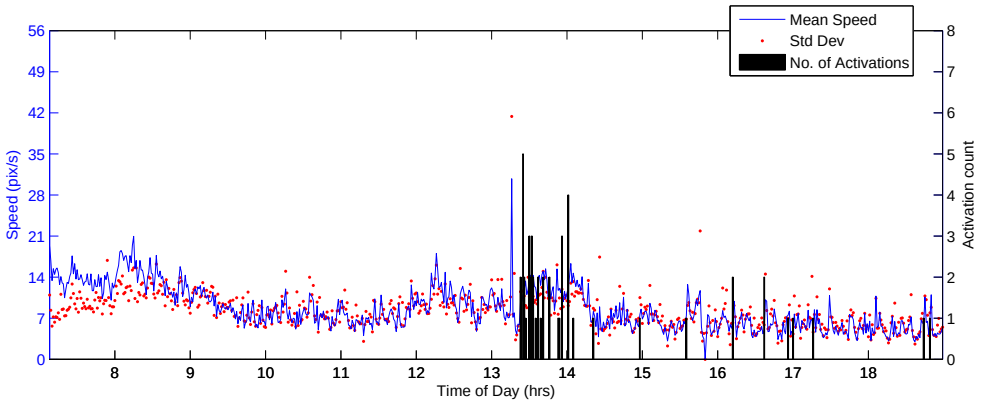

(xxxi) 26 February

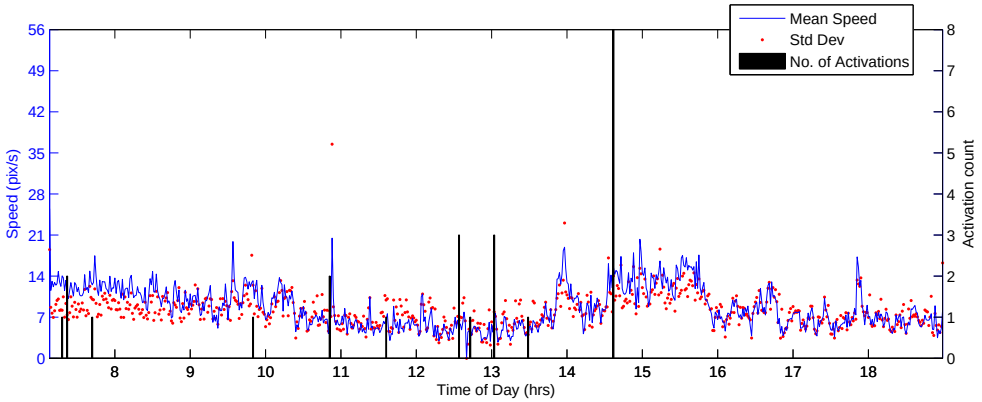

(xxxii) 27 February

Figure C.1: Continued.

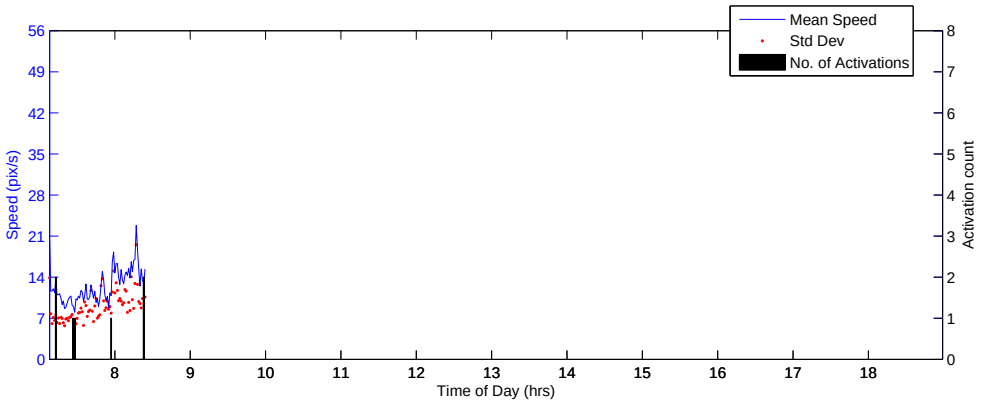

(xxxiii) 28 February

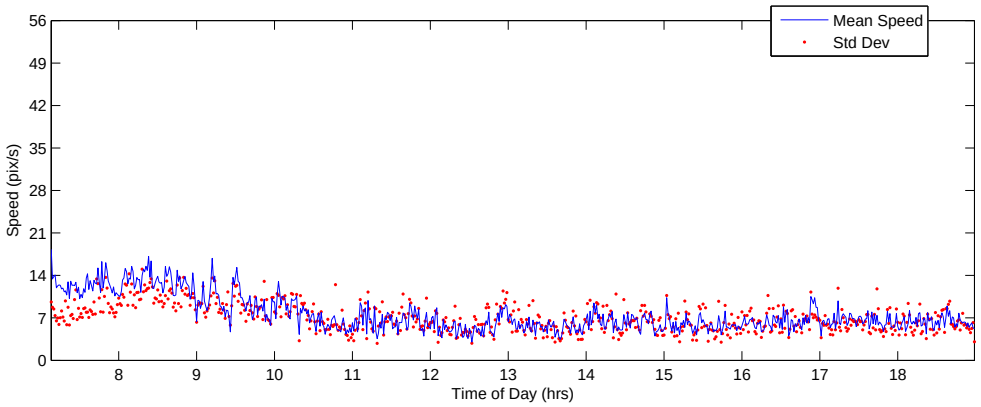

(xxxiv) 1 March

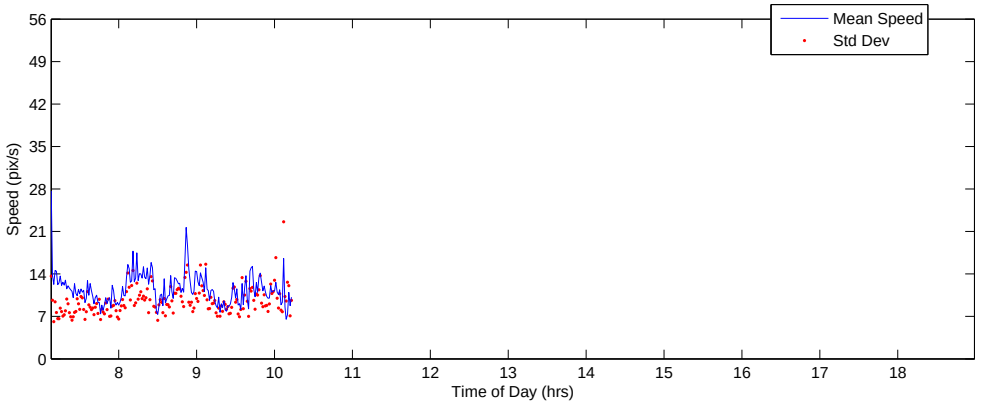

(xxxv) 2 March

Figure C.1: Continued.

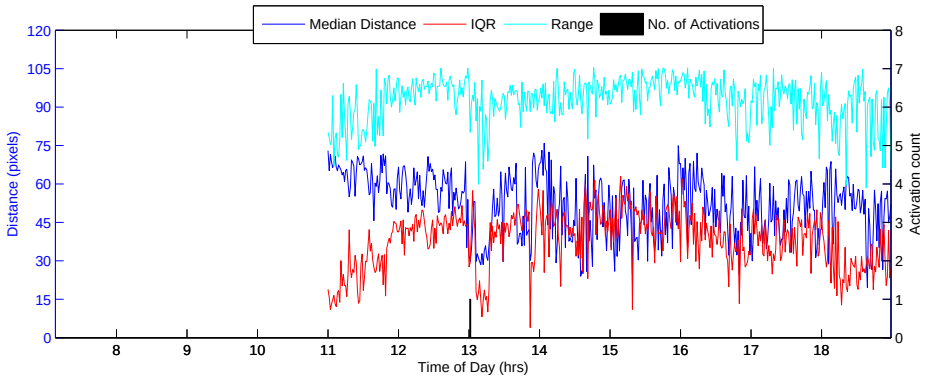

(i) 27 January

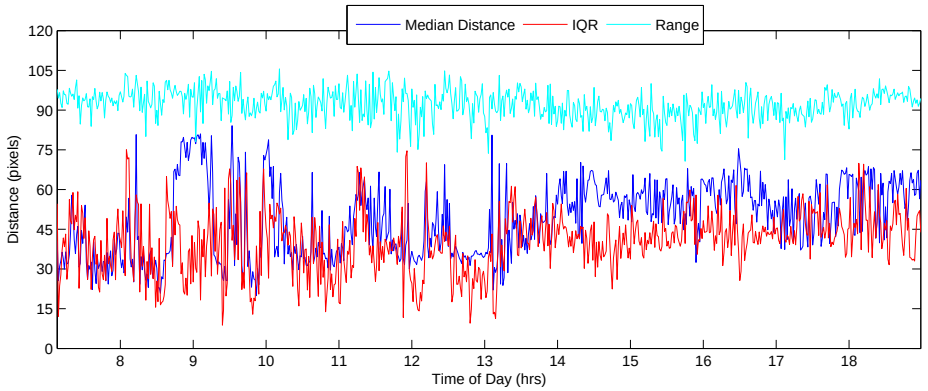

(ii) 28 January

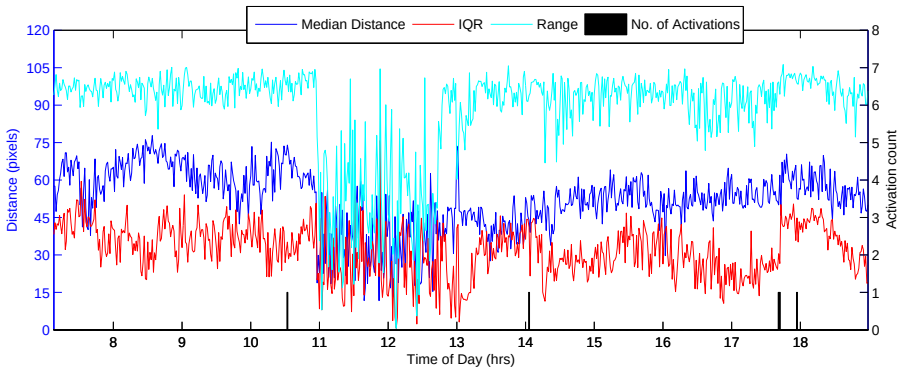

(iii) 29 January

Figure C.2: Distance from the feeding area of 10 fish in a research tank during 35 days (27 Jan - 2 March 2010).

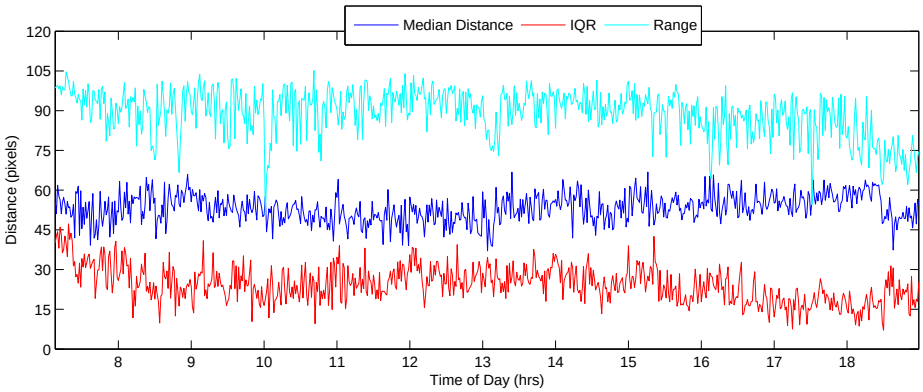

(iv) 30 January

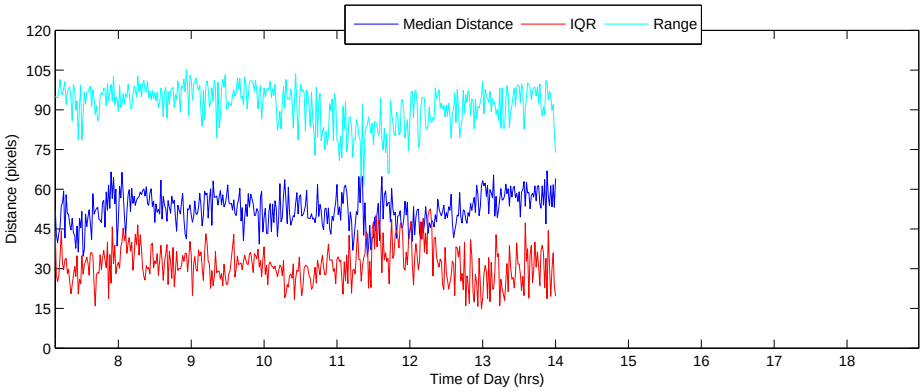

(v) 31 January

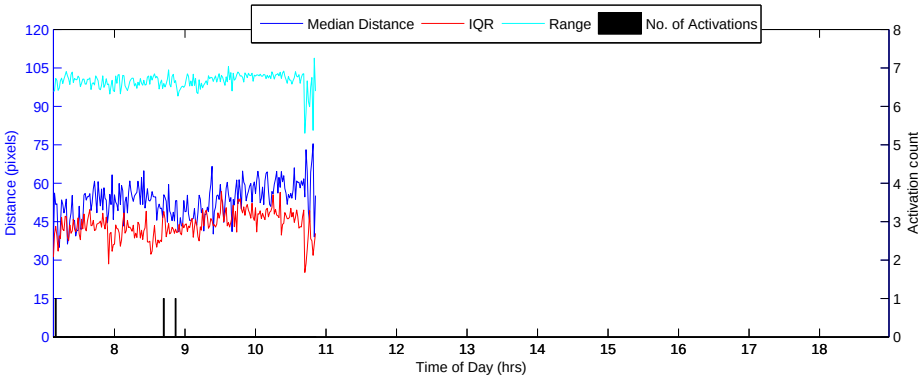

(vi) 1 February

Figure C.2: Continued.

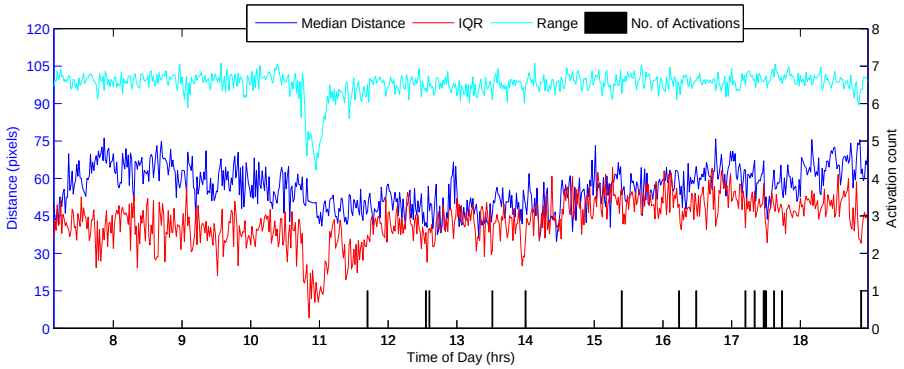

(vii) 2 February

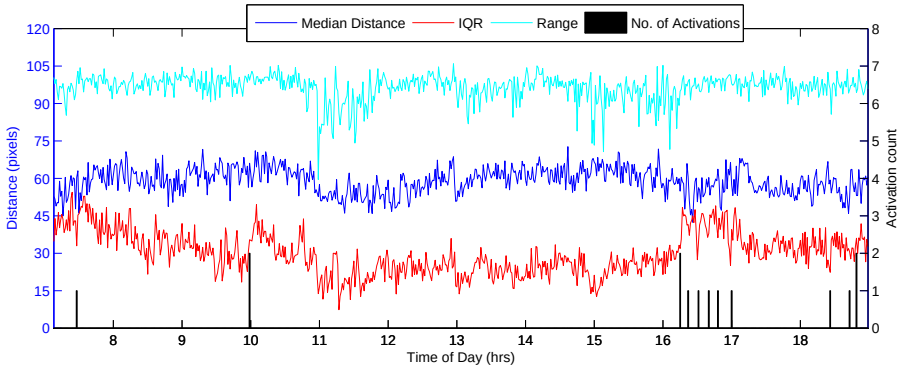

(viii) 3 February

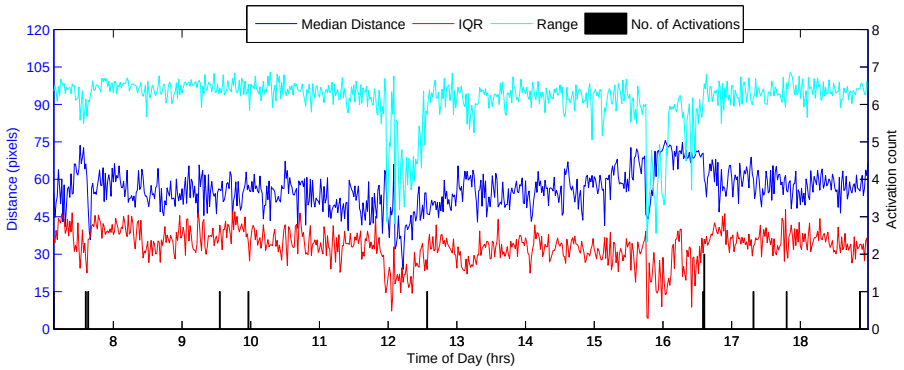

(ix) 4 February

Figure C.2: Continued.

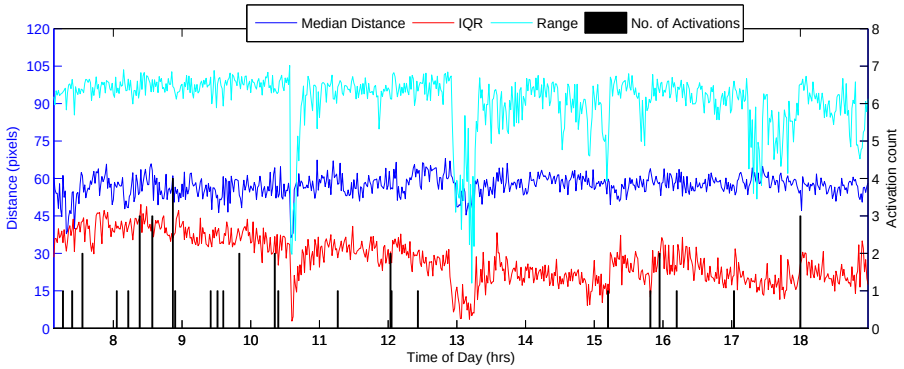

(x) 5 February

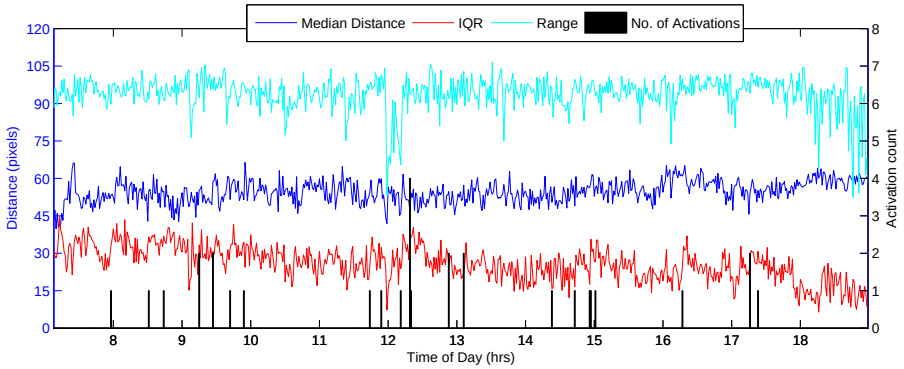

(xi) 6 February

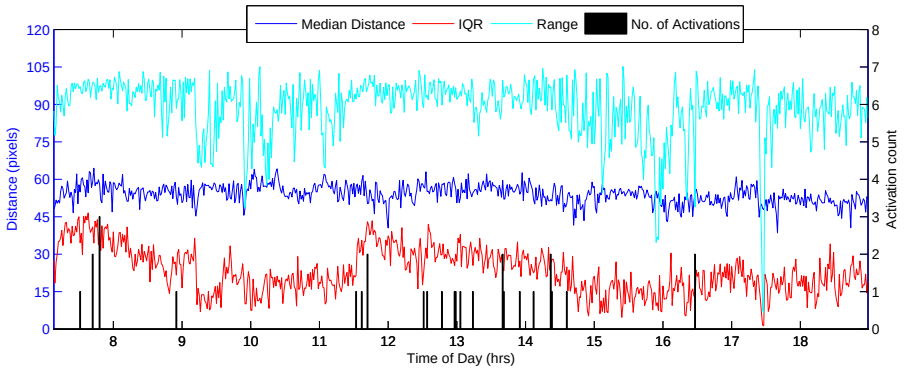

(xii) 7 February

Figure C.2: Continued.

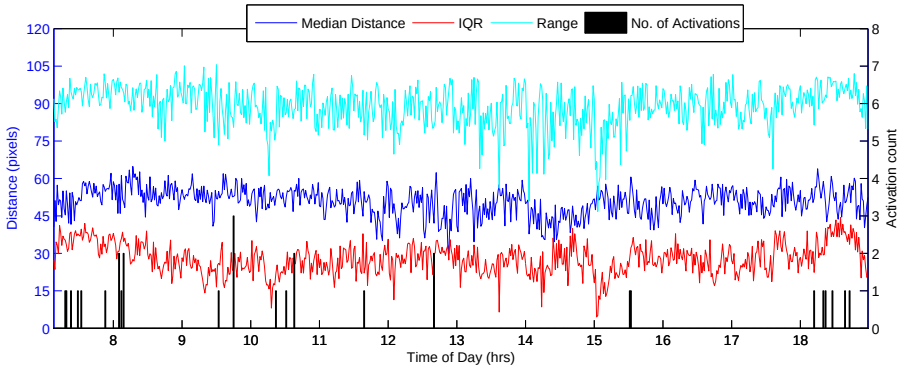

(xiii) 8 February

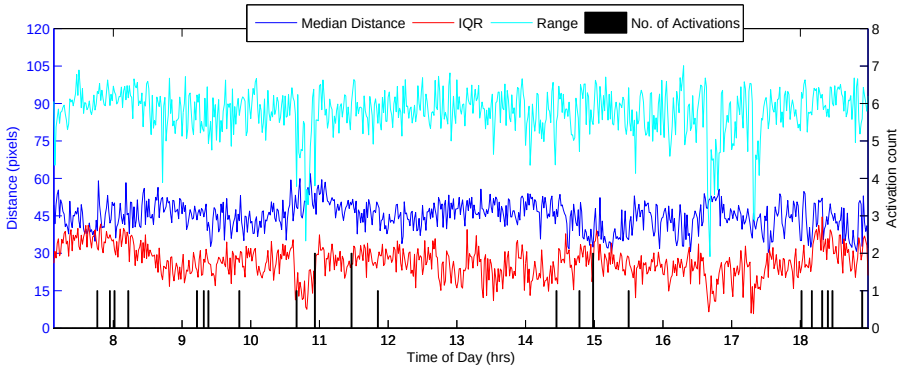

(xiv) 9 February

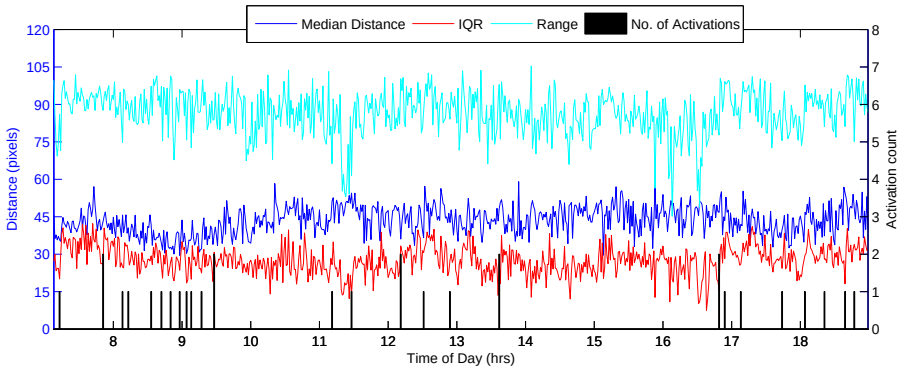

(xv) 10 February

Figure C.2: Continued.

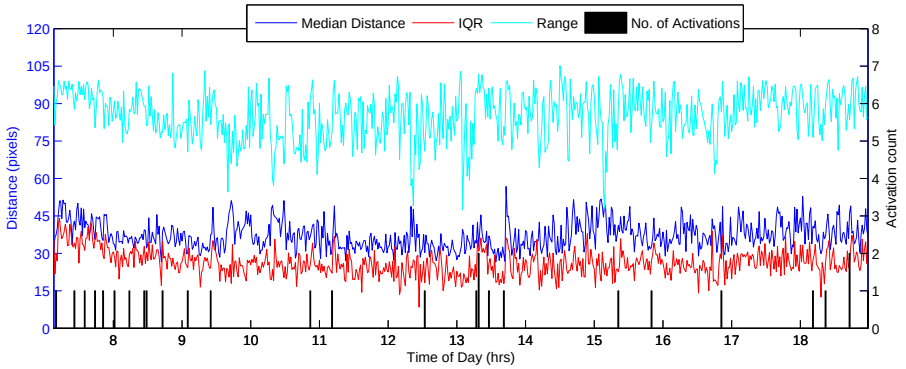

(xvi) 11 February

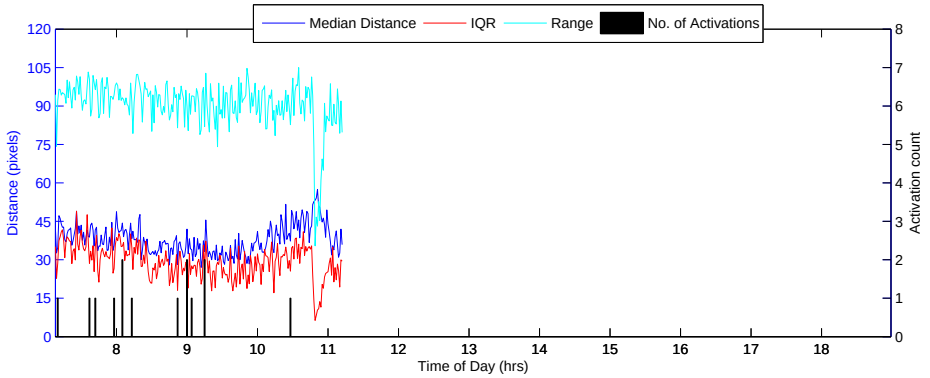

(xvii) 12 February

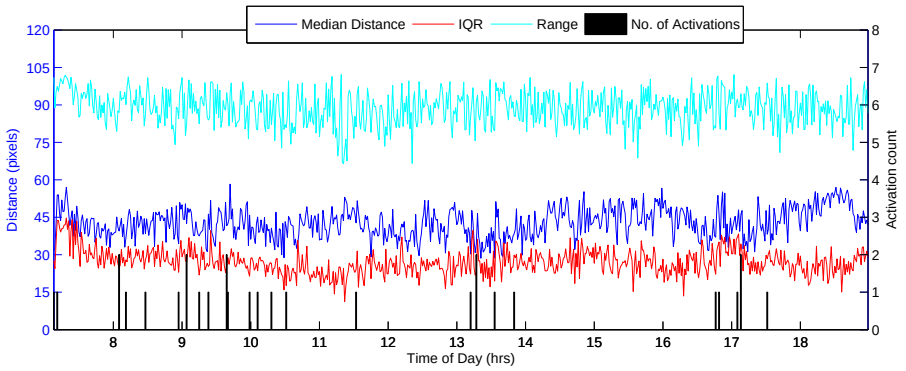

(xviii) 13 February

Figure C.2: Continued.

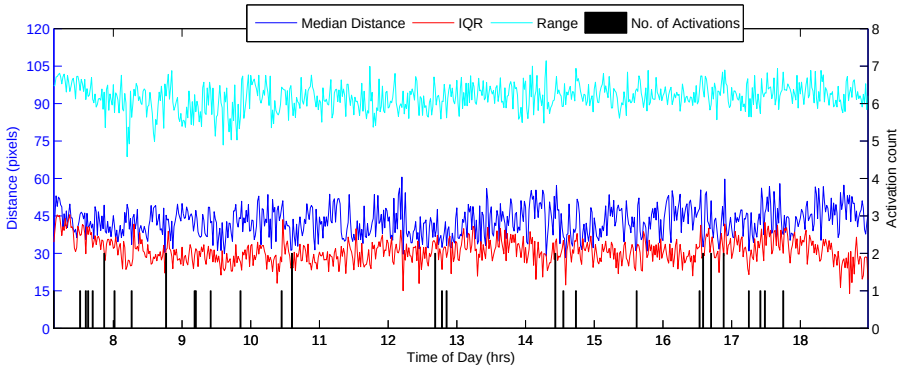

(xix) 14 February

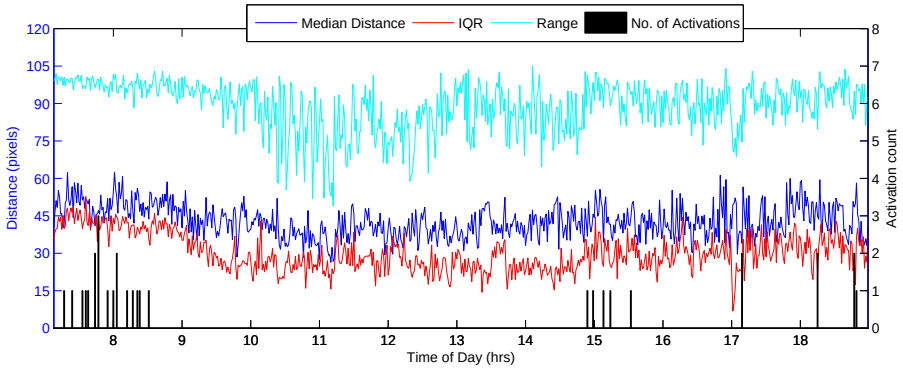

(xx) 15 February

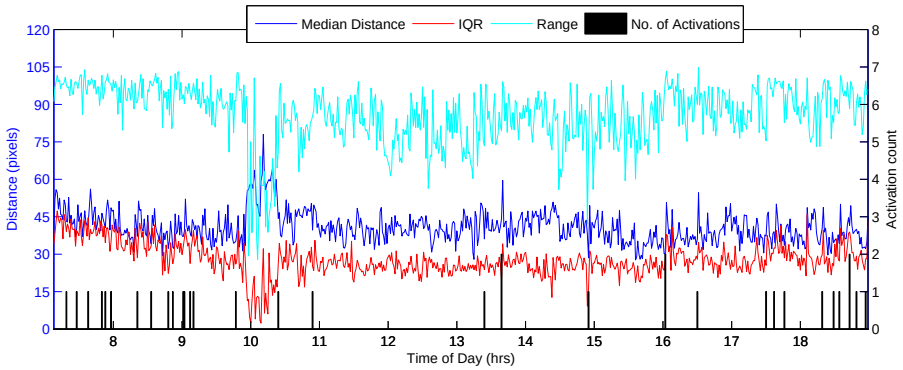

(xxi) 16 February

Figure C.2: Continued.

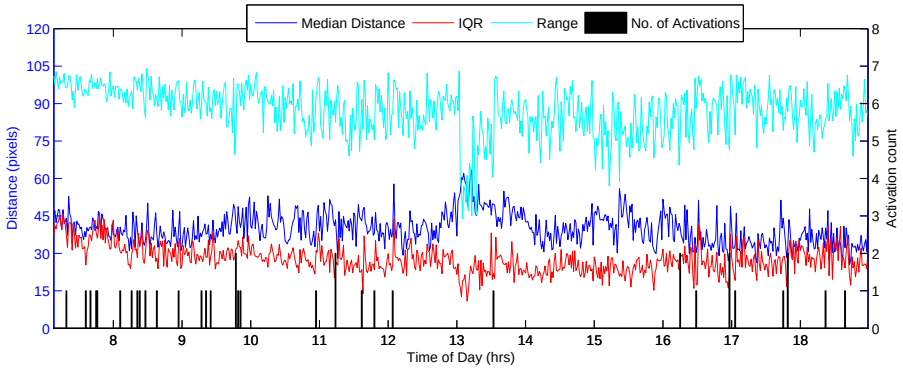

(xxii) 17 February

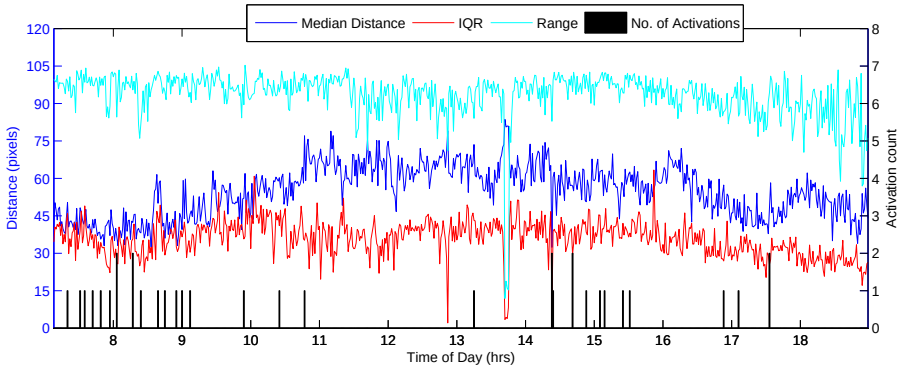

(xxiii) 18 February

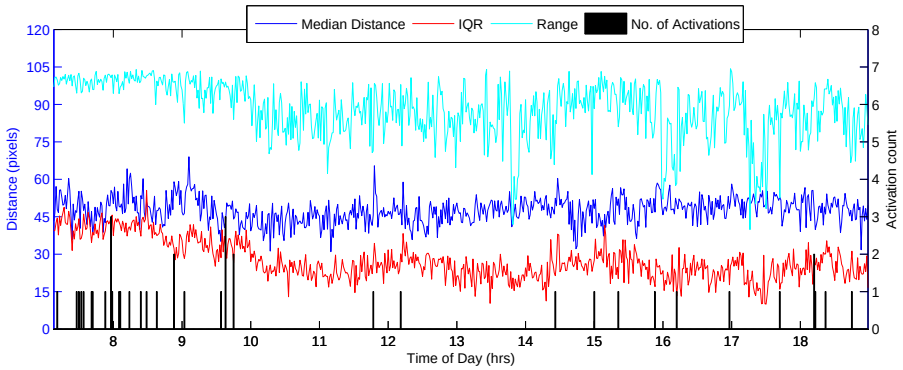

(xxiv) 19 February

Figure C.2: Continued.

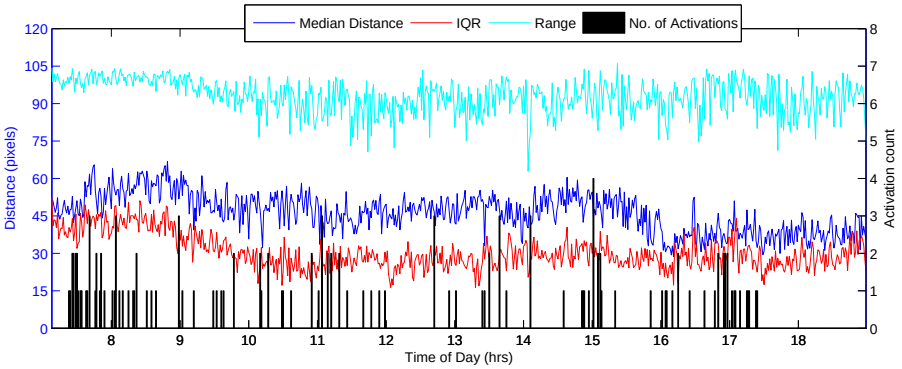

(xxv) 20 February

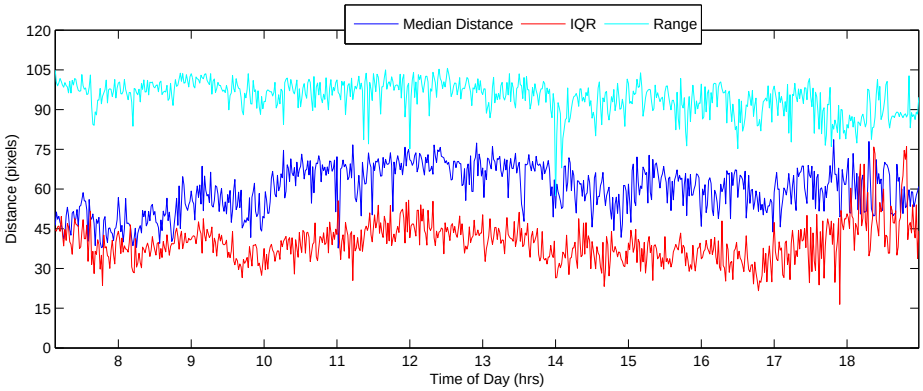

(xxvi) 21 February

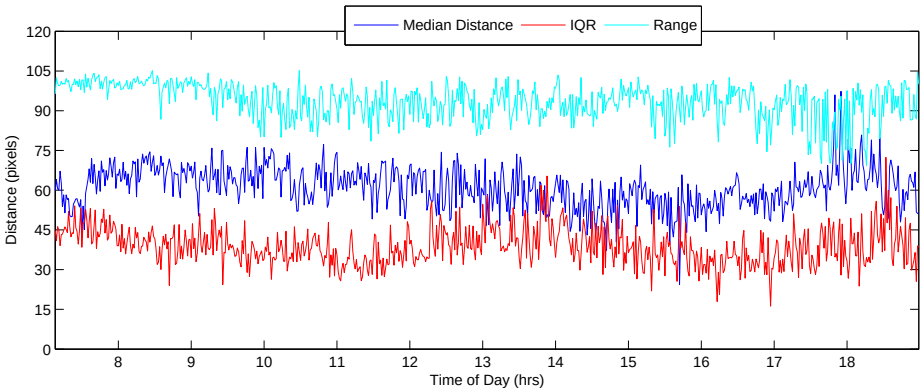

(xxvii) 22 February

Figure C.2: Continued.

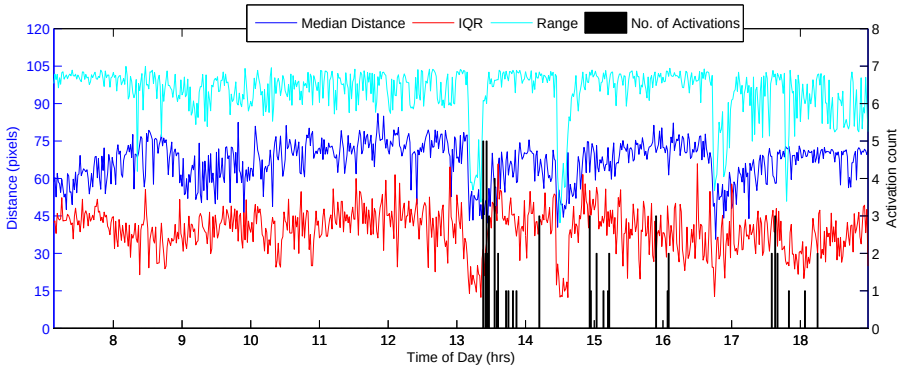

(xxviii) 23 February

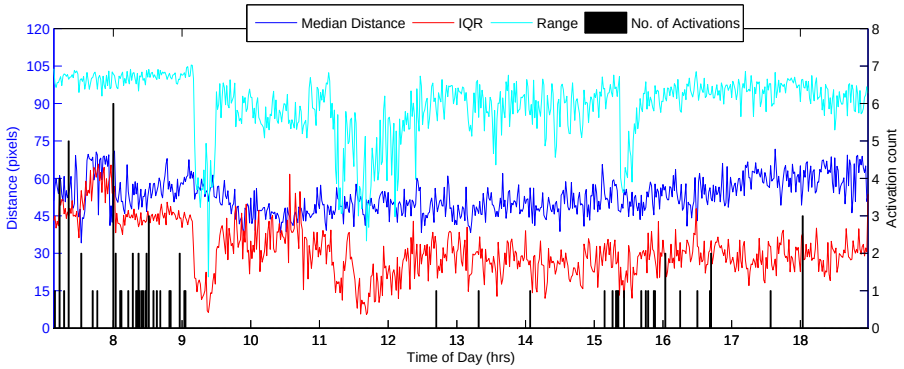

(xxix) 24 February

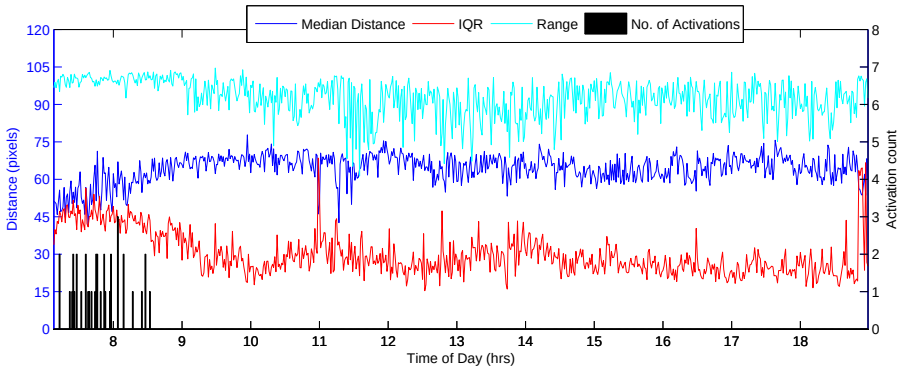

(xxx) 25 February

Figure C.2: Continued.

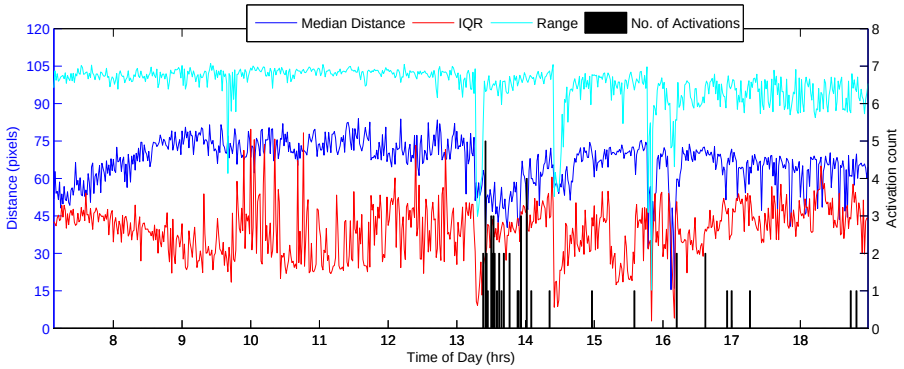

(xxxi) 26 February

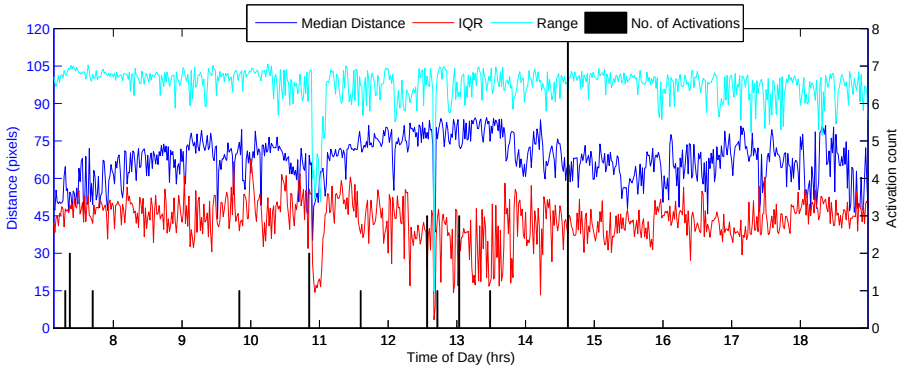

(xxxii) 27 February

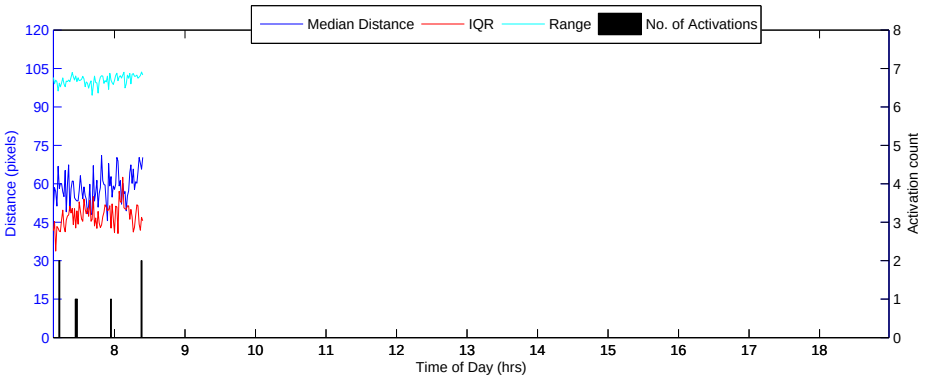

(xxxiii) 28 February

Figure C.2: Continued.

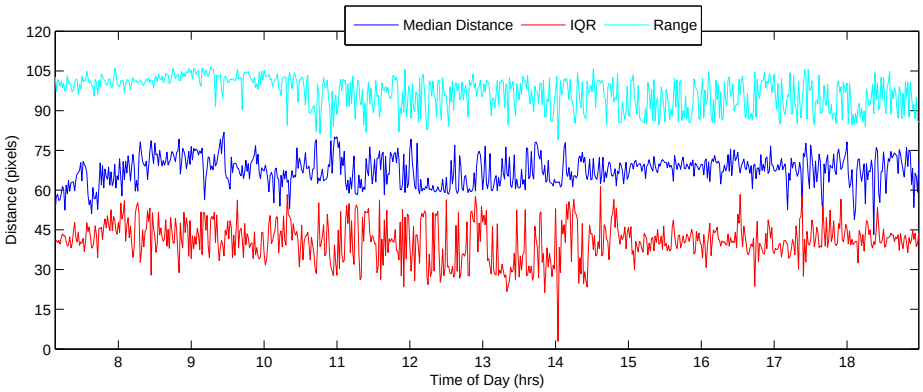

(xxxiv) 1 March

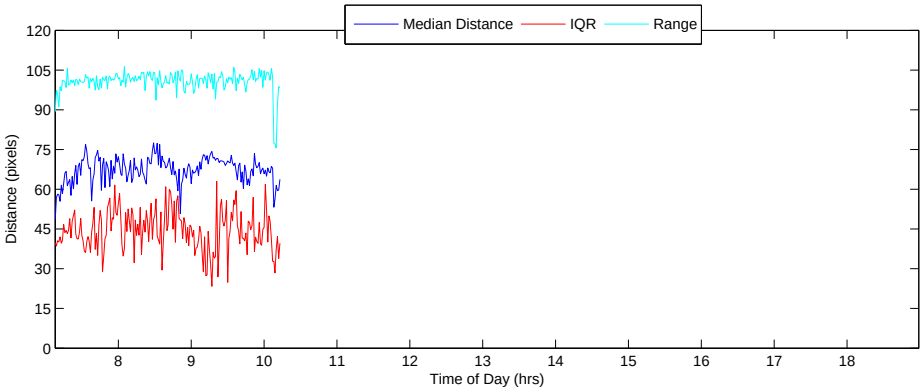

(xxxv) 2 March

Figure C.2: Continued.

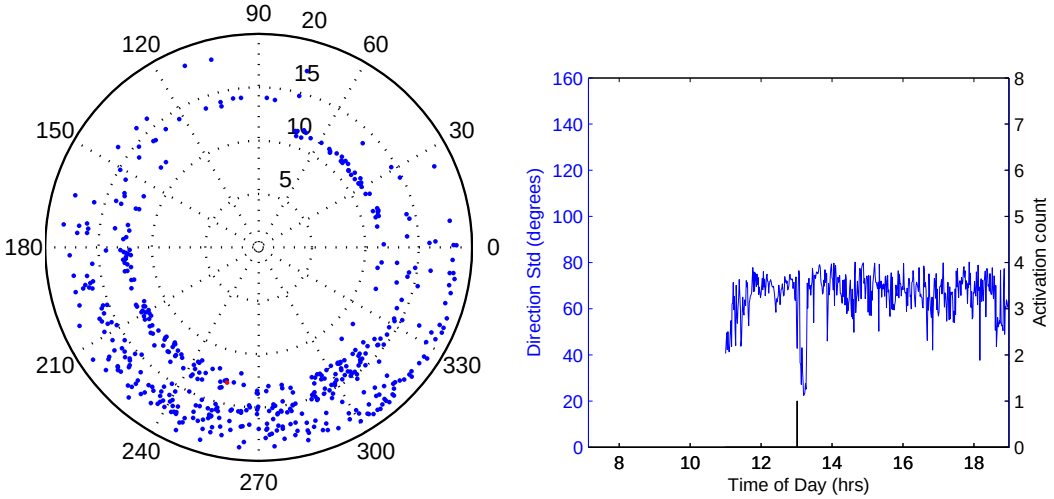

(i) 27 January

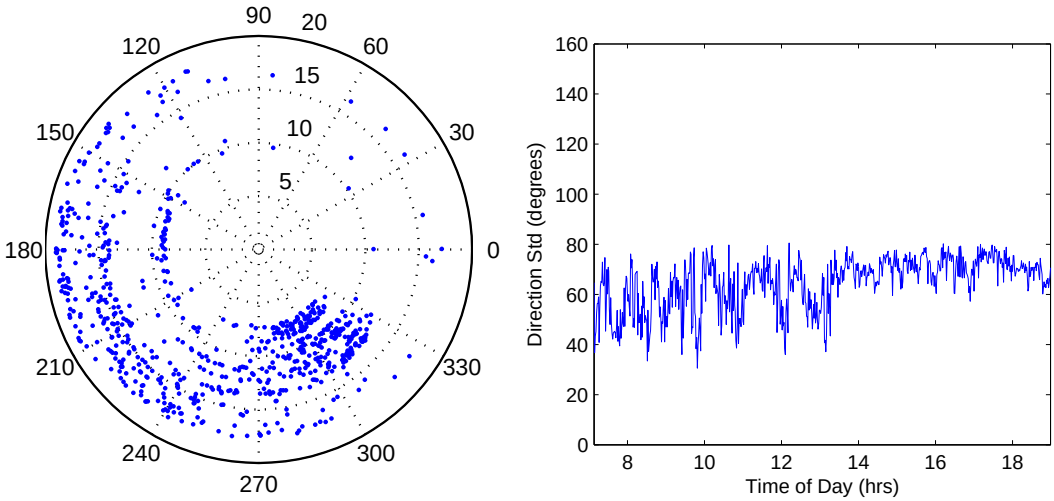

(ii) 28 January

Figure C.3: Circular mean direction (left image) and circular standard deviation (right image) of group of fish from the centre of a tank between 27 Jan and 2 Mar 2010. Red data points indicate direction during feeder activations.

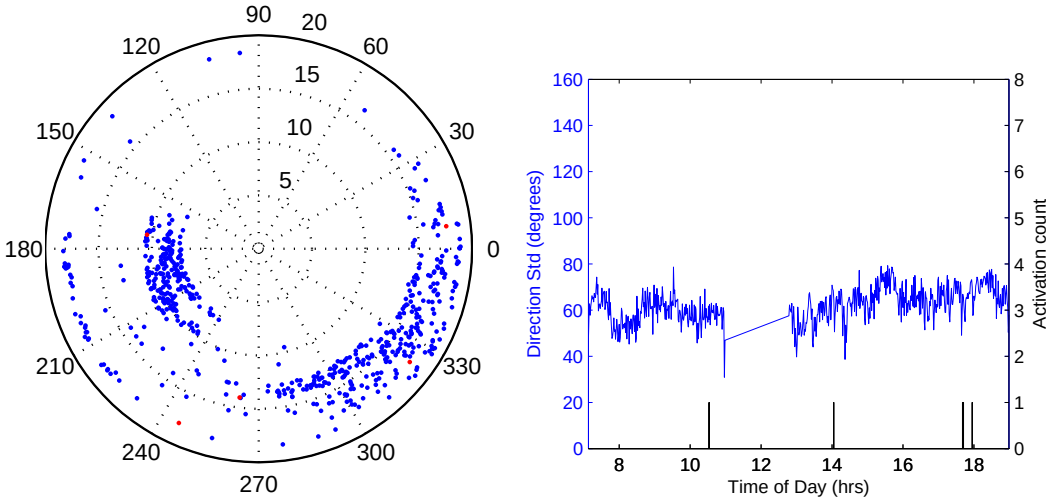

(iii) 29 January

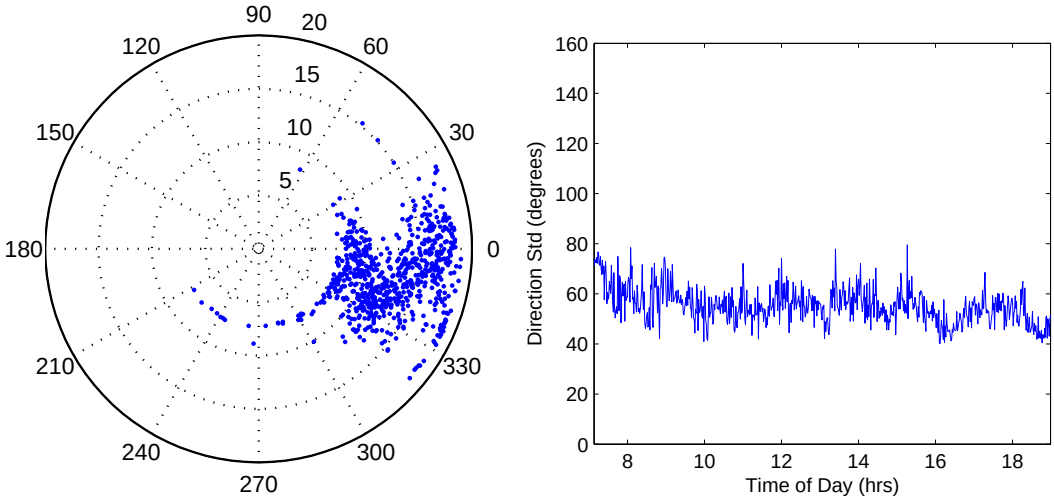

(iv) 30 January

Figure C.3: Continued.

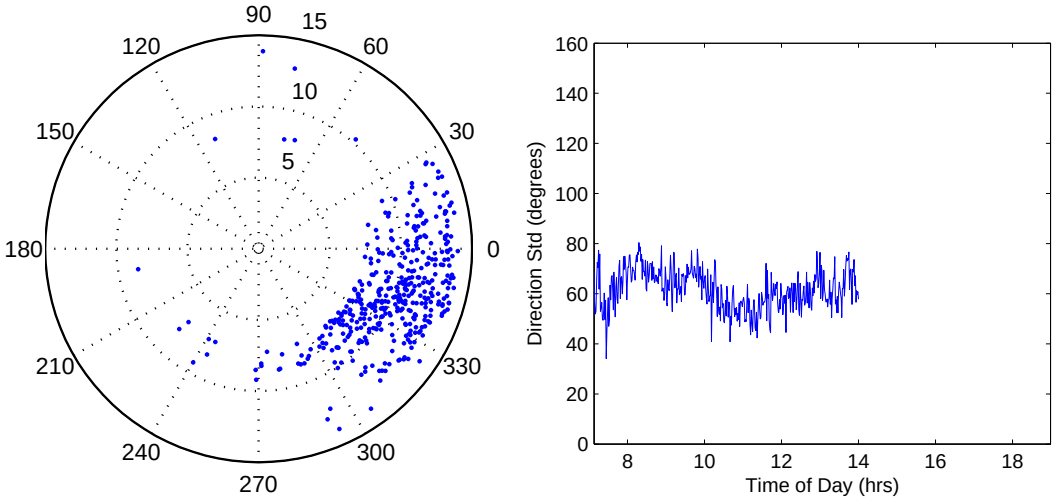

(v) 31 January

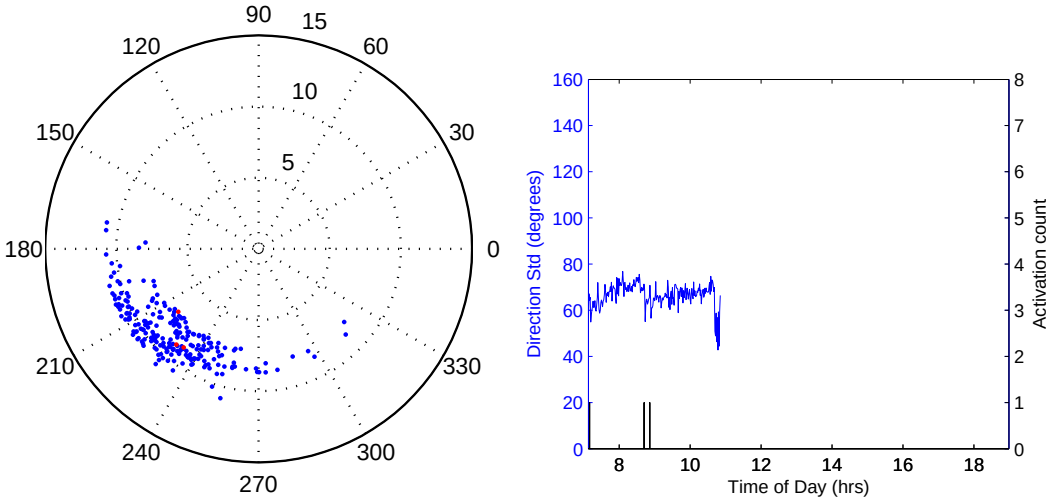

(vi) 1 February

Figure C.3: Continued.

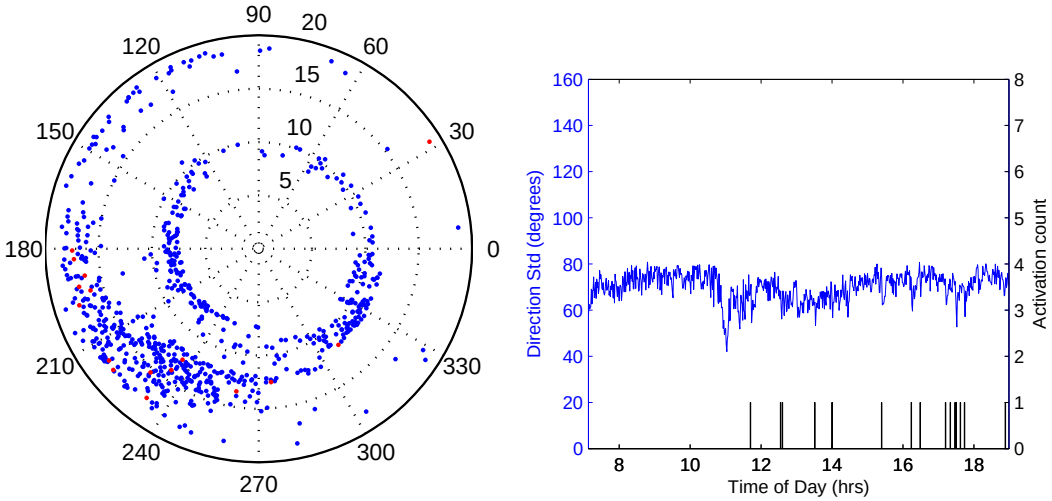

(vii) 2 February

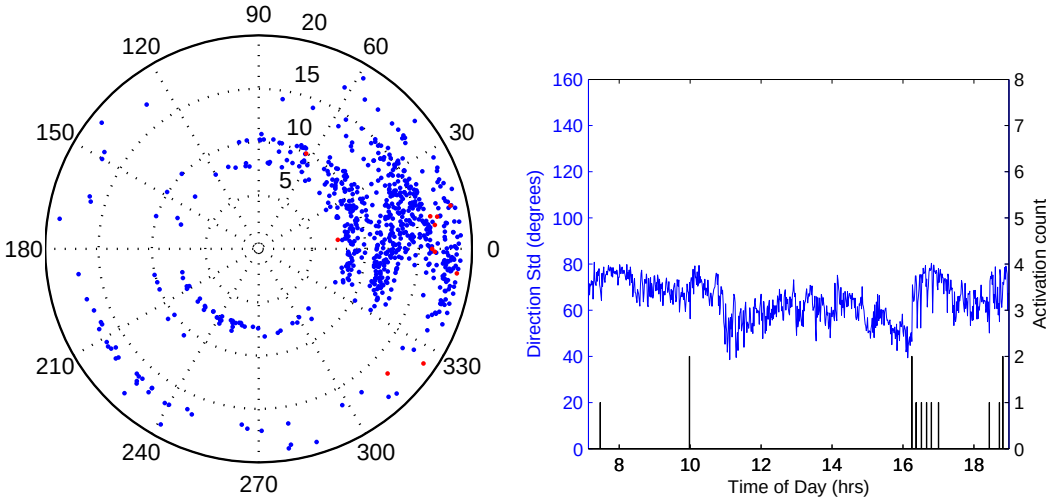

(viii) 3 February

Figure C.3: Continued.

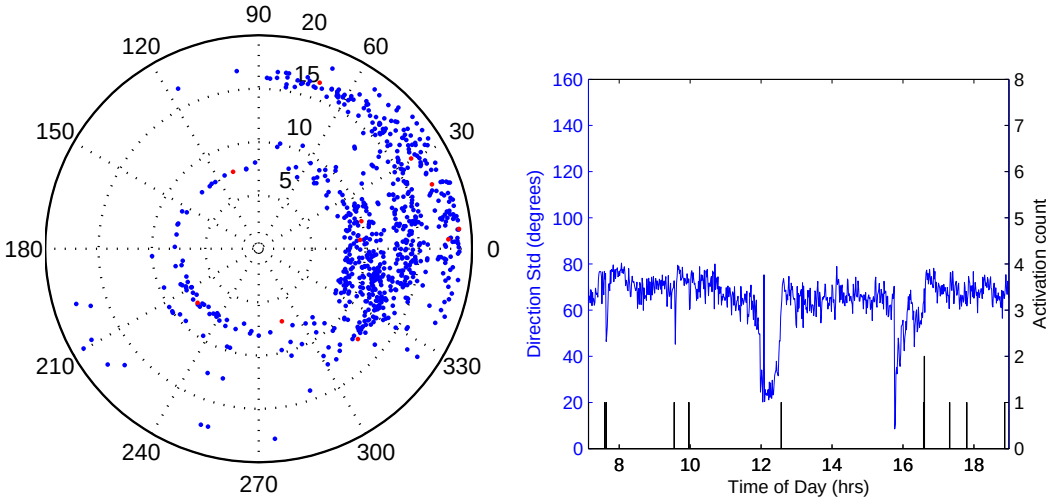

(ix) 4 February

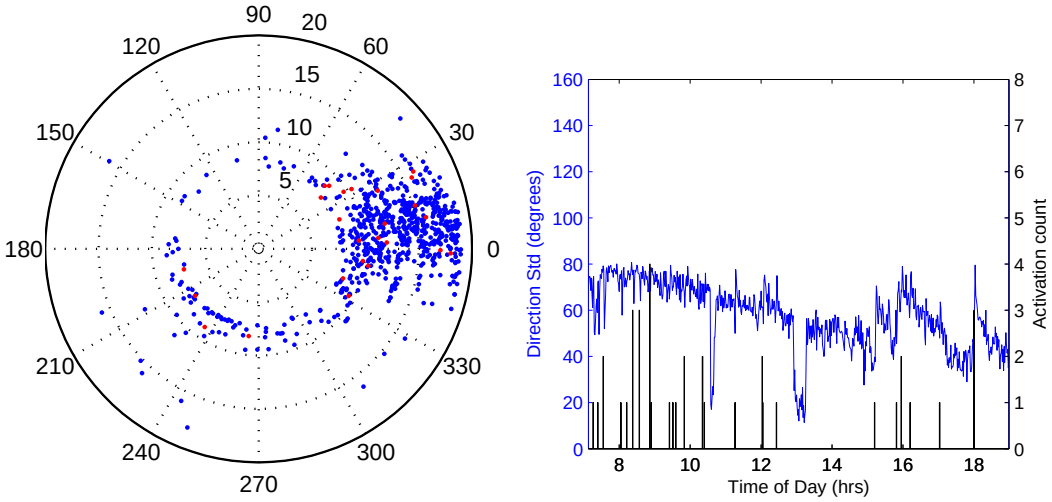

(x) 5 February

Figure C.3: Continued.

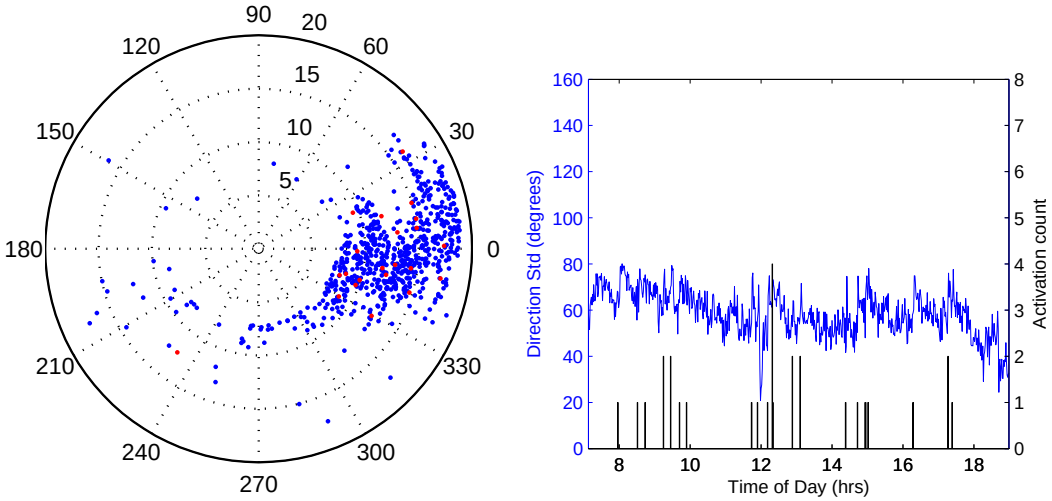

(xi) 6 February

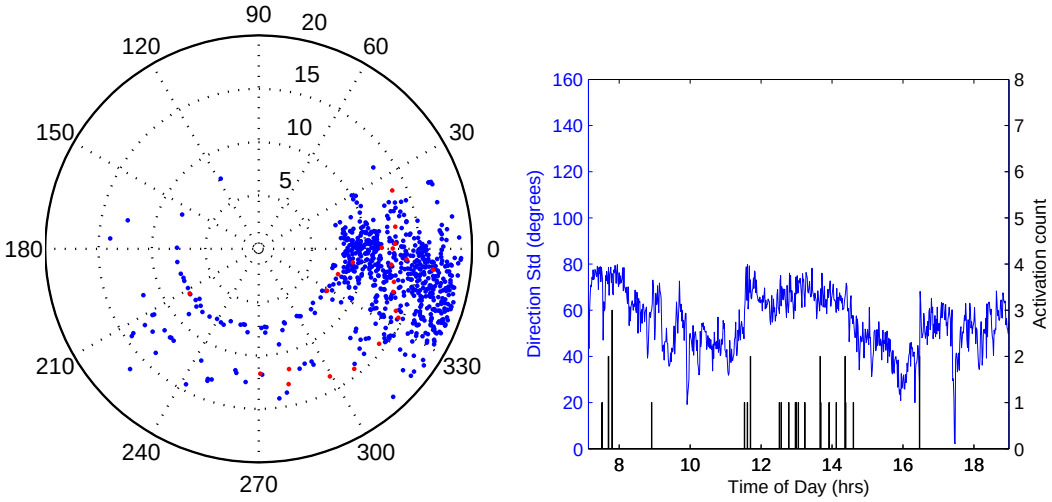

(xii) 7 February

Figure C.3: Continued.

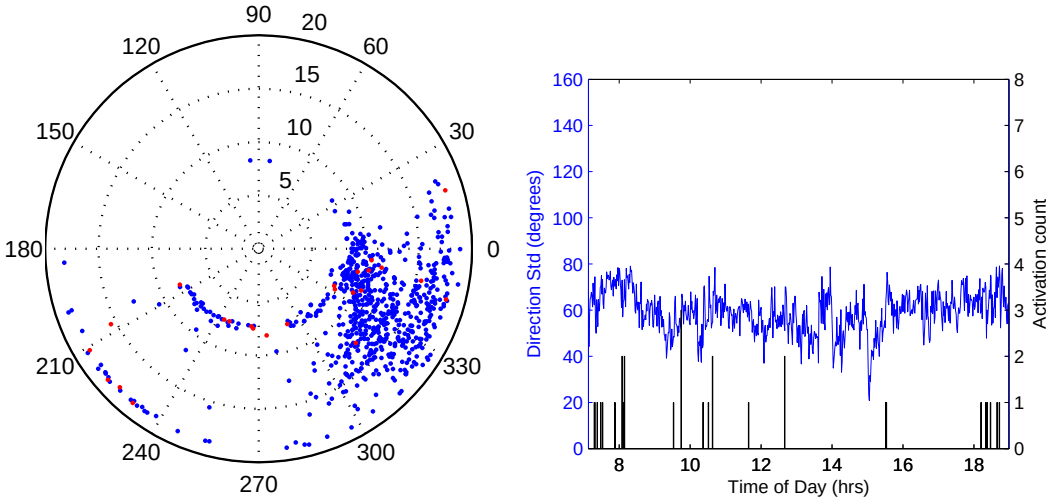

(xiii) 8 February

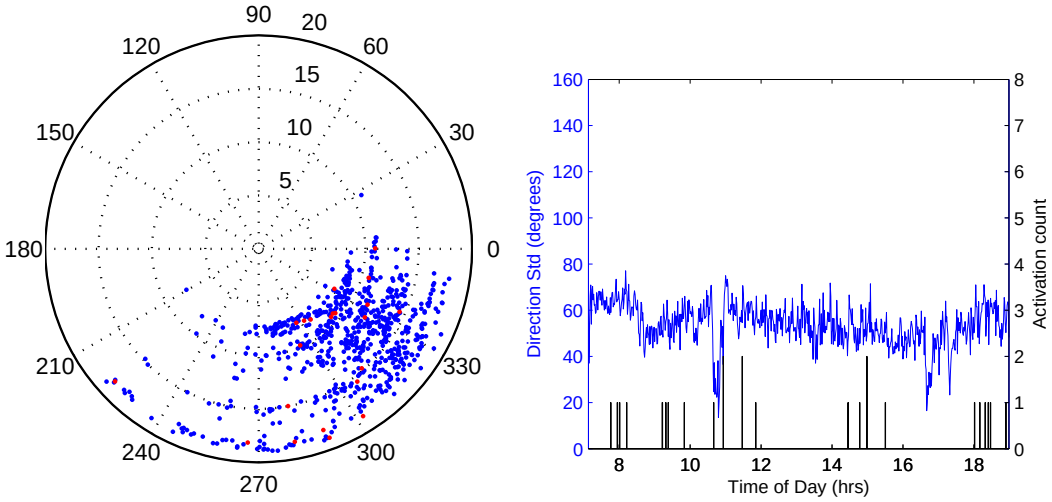

(xiv) 9 February

Figure C.3: Continued.

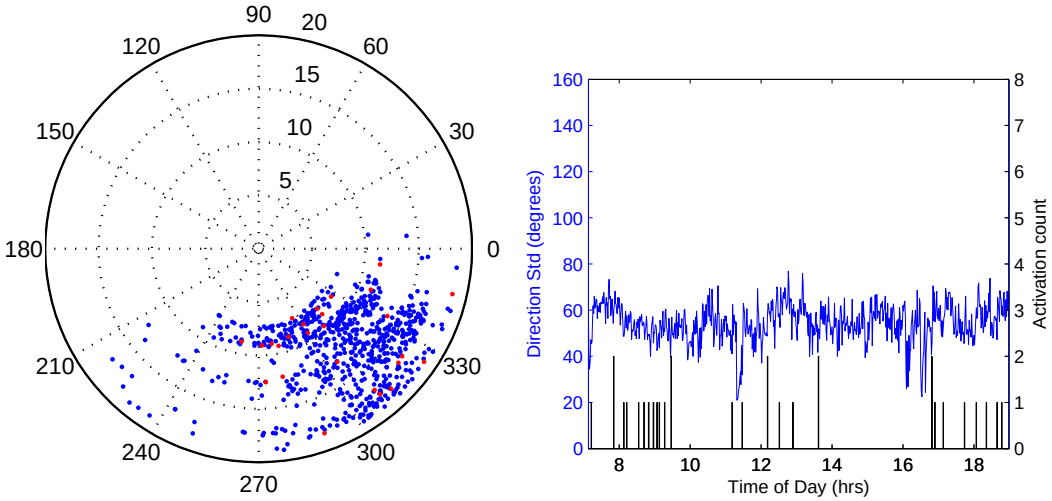

(xv) 10 February

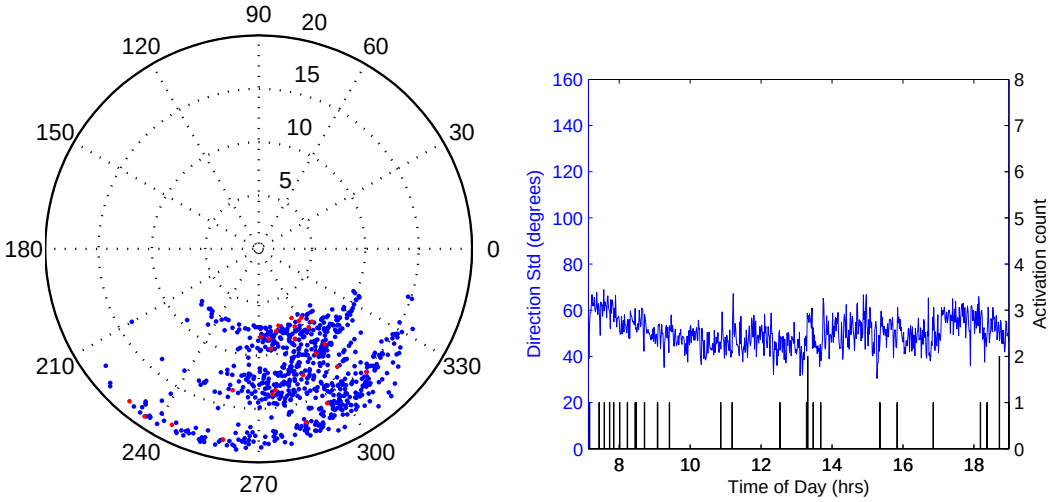

(xvi) 11 February

Figure C.3: Continued.

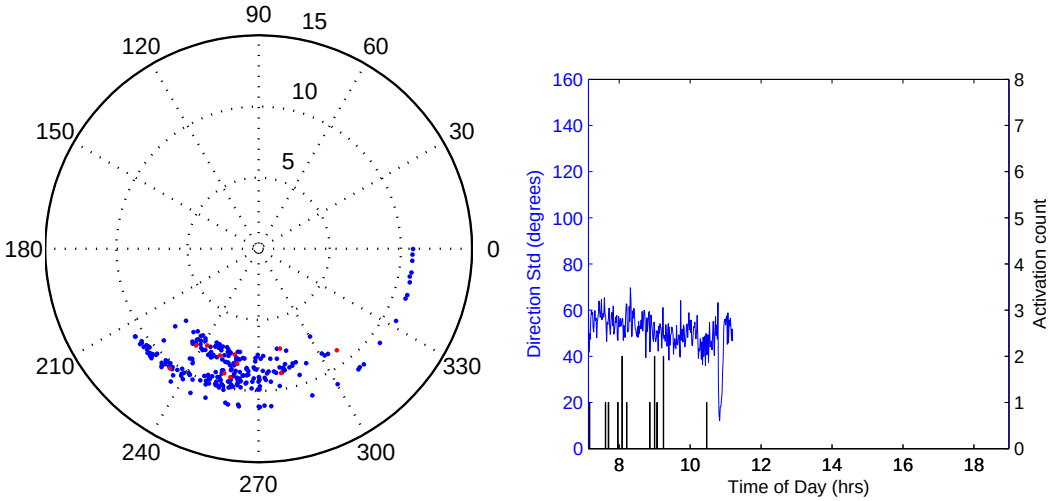

(xvii) 12 February

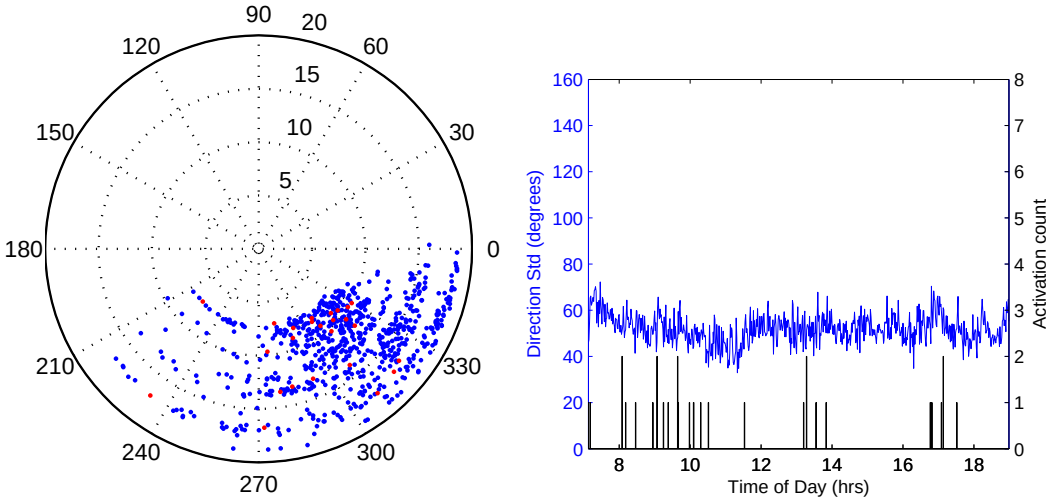

(xviii) 13 February

Figure C.3: Continued.

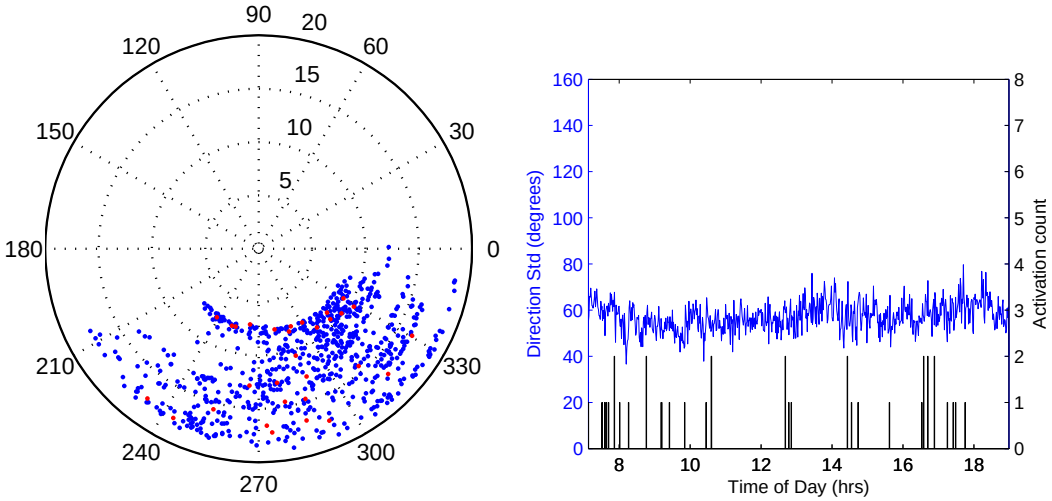

(xix) 14 February

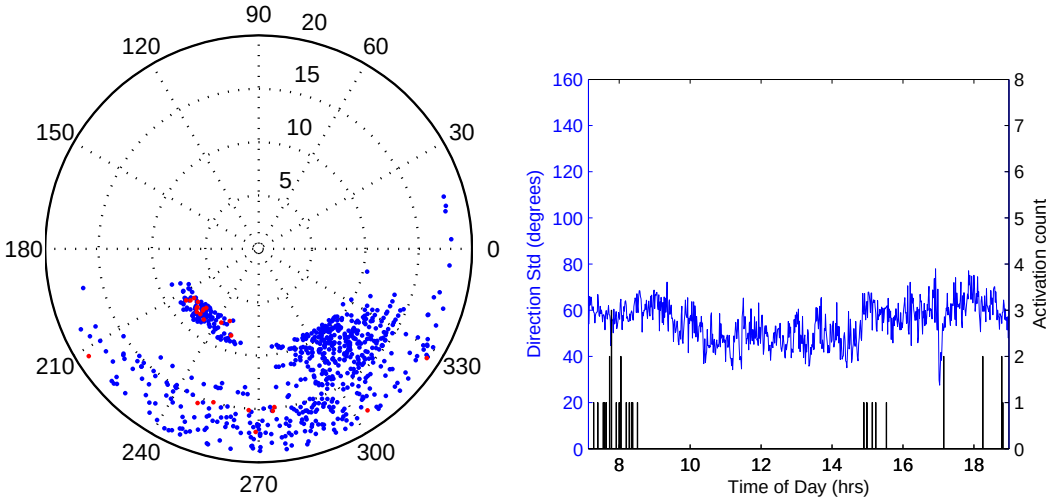

(xx) 15 February

Figure C.3: Continued.

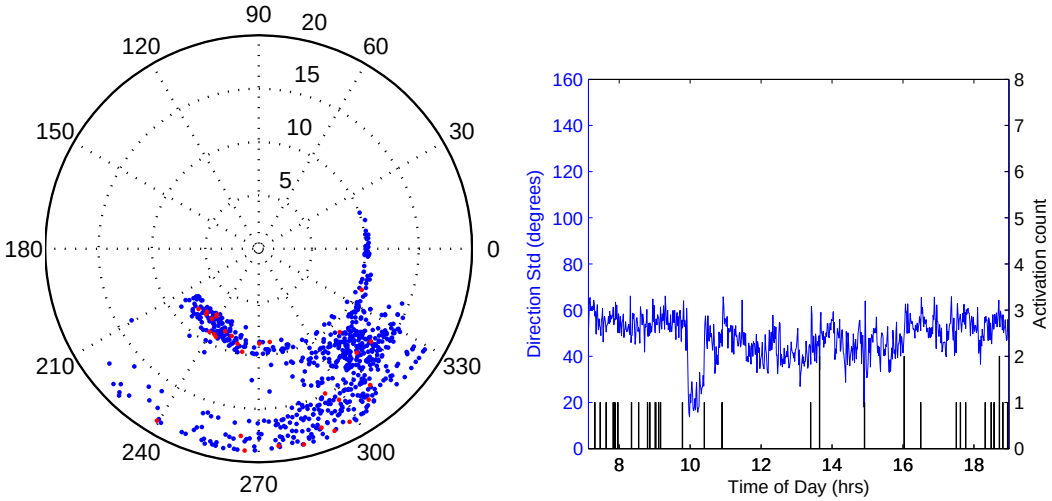

(xxi) 16 February

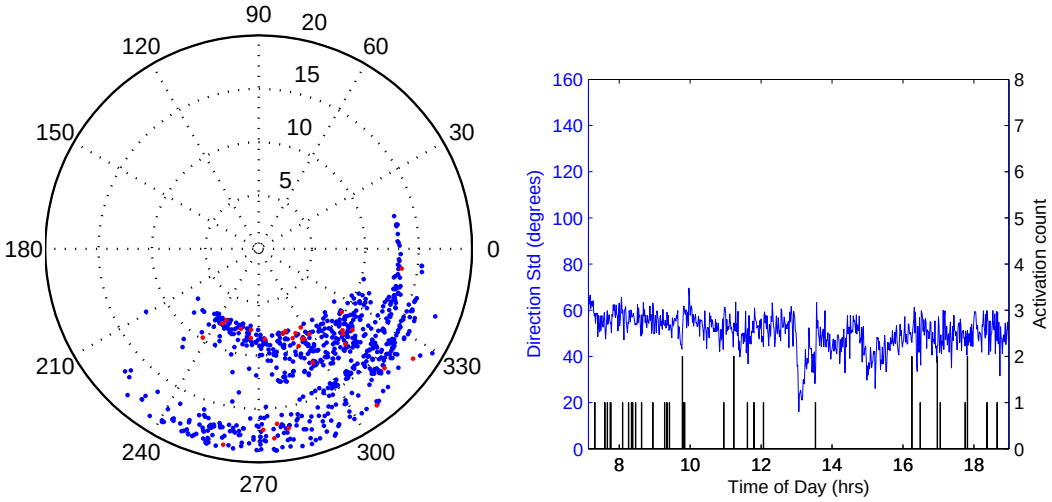

(xxii) 17 February

Figure C.3: Continued.

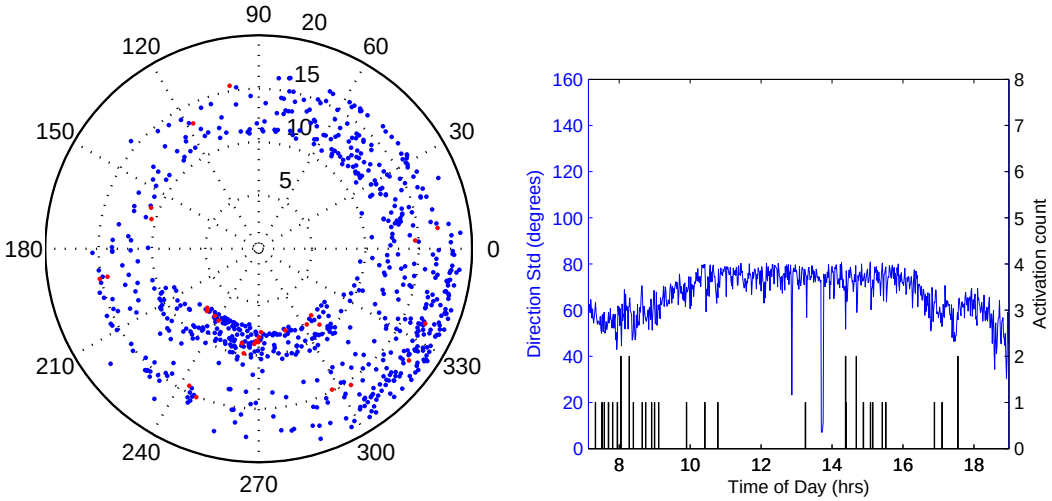

(xxiii) 18 February

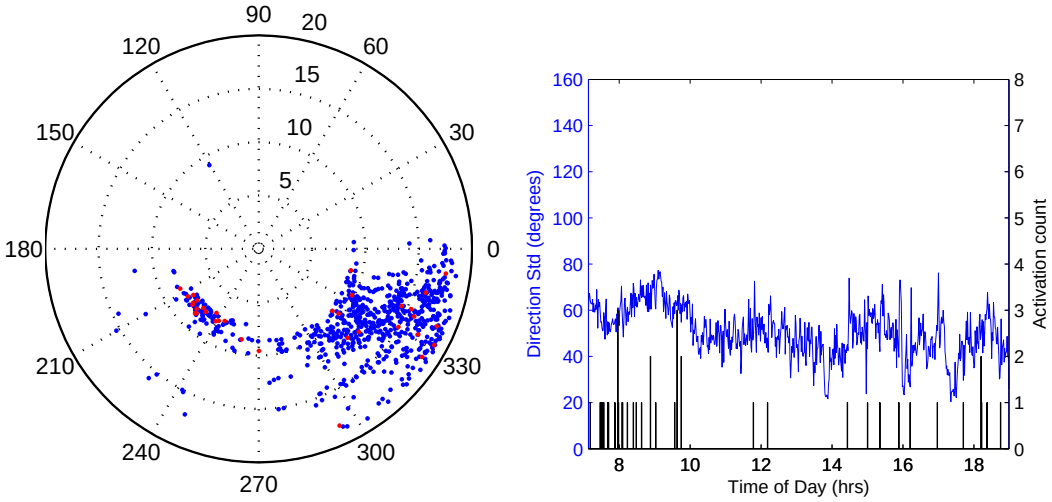

(xxiv) 19 February

Figure C.3: Continued.

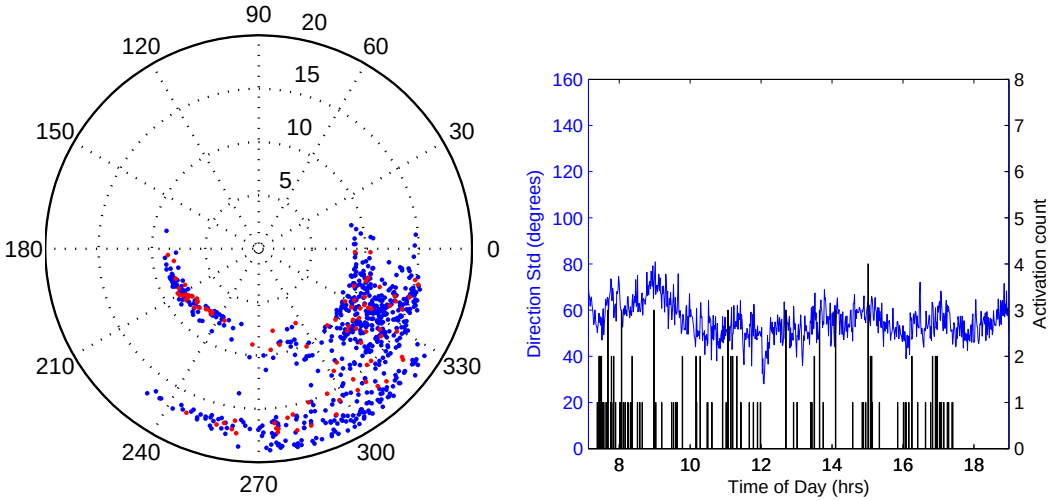

(xxv) 20 February

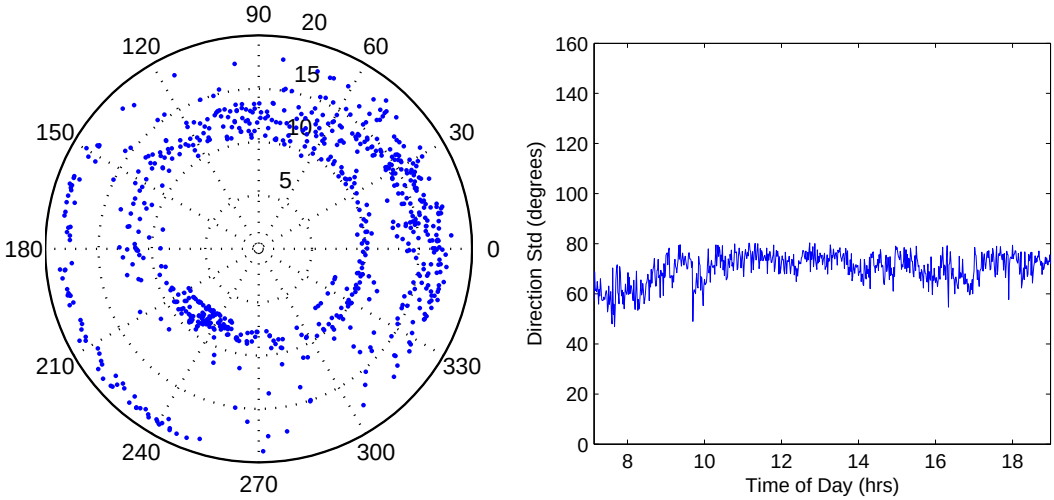

(xxvi) 21 February

Figure C.3: Continued.

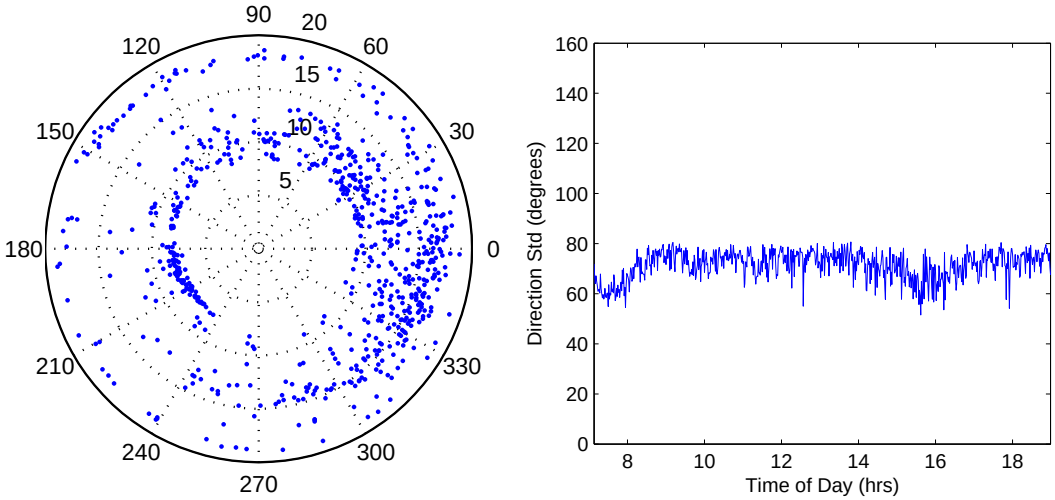

(xxvii) 22 February

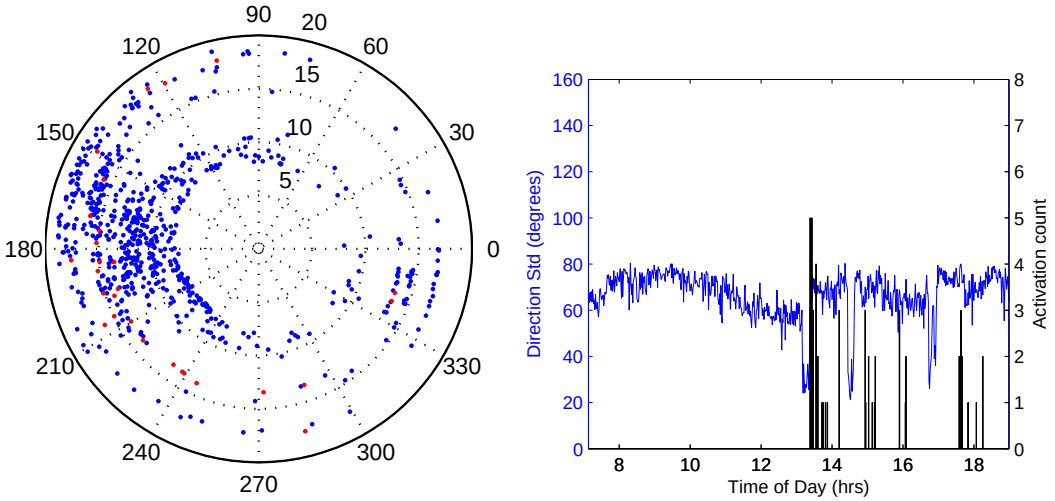

(xxviii) 23 February

Figure C.3: Continued.

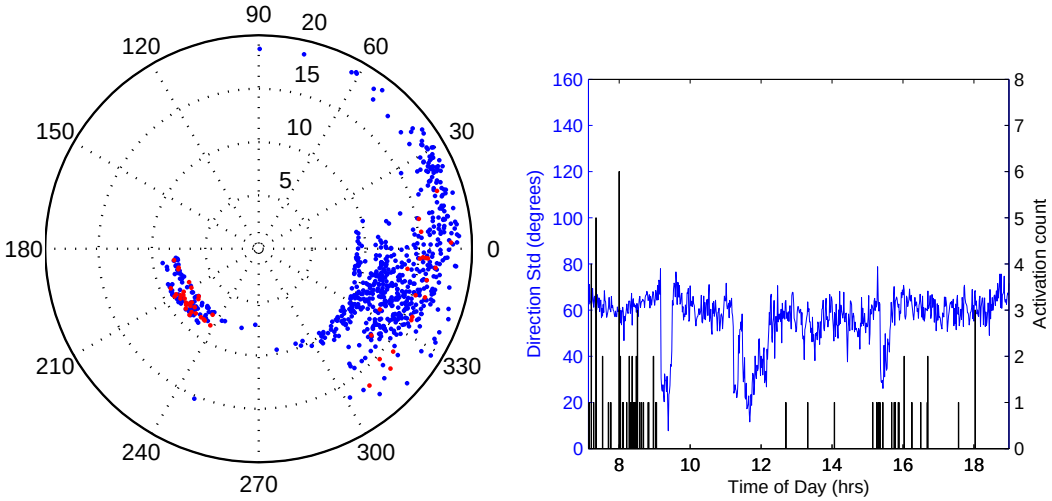

(xxix) 24 February

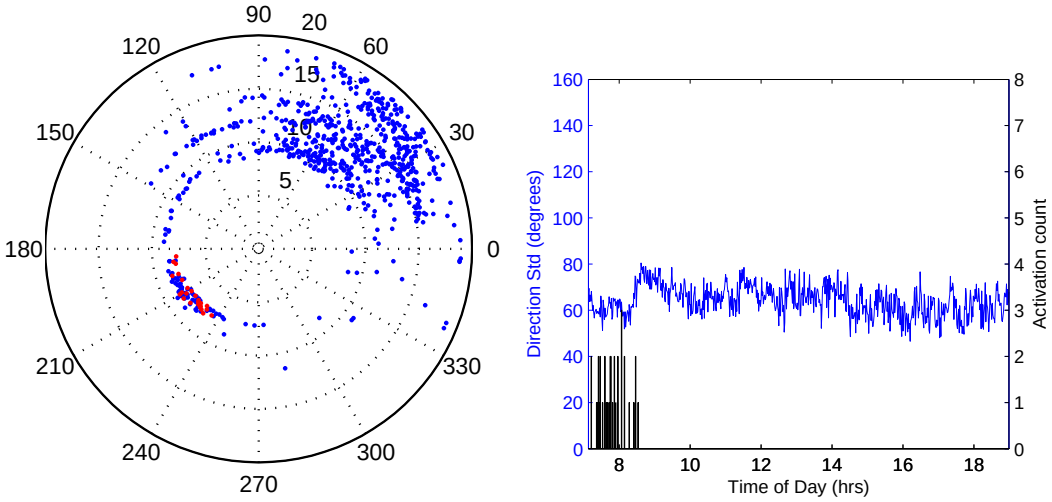

(xxx) 25 February

Figure C.3: Continued.

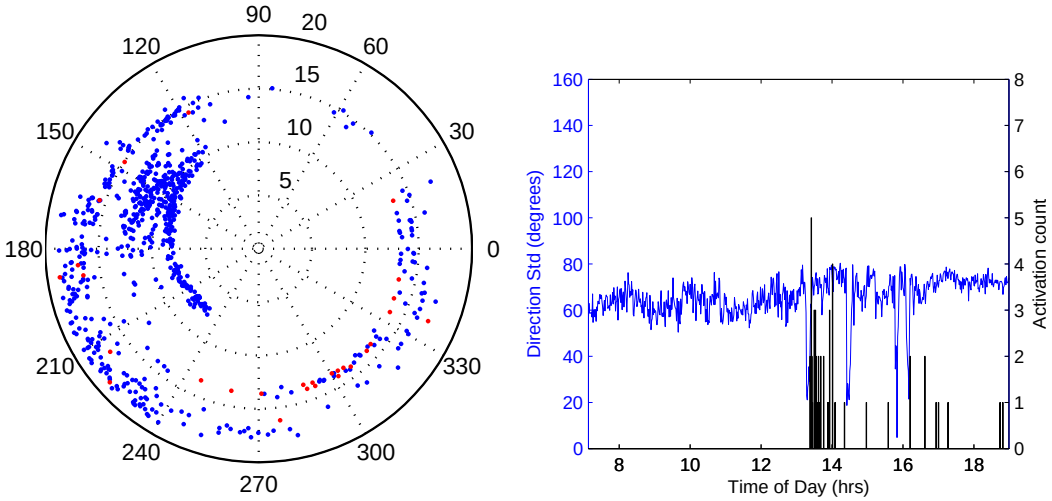

(xxxi) 26 February

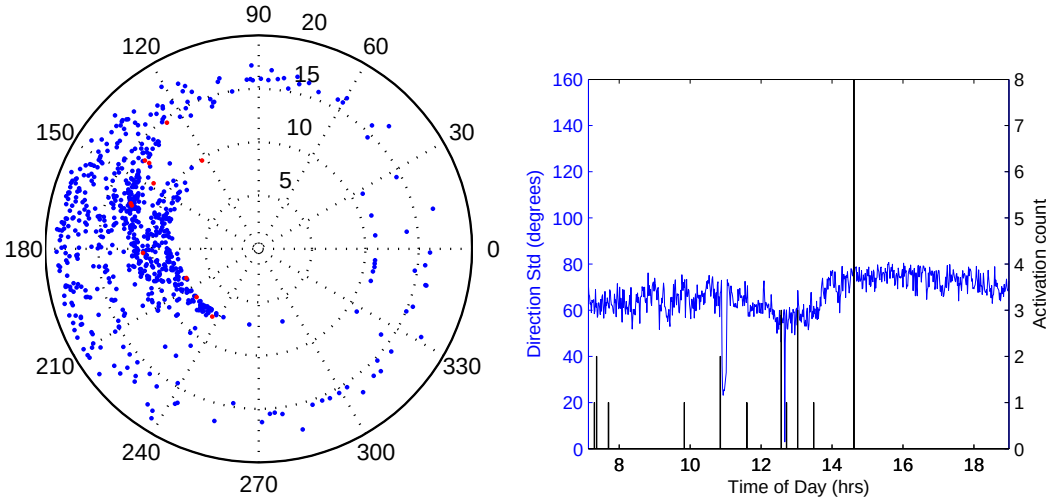

(xxxii) 27 February

Figure C.3: Continued.

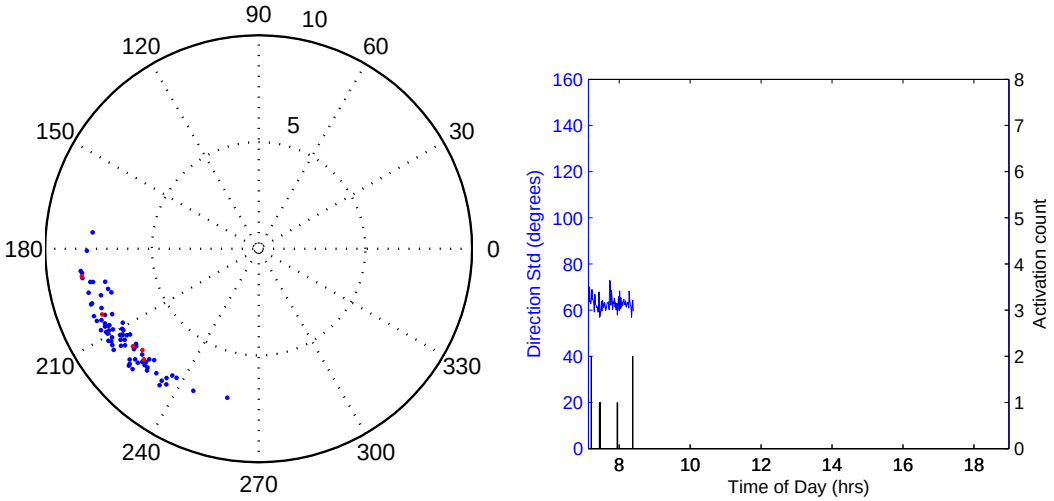

(xxxiii) 28 February

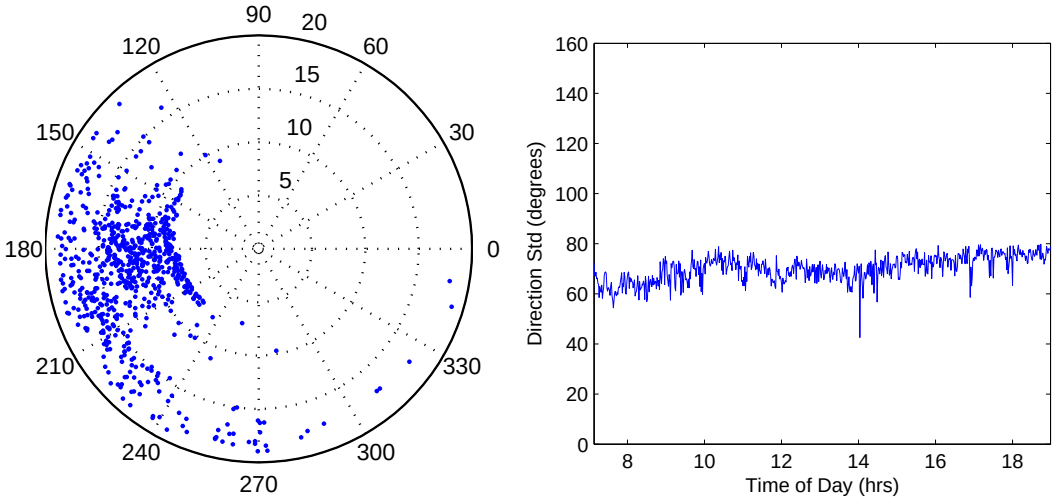

(xxxiv) 1 March

Figure C.3: Continued.

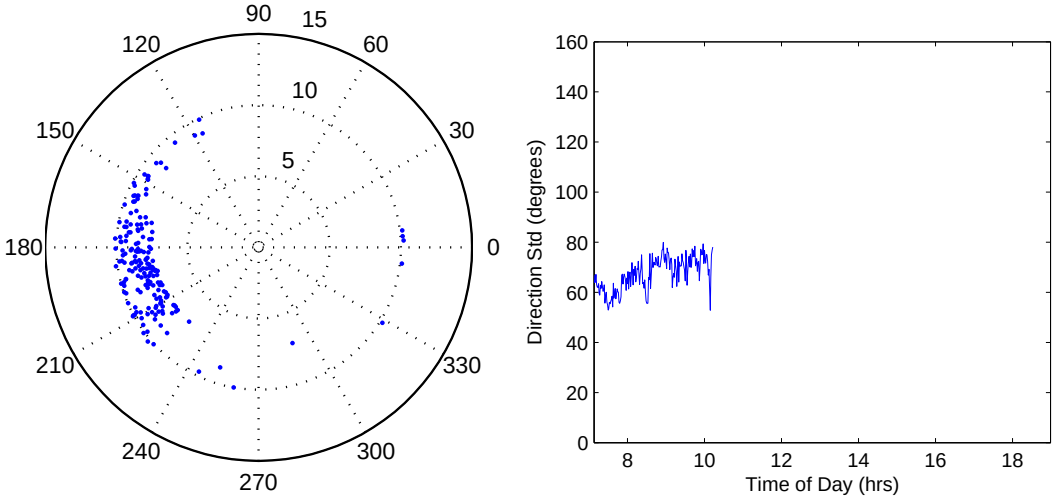

(xxxv) 2 March

Figure C.3: Continued.

References

Alanärä, A., Burns, M., and Metcalfe, N. (**2001**). "Intraspecific Resource Partitioning in Brown Trout: the Temporal Distribution of Foraging is Determined by Social Rank." *Journal of Animal Ecology*, 70(6): 980–986.

Ali, S. and Shah, M. (**2008**). "Floor Fields for Tracking in High Density Crowded Scenes." In *Proceedings of 10th European Conference on Computer Vision*, pages 1–14. Marseille, France.

Andrew, J. E., Holm, J., Kadri, S., and Huntingford, F. A. (**2004**). "The Effect of Competition on the Feeding Efficiency and Feed Handling Behaviour in Gilthead Sea Bream (*Sparus aurata* L.) Held in Tanks." *Aquaculture*, 232(1-4): 317–331.

Andrew, J. E., Noble, C., Kadri, S., Jewell, H., and Huntingford, F. A. (**2002**). "The Effect of Demand Feeding on Swimming Speed and Feeding Responses in Atlantic Salmon (*Salmo salar* L.), Gilthead Gea Bream (*Sparus aurata* L.) and European Sea Bass (*Dicentrarchus labrax* L.) in Sea Cages." *Aquaculture Research*, 33(7): 501–507.

Ang, K. P. and Petrell, R. J. (**1997**). "Control of Feed Dispensation in Seacages Using Underwater Video Monitoring: Effects on Growth and Food Conversion." *Aquacultural Engineering*, 16(1-2): 45–62.

Ang, K. P. and Petrell, R. J. (**1998**). "Pellet Wastage, and Subsurface and Surface Feeding Behaviours Associated with Different Feeding Systems in Sea Cage Farming of Salmonids." *Aquacultural Engineering*, 18(2): 95–115.

Arulampalam, M. S., Maskell, S., Gordon, N., and Clapp, T. (**2002**). "A Tutorial on Particle Filters for Online Nonlinear/Non-Gaussian Bayesian Tracking." *IEEE Transactions on Signal Processing*, 50(2): 174–188.

Ashley, P. J. (**2007**). "Fish Welfare: Current Issues in Aquaculture." *Applied Animal Behaviour Science*, 104(3-4): 199–235.

Bailey, J. and Alanärä, A. (**2006**). "Mapping the demand-feeding pattern of hatchery-reared rainbow trout, *Oncorhynchus mykiss* (Walbaum)." *Aquaculture*, 254(1-4): 355–360.

Bar-Shalom, Y. and Li, X.-R. (**1995**). *Multitarget-multisensor Tracking : Principles and Techniques*. The Authors, Storrs, Connecticut.

Bar-Shalom, Y. and Tse, E. (**1975**). "Tracking in a Cluttered Environment with Probabilistic Data Association." *Automatica*, 11: 451–460.

Baras, E. and Lagardère, J.-P. (**1995**). "Fish Telemetry in Aquaculture: Review and Perspectives." *Aquaculture International*, 3(2): 77–102.

Batschelet, E. (**1981**). *Circular Statistics in Biology*. Mathematics in biology. Academic Press, London.

Baumgartner, L., Reynoldson, N., Cameron, L., and Stanger, J. (**2006**). *Assessment of a Dual-frequency Identification Sonar (DIDSON) for Application in Fish Migration Studies*. Technical report, NSW Department of Primary Industries.

Bégout Anras, M.-L. and Lagardère, J. P. (**2004**). "Measuring Cultured Fish Swimming Behaviour: First Results on Rainbow Trout Using Acoustic Telemetry in Tanks." *Aquaculture*, 240(1-4): 175–186.

Bellman, R. E. (**1957**). *Dynamic programming*. Princeton University Press.

Blackman, S. S. and Popoli, R. (**1999**). *Design and Analysis of Modern Tracking Systems*. Artech House, Boston, Mass.

Blyth, P., Purser, G., and Russell, J. (**1993**). "Detection of Feeding Rhythms in Sea-caged Atlantic Salmon Using New Feeder Technology." In H. Reinersten, L. A. Dahle, L. Jørgensen, and K. Tvinnereim, editors, *Fish Farming Technology Conference*, pages 209–215. A.A.Balkema, Rotterdam.

Blyth, P. J., Kadri, S., Valdimarsson, S. K., Mitchell, D. F., and Purser, G. J. (**1999**). "Diurnal and seasonal variation in feeding patterns of Atlantic salmon, *Salmo salar* L., in sea cages." *Aquaculture Research*, 30(7): 539–544.

Boult, T. E., Micheals, R. J., Gao, X., and Eckmann, M. (**2001**). "Into the Woods: Visual Surveillance of Noncooperative and Camouflaged Targets in Complex Outdoor Settings." *Proceedings of the IEEE*, 89(10): 1382–1402.

Brännäs, E. and Alanärä, A. (**1993**). "Monitoring the Feeding Activity of Individual Fish with a Demand Feeding System." *Journal of Fish Biology*, 42(2): 209–215.

Brännäs, E., Alanärä, A., and Magnhagen, C. (**2001**). "The Social Behaviour of Fish." In L. Keeling and H. Gonyou, editors, *Social Behaviour in Farm Animals*, pages 275–304. CABI Publishing.

Branson, E. (**2008**). *Fish Welfare*. Blackwell, Oxford.

Bratland, S., Stien, L., Braithwaite, V., Juell, J.-E., Folkedal, O., Nilsson, J., Oppedal, F., Fosseidengen, J., and Kristiansen, T. (**2010**). "From Fright to Anticipation: Using Aversive Light Stimuli to Investigate Reward Conditioning in Large Groups of Atlantic Salmon (*Salmo salar*)." *Aquaculture International (online)*.

Breit, H. and Rigoll, G. (**2001**). "Improved Person Tracking Using a Combined Pseudo-2D-HMM and Kalman Filter Approach with Automatic Background State Adaptation." In *Proceedings of the International Conference on Image Processing, 2001*, volume 2, pages 53–56 vol.2.

Bridger, C. and Booth, R. (**2003**). "The Effects of Biotelemetry Transmitter Presence and Attachment Procedures on Fish Physiology and Behavior." *Reviews in Fisheries Science*, 11(1): 13–34.

Brown, C., Laland, K. N., and Krause, J. (**2006**). *Fish Cognition and Behavior*. Fish and aquatic resources series ; 11. Blackwell, Oxford, England, 1st edition.

Buehren, M. (**2009**). "Functions for the Rectangular Assignment Problem." URL `http://www.mathworks.com/matlabcentral/fileexchange/6543`.

Cai, J. and Walker, R. (**2008**). "Robust Motion Estimation for Camcorders Mounted in Mobile Platforms." In *Proceedings of Digital Image Computing: Techniques and Application*, pages 491–497.

Cai, J. and Walker, R. A. (**2009**). "Robust Video Stabilisation Algorithm using Feature Point Selection and Delta Optical Flow." *IET Computer Vision*, 3(4): 176–188.

Cai, Y. (**2005**). *Robust Visual Tracking for Multiple Targets*. Master's thesis, University of British Columbia.

Chien, S.-Y., Huang, Y.-W., Hsieh, B.-Y., Ma, S.-Y., and Chen, L.-G. (**2004**). "Fast Video Segmentation Algorithm with Shadow Cancellation, Global Motion Compensation, and Adaptive Threshold Techniques." *IEEE Transactions on Multimedia*, 6(5): 732–748.

Collins, R., Lipton, A., Kanade, T., Fujiyoshi, H., Duggins, D., Tsin, Y., Tolliver, D., Enomoto, N., and Hasegawa, O. (**2000**). *A System for Video Surveillance and Monitoring*. Technical Report CMU-RI-TR-00-12, Robotics Institute, Carnegie Mellon University.

Comaniciu, D. and Meer, P. (**2002**). "Mean Shift: a Robust Approach Toward Feature Space Analysis." *IEEE Transactions on Pattern Analysis and Machine Intelligence*, 24(5): 603–619.

Conti, S. G., Roux, P., Fauvel, C., Maurer, B. D., and Demer, D. A. (**2006**). "Acoustical Monitoring of Fish Density, Behavior, and Growth Rate in a Tank." *Aquaculture*, 251(2-4): 314–323.

Cootes, T. and Taylor, C. (**2001**). "Statistical Models of Appearance for Medical Image Analysis and Computer Vision." In *SPIE Medical Imaging 2001*, volume 4322, pages 236–248.

Cootes, T., Taylor, C., Cooper, D., and Graham, J. (**1995**). "Active Shape Models - Their Training and Application." *Computer Vision and Image Understanding*, 61(1): 3859.

Costa, C., Loy, A., Cataudella, S., Davis, D., and Scardi, M. (**2006**). "Extracting Fish Size using Dual Underwater Cameras." *Aquacultural Engineering*, 35(3): 218–227.

Covès, D., Beauchaud, M., Attia, J., Dutto, G., Bouchut, C., and Bégout, M. L. (**2006**). "Long-term Monitoring of Individual Fish Triggering Activity on a Self-feeding System: An Example Using European Sea Bass (*Dicentrarchus labrax*)." *Aquaculture*, 253(1-4): 385–392.

Cox, J., Ingemar and Hingorani, L., Sunita (**1996**). "An Efficient Implementation of Reid's Multiple Hypothesis Tracking Algorithm and Its Evaluation for the Purpose of Visual Tracking." *IEEE Transactions on Pattern Analysis and Machine Intelligence*, 18(2): 138–150.

Cubitt, K. F., Churchill, S., Rowsell, D., Scruton, D. A., and McKinley, R. S. (**2003**). "3-dimensional Positioning of Salmon in Commercial Sea Cages: Assessment of a Tool for Monitoring Behaviour." In M. Spedicato, G. Lembo, and G. Marmulla, editors, *Proceedings of the Fifth Conference on Fish Telemetry*. Ustica, Italy.

Czyz, J., Ristic, B., and Macq, B. (**2005**). "A Color-based Particle Filter for Joint Detection and Tracking of Multiple Objects." In *IEEE International*

Conference on Acoustics, Speech, and Signal Processing, 2005, volume 2, pages 217–220.

Czyz, J., Ristic, B., and Macq, B. (**2007**). "A Particle Filter for Joint Detection and Tracking of Color Objects." *Image and Vision Computing*, 25(8): 1271–1281.

Damsgård, B., Juell, J.-E., and Braastad, B. O. (**2006**). *Welfare in Farmed Fish*. Technical report, Norwegian Institute of Fisheries and Aquaculture Research.

Daum, F. and Huang, J. (**2003**). "Curse of Dimensionality and Particle Filters." In *Proceeding of IEEE Aerospace Conference*, volume 4.

Davies, E. R. (**2005**). *Machine Vision : Theory, Algorithms, Practicalities*. Elsevier, Amsterdam ; Boston, 3rd edition.

Dempster, T., Juell, J.-E., Fosseidengen, J. E., Fredheim, A., and Lader, P. (**2008**). "Behaviour and Growth of Atlantic salmon (*Salmo salar* L.) Subjected to Short-term Submergence in Commercial Scale Sea-cages." *Aquaculture*, 276(1-4): 103–111.

DeVries, P., Goetz, F., Fresh, K., and Seiler, D. (**2004**). "Evidence of a lunar gravitation cue on timing of estuarine entry by Pacific salmon smolts." *Transactions of the American Fisheries Society*, 133(6): 1379–1395.

Doucet, A. and Freitas, N. d. (**1998**). "MATLAB Code for Systematic Resampling."

Doucet, A., Godsill, S., and Andrieu, C. (**2000**). "On Sequential Monte Carlo Sampling Methods for Bayesian Filtering." *Statistics and Computing*, 10: 197–208.

Duarte, S., Reig, L., and Oca, J. (**2009**). "Measurement of Sole Activity by Digital Image Analysis." *Aquacultural Engineering*, 41(1): 22–27.

Dunn, Z. (**2008**). *Improved Feed Utilisation in Cage Aquaculture by Use of Machine Vision*. Master thesis, Stellenbosch University.

Fischer, P., Kautz, H., Weber, H., and Obergfell, W. (**2001**). "The Use of Passive Integrated Transponder Systems (PIT) Triggered by Infrared-gates for Behavioural Studies in Nocturnal, Bottom-dwelling Fish Species." *Journal of Fish Biology*, 58(1): 295–298.

Gélineau, A., Corraze, G., and Boujard, T. (**1998**). "Effects of Restricted Ration, Time-restricted Access and Reward Level on Voluntary Food Intake, Growth and Growth Heterogeneity of Rainbow Trout (*Oncorhynchus mykiss*) Fed on Demand with Self-feeders." *Aquaculture*, 167(3-4): 247–258.

Gonzalez, R. C. and Woods, R. E. (**2008**). *Digital Image Processing*. Pearson/Prentice Hall, Harlow, 3rd edition.

Gonzalez, R. C., Woods, R. E., and Eddins, S. L. (**2004**). *Digital Image Processing Using MATLAB*. Pearson Prentice Hall, Upper Saddle River, N. J.

Gordon, N., Salmond, D., and Smith, A. (**1993**). "Novel Approach to Nonlinear/Non-Gaussian Bayesian State Estimation." *IEE Proceedings F: Radar and Signal Processing*, 140(2): 107–113.

Hedenskog, M., Petersson, E., and Järvi, T. (**2002**). "Agonistic behavior and growth in newly emerged brown trout (*Salmo trutta* L) of sea-ranched and wild origin." *Aggressive Behavior*, 28(2): 145–153.

Herbert, N., Kadri, S., and Huntingford, F. (**2011**). "A moving light stimulus elicits a sustained swimming response in farmed Atlantic salmon, *Salmo salar* L." *Fish Physiology and Biochemistry*, 37(2): 317–325.

Hillier, F. S. and Lieberman, G. J. (**2010**). *Introduction to operations research*. McGraw-Hill Higher Education, Boston, 9th edition.

Hu, M., Ali, S., and Shah, M. (**2008**). "Detecting Global Motion Patterns in Complex Videos." In *19th International Conference on Pattern Recognition*. Tampa, Florida.

Huntingford, F. A. and Kadri, S. (**2008**). "Welfare and Fish." In E. Branson, editor, *Fish Welfare*, pages 19–31. Blackwell, Oxford.

Hvidsten, N. A., Jensen, A. J., Vivas, H., Bakke, O., and Heggberget, T. G. (**1995**). "Downstream migration of Atlantic salmon smolts in relation to water flow, water temperature, moon phase and social interaction." *Nordic Journal of Freshwater Research*, 70: 38–48.

Isard, M. (**1998**). *Visual Motion Analysis by Probabilistic Propagation of Conditional Density*. D.Phil thesis, Oxford University.

Israeli, D. and Kimmel, E. (**1996**). "Monitoring the behavior of hypoxia-stressed *Carassius auratus* using computer vision." *Aquacultural Engineering*, 15(6): 423–440.

Jang, D.-S., Jang, S.-W., and Choi, H.-I. (**2002**). "2D Human Body Tracking with Structural Kalman Filter." *Pattern Recognition*, 35(10): 2041–2049.

Jin, Y., Fayad, L., and Laine, A. (**2001**). "Contrast Enhancement by Multiscale Adaptive Histogram Equalization." In *Proceedings of SPIE - Wavelets: Applications in Signal and Image Processing IX*, volume 4478, pages 206–213.

Juell, J.-E. (**1995**). "The behaviour of Atlantic salmon in relation to efficient cage-rearing." *Reviews in Fish Biology and Fisheries*, 5(3): 320–335.

Juell, J.-E. and Fosseidengen, J. E. (**2004**). "Use of Artificial Light to Control Swimming Depth and Fish Density of Atlantic salmon (*Salmo salar*) in Production Cages." *Aquaculture*, 233(1-4): 269–282.

Julier, S. and Uhlmann, J. (**1997**). "A New Extension of the Kalman Filter to Nonlinear Systems." In *Int. Symp. Aerospace/Defense Sensing, Simul. and Controls*. Orlando, FL.

Kadri, S., Huntingford, F. A., Metcalfe, N. B., and Thorpe, J. E. (**1996**). "Social Interactions and the Distribution of Food Among One-sea-winter Atlantic Salmon (*Salmo salar*) in a Sea-cage." *Aquaculture*, 139(1-2): 1–10.

Kadri, S., Metcalfe, N. B., Huntingford, F. A., and Thorpe, J. E. (**1991**). "Daily Feeding Rhythms in Atlantic Salmon in Sea Cages." *Aquaculture*, 92: 219–224.

Kalman, R. E. (**1960**). "A New Approach to Linear Filtering and Prediction Problems." *Transactions of the ASME - Journal of Basic Engineering*, 82: 35–45.

Kato, S., Nakagawa, T., Ohkawa, M., Muramoto, K., Oyama, O., Watanabe, A., Nakashima, H., Nemoto, T., and Sugitani, K. (**2004**). "A Computer Image Processing System for Quantification of Zebrafish Behavior." *Journal of Neuroscience Methods*, 134(1): 1–7.

Kato, S., Tamada, K., Shimada, Y., and Chujo, T. (**1996**). "A Quantification of Goldfish Behavior by an Image Processing System." *Behavioural Brain Research*, 80(1-2): 51–55.

Koehn, J. D. (**1999**). "Why Use Radio Tags to Study Freshwater Fish?" In D. A. Hancock, D. C. Smith, and J. D. Koehn, editors, *Workshop on Fish Movement and Migration*, pages 24–32. Bendigo,Victoria.

Kreucher, C., Kastella, K., and Hero, A. O. (**2005**). "Multitarget Tracking Using the Joint Multitarget Probability Density." *IEEE Transactions on Aerospace and Electronic Systems*, 41(4): 1396–1414.

Kristiansen, T. S., Fernö, A., Holm, J. C., Privitera, L., Bakke, S., and Fosseidengen, J. E. (**2004**). "Swimming Behaviour as an Indicator of Low Growth Rate and Impaired Welfare in Atlantic Halibut (*Hippoglossus hippoglossus* L.) Reared at Three Stocking Densities." *Aquaculture*, 230(1-4): 137–151.

Lagardère, J. P., Mallekh, R., and Mariani, A. (**2004**). "Acoustic Characteristics of Two Feeding Modes Used by Brown Trout (*Salmo trutta*), Rainbow Trout (*Oncorhynchus mykiss*) and Turbot (*Scophthalmus maximus*)." *Aquaculture*, 240(1-4): 607–616.

Lumley, T., Diehr, P., Emerson, S., and Chen, L. (**2002**). "The Importance of the Normality Assumption in Large Public Health Data Sets." *Annual Review of Public Health*, 23: 151–169.

Martinez-de Dios, J. R., Serna, C., and Ollero, A. (**2003**). "Computer Vision and Robotics Techniques in Fish Farms." *Robotica*, 21(3): 233–243.

Mathworks (**2009**). "Documentation for MathWorks Products, R2009b." URL `http://www.mathworks.com`.

McKinnon, D., Trott, L., Duggan, S., Brinkman, R., Alongi, D., Castine, S., and Patel, F. (**2008**). *Environmental Impacts of Sea Cage Aquaculture in a Queensland Context - Hinchinbrook Channel Case Study.* Technical report, Australian Institute of Marine Science.

Michel, A. P. M., Croff, K. L., McLetchie, K. W., and Irish, J. D. (**2002**). "A Remote Monitoring System for Open Ocean Aquaculture." In *Proceedings of Oceans 2002 Conference*, volume 4, pages 2488–2496.

Miller, N. and Gerlai, R. (**2007**). "Quantification of Shoaling Behaviour in Zebrafish (*Danio rerio*)." *Behavioural Brain Research*, 184(2): 157–166.

Munkres, J. (**1957**). "Algorithms for the Assignment and Transportation Problems." *Journal of the Society for Industrial and Applied Mathematics*, 5(1): 32–38.

Naiberg, A. (**1994**). *A Unified Recognition and Stereo Vision System for Size Assessment.* Master thesis, University of British Columbia.

Noble, C., Kadri, S., Mitchell, D. F., and Huntingford, F. A. (**2007**). "The Impact of Environmental Variables on the Feeding Rhythms and Daily Feed Intake of Cage-held 1+ Atlantic Salmon Parr (*Salmo salar* L.)." *Aquaculture*, 269(1-4): 290–298.

Oppedal, F., Dempster, T., and Stien, L. (**2011**). "Environmental Drivers of Atlantic Salmon Behaviour in Sea-cages: a Review." *Aquaculture*.

Orderud, F. (**2005**). "Comparison of Kalman Filter Estimation Approaches for State Space Models with Nonlinear Measurements." In *Proceedings of Scandinavian Conference on Simulation and Modeling*.

Otsu, N. (**1979**). "A Threshold Selection Method from Gray-Level Histograms." *IEEE Transactions on Systems, Man, and Cybernetics*, 9(1): 62–66.

Pérez, P., Hue, C., Vermaak, J., and Gangnet, M. (**2002**). "Color-Based Probabilistic Tracking." In *Proceedings of the 7th European Conference on Computer Vision-Part I*, volume 2350, pages 661–675. Springer-Verlag.

Petersson, E. and Järvi, T. (**2006**). "Anti-predator Response in Wild and Sea-ranched Brown Trout and Their Crosses." *Aquaculture*, 253(1-4): 218–228.

Petrell, R. J. and Ang, K. P. (**2001**). "Effects of Pellet Contrast and Light Intensity on Salmonid Feeding Behaviours." *Aquacultural Engineering*, 25(3): 175–186.

Petrell, R. J., Shi, X., Ward, R. K., Naiberg, A., and Savage, C. R. (**1997**). "Determining Fish Size and Swimming Speed in Cages and Tanks using Simple Video Techniques." *Aquacultural Engineering*, 16(1-2): 63–84.

Pizer, S. M., Amburn, E. P., Austin, J. D., Cromartie, R., Geselowitz, A., Greer, T., Romeny, B. t. H., Zimmerman, J. B., and Zuiderveld, K. (**1987**). "Adaptive Histogram Equalisation and Its Variations." *Computer Vision, Graphics and Image Processing*, 39: 355–368.

Poore, A. P., Rijavec, N., Barker, T. N., and Munger, M. L. (**1993**). "Data Association Problems Posed as Multidimensional Assignment Problems: Algorithm Development." In I. Kadar and V. Libby, editors, *Proceedings of SPIE - Signal Processing, Sensor Fusion, and Target Recognition II*, volume 1955, pages 172–182. SPIE, Orlando, FL, USA.

Prentice, E. F., Flagg, T., McCutcheon, C., Brastow, D., and Cross, D. (**1990**). "Equipment, Methods and an Automated Data-Entry Station for PIT Tagging." In R. C. H. N. C. Parker, A. E. Giorgi and D. Jester,

editors, *Fish-Marking Techniques*, pages 335–340. American Fisheries Society, Bethesda, Maryland.

Purser, J. and Forteath, N. (**2003**). "Salmonids." In J. Lucas and P. Southgate, editors, *Aquaculture: Farming of Aquatic Animals and Plants*, pages 295–320. Blackwell Publishing, Oxford.

Reid, D. (**1979**). "An Algorithm for Tracking Multiple Targets." *Automatic Control, IEEE Transactions on*, 24(6): 843–854.

Rillahan, C., Chambers, M., Howell, W. H., and Watson III, W. H. (**2009**). "A Self-contained System for Observing and Quantifying the Behavior of Atlantic Cod, *Gadus morhua*, in an Offshore Aquaculture Cage." *Aquaculture*, In Press, Corrected Proof.

Ristic, B. (**1998**). "MATLAB Code for Modified Munkres Algorithm for Optimal Assignment."

Ristic, B. (**2007**). "Tracking and Data Fusion Short Course."

Ristic, B., Arulampalm, S., and Gordon, N. (**2004**). *Beyond the Kalman Filter : Particle Filters for Tracking Applications*. Artech House, Boston, MA.

Rosin, P. and Ellis, T. (**1995**). "Image Difference Threshold Strategies and Shadow Detection." In *Proceedings of the British Conference on Machine Vision, 1995*, volume 1. BMVA Press, Birmingham, UK.

Salmond, D. J. and Birch, H. (**2001**). "A Particle Filter for Track-Before-Detect." In *Proceedings of the 2001 American Control Conference*, volume 5, pages 3755–3760.

Smith, I., Metcalfe, N., Huntingford, F., and Kadri, S. (**1993**). "Daily and Seasonal Patterns in the Feeding Behaviour of Atlantic Salmon (*Salmo Salar* L.) in a Sea Cage." *Aquaculture*, 117(1-2): 165–178.

Stenger, B., Mendonca, P., and Cipolla, R. (**2001**). "Model-based Hand Tracking Using an Unscented Kalman Filter." In *Proceedings of the British Machine Vision Conference*. Manchester, UK.

Stien, L. H., Bratland, S., Austevoll, I., Oppedal, F., and Kristiansen, T. S. (**2007**). "A Video Analysis Procedure for Assessing Vertical Fish Distribution in Aquaculture Tanks." *Aquacultural Engineering*, 37(2): 115–124.

Tillett, R., McFarlane, N., and Lines, J. (**2000**). "Estimating Dimensions of Free-Swimming Fish Using 3D Point Distribution Models." *Computer Vision and Image Understanding*, 79(1): 123–141.

Welch, G. and Bishop, G. (**1995**). *An Introduction to the Kalman Filter*. Technical Report TR 95-041, University of North Carolina. Updated 04/07/2006.

Welch, G. and Bishop, G. (**2001**). "An Introduction to the Kalman Filter - Course 8." In *SIGGRAPH 2001*.

Weng, S.-K., Kuo, C.-M., and Tu, S.-K. (**2006**). "Video Object Tracking Using Adaptive Kalman Filter." *Journal of Visual Communication and Image Representation*, 17(6): 1190–1208.

Williams, R., Lambert, T., Kelsall, A., and Pauly, T. (**2006**). "Detecting Marine Animals in Underwater Video: Let's Start with Salmon." In *Proceedings of 12th Americas Conference on Information Systems*. Mexico, Acapulco.

Williamson, J. R. (**1996**). "Gaussian ARTMAP: A Neural Network for Fast Incremental Learning of Noisy Multidimensional Maps." *Neural Networks*, 9: 881–897.

Xu, J., Liu, Y., Cui, S., and Miao, X. (**2006**). "Behavioral Responses of Tilapia (*Oreochromis niloticus*) to Acute Fluctuations in Dissolved Oxygen Levels as Monitored by Computer Vision." *Aquacultural Engineering*, 35(3): 207–217.

Xu, L. Q., Landabaso, J. L., and Lei, B. (**2004**). "Segmentation and Tracking of Multiple Moving Objects for Intelligent Video Analysis." *BT Technology Journal*, 22(3): 140–150.

Yamauchi, K., Koide, N., Adachi, S., and Nagahama, Y. (**1984**). "Changes in seawater adaptability and blood thyroxine concentrations during smoltification of the masu salmon, *Oncorhynchus masou*, and the amago salmon, *Oncorhynchus rhodurus*." *Aquaculture*, 42(3-4): 247–256.

Index